U. S. ARMY ELECTRONICS COMMAND

Fort Monmouth, New Jersey

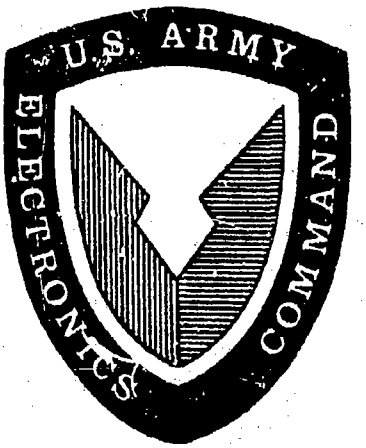

PROCEEDINGS OF THE ECOM-ARO WORKSHOP ON ELECTRICALLY SMALL ANTENNAS

6 and 7 MAY 1976,
FORT MONMOUTH, NEW JERSEY,

EDITED BY G. GOUBAU AND F. SCHWERING

October 1976

Approved for public release;
distribution unlimited

DISCLAIMER

The findings in this report are not to be construed as an official Department of the Army position, unless so designated by other authorized documents.

The citation of trade names and names of manufacturers in this report is not to be construed as official Government indorsement or approval of commercial products or services referenced herein.

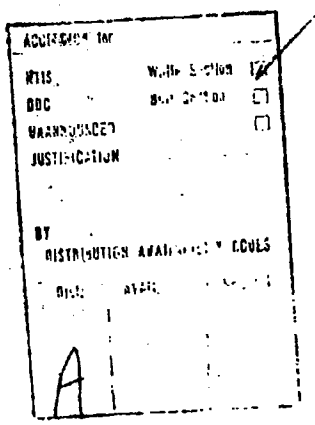

PROCEEDINGS OF THE WORKSHOP ON ELECTRICALLY SMALL ANTENNAS 6 AND 7 MAY 1976

SPONSOR

U. S. ARMY RESEARCH OFFICE
DURHAM, NORTH CAROLINA

HOST

COMMUNICATIONS/AUTOMATIC DATA PROCESSING LABORATORY
U. S. ARMY ELECTRONICS COMMAND
FORT MONMOUTH, NEW JERSEY

Approved for public release;
distribution unlimited

These Proceedings are dedicated to the memory of
our late colleague

D R . K U R T I K R A T H

He will be remembered for
his great interest in his fellow man,
his innovative ability, and
his dedication to his profession.

FOREWORD

Antennas to be used for communication in Army tactical situations have to satisfy the requirements of low visibility and low vulnerability. At wavelengths in the HF and VHF ranges--the frequency bands commonly used for tactical radio communications--these constraints require the use of *electrically small antennas*. As is well known, the design of such antennas requires sophistication if acceptable electrical performance is to be achieved.

The purpose of the Workshop was to bring together antenna scientists from universities, industries, and government laboratories to discuss the capabilities, fundamental limitations, and design trade-offs of electrically small antennas, and to provide a forum for the presentation of new ideas for improving antenna performance.

Special attention has been given to active antenna techniques, which up to now have not been used by the Army to a large extent, and to the problem of controlling or utilizing the interaction of electrically small antennas with complex platform environments such as provided by tanks, helicopters, and manpack sets.

The Workshop was suggested and sponsored by the U. S. Army Research Office, Durham, N. C. The Communications Research Technical Area, Communications/Automatic Data Processing Laboratory, ECOM, Fort Monmouth, organized and hosted the conference.

TABLE OF CONTENTS

AGENDA

WORKSHOP ON ELECTRICALLY SMALL ANTENNAS

6 and 7 May 1976

U. S. Army Electronics Command
Fort Monmouth, New Jersey

Sponsored by The U. S. Army Research Office

Conducted by The Communications/ADP Laboratory of ECOM

Chairman: G. Goubau Co-Chairman: F. Schwering

THURSDAY, 6 MAY 1976 - Morning

0800-0830 REGISTRATION

INTRODUCTION

0830-0845 OPENING REMARKS
Col. D. A. Slingerland, Director, Comm/ADP Laboratory

0845-0900 BACKGROUND AND PURPOSE OF WORKSHOP
F. Schwering, ECOM

INVITED PAPERS

0900-0930 ANTENNA REQUIREMENTS FOR THE MODERN WARFARE BATTLEFIELD
Captain K. N. Graham, U. S. Army Signal School.*

0930-1000 AN OVERVIEW OF ELECTRICALLY SMALL ANTENNAS WITHIN THE NAVY
M. S. Kvigne, Naval Electronics Laboratory Center.

1000-1020 INTERMISSION

1020-1050 INTRODUCTION TO THE CONCEPT OF SMALL ANTENNAS
H. A. Wheeler, Hazeltine Corporation.

1050-1120 ELECTRICALLY SMALL ANTENNA STUDIES AT OHIO STATE UNIVERSITY
C. H. Walter, Ohio State University

* Paper presented by Master Sergeant A. Donohue, U. S. Army Signal School.

THURSDAY, 6 MAY 1976

1120-1150 ELECTRICALLY SMALL ACTIVE RECEIVING ANTENNAS

H. H. Meinke, Technical University, Munich, Germany.

1150-1400 RECESS FOR LUNCH

PASSIVE ANTENNAS, SESSION I

1400-1415 AN ERROR ANALYSIS FOR THE WHEELER METHOD OF MEASURING THE RADIATION EFFICIENCY OF ELECTRICALLY SMALL ANTENNAS

G. S. Smith, Georgia Institute of Technology.

1415-1435 A REVIEW OF INDUCTIVELY LOADED ANTENNAS

R. C. Hansen, R. C. Hansen, Inc.

1435-1450 A LOW PROFILE REMOTE-TUNED DIPOLE ANTENNA FOR THE 30-80 MHz RANGE

D. V. Campbell, ECOM.

1450-1505 MULTI-ELEMENT MONOPOLE ANTENNAS

G. Goubau ECOM Consultant.

1505-1525 INTERMISSION

1525-1555 DISCUSSION PERIOD

Moderator: R. C. Hansen

1555-1610 AN EXPERIMENTAL AND THEORETICAL INVESTIGATION OF THE CIRCULAR DISC, PRINTED CIRCUIT ANTENNA

S. A. Long and L. C. Shen, University of Houston.

1610-1630 PHYSICAL LIMITATIONS OF THE MULTIMODE CURRENT RING DF ANTENNAS

J. J. H. Wang, Georgia Institute of Technology.

1630-1645 LONG WIRE ANTENNA PERFORMANCE

G. Lane, USACEEIA

AIR FORCE VLF COMMUNICATION ANTENNAS

P. R. Franchi, Rome Air Development Center.†

†Paper not formally presented, but included in these Proceedings.

THURSDAY, 6 MAY 1976

THE UMBRELLA TOP-LOADED VERTICAL RADIATOR FOR USE AT MEDIUM FREQUENCIES

J. S. Belrose, Dept. of Communications, Ottawa, Canada.†

ELECTRICALLY SMALL ANTENNAS: THEORY AND EXPERIMENT

J. S. Belrose, Dept. of Communications, Ottawa, Canada.†

ELECTRICALLY SMALL COMPLEMENTARY PAIR ANTENNAS AND SCATTERERS

K. G. Schroeder, The Aerospace Corporation.†

1645-1715 DISCUSSION PERIOD

Moderator: R. C. Hansen

1730-1830 SOCIAL HOUR

1830-2000 DINNER

SPEAKER: R. Mittra

DEMONSTRATIONS AND DISCUSSIONS

2000-2030 SOME EXAMPLES OF SMALL, LOW-NOISE, HIGHLY LINEAR ACTIVE ANTENNAS PRODUCED IN QUANTITY FOR VARIOUS APPLICATIONS

H. K. Lindenmeier and F. Landstorfer, Technical University of Munich.

2030-2045 TRADE-OFFS IN THE DESIGN OF A SMALL ACTIVE ANTENNA FOR TELEVISION RECEPTION

J. J. Gibson, RCA.

2045-2100 VHF MANPACK LOG PERIODIC ANTENNA

J. C. Davis, DHV Inc.

2100-2130 DISCUSSION PERIOD

†Papers not formally presented, but included in these Proceedings.

FRIDAY, 7 MAY 1976 - Morning

PASSIVE ANTENNAS, SESSION II

0830-0900 A TECHNIQUE FOR CALCULATING THE RADIATION AND IMPEDANCE CHARACTERISTICS OF ANTENNAS MOUNTED ON A FINITE GROUND PLANE OR OTHER STRUCTURES

R. Mittra, Y. Rahmat-Samii and P. Parhami, Univ. of Illinois.

0900-0915 RF TRANLINE ANTENNA FOR VEHICLES

J. E. Brunner and J. R. Gruber, Cincinnati Electronics Corp.

0915-0930 PREDICTION AND MEASUREMENT OF HF ANTENNA RADIATION PATTERNS OF HELICOPTERS

L. N. Medgyesi-Mitschang, McDonnell Douglas Research Labs.; and J. Brune, ECOM.

0930-0945 SCALE MODEL TEST RESULTS FOR AN ELECTRCIALLY-SMALL LOOP ON A UH-1D AIRCRAFT

H. H. Jenkins and B. J. Wilson, Georgia Institute of Technology; and L. Scott, ECOM.

COMPUTER MODELLING OF SMALL ANTENNAS ON AIRCRAFT

J. J. H. Wang, Georgia Institute of Technology.†

0945-1005 INTERMISSION

1005-1035 DISCUSSION PERIOD

Moderator: R. Mittra

1035-1050 LOW PROFILE VHF ANTENNA FOR ARMOR

J. E. Brunner and G. Seward, Cincinnati Electronics Corp.

1050-1105 SLOT ANTENNAS FOR VEHICULAR COMMUNICATION IN THE VHF RANGE

K. Ikrath, ECOM.

1105-1120 WIRE ANTENNAS IN THE PRESENCE OF MATERIAL BODIES

E. H. Newman, Ohio State University.

1120-1135 COUPLING OF SMALL ANTENNAS WITH HUMAN BODY

K.-M. Chen and D. P. Nyquist, Michigan State University.

1135-1150 EXPERIMENTAL INVESTIGATION OF MANPACK WHIP ANTENNAS: ANTENNA CHARACTERISTICS AND PROXIMITY EFFECTS

J. Mink, ECOM.

†Paper not formally presented, but included in these Proceedings.

FRIDAY, 7 MAY 1976

1150-1220 DISCUSSION PERIOD

Moderator: R. Mittra

1220-1400 LUNCH RECESS

FRIDAY, 7 MAY 1976 - AFTERNOON

ACTIVE ANTENNAS

1400-1425 A SUPERCONDUCTIVE H-FIELD ANTENNA SYSTEM

Nancy K. Welker and F. D. Bedard, Laboratory for Physical Sciences.

1425-1445 AN APPROACH TO SHIPBOARD HF RECEIVING ANTENNA SYSTEMS

R. K. Royce, Naval Research Laboratory.

1445-1505 APPLICATION OF ACTIVE-IMPEDANCE MATCHING TO ELECTRICALLY SMALL RECEIVING ANTENNAS

A. J. Bahr, Stanford Research Institute.

1505-1525 INTERMISSION

1525-1555 DISCUSSION PERIOD

Moderator: C. H. Walter

1555-1615 ELECTRICALLY SMALL ANTENNAS WITH LOADING MATERIALS AND WITH ACTIVE ELEMENTS

J. A. M. Lyon and R. E. Hiatt, The University of Michigan.

1615-1630 SHORT, ACTIVE, HIGH-FREQUENCY ANTENNA AS AN E-FIELD PROBE

E. F. Laine, Lawrence Livermore Laboratory.

1630-1700 DISCUSSION PERIOD

Moderator: C. H. Walter.

1700 CONCLUDING REMARKS AND ADJOURNMENT.

OPENING REMARKS

Colonel D. A. Slingerland, Director of the Communications/Automatic Data Processing Laboratory, ECOM, opened the Workshop and welcomed the conference attendees. He thanked the Army Research Office for suggesting and sponsoring this meeting, and by referring to practical examples, underscored the Army's need for compact tactical communication antennas of high electrical performance. He concluded his welcoming address by a surprise demonstration of a novel and highly advanced antenna model representing the ultimate goal in electrical smallness: the invisible antenna of zero dimensions.

WORKSHOP ON ELECTRICALLY SMALL ANTENNAS: BACKGROUND AND PURPOSE

F. SCHWERING

Communications/Automatic Data Processing Laboratory
U. S. Army Electronics Command, Fort Monmouth, New Jersey 07703

Due to the use of integrated circuit technology, the physical size of tactical radio communication equipment has become smaller and smaller in recent years. The antennas operating with this equipment have, in most cases, still a rather conventional size, i.e., linear dimensions in the order of several feet at VHF and of several 10's of feet at HF. The HF and VHF bands, covering the frequency range from 3 to 300 MHz, are those commonly used in tactical communication.

The interest of the Army in reducing the size of tactical antennas is not merely a matter of conforming with a general trend to smaller, more compact devices, for antennas to be used in tactical situations have to satisfy certain requirements concerning their mechanical structure, notably those of low visibility and low vulnerability. Manpack antennas, for example, should be as inconspicuous as possible to enemy observers, and armored-vehicle antennas should be hardened against small arms fire and the shock waves and fragments of artillery shell explosions. Both constraints require compact, low silhouette antennas. At wavelengths in the HF and VHF ranges, this means, in practice, electrically small antennas. According to a commonly used definition, the term "electrically small antenna" implies dimensions in the order of 1/10 of a wavelength or less.

Apart from the need for compact antennas in tactical communications, an area of primary interest to the Communications/ADP Laboratory, a number of further applications in Army electronics systems is seen for small antennas. Examples include DF systems to be deployed near front lines, remote battlefield sensors, electronic warfare and camouflage techniques, and munition control systems, to name a few. The Navy and Air Force have corresponding requirements for small antennas though, naturally, for different purposes and under different constraints. The Armed Services requirements will be discussed in some detail by two invited speakers: Master Sgt Donohue of the Army Signal School will present the Army requirements, and Dr. Kvigne of NELC will give an overview on Navy problems in this area.

As every antenna engineer knows, electrically small antennas pose a major problem in regard to their electrical performarce. The radiation resistance of these antennas decreases rapidly with size and tuning and matching becomes very difficult and inefficient. As a consequence, the antenna performance deteriorates and performance parameters, such as radiation efficiency, S/N-ratio, and bandwidth, tend to decrease to unacceptable levels.

Designing compact antennas which are efficient in spite of their smallness is a very difficult task which requires both understanding of their capabilities and fundamental limitations, and familiarity with advanced methods for enhancing antenna performance. The main purpose of the Workshop is to provide a forum for the presentation and discussion of papers on the theory and practice of these antennas.

To present an in-depth exposition of the fundamentals of small antennas, their limitations and trade-offs, we have invited Dr. Wheeler who has written papers on this subject which have become classics. We are grateful to Dr. Wheeler for having accepted our invitation.

Two more invited papers will be presented this morning. Professor Walter will report on the extensive research program on electrically small antennas under way at Ohio State University and Professor Meinke will present results of his pioneering work in the area of active antennas. I would like to express our thanks to Prof. Walter, and to Prof. Meinke, who has come all the way from Munich to participate in this conference.

The first session on passive antennas, this afternoon, will be concerned primarily with techniques for improving the performance of small antennas and overcoming - as far as this is possible - their limitations. The session on active antennas tomorrow afternoon will, in effect, address the same subject though by a different approach: the use of active devices integrated with the radiating element or the tuning networks of antennas.

Up to now, active antennas have not been widely used by the Army. However, it appears that they have the potential for solving a number of problems, in particular, in the area of electrically small antennas. An example is the bandwidth problem. Small antennas of simple construction, such as stubs or loops, are inherently narrow band devices. This may be an advantage for certain applications; also, these antennas, of course, are tunable over a broad frequency band by using conventional variable reactive networks. But for other applications, antennas with a wide <u>instantaneous</u> bandwidth are required. Examples include antijamming and signal camouflaging methods such as spread spectrum techniques and fast frequency hopping (FFH).

As the recent literature and papers to be presented at this conference show, the use of active tuning networks provides a solution to this problem, not just in principle, but a practical solution.

Because of this and similar capabilities of active antenna techniques, this Workshop has been seen as an appropriate occasion to discuss these antennas in some detail and assess their potential for Army applications. In addition to the Friday afternoon session on this subject, models of active antennas will also be demonstrated and further discussed during the after dinner session tonight.

The second session on passive antennas, tomorrow morning, will be concerned with proximity effects, i.e., with small antennas radiating in the presence of their platform environments.

In one respect, electrically small antennas are easy to understand. Their radiation patterns in free space (or when operating above a large plane ground screen) are those of an electrical dipole, a magnetic dipole, or a combination of these two basic radiators. Unfortunately, Army antennas do not radiate in free space, but are usually attached to structures like helicopters, tanks, or manpack sets carried by soldiers. Small antennas have strong near fields and, therefore, tend to strongly interact with their platform environments. As the before mentioned examples show, typical Army platforms are everything else but simple in structure and, hence, proximity effects present us with another complex problem. To complicate things even further, these platforms usually have dimensions in the order of a wavelength somewhere in the upper HF to lower VHF regions. But on the other hand, this may be used to advantage by exciting the total structure to radiate as an antenna. As several papers of this session show, in this way an efficient radiating system can be obtained with radiation patterns that in the HF-range are predictable and in the VHF-range even become steerable.

The complicated structure of typical Army platforms entails that analytical studies of proximity effects have to rely to a large extent on advanced computer modeling techniques such as those described or utilized in the theoretical papers of this session. As an introduction to this session, Professor Mittra will give an overview of several existing methods and a new approach that may serve as the basis for the development of versatile and accurate, but numerically efficient, computer codes.

In summary, electrically small antennas require sophistication in their design. Much progress has been made in recent years (and also in not so recent years) in the conceptual understanding of these antennas and

in practical methods for overcoming their limitations. The purpose of the Workshop is to discuss the theory and practical design of these antennas, their fundamentals and enhancement techniques, in particular in view of possible applications to tactical Army antennas (though the discussion shall not be limited to a specific application). I hope that we will have an interesting conference - the quality of the papers to be presented makes me rather confident on this point - and that this meeting will be professionally rewarding to all participating in it.

ANTENNA REQUIREMENTS FOR THE MODERN WARFARE BATTLEFIELD

Excerpts from Presentation
by
Master Sergeant A. Donohue
Directorate of Combat Development
U.S. Army Signal School
Fort Gordon, Georgia

The Army is now largely an armored-mechanized force. In order to maximize combat effectiveness and survivability, Army tankers have developed new doctrinal concepts on "how to fight". These concepts are based on maximum use of protective terrain to conceal movement and firing position. This requires low-profile antennas which do not compromise the position of the tank. The Army is studying a two phase approach to reduce the size of tactical VHF antennas in order to reduce the vulnerability of its combat vehicles. The first such effort involves shortening the whip length of the present vehicular antenna, AS-1729/VIC, to half its present length of 10 feet. This low-risk development will result in the fielding of a five foot whip antenna late in 1977. This new antenna is being eagerly awaited by field commanders, and will provide a significant increase in their operational capabilities. However, a longer term, final solution for VHF vehicular antennas is required by the Army. It is envisioned that this new antenna will blend with the silhouette of the vehicle on which it is mounted to further reduce the visual signature of the vehicle. Ways to reinforce the antenna to provide blast and fragmentation damage resistance must be incorporated into the design efforts for such an antenna. Several designs are being considered by industry and the Electronics Command. The multiturn loop, vehicular slot, and short top-loaded monopole designs have shown great promise toward meeting the Army's goals.

The Army is also vitally interested in increasing the capability of our forces that employ radios in the high frequency range from 3-30 MHz. Military operations over extended distances and during wide-ranging independent operations necessitate looking at ways to develop more efficient, yet highly mobile, omni-directional and directional high frequency arrays.

In summary, success on the battlefield will, in the future, rest with the combatant with the greatest mobility and wisest tactics. He must move, shoot and communicate without drawing attention and enemy fire on his position because of large, conspicuous antenna systems. Development and fielding of electrically small antennas for use by our combat forces will contribute greatly to the field commander's mission-winning on the modern battlefield.

The speaker stressed that the development of low-profile antennas should proceed at an accelerated pace, as survivability on the battlefield requires it.

AN OVERVIEW OF ELECTRICALLY SMALL ANTENNAS WITHIN THE NAVY

Marlan S. Kvigne
Naval Electronics Laboratory Center
San Diego, California

ABSTRACT

The Navy ship antenna environment, the past and present HF and VHF Navy investigations concerning small antennas will be discussed. The trends of the future will also be discussed.

NAVY ANTENNA ENVIRONMENT

The ship topside environment is a major factor to be considered when thinking of a Navy antenna system. In general, the area available for antenna placement is small and the number of antennas required is large. Any antenna system must be judged on the basis of how much it contributes to the total ship combat effectiveness. [1]

At present most Navy HF and VHF systems require omnidirectional coverage with the ability to provide a specified grade of service at a specified maximum range. In addition, certain subsets of the electromagnetic (EM) system must be capable of simultaneous operation and the operating envelopes of all nonradiating systems must be respected.

Because of the large number of antennas required in such a small space, many special constraints and considerations are involved in the selection of an antenna system. In the high-antenna-density environment typical of most ships, mutual coupling between antennas is a potential source of system degradation. Undesirable effects of mutual coupling include distortion of radiation patterns, alteration of antenna feedpoint impedances, and the transfer of rf energy from one antenna to the other. In addition, coupling to the superstructure (acting as a parasitic element) may or may not be desirable.

Most ships require the simultaneous operation of several HF transmitters, each with a power in excess of 1 KW. This dictates concern for HERO and RADHAZ. Since receivers must also operate simultaneously, they must be protected with a suitable rf distribution system and the whole ship topside environment freed of unintentional sources of radiation whose frequency might fall directly upon the receiver center frequency. Ships are deployed for long periods of time with little chance for antenna maintenance or adjustment. This implies a need for simple, inexpensive, easily maintainable antenna systems. In addition, shipboard salt and stack gas environments are highly corrosive to antenna systems.

To further complicate the situation, relative system priority influences antenna placement. For instance, the more stringent requirements of the Navy Tactical Data System Antennas make it necessary that this antenna requirement be satisfied even if other antennas must be assigned less than optimum locations.

As can be seen, Navy ship antenna needs are mission-dependent and hence are tailored to individual ships. Since a ship has few antenna locations which can meet all of the requirements, and a highly efficient electrically small antenna has not been developed which meets all of the EM constraints, the following Navy antenna trends have evolved. Most systems make use of a few broadband antennas with multicouplers to satisfy the large circuit requirements. This system is used for both receiving and transmitting antennas and physical seperation plus the filter selectivity is used to obtain the desired isolation. Fan antennas which excite the ship superstructure are used for the lower HF broadband systems and "fat" monopoles for the higher HF frequencies. "Fat" dipoles are generally used for broadband VHF applications. For single circuit applications, whips are generally used in both bands. [2 through 8]

Navy aircraft and submarines generally do no employ broadband systems. Submarines utilize tuned monopoles and aircraft utilize tuned slots or wires.

ANTENNA INVESTIGATIONS

In an attempt to find better broadband antennas and suitable electrically small antenna for Navy/Marine Corps applications, several investigations have been undertaken during the last years. Discussions of some of the recent salient investigations are presented in the following paragrpahs.

Antenna Research Associates, Inc. Miniloop Antenna [9] The MLA-1 Miniloop antenna system employs a tuned one-turn main loop coupled to an untuned one-turn feed loop. The feed loop terminates a 50 ohm coaxial transmission line which is routed up the inside of a hollow supporting mast. The center of the loop proper is approximately 11 feet above the supporting platform. The main loop has a mean radius of 3 feet and a conductor diameter of 4 inches. Tuning is accomplished by remote control of a variable vacuum capacitor located at the top of the loop. The tuning range is 1.8 to 14.5 MHz for the MLA-1/E and 2.25 to 16.5 MHz for the MLA-1/D. The only difference between the two models is the value of the tuning capacitor.

Positioning of the miniloop is accomplished by rotating it about its vertical axis either manually or with an optional remotely controlled rotator. In a clear location it has a figure-8 azimuthal pattern in the horizontal plane.

An evaluation was conducted on this antenna and it was found to have vibration problems and have some potential tuning problems. Scale brass models indicated that a ship's superstructure could have an adverse impact on pattern performance.

Ohio State University HF Multiturn Loop (MTL) Antenna [10] In an attempt to obtain an ultra small HF shipboard antenna, Ohio State University proposed to develop a feasibility model of an antenna with the following characteristics:

Tuning range:	2 to 10 MHz	Input power:	1 KW
Efficiency range:	1% to 30%	Size of coil:	12" X 26" X 26"
Bandwidth:	3 KHz min. (3 dB)	Weight:	50 lbs
Impedance over tuning range:	Adjustable to exactly 50 ohms		

This development was procured and the antenna evaluated for shipboard application.

The evaluation found the following: Its inherent nature is that of a high Q, low profile, horizontal magnetic dipole with a significant horizontally polarized radiation component at high elevation angles and vertically polarized component have a cos θ pattern in all vertical planes where θ is the elevation angle. However its shipboard applicability could be limited by low efficiency, tuning and matching difficulties, and the rapid deterioration of the radiation pattern in a "confused" ship topside environment (its coupling is directional in nature).

Normal Mode Helix Antenna [11] To overcome the difficulty of Ohio State MTL pattern deterioration in a complex shipboard environment and some of its tuning deficiences, it was felt that a vertical version of the Ohio State MTL with a different tuning configuration held promise. Several models were constructed and evaluated. Findings indicated similar efficiency, tuning, and matching limitations, but patterns and coupling of a short vertical dipole with little horizontally polarized radiation at the high elevation angles.

Broadband VHF Antenna Development [12] It has become apparent over the past several years that the AS-2231 antenna associated with the shipboard 30-76 MHz AN/SRA-60 has serious deficiencies. To overcome these deficiencies on electrical feasibility model development was undertaken to produce a replacement. In addition to the shipboard application, it was hoped the new antenna would be useful for Marine Corps fixed and mobile applications.

This development resulted in a "fat" dipole with balun for ship and fixed command post deployment. Each dipole element consists of four equispaced whips approximately 5 1/2 feet long for a total length of 12 feet and a weight of 50 lbs. A monopole version consisting of three equispaced 5 1/2 foot whips for vehicular use was also designed. The dipole version is currently undergoing field testing.

Low Profile Antenna for the AN/PRC-25,77 [13, 14, 15] Ohio State University proposed to utilize their MTL antenna on the AN/PRC-25, 77 to replace the 3 foot AT-982 whip, thereby reducing the profile of the radiomen and hopefully his casualty rate in combat. The proposed development was procured and resulted in a 6" packaged MLT antenna add-on to the battery case of the 25 or 77. The unit has fully automatic tuning, which responds to changes in the local environment. This unit has not been evaluated yet, but preliminary results indicate slightly reduced efficiency and a slightly directional pattern characteristic.

AN/PRC-104 Antenna Study [16] An investigation was undertaken to see if it was possible to improve the performance of the AN/PRC-104 radio set by utilizing a different antenna with the existing tuner. The AN/PRC-104 is a manpackable, 2 to 30 MHz, 20 watt transceiver with an 8 foot whip designed and produced by Hughes Aircraft Company. Antennas studied were the 8 foot whip, 8 foot sleeve monopole, 8 foot centerfed dipole, a Southcom International, Inc. centerloaded antenna, a 10 foot whip, and an Ohio State Multiturn loop. The effects of skin contact on the packset, absorption by the body, and lossy ground were studied. The impedance of the antenna system on a radioman was determined for each of the above situations. Findings indicate the tuner of the AN/PRC-104 is designed for an 8 foot whip in a manpack configuration and

as such does lend itself to other antennas. Best performance appears to result if the body is shielded with conductor and an 8 foot whip is utilized. Next followed the 8 foot whip without the body conductor and then all other antennas tested providing equal or poorer performance.

Multielement Element Investigations Antenna diversity has been investigated and utilized as a means of overcoming HF fading associated with skywave channels. In addition, multiple omnidirectional antennas suffering superstructure blockage have been fed in phase in an attempt to overcome the blockage. Adaptive antennas have been investigated as a means of overcoming ship blockage to HF antennas. These studies have been conducted only on scale brass models. Full scale field tests have been conducted at VHF frequencies for sensor applications [17].

Miscellaneous Investigations In addition to surface ship and Marine Corps antennas, work has occurred concerning antennas for other platforms. The dogleg antenna was developed for the P-3 and the efficiency and impedance of most submarine HF antennas was measured [18]. Active antenna efforts have been minimal at NELC due to concern for non linear emissions and interactions.

TUNING, MATCHING, AND DECOUPLING

Each of the above antenna systems has an associated tuning or matching network which has been developed or investigated. Because there are so many antenna systems on board a ship, coupling between them is of prime concern. Filters and multicouplers (AN/SRA-16, 34, 49, 56, 57, 58, 60, etc.) have been developed for use with broadband antennas to aid in achieving the desired isolation. Further developments have been undertaken to enhance existing capabilities and solve unknown problems during recent years. Some of the salient efforts are summarized in the following paragraphs.

NRL Base Tuner An HF base tuner is under development at NRL which incorporates a tuned circuit to provide increased rejection and improved ability to tune in the presence of other tuners and transmitters. This tuner is an alternative to the AN/URA-38 and is capable of tuning a vertical 35 foot whip over a 2-30 MHz range with a minimum efficiency of 10%. An automatic digital control mechanism is used for tuning and the whole system is still under development.

NRL Small Ship RF Distribution System (SSDS) A transmit multicoupler tailored specifically for small ships is currently under development at NRL. The multicoupler is a unified five channel package which divides the HF band into two ranges, 2-8 and 8-30 MHz. Two antennas are required, one for each range with a 4:1 or better VSWR. The two antennas are connected directly to the combined multicoupler unit. The five input channels of the multicoupler are configured so that transmitters connected ot four of the channels may be operated in either the 2-8 or 8-30 MHz range as desired, with each output combined and connected to the appropriate antenna. The fifth channel is operable only in the 2-8 MHz range. All five transmitters may therefore be operated in any combination from all five in the 2-8 MHz band to one in the 2-8 MHz and four in the 8-30 MHz bands.

8 Channel AN/SRA-60 [19] The existing shipboard 30-75 MHz multicoupler AN/SRA-60, is a four channel device. An investigation was undertaken to determine if it would be possible to increase the capacity to eight channels

and thereby reduce the required antennas by a factor of two. Findings indicated it would be possible with repackaging to make an 8 channel AN/SRA-60 with insertion loss similar to that obtained in the four channel mode but with adjacent channel frequency spacing increased to 3%.

10 Channel VHF Multicoupler for the Marine Corps [20] In order to alleviate the collocation problems associated with the amphibious command tractor, LVTC-7, and fixed command posts, a development was undertaken to determine if a multicoupler was a feasible solution to some of the problems. Since the AN/SRA-60 is too large and cumbersome for this application, a totally new concept was pursued. As a result, a manually tuned, 10 channel electrical feasibility model was constructed which is capable of 3% adjacent channel frequency separation and less than 2 dB insertion loss when used with a 2:1 VSWR antenna in the 30-76 MHz band. It is capable of 70 watts per channel and is currently undergoing limited field tests.

Marine Corps Tactical Communications Inline Filter (30-76 MHz) [21] As an adjunct to the 10 channel VHF multicoupler an inline filter was designed, constructed, and tested in a limited manner. The device is fully automatic, capable of automatic tune upon application of transmitter power or operator indicating the desired receive frequency. The filter is intended to alleviate the receiver overload and transmitter intermodulation problems associated with the RT-524 transceiver which cause degraded VHF communications.

Combination Antenna Receive Transmit System (CARTS) [22] In order to reduce the number of antennas to a minimum and capitalize on the prime shipboard antenna locations available, a coupler isolator (CU-2113 (XG-1)/SRC) has been developed which uses a ship's transmitting antenna to be used simultaneously and independent of the transmit function for receiving over the VLF, LF, MF, and HF frequency bands.

The coupler-isolator is designed for installation in the transmission line between the ship's 2-6 MHz transmitting multicoupler (near multicoupler output) and the broadband 2-6 MHz antenna. There are two decoupled receiving outputs on the CU-2113. One is used for receiving in the HF range, 2-30 MHz; the other for receiving at VLF-LF-MF frequencies 10 KHz to 2 MHz. Connection of the CARTS decoupled (receive) outputs to the receivers used should be made through a receive multicoupler. The multicoupler will give protection to receivers and provide the multiple receive channels needed.

Antenna Location Techniques In addition to those hardware techniques described above, antenna location and configuration are utilized to provide a suitable antenna to antenna decoupling and the desired impedance match. Scale brass modeling and computer simulation are two technologies which are used extensively to aid in the determination of antenna locations and configurations.

DIRECTIVE AND BROADBAND ANTENNAS

As indicated above, the Navy relies extensively on broadband antennas and their state of development is quite advanced. However, most are omnidirectional and tailored to individual ships and in general are not

electrically small. The Log Periodic antenna has been investigated for directional broadband applications for ship and shore. Navy ship and aircraft antenna systems are currently being investigated to determine their impact on frequency hopped communication systems.

COMPUTER MODELING

Computer modeling is utilized extensively in the analysis and design of Navy HF and VHF antennas. The MB Associate's code, called AMP, is the preferred code. This code or other method of moments codes have been utilized to investigate antenna near fields, the minileop antenna, the multitune loops, the HF broadband antenna, HF manpack antennas, and shore station antennas. AMP was used to determine the near fields of the HF antennas of the Patrol Hydrafoil Missile Ship (PHM) and recently the complete integrated antenna system, including the complex superstructure was computer modeled to provide a new ship preliminary design antenna configuration. [23, 24]

Computer modeling appears to be applicable where a basic knowledge of antenna impedance, patterns, near fields, and coupling, including the effects of a complex environment are needed in a relatively short time. It does not appear to be cost effective where large amounts of data are required and the time schedule is less stringent, as other techniques are more advantageous.

FUTURE TRENDS

Future trends appear to be along the line of reducing the size of existing systems without sacrificing efficiency, isolation, or bandpass characteristics. New systems must be able to function in the environment and contribute to the overall platform effectiveness, be inexpensive and easily maintainable, and preferably be simple. It should be noted that findings concerning all three of the small individual HF antennas discussed above found that each had less than a 2-30 MHz tuning range and potential tuning problems. These limitations are perhaps more detrimental than the low efficiency.

Specifically, there appears to be a need for broadband receive antennas for the 2 to 30 MHz, 30 to 300 MHz, and other selected bands. These must be small, able withstand the ship environment and be tailored to fit in it, and meet the electrical specification of the environment and the particular system. As always, it would be nice if these antennas were highly efficient, had almost zero volume and size, were extremely broadband, and had an omnidirectional pattern with some gain. Realistically, these are desires and the deployed antenna will be a compromise of the necessary parameters.

1. NELC TD 356 "Shipboard Antenna and Topside Arrangement Guidance," D. W. DuBrul and L. M. Peters, 1 September 74.

2. NELC TR 1712 "Shipboard HF Receiving Antenna System Design Criteria," W. E. Gustafson and W. M. Chase, 2 June 1970

3. NELC TR 1808 "HF Shipboard Antenna System Design and Utilization Criteria," J. M. Horn and W. E. Gustafson, 1 December 1971

4. NELC TR 1855 "Shipboard HF Transmitting Antenna System Design and Utilization Criteria for Ionospheric Path Circuits," H. W. Guyader and J. M. Horn, 2 Jan 73

5. NELC TR 1914 "HF Antenna System for a Small High-Speed Ship," I. C. Olson and H. K. Lanoakov, 10 July 1974

6. NELC TD 300 "Optimum HF RF Distribution System for Small-Ship Communication," J. M. Horn, J. Watson, and R. D. Smith, 25 June 1974

7. NELC TN 2955* "VLF/UHF Antenna Concepts for Small and High-Speed Ships," J. M. Horn and J. W. Watson, 15 May 1975

8. NELC TD 446 "HF Receiving Design Study for Small Ships," J. L. Lievens and A. R. Evans, 15 August 1975

9. NELC TD 317 "MLA 1 Miniloop Antenna: A Technical Evaluation," D. W. DuBrul and J. L. Lievens, 10 May 1974

10. NELC TD 339 "Multiturn HF Loop Antenna for Shipboard Applications: An Evaluation, J. W. Rockway and W. M. Chase, 25 July 1974

11. NELC TN ----* "HF Normal Mode, Tunable Helix Antenna Development," J. W. Rockway, J. C. Logan, and W. M. Chase, to be published

12. NELC TN ----* "VHF Broadband Antenna Development," L. A. Thowless, to be published

13 NELC TN 2354* "Multiturn Loop Antenna Test and Evaluation," M. S. Kvigne, 11 April 1973

14. Ohio State University Technical Report 3824-1, "The Development of a Multiturn Loop Antenna for the AN/PRC-77," R. J. Davis, December 1974

15. Ohio State University Final Report 3824-2, "The Man-Pack Loop Antenna System," P. Bokley, R. J. Davis, and C. H. Walter, December 1974

16. NELC TR 1980, "AN/PRC-104 Antenna Study, Final Report," J. C. Logan, 3 February 1976

17. NELC TD 451, "Remote Unattended Ground Sensor Adaptive Array Antenna Evaluation," P. M. Hansen, 17 September 1975

18. NELC TD 453, "Submarine Antenna Measurements," volumes 1 through 6, L. A. Thowless and R. A. Hills, 1 April 1975

19. NELC TR 1925, "Eight-Channel Combining for the AN/SRA-60(V) Antenna Coupler Group: A feasibility Study," J. L. Lievens, 24 June 1974

20. NELC TD 454 "Development of a Ten-Channel 30 to 76 MHz Multicoupler for the Marine Corps LVTC-7 Command Amphibious Tractor," J. E. Kershaw, 1 October 1975

21. NELC TN 3044* "Marine Corps Tactical Communications Inline Filter (30-76 MHz)," J. E. Kershaw, 19 Sept 1975

22. NELC TD 437, "CU-2113(XG-1)/SRC Coupler-Isolator: Technical Evaluation," I. C. Olson and J. L. Lievens, 31 July 1974

23. NELC TN 3137* "Antenna Mathematical Modeling vs Brass Scale Modeling," D. W. DuBrul and J. W. Rockway, 9 March 1976

24 NELC TD 359 "Applications of Thin Wire Modeling Technique to Antenna Analysis, J. W. Rockway and J. C. Logan, 11 October 1974

*NELC Technical Notes (TN) are working papers giving tentative information about work in progress which is tentative and formally unpublished at NELC.

Small Antennas

HAROLD A. WHEELER, LIFE FELLOW, IEEE

Abstract—A small antenna is one whose size is a small fraction of the wavelength. It is a capacitor or inductor, and it is tuned to resonance by a reactor of opposite kind. Its bandwidth of impedance matching is subject to a fundamental limitation measured by its "radiation power factor" which is proportional to its "effective volume". These principles are reviewed in the light of a quarter-century of experience. They are related to various practical configurations, including flush radiators for mounting on aircraft. Among the examples, one extreme is a small one-turn loop of wide strip, tuned by an integral capacitor. The opposite extreme is the largest antenna in the world, which is a "small antenna" in terms of its operating wavelength. In each of these extremes, the radiation power factor is much less than one percent.

I. Introduction

A "SMALL ANTENNA" is here defined as one occupying a small fraction of one radiansphere in space. Typically its greatest dimension is less than $\frac{1}{4}$ wavelength (including any image in a ground plane). Some of its properties and available performance are limited by its size and the laws of nature. An appreciation of these limitations has proved helpful in arriving at practical designs.

The radiansphere is the spherical volume having a radius of $1/2\pi$ wavelength [10]. It is a logical reference here because, around a small antenna, it is the space occupied mainly by the stored energy of its electric or magnetic field.

Some limitations are peculiar to a passive network, where the concepts of efficiency, impedance matching and frequency bandwidth are essential and may be the controlling factors in performance evaluation. This discussion is directed mainly to these limitations in relation to small size. This subject has been on the record for a quarter-century but is still too little taught and appreciated. It centers around the term, "radiation power factor" and its proportionality to volume [2].

As in any area of engineering compromise, there have been some ingenious developments for realizing some qualities at the expense of others. A valid comparison of alternatives requires careful description and evaluation in terms of well defined quantities, especially in the use of terms such as efficiency and impedance matching. Also in the size comparison of circuits qualified for high power or low power [11].

An outline of some of the relevant principles will be followed by a brief reference to the background in the use of an amplifier with a small antenna for reception. Then the principal topic will be introduced in terms of the bandwidth limitations of impedance matching with a resonant circuit, which is a tuned antenna circuit in this discussion.

Manuscript received July 29, 1974. The paper was presented at the Twenty-Third Annual USAF Antenna Symposium, October, 1973.

The author is with the Hazeltine Corporation, Greenlawn, NY 11740.

TABLE I
COMPARISON OF TOPICS OF EFFICIENCY AND AMPLIFICATION

EFFICIENCY	TOPIC	AMPLIFICATION
PASSIVE	LINEAR NETWORK	ACTIVE
ESSENTIAL	IMPEDANCE MATCHING	OPTIONAL
NO	TOLERANCE OF LOSSES	YES
THERMAL	NOISE	AMPLIFIED
NO	POWER LIMITING	YES

The radiation power factor will be reviewed in concept and in some applications to typical antennas in the form of capacitors and inductors. Some special applications will be described for flush mounting and for VLF transmission and reception. In every case, the efficiency and/or bandwidth is seen to be limited ultimately by size.

II. Principles

Table I shows a comparison between efficiency and amplification, referring to some topics relevant to small antennas. Its purpose is to emphasize the distinction between efficiency and amplification, the former being the basis for this presentation. The relations in this table may help to bring out the accepted meanings of various terms.

Efficiency implies the utilization of the amount of radiated signal power that can be intercepted by the receiver. If the antenna is small, the greatest power transfer to a circuit requires impedance matching. This is achieved in a passive network by tuning the antenna and coupling to the circuit.

Amplification implies the utilization of the intercepted signal, but the excitation of the amplifier may not require impedance matching in the active network. This may facilitate a wideband design, as in one example to be shown. However, the amplifier may add much to the thermal noise generated in the antenna dissipation.

In a linear network, efficiency is associated with a passive network, while amplification is associated with an active network. In a weak-signal receiver, linearity is not a primary problem. In a power transmitter, however, an active network imposes an upper limit.

In general, efficiency is reduced by losses. This is particularly true in a small antenna where the radiation power factor is small and may be far exceeded by the loss power factor. In a weak-signal receiver, an amplifier can make up for losses in respect to signal strength, but only with increasing background of thermal noise. In a power transmitter, the power rating must be increased to cover losses.

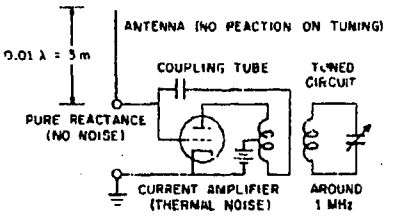

Fig. 1. Small antenna with wideband coupling tube, used in broadcast receivers (1928).

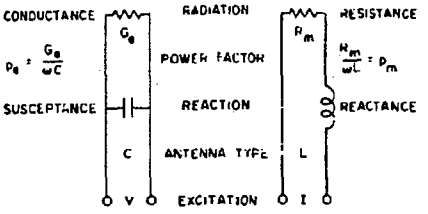

Fig. 2. Radiation power factor of small antenna.

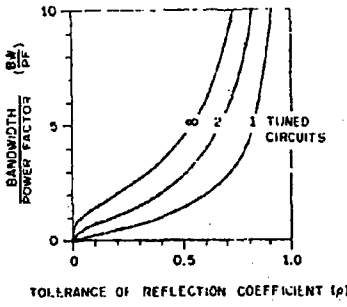

Fig. 3. Bandwidth of matching with tuned circuits.

These relations are emphasized because there have been some invalid ratings of small antennas associated with active devices serving as amplifiers. The greatest confusion has been associated with transmitters, by ignoring the power limitations imposed by small active devices. These limitations are not avoided by any particular relation between the small antenna and the amplifier.

III. Background

The wideband utilization of a small antenna was accomplished in a receiver about a half-century ago. That history is relevant to the more recent proposals using an amplifier in conjunction with a small antenna [11].

Fig. 1 shows a circuit that was commonly used in radio broadcast receivers about 1928. It operated over a frequency ratio of 1:3. A short wire is simply connected to the grid of the first tube. It bears a striking resemblance to some recent proposals, but using a tube instead of a transistor, and at lower frequencies. It substituted amplification for antenna tuning. It increased the noise threshold and also suffered from crossmodulation of all signals by any one strong signal. Then the pendulum swung and it was superseded by double tuning ahead of the first tube. The tuning yielded efficiency over noise and also preselection against crossmodulation.

IV. Frequency Bandwidth of Impedance Matching

There are limitations on the frequency bandwidth of impedance matching between a resonant circuit (antenna) and a generator or load. A quarter-century has elapsed since these limitations were developed and clearly stated [5]. In contrast to the history of small antennas, these limitations have been widely taught and appreciated.

The bandwidth of matching, within any specified tolerance of reflection, is proportional to the resonance bandwidth of the resonant circuit. A small bandwidth is logically expressed in terms of the power factor of its reactance, in the manner taught to the writer by Prof. Hazeltine just 50 years ago [1]. Its common expression in terms of $1/Q$ is neither logical nor helpful in clear exposition. The term dissipation factor is numerically equal to power factor but is counterdescriptive of a useful load (as here).

Fig. 2 shows the circuit properties of a small antenna, describing its radiation power factor (PF). The antenna may behave as a capacitor (C) or inductor (L), and either is to be resonated by a reactor of the opposite kind. Dissipation (other than radiation) is here ignored, because it is treated in the earlier paper [2]. The nominal bandwidth of the resonator is the PF (p) times the frequency of resonance, as usual.

Fig. 3 is the bandwidth of matching within any specified tolerance of reflection (ρ) as given in 1948 by Fano [5]. It is graphed in the terms of the present discussion. For each graph, the number of tuned circuits includes the antenna circuit and any that are added for increasing the bandwidth of matching. The added circuits are taken to be free of dissipation. Usually double tuning is used, in which case the added circuit can reduce the reflection coefficient to the square of its value for single tuning.

V. The Radiation Power Factor

The term "radiation power factor" is a natural one introduced by the author in 1947 [2]. It is descriptive of the radiation of real power from a small antenna taking a much larger value of reactive power. It is applicable alike to either kind of reactor and its value is limited by some measure of the size in either kind.

Fig. 4 shows small antennas of both kinds (C and L) occupying equal cylindrical spaces [2]. They are here used for introducing the relation between radiation PF and size.

A small antenna of either kind is basically a reactor with some small value of PF associated with useful radiation. The latter depends primarily on its size relative to the wavelength (λ), as discovered by the writer [2]. The size may be stated relative to the radianlength ($\lambda/2\pi$) in terms of either of two values of reference volume:

$$\text{radiancube} = V_c = \left(\frac{\lambda}{2\pi}\right)^3 = \frac{1}{4\pi} V_s \qquad (1)$$

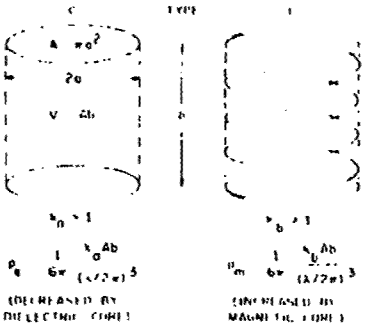

Fig. 4. Radiation power factor in terms of equivalent volume.

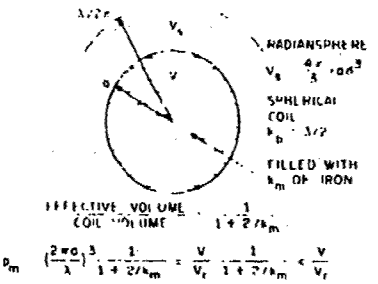

Fig. 5. Spherical coil with magnetic core.

or

$$\text{radiansphere} \qquad V_r = \frac{4\pi}{3}\left(\frac{\lambda}{2\pi}\right)^3 \qquad \frac{4\pi}{3} V_r \tag{2}$$

The former was used in the writer's first paper. The latter is particularly significant in radiation because it defines the space in which the reactive power density exceeds the radiation power density [10]. Also the latter is convenient if the antenna is spherical [9] or its effective volume is expressed as a sphere.

In either type of antenna, the radiation PF is found to be proportional to volume and also to a shape factor. The cylindrical volume ($V = Ah$) is here multiplied by a shape factor (k_a or $k_b > 1$) to give the effective volume ($V' = k_a Ah$ or $k_b Ah$). Then the general formula is

$$\text{rad PF} \qquad p = \frac{1}{6\pi}\frac{V'}{V_r} = \frac{2}{9}\frac{V'}{V_s}. \tag{3}$$

The effective volume may be stated as a sphere of radius (a'), in which case

$$V' = \frac{4\pi}{3} a'^3, \quad p = \frac{2}{9}\left(\frac{2\pi a'}{\lambda}\right)^3, \quad a' = \frac{\lambda}{2\pi}\left(\frac{9}{2} p\right)^{1/3}. \tag{4}$$

It is noted in passing that a certain shape of self-resonant coil radiates equally as both C and L, in which case the total radiation PF is double either one [3].

There is one theoretical case of a small coil which has the greatest radiation PF obtainable within a spherical volume. Fig. 5 shows such a coil and its relation to the radiansphere (V_r) [9], [10]. The effective volume of an empty spherical coil has a shape factor $3/2$. Filling with a perfect magnetic core ($k_m = \infty$) multiplies the effective volume by 3

$$p_m = \frac{2}{9}\frac{(3)(3/2)V_r}{V_s} = \frac{V_r}{V_s} = \left(\frac{2\pi a}{\lambda}\right)^3. \tag{5}$$

This is indicated by the shaded sphere (a).

This idealized case depicts the physical meaning of the radiation PF that cannot be exceeded. Outside the sphere occupied by the antenna, there is stored energy or reactive power that conceptually fills the radiansphere [10], but there is none inside the antenna sphere. The reactive power density, which is dominant in the radiation within the radiansphere, is related to the real power density, which is dominant in the radiation outside.

In a rigorous description of the electromagnetic field from a small dipole of either kind, the radiation of power in the far-field is accompanied by stored energy which is mostly located in the near-field (within the radiansphere) [4], [10]. The small spherical inductor in Fig. 5 is conceptually filled with perfect magnetic material, so there is no stored energy inside the sphere. This removes the "avoidable" stored energy, leaving only the "unavoidable" amount outside the inductor but mostly inside the radiansphere. This unavoidable stored energy is what imposes a fundamental limitation on the obtainable radiation PF.

One of the fallacies in some studies has been the provision of dielectric or magnetic material outside of the space occupied by the antenna conductors, without including that material in rating the size of the antenna. The fundamental limitations are based on the size of all the material structure which forms the antenna. Likewise, such material would naturally be included in a practical evaluation of the size. Fig. 5 shows the empty space outside the antenna but inside the radiansphere (V_r) which space is filled with stored energy and therefore reduces the radiation PF of the antenna.

VI. Application to Typical Antennas

The radiation PF may be evaluated for any kind of small antenna. From its value, we may state the effective volume of the antenna, as formulated (4):

$$V' = 6\pi p V_r, \quad \tfrac{2}{3} p V_s, \quad a' = \frac{\lambda}{2\pi}\left(\tfrac{9}{2} p\right)^{1/3}.$$

This is a useful quantity which can be shown on a space drawing. It gives a direct comparison of the bandwidth capability of different structures. It will be shown for C and L antennas of elementary configurations. It will be drawn as a dashed circle the size of the spherical effective volume.

Fig. 6 shows some examples of an electric dipole with a linear axis of symmetry. A thin wire (a) and a thick conical conductor (b) differ greatly in the occupied volume, but much less in effective volume. The latter is influenced most by length and less by the smaller transverse dimensions.

Fig. 6(c) shows a pair of separated discs [2], which is found to approach the greatest effective volume for some shapes within limited length and diameter. However, any

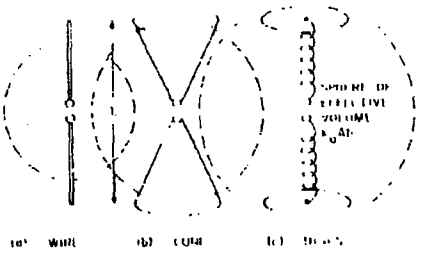

Fig. 6 Effective volume of axial electric dipole

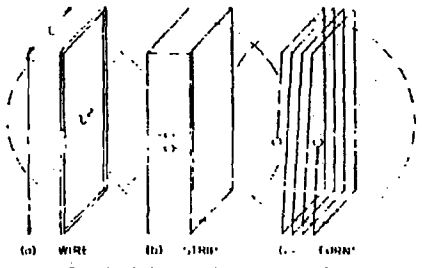

Fig. 7. Effective volume of square loop.

intermediate connecting wires would detract from this rating. The full value of the radiation PF can be realized by the use of a tunny inductor distributed along the axial line between the discs. It is proportioned to conform to the natural pattern of electric potential, thereby contributing no extra amount to the stored electric energy. A coil of small diameter may be used to avoid extra (cross-polarized) radiation therefrom. The spherical effective volume may extend beyond the length between the discs, as shown. This occurs if the disc diameter exceeds $\frac{1}{4}$ the length ($2a > b/4$), as in the example shown. This may be interpreted as a "sphere of influence" extending beyond the antenna structure.

In further reference to Fig. 6(c), there is a pair of end electrodes which will give the greatest radiation PF within a cylindrical boundary. At each end, a hollow cup is connected with its open end toward the center. Its depth is proportioned to maximize the radiation PF. Also greater value can be obtained by simple conductors subject to the stated constraints.

Fig. 7 shows some examples of a loop inductor on a square frame. A thin wire (a) and a wide strip (b) differ rather little in effective volume, because it is influenced most by the size of the square. A multiturn loop (c) has nearly the same effective volume as one turn occupying the same space. This is one of the principal conclusions presented in the writer's first paper [2]. It superseded several inaccurate evaluations based on the concept of "effective height" of a number of turns, irrespective of their width and spacing.

Reference again to Fig. 4, the shape factors are related to the shape in opposite ways for the two kinds (*C* and *L*).

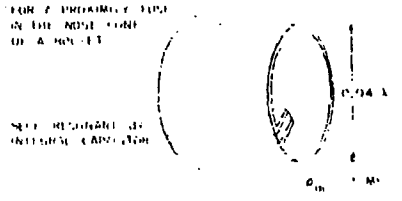

Fig. 8. One-turn loop of wide strip.

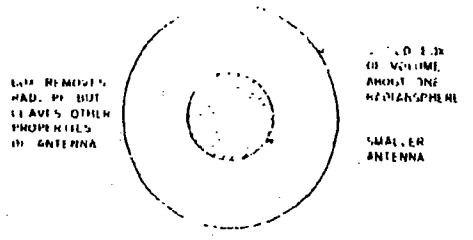

Fig. 9 Radiation shield for use in measuring radiation power factor.

With greater ratio of length/diameter ($b/2a$), one factor (k_a for *C*) is greater and the other (k_b for *L*) is smaller. Therefore the utilization of volume is greater for the *C* type made of a long wire or for the *L* type made of a "short coil" or loop. These are exemplified in Figs. 6 and 7. Each of these has large and small dimensions, and the smaller dimensions may be less significant in a practical allocation of space.

In the writer's experience, the concept of radiation PF was first applied to the design of a very small loop antenna for coaxial location in the nose cone of a small rocket. Fig. 8 shows the resulting one turn of wide strip. It superseded some attempts to design a multiturn loop. It is resonated by an integral capacitor made of a ceramic slab metallized on both faces. It proved superior in performance, simplicity, and reproducibility. It may have been the smallest antenna then known to realize about 50 percent radiation efficiency, the size being stated in fractions of the wavelength. Its diameter and length were about 0.04 wavelength so its radius was about 0.12 radianlength. It was measured by a method to be described here.

For efficiency of radiation, a small antenna of one kind is associated by a reactor of the opposite kind. Then

$$\text{radiation efficiency} = \frac{\text{radiation PF}}{\text{rad PF} + \text{loss PF}} \qquad (6)$$

In a very small antenna, the radiation and loss power factors may be so small that their ratio is difficult to measure. In any case, how would they be separated in measurement? Direct measurement of radiated power is laborious. Another method was developed, using a "radiation shield" [10].

Fig. 9 shows the concept of the radiation shield. Its purpose is to avoid radiation of power while leaving the inherent dissipation in the resonant circuit of the small antenna. The shield is a box with conductive walls for preventing radiation. Its size and shape are noncritical.

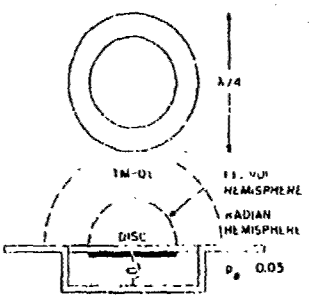

Fig. 10. Flush disc capacitor.

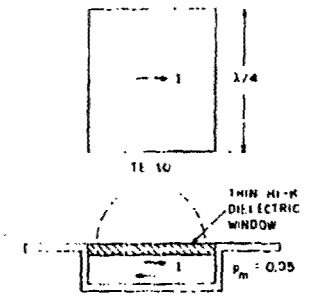

Fig. 11. Flush cavity inductor with dielectric window.

but the theoretical ideal is a radiansphere as indicated. It should be much larger than the antenna to be shielded, so as to retain substantially the reactance and loss PF of the antenna. Then the PF is measured with and without the shield, for evaluating the power efficiency of the useful radiation [10]. In the design shown in Fig. 8, the circuit was included in an oscillator, so the effect of the shield on the amplitude of oscillation could be interpreted in terms of radiation efficiency.

VII. Flush Antennas

A useful family of small antennas comprises those that are recessed in a shield surface, such as a ground plane or the skin of an aircraft. Some may be inherently flush designs, while others may be suited for operation adjacent to a shield surface, whether recessed or not. The antenna may be *C* or *L* type, either one radiating in a polarization compatible with the shield surface.

Fig. 10 shows a flush disc capacitor. (It is sometimes termed an "annular slot.") This capacitor in the flush mounting may be compared with the same capacitor just above the surface. The recessing somewhat reduces the radiation PF. The remaining effective volume is that of a hemisphere indicated by the dashed semicircle. Its size is comparable with that of the disc. The cylindrical walls may be regarded as a short length of waveguide beyond cutoff, operating in the lowest TM mode (circular TM-01, as shown, or rectangular TM-11). The capacitor may be resonated by an integral inductor as shown. In any cavity, there is a size and shape of disc that can yield the greatest radiation PF. The primary factor is the size of the cavity.

The evaluation of a flush antenna includes the shield surface. It is necessary first to evaluate the radiation PF by some method of computation. Then it can be stated in terms of a volume ratio. Here we consider the half-space of radiation and show the hemisphere of $\frac{1}{2}V'$ which may then be compared with the half-radiansphere, $\frac{1}{2}V_r$. The radii are retained (a' and r, 2π). An antenna located on the surface (not recessed) could be considered with its image to yield the complete sphere of V' to be compared with the radiansphere V_r. Then $\frac{1}{4}$ of each may be shown above the shield plane, as for the flush antenna.

The disc capacitor radiates in the same mode as a small vertical electric dipole, by virtue of vertical electric flux from the disc. This is vertical polarization on the plane of the shield, with omnidirective radiation. The other examples of a flush antenna, to be shown here, radiate as a small horizontal magnetic dipole, by virtue of magnetic flux leaving the cavity on one side and returning on the other side. This is vertical polarization but directive in a figure-eight pattern. Omnidirective radiation can be provided by quadrature excitation of two crossed modes in the same cavity. The radiation PF of either kind is reduced by recessing, but the magnetic dipole suffers less reduction.

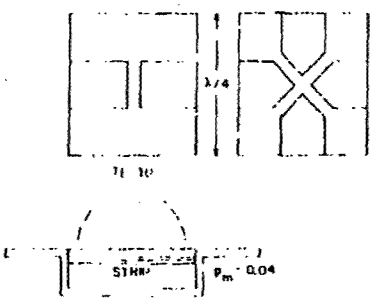

Fig. 12. Flush strip inductor.

Fig. 11 shows an idealized cavity resonator which radiates as an inductor. The cavity is covered by a thin window of high-k dielectric which serves two purposes. It completes the current loop indicated by the arrows (I). Also it provides, in effect, series capacitance which resonates the current loop. The cylindrical walls and the aperture excitation may be regarded as the lowest (cutoff) TE mode (circular TE-11), or rectangular TE 10 or TE-01, as shown). Each of these modes has two crossed orientations, of which one is indicated by the current loop. The continuous dielectric sheet on a square (or circular) cavity resonates the two crossed modes. Because each resonance is in the lowest mode, it involves the smallest amount of stored energy relative to radiated power, and therefore the greatest value of radiation PF.

Fig. 12 shows some practical designs which yield nearly the same performance by the use of conductive strips on ordinary (low-k) dielectric windows. (High k dielectric is not required.) Here the radiating inductor (strip) and the resonating series capacitor (gap) are apparent. The two

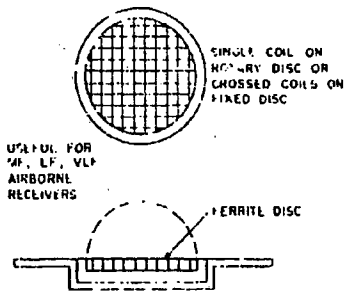

Fig. 13. Flush inductor on thin ferrite disc.

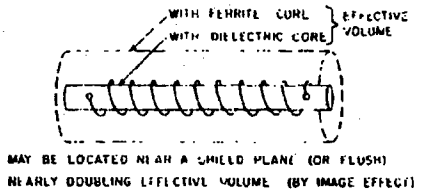

Fig. 14. Long coil on ferrite rod.

alternatives are shown, one mode or a pair of crossed modes. Practical designs about $\lambda/4$ square have been made with radiation PF about 0.04. This is about the largest size that follows the rules of a small antenna.

The required coupling with any of the resonant antennas in Figs. 10-12 may be provided by another (smaller) resonator located within the cavity. This enables the bandwidth of matching shown by the intermediate graph in Fig. 3. Each of these is suited for self-resonance, and requires some depth of activity to hold down the extra amount of energy storage in this nonradiating space.

Fig. 13 shows a flush inductor made of crossed coils on a thin magnetic disc. At medium or low frequencies (MF, LF, VLF) the available ferrite materials [12] can provide a magnetic core which is a return path nearly free of extra energy storage, even in the thin disc; also which adds very little dissipation. The required depth of cavity is then only sufficient to take the disc thickness with some margin. Relative to the wavelength at the lower frequencies, the antenna is too small to enable high efficiency, even at its frequency of resonance, so it is useful only for reception. A rotary coil or crossed coils can be used for a direction finder or omnidirectional reception. The principal application is on the skin of an aircraft.

Fig. 14 shows the ferrite-rod inductor which is the antenna most commonly used in small broadcast receivers (MF, around 1 MHz). The ferrite rod greatly increases the effective volume of a thin coil, as indicated. The effective volume is then determined primarily by the length, rather than the diameter, of the coil. Like the ferrite disc, this can be used close (parallel) to a shield surface or recessed in the surface.

Here we may note that a long coil with its small shape factor ($k_s \to 1$), can have its effective volume greatly

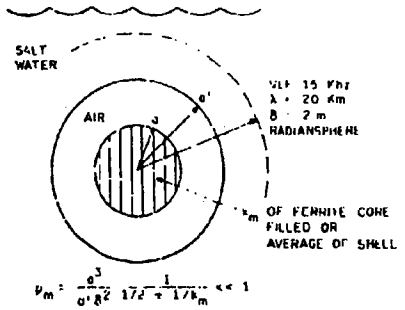

Fig. 15. Inductor in radome submerged in sea water.

increased by a ferrite core. On the other hand, a parallel-plate capacitor, with its small shape factor ($k_s \to 1$), can only have its effective volume decreased by a dielectric core. This is one respect in which the inductor offers more opportunity in design. In another respect, the number of turns can be used to set the impedance level, a freedom that may be desired but is unavailable in a simple capacitor.

If a long coil as a magnetic dipole were filled with perfect magnetic material, its effective volume would be comparable with that of an equally long conductor as an electric dipole. If the coil had many turns, they could theoretically be distributed (crowded toward the ends) to give an effective volume greater than that of a pair of discs far apart, Fig. 6(a). If the coil is not too thin, this result can be approximated at the lower frequencies with many turns on a ferrite core.

VIII. Antennas for VLF

The greater the wavelength, the more relevant may be the concept of a small antenna. Current activities go as low as 10 kHz with a wavelength of 30 km. Even the largest of transmitter antennas is small in terms of this wavelength, or its radianlength of 5 km. For underwater reception, however, the radianlength or skin depth in salt water is only a few meters, so a small antenna may occupy a substantial fraction of this size. The latter will be discussed first, as another example of a small inductor.

For submarine reception of VLF signals in salt water, an inductor in a hollow cavity (radome) is the preferred type [8]. As compared with a capacitor, its efficiency is greater because the conductivity of the water causes near-field losses in response to electric field but not magnetic field. Also there is no need for conductive contact with the water.

Fig. 15 shows an idealized small antenna in a submarine cavity [8], [9]. It is a spherical coil with a magnetic core, as shown in Fig. 5. In the water, the radianlength is equal to the skin depth (δ). At 15 kHz, this is about 2 m. The size of the cavity is much less, and the coil still less, so it is a small antenna in this environment. The radiation PF indicates two qualities, the desired coupling to the medium and the undesired dissipation in the medium. The former is proportional to the coil volume, and is increased by the magnetic core. The latter is decreased by increasing the

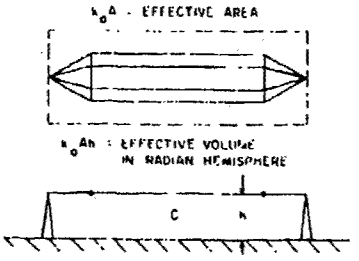

Fig. 16. Large flat-top capacitor which is still small relative to wavelength.

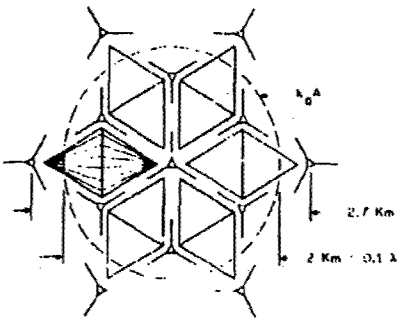

Fig. 17. Large VLF antenna (plan view)

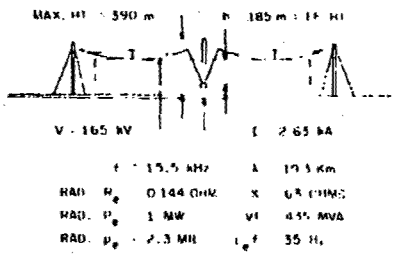

Fig. 18. Large VLF antenna (elevation view).

cavity radius. The coil is in the vertical plane for vertical polarization. Crossed coils may be used for omnidirective reception and direction finding.

For efficient transmission at the lower frequencies, one of the early simple types is the one shown in Fig. 16 [7]. It is a "flat-top" grid of wires forming a capacitor with ground as the lower conductor. In the terms of small antennas, it may be described in the manner indicated. The effective height (h) is related to the radiation resistance. The capacitance enables the statement of an effective area (k_0A) as noted. The effective volume (k_0Ah) in half-space is compared with $\frac{1}{2}$ radiansphere to determine the radiation PF. It is notable that the grid of many wires may provide an effective area greater than that of the grid, in spite of the much smaller area of conductor.

As an extreme example, we shall consider the latter one of the two largest antennas in the world. They are the Navy transmitters located at Cutler, Me., (NAA) and Northwest Cape, Australia, (NWC). The latter was commissioned in 1967. It is taken as an example because it is the simpler. Figs. 17 and 18 show the plan and elevation views of the structure. It operates down to about 15 kHz, a wavelength of 20 km.

The lowest "specification" frequency determines the required size. At this frequency, the following statistics are relevant:

frequency	15.5 kHz
wavelength	$\lambda = 19.3$ km
extreme diameter	2.7 km = $\frac{1}{7}\lambda$
center-tower height	390 m
effective height	185 m = $\frac{1}{104}\lambda$
capacitance	0.163 μF
effective area	3.4 (km)^2
effective volume	$V = 0.63$ (km)^3
radiation resistance	$R_r = 0.144\ \Omega$
reactance	$X_c = 0.3\ \Omega$
radiation PF	$p_e = 2.3$ mils
loss PF	< 2.3 mils
efficiency	> 0.50
resonance bandwidth	134 Hz
radiated power	1 MW
input power	2 MW
reactive power	435 MVA
voltage	165 kV
current	2.63 kA.

Particularly spectacular are the reactive power of 435 MVA in the air dielectric, and the real power of 2 MW delivered to a resistance of about 0.3 Ω. Less than half of this resistance is budgeted to all losses, including the ground connection and the tuning inductor. The small value of radiation PF (2.3 mils) well qualifies this structure as a "small antenna." The choice of a capacitor (rather than an inductor) was influenced by the need for omnidirective coverage.

The effective volume is diagramed in the form of a cylinder bounded by the dashed lines. Fig. 17, the effective area is a circle including more area than the grid of wires. In Fig. 18, the effective height is reduced by two practical considerations. The top level is lower than the top wires by the effect of the downlead (48 wires around the central tower). The bottom level is higher than the ground, by the effect of the grounded towers and guy wires (each tower having 3 at each of 4 or 5 levels). The resulting effective height is about $\frac{1}{2}$ the average height of the 13 towers. The radiation PF is related to this effective volume by (3) adapted to half space above ground. (The effective volume is compared with 1 radiansphere.)

IX. Conclusion

The principles of small antennas can be described in simple terms, both mathematically and pictorially. They are helpful in the understanding and design of practical antennas in either type, capacitor or inductor. While the two types have a common rating in terms of effective volume,

there are differences that may give either an advantage in size or other practical considerations. For any configuration, the efficiency and/or bandwidth is ultimately limited by size relative to the wavelength.

Acknowledgment

By way of acknowledgment, the author is indebted to various groups for opportunities to apply the principles of small antennas. The first example was the one-turn loop of Fig. 8 which was developed in collaboration with Seymour Berkoff at Emerson Radio and Phonograph Corp., in 1948 (for use by NBS in a proximity fuse). In the design of the large VLF antennas for the Navy by DECO at Leesburg, Va. (now DECO Communications Dep. of Westinghouse), the author was active in 1956–1957 as consultant to the late Lester H. Carr and his group, including William S. Alberts who kindly provided the information for Figs. 17 and 18. The flush inductor of Fig. 12 was developed in several forms at Wheeler Laboratories during the period 1964–1970, for use on rockets and aircraft. The work was supported by various agencies, including Bell Telephone Laboratories (for Army Ordnance), Air Systems Division of the Air Force, and Naval Air Development Center. Other examples in the text are based on specific studies and proposals made in various situations during the past quarter century. The writer is grateful to his associate, Alfred R. Lopez, for helpful discussions relating to this paper.

References

[1] L. A. Hazeltine, "Discussion on 'The shielded Neutrodyne receiver'," *Proc. IRE*, vol. 14, pp. 395–412, June 1926. (Introduction of p = "natural power factor of the resonant circuit as a whole." Used as a reference for bandwidth.)

[2] H. A. Wheeler, "Fundamental limitations of small antennas," *Proc. IRE*, vol. 35, pp. 1479–1484, Dec. 1947. (The first paper on the radiation power factor of C and L radiators of equal volume.)

[3] ———, "A helical antenna for circular polarization," *Proc. IRE*, vol. 35, pp. 1484–1488, Dec. 1947. (Coil with equal I and M radiation P[illegible].)

[4] L. J. Chu, "Physical limitations of omni-directional antennas," *J. Appl. Phys.*, vol. 19, pp. 1163–1175, Dec. 1948.

[5] R. M. Fano, "Theoretical limitations on the broadband matching of arbitrary impedances," *J. Franklin Inst.*, vol. 249, pp. 57–83, 139–154, Jan., Feb. 1950. (Tolerance and bandwidth, graphs p. 144.)

[6] J. R. Wait, "The magnetic dipole antenna immersed in a conducting medium," *Proc. IRE*, vol. 40, pp. 1244–1245, Oct. 1952. (In a spherical cavity.)

[7] H. A. Wheeler, "Fundamental relations in the design of a VLF transmitting antenna," *IRE Trans. Antennas Propagat.*, vol. AP-6, pp. 120–122, Jan. 1958. (Effective area, Radiation power factor.)

[8] ———, "Fundamental limitations of a small VLF antenna for submarines," *IRE Trans. Antennas Propagat.*, vol. AP-6, pp. 123–125, Jan. 1958. (Inductor in a cavity. Radiation power factor.)

[9] ———, "The spherical coil as an inductor, shield, or antenna," *Proc. IRE*, vol. 46, pp. 1595–1602, Sept. 1958; correction, vol. 48, p. 924, Mar. 1960. (Ideal sphere inductor. Subnar ne coil.)

[10] ———, "The radiansphere around a small antenna," *Proc. IRE*, vol. 47, pp. 1325–1331, Aug. 1959. (Ideal sphere inductor. Radiation shield.)

[11] J. H. Dunlavy and R. C. Reynolds, "Electrically small antennas," in *23rd Ann. USAF Antenna Symp.*, Oct. 1972. (Examples of passive and active antennas. The most recent paper in this publication series.)

[12] C. E. Owens, "A survey of the properties and applications of ferrites below microwave frequencies," *Proc. IRE*, vol. 44, pp. 1234–1248, Oct. 1956. (Around 1 MHz, antenna cores.)

ELECTRICALLY SMALL ANTENNA STUDIES AT OSU

by

C.H. Walter

The Ohio State University ElectroScience Laboratory
Department of Electrical Engineering
Columbus, Ohio 43212
April 1976

ABSTRACT

This paper describes work at The Ohio State University ElectroScience Laboratory on studies related to electrically small antennas. Recent work includes the development of techniques for measuring efficiency, the development of efficient elements for transmitting applications at HF and VHF and studies of reduced-size arrays of small elements. In addition some earlier work on the integration of active circuitry to antennas is described.

INTRODUCTION

This paper describes work at the Ohio State University on studies related to electrically small antennas. The scope of the work includes efficiency measuring techniques and theoretical and experimental studies of basic radiating elements and reduced-size arrays of small elements. In addition some earlier work on the integration of circuits and antenna elements that may be useful for small antennas is included.

EFFICIENCY MEASURING TECHNIQUES

One of the most difficult and important problems associated with electrically small antennas is the determination of antenna efficiency. Although theoretical analyses such as an integral equation formulation with Moment Method solution are useful, an experimental approach has the advantage of including unforeseen and/or hidden loss factors that may not or could not have been included in the theoretical model. Examples of this would include solder joint loss, lossy film on the conductors and losses in tuning and matching components.

The pattern integration and gain comparison methods usually provide reliable methods for measuring antenna efficiency but the time required may be prohibitive when a parameter study is to be made in order to optimize the antenna in some way. Thus other experimental techniques have been explored and two of these, the Wheeler Cap Method and the Q Method, have been found to be quite useful for rapid parametric studies.

A. Wheeler Cap Method

If we define R_R to be the antenna radiation resistance and R_L the antenna loss resistance, the quantity R_R+R_L may be determined by measuring the antenna input impedance. Wheeler[1] suggests that enclosing the antenna with a conducting sphere a radian length (about one-sixth wavelength) in radius will eliminate R_R from the input impedance without significantly changing R_L. This assumes that the conducting sphere causes no change in the current distribution on the antenna. If this assumption is correct, the real part of the input impedance with the sphere in place will be R_L. Thus by making two impedance measurements, one without the sphere and one with the sphere in place, the antenna efficiency can be determined using the relation

$$E_W = \frac{R_R}{R_R+R_L}$$

Using standard equipment such as a network analyzer (with Smith chart overlay) one can quickly and easily measure R_L+R_R and R_L and therefore efficiency. A typical test configuration is illustrated in Fig. 1 for a VHF multiturn loop (MTL) antenna. The antenna is shown larger than scale for clarity. The cap may be cubic in shape. It was determined that the shape of the conducting cap was not critical and no real difference (plus or minus 2 percent) could be determined in measured efficiency whether the cap was copper or aluminum. The effect of reducing cap size was to increase input reactance but, so long as accurate values of input resistance could be determined, there was no appreciable change in measured efficiency. A larger cap makes input resistance easier to read and the 18" x 18" x 18" aluminum cap in Fig. 1 was used in measurements at 160-240 MHz.

Measured results from the Wheeler Cap method have been compared with results from pattern integration and gain comparison methods. Comparison with pattern integration data showed differences of up to 25% and Fig. 2 shows a comparison with data from gain measurements. For the data in Fig. 2 the efficiency by the Wheeler Cap method was obtained from the structure of Fig. 1 whereas the gain comparison method utilized a 20' x 20' groundplane. This may account for some of the discrepancy in the data.

It is concluded that the Wheeler Cap method can accurately predict the relative efficiencies of two antennas and to also yield a reasonable approximation to the absolute efficiency. The major advantage of the method is that the measurement is quick and easy. At the lower frequencies it is limited by the size of the conducting cap that one is willing to construct. Caps as large as 15' x 15' x 10' have been used for HF antennas from 4-30 MHz.

B. The Q Factor Method

A second method for measuring antenna efficiency is based on a comparison of measured to ideal Q. The Q of a realizable antenna is defined as

$$(2) \qquad Q_{RL} = \frac{\omega \times \text{peak energy stored}}{\text{average power radiated + average power dissipated}}$$

and the Q of the ideal, lossless antenna is

$$(3) \qquad Q_R = \frac{\omega \times \text{peak energy stored}}{\text{average power radiated}} .$$

If the current distributions on the realizable and on the ideal antenna are considered to be the same, then the stored energies will also be the same, and the efficiency of the realizable antenna is simply the ratio

$$(4) \qquad E_Q = \frac{Q_{RL}}{Q_R} = \frac{\text{power radiated}}{\text{power radiated + power dissipated}} .$$

Q_{RL} can be determined by measuring the impedance bandwidth of the actual antenna. Q_R for the ideal lossless antenna can be found from the results of Chu[2] and Harrington[3] where the antenna is considered to radiate a number of spherical waveguide modes emanating from a spherical surface surrounding the antenna. For an electrically small MTL antenna the size of the spherical surface is taken as the smallest sphere which encompasses the MTL and the tuning and matching capacitors (see Fig. 1), and the distribution of spherical waveguide modes is taken as the lowest order TM_{01} mode only. The solid curve of Fig. 3 shows the ideal Q_R of an antenna which can be enclosed by a sphere of minimum radius a, and which radiates the TM_{01} mode only. This curve was used to obtain Q_R for all of the MTL considered here. The dashed curve in Fig. 3 is the ideal Q_R of an antenna which radiates equal amounts of the TE_{01} and TM_{01} modes[3].

A comparison of efficiencies by the Wheeler and Q methods is shown in Table I. In this set of measurements five MTL antennas, each with a different number of turns, were made from No. 18 tin-coated copper wire. For each MTL, Table I lists the number of turns in the loop (N), 2π times the radius a in wavelengths of the smallest sphere which could completely enclose the MTL and its feed and matching capacitors, the Wheeler efficiency, and the Q efficiency. Table I shows that for $ka \leq 0.156$ the Wheeler method and the Q method yield approximately the same efficiency. For larger ka the antenna can radiate significant amounts of higher order modes, and the methods for choosing the radius a and the modal distribution fail, and thus the Q method fails as used here. In Table I this is illustrated by a Q efficiency of 122 percent for ka = 0.236.

Although it is not a fundamental limitation, determining the higher order modes radiated by an antenna is sufficiently difficult that the Q method is in practice limited to electrically small antennas. Our experience with this method indicates that if absolute efficiency is desired, it is reasonable to use the Q method to measure MTL efficiency for $ka \approx 0.2$. If only relative efficiency is important, the method can be applied for ka somewhat greater than 0.2.

Both the Wheeler method and the Q method are easy to apply. They have been found to accurately predict relative changes in efficiency, and to a lesser extent absolute efficiency. Further, they are applicable at HF and VHF frequencies where the standard pattern integration technique may become impractical. The Wheeler method is limited on the low frequency end by the size of the cap that one is willing to construct. Provided that the impedance of the antenna can be accurately measured, we see no lower frequency limit for the Q method.

TABLE I
A COMPARISON OF WHEELER AND Q EFFICIENCY
FOR VARIOUS SIZE MTL

N	ka	E_W (percent)	E_Q (percent)
6	0.056	6	4
4	0.076	10	12
3	0.118	26	34
2	0.156	46	47
1	0.286	84	122

ELECTRICALLY SMALL RADIATING ELEMENTS

An electrically small antenna is an antenna whose maximum dimension is much less than the wavelength. We shall adopt the definition used by Shelkunoff and Friis[4] in which an electrically small antenna is one-eighth wavelength or less in maximum extent. Except for pattern distorting effects of finite ground plane or support structure the pattern of a small antenna is essentially that of the classic elemental dipole which in free space and with current flow along the z-axis in a conventional spherical coordinate system has a sine field pattern and a directivity (directive gain) of 1.5.

There are two basic types of electrically small antennas. These are the electric element, which couples to the electric field and is referred to as a capacitive antenna, and the magnetic element (electric loop), which couples to the magnetic field and is referred to as an inductive antenna.

Electrically small antenna are generally categorized as one of the other of these two basic types although many practical small antennas are some combination of the two types. The categorization is done on the basis that the antenna is principally an electric or magnetic element. Of these two basic types the electric element can be considered to be the most fundamental since the loop, or in general any wire antenna, can be constructed from a superposition of electric elements.

Some examples of small electric dipole or capacitive antennas are given in Fig. 4 and some examples of small loop or inductive antennas are given in Fig. 5.

The representation of a small antenna by means of a capacitor or inductor is a convenient application of lumped circuit concepts to antennas and is a justifiable approximation for many small antennas. Many successful antennas, particularly for VLF-HF applications, have been developed on this basis and a good summary of capacitive and inductive antennas has been given by Wheeler[5]. However, modern high-speed digital computers now enable the antenna engineer to analyze, with almost any degree of accuracy, small antennas of arbitrary form such as those shown in Figs. 4 and 5.

In the definition of the small antenna it is implied that the antenna is operated at a frequency or frequencies well below its first natural resonance. This is usually true but some small antennas utilize multiturn loop, spiral, or folded configurations as shown in Figs. 4 and 5 wherein it is possible to have a conducting element of sufficient electrical length to operate at or above the first natural resonance, but still not have the maximum dimension of the antenna structure exceed one-eighth wavelength.

Design data in the form of impedance, efficiency and patterns of many of the configurations in Figs. 4 and 5, as well as others, have been obtained at the Ohio State University and are contained in part in References [6-12]. The data generally were HF and VHF designs and are too extensive to include here. Some of these data have been obtained experimentally using the efficiency method described above. Most of the data, however, have been obtained by numerical analysis primarily using the Method of Moments[9]. In many cases, effects of environment on the antenna performance are included such as lossy earth beneath body, vehicle, etc.

An interesting example of a small antenna coupling to a complex structure is shown in Fig. 6. This is the case of a small, simple turn loop efficiency side which in free space has an efficiency of about 7 %. When mounted on the side of conductor, the efficiency is drastically increased by virtue of coupling to and radiation from the nearby structure. The point here is that even though the efficiency of a small antenna may be low, when it is located near a large practical structure such as a land or plane it can couple to modes on the structure which greatly increases the radiation efficiency.

REDUCED SIZE ARRAYS

Use of superdirective designs at HF and lower frequencies is not practical due to the high ambient noise level. However, gains of 3 to 5 dB over an order of magnitude or greater is possible at [illegible] including height reduction of three or more using electrically [illegible] extent reduction of three or more using superdirective array designs with tolerance constraint.

A study has been made to examine the properties of antenna arrays for increased directivity and to develop an analysis for such arrays suitable for engineering design form to illustrate receiving system trade offs in terms of electrical and mechanical parameters and tolerances [11]. For receiving the factor of primary interest is the system signal to noise ratio. The signal to noise ratio (SNR) of a receiving array is equal to the product of the directive gain and the ratio of incident signal power to incident noise power if the system is background noise limited, and if the background noise is uniformly distributed in space. Receiving systems tend to be background noise limited at frequencies below approximately 30 MHz.

The SNR is probably the most important parameter describing and limiting the performance of a receiving system. There are several possible procedures for increasing the SNR. Although decreasing the external noise will increase the SNR, except to the extent that changing the location of the receiving array will also change the noise, one usually has no control over the external noise environment. Increasing the signal power [illegible] will, of course, increase the

SNR. However, often the designer of a receiving system has little or no control over N_{ext}. Finally, one can increase the SNR by increasing the directive gain in the direction of the incident signal, $D(\theta_M,\phi_M)$.

The most common approach for increasing $D(\theta_M,\phi_M)$ is to space the array elements at approximately $\lambda/2$, and feed the elements with constant amplitude and with the proper phase so that radiation from the direction (θ_M,ϕ_M) adds in phase. Depending on the array geometry and the number of array elements, spacing the elements $\lambda/2$ apart will often result in arrays of several wavelengths in extent. At 2 MHz, $\lambda = 150$ meters and arrays on the order of 1000 meters or larger could be required to obtain an acceptable $D(\theta_M,\phi_M)$ and SNR.

It is well known that the constant amplitude linear phase taper method for feeding arrays does not maximize the directive gain and significant improvements in directive gain can be achieved for arrays with element spacings closer than the usual $\lambda/2$; however, designing for maximum directive gain will not lead to as useful results as designing for near maximum directive gain by imposing a constraint on electrical and mechanical tolerances. By designing for maximum directive gain subject to a constraint called sensitivity factor one can trade increased directivity for lower efficiency, higher tolerances, and greater bandwidth[13].

Directive gains for 10 element circular arrays for various array radii R/λ as a function of sensitivity factor K are shown in Fig. 7 and the pattern in the plane of the array for an array diameter of 0.1λ and a sensitivity factor K = 30 is shown in Fig. 8.

INTEGRATED ANTENNAS AND CIRCUITS

Some early studies at Ohio State considered mixers, amplifiers and phase shifters as integral parts of antennas such as dipoles, log-periodic dipole arrays and conical spirals[14-17]. The concept of integrated antenna-circuitry design is one of combining certain antenna functions with certain circuit functions in a single structure. Some of the advantages offered by integrated design over conventional separated design are improved electrical performance, increased reliability, reduced number of components and more compact packaging.

An example of a dipole with integrated solid state amplifier is illustrated in Fig. 9. Such a device is compact, relatively inexpensive, can be designed to have high gain with low noise, and can be used singly or in arrays where the element gains may be controlled independently.

These techniques can be used in electrically small antennas to obtain better impedance matching and better overall system performance with regard to some parameter such as SNR or efficiency. For example, the MIC illustrated in Fig. 1 makes use of two integral capacitors for tuning and matching. Varying capacitor C_A in Fig. 1 changes the resonant frequency of the antenna and C_B is adjusted to give a real input impedance at some level such as, 50 Ω. The use of integral tuning and matching in this case results in a simpler and more efficient antenna than having an external network for this purpose. Feedback circuitry can be added to keep the antenna tuned automatically[18].

REFERENCES

[1] H.A. Wheeler, "The radiansphere around a small antenna," Proc. IRE, pp. 1325-1331, Aug. 1959.

[2] L.J. Chu, "Physical limitations of omni-directional antennas," J.A.P., vol. 19, pp. 1163-1175, Dec. 1948.

[3] R.G. Harrington, Time Harmonic Electromagnetic Fields, New York: McGraw-Hill, pp. 264-316, 1961.

[4] S.A. Schelkunoff and H.T. Friis, Antennas: Theory and Practice. John Wiley and Sons, 1952.

[5] H.A. Wheeler, "Fundamental limitations of small antennas," Proc. IRE, pp. 1479-1488, Dec. 1947.

[6] "Final report for a study of controlled radiation from an aircraft structure at high frequencies," Ohio State University ElectroScience Laboratory, Dep. Elec. Eng., Rep. 2833-1, 16 Feb. 1970; prepared under Contract N00123-69-C-2472 for U.S. Navy Purchasing Office.

[7] D.S. Irons, Jr. and W.D. Burnside, "Final technical report for phase III, 'antennas for mine detection systems,'", Ohio State University ElectroScience Laboratory, Dep. Elec. Eng., Rep. 2857-9, May 1971; prepared under Contract DAAK02-C-0638 for U.S. Army Mobility Equipment Research and Development Center. (AD 888 410L)

[8] P. Bohley and E.H. Newman, "Development of a VHF multiturn loop antenna for seismic sensor systems," Ohio State University ElectroScience Laboratory, Dep. Elec. Eng., Rep. 3281-2, Mar. 1973; prepared under Contract DAAG39-72-C-0041 for Harry Diamond Laboratories. (AD 759 508)

[9] C.H. Walter and E.H. Newman, "Electrically small antennas," Ohio State University ElectroScience Laboratory, Dep. Elec. Eng., Report 3281-3, Feb. 1974; prepared under Contract DAAG39-72-C-0041 for Harry Diamond Laboratories. (AD 775 855) (HDL-TR-041-1)

[10] E.H. Newman, J.H. Richmond, G.K. Chan and C.H. Walter, "Small antennas for nose tip applications," Final Report, Ohio State University ElectroScience Laboratory, Dep. Elec. Eng., Rep. 3281-5, April 1974; prepared under Contract DAAG39-72-C-0041 for Harry Diamond Laboratories. (AD 778 204) (HDL-TR-041-3)

[11] G.A. Thiele, R. Sunderland and C. Donn, "Electrically small antennas for nose cone applications," Ohio State University ElectroScience Laboratory, Dep. Elec. Eng., Rep. 3578-1, Mar. 1973; prepared under Contract F04701-72-C-0180 for Space and Missile Systems Organization. (AD 526 402L) (SAMSO-TR-73-182)

[12] C.H. Walter, P. Bohley and R. Caldecott, "Development of the multiturn loop antnena at H.F. for shipboard application," Ohio State University ElectroScience Laboratory, Dep. Elec. Eng., Rep. 3518-1, Dec. 1973; prepared under Contract N00024-73-C-1023 for Naval Ship Systems Command. (AD 771 729)

[13] E.H. Newman, J.H. Richmond and C.H. Walter, "Superdirective array study," Ohio State University ElectroScience Laboratory, Dep. Elec. Eng., Report 3955-2, Sept. 1975; prepared under Contract DAAB03-74-C-0516(1433) for Department of the Army.

[14] "Final Engineering Report," Ohio State University Antenna Laboratory, Dep. Elec. Eng., Rep. 1566-24, 20 Dec. 1965; prepared under Contract AF 33(657)-10386 for Air Force Avionics Laboratory. (AD 476 943)

[15] J.R. Copeland, W.J. Robertson and R.G. Verstraete, "Antennafier arrays," IEEE Trans. on Antennas and Propagation, Vol. AP-12, No. 2, Mar. 1964.

[16] "Final report (techniques for integrating solid state circuitry into antennas).", Ohio State University ElectroScience Laboratory, Dep. Elec. Eng., Rep. 2142-20, Jan. 1969; prepared under Contract AF 33(615)-3884 for Air Force Avionics Laboratory. (AD 849 118)

[17] P. Agrawal, E.H. Newman, G.A. Thiele, M. Van deWelle, N.A. Walker and C.H. Walter, "Antennas with solid state circuitry," Ohio State University ElectroScience Laboratory, Dep. Elec. Eng., Rep. 2744-2, Mar. 1972; prepared under Contract F33615-69-C-1197 for Air Force Avionics Laboratory. (AD 893 437L) (AFAL-TR-72-87)

[18] P. Bohley, R.J. Davis and C.H. Walter, Final report, "Man pack loop antenna system," Ohio State University ElectroScience Laboratory, Dep. Elec. Eng, Rep. 3864-2, Dec. 1974, prepared under Contract N00123-74-C-0645 for Naval Regional Procurement Office. (AD/A 006 278)

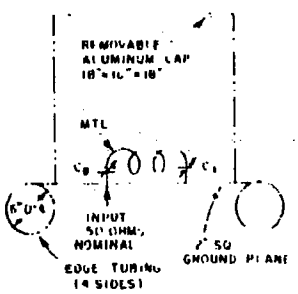

Fig. 1. System for measuring MTL efficiency.

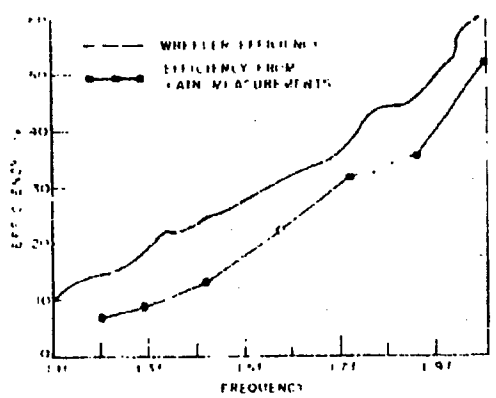

Fig. 2. Comparison of MTL efficiency from Wheeler method and gain measurements.

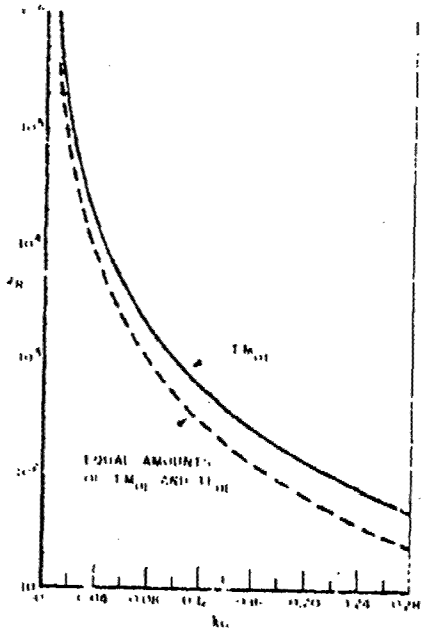

Fig. 3. Theoretical ideal Q as function of $2\pi a/\lambda$.

Fig. 4. Examples of small electric dipole or capacitive antennas.

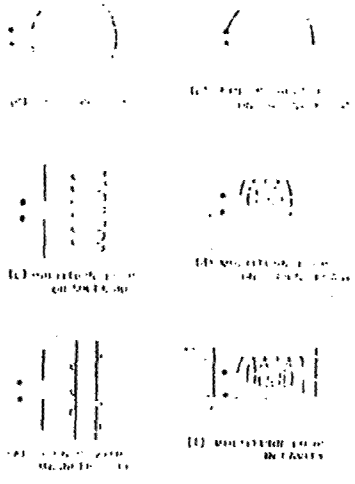

Fig. 5. Examples of small magnetic dipole (loop) or inductive antennas.

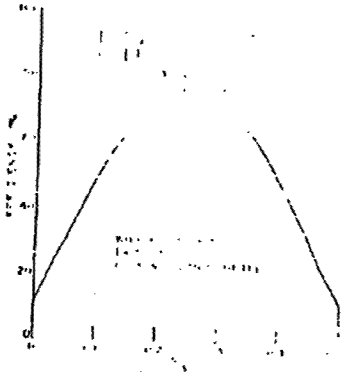

Fig. 6. Increased efficiency of a small loop by coupling to a nearby structure.

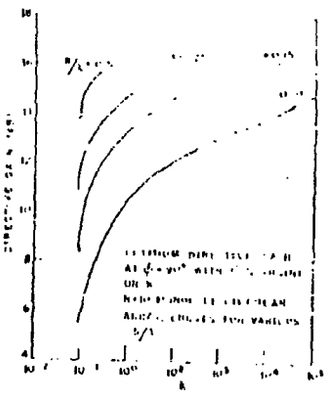

Fig. 7. Optimum directive gain versus the sensitivity factor for a 10 element circular array.

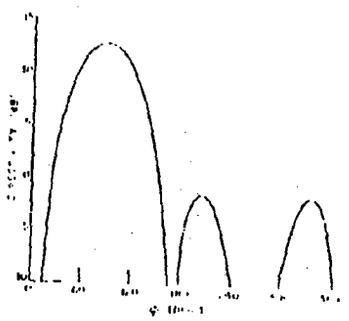

Fig. 8. H-plane pattern for a 10 element circular array with R = 0.05 and k = 30.

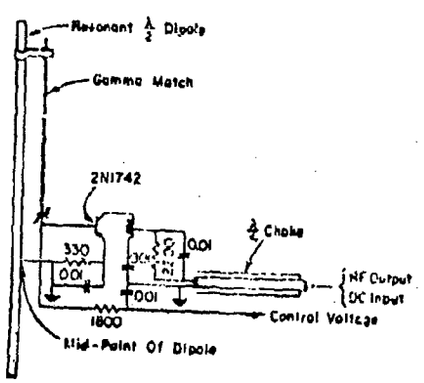

Fig. 9. A dipole antenna with integrated solid state amplifier.

ELECTRICALLY SMALL ACTIVE RECEIVING ANTENNAS

by

HANS H. MEINKE

Technical University
of Munich, Germany

ABSTRACT

An electrically short monopole is directly combined with a field-effect transistor to form a broadband active antenna. A curve of optimum antenna height depending on frequency is given. At frequencies below 1 MHz, the optimum monopole height decreases with decreasing frequency due to increasing external noise. Linearity and lightning protection are additional requirements for active antennas for which solutions are presented.

Electrically small

active receiving antennas

The active antenna in its basic form consists of a passive antenna and an integrated amplifying device. Here I discuss the most simple case of a short monopole which is directly connected to the input of a fieldeffect-transistor. In Fig.1 the monopole acts as a source which feeds the transistor. The antenna has a emf V_A which is $V_A = E \cdot h_{eff}$; E = electrical fieldstrength, h_{eff} = effective height. The monopole has a capacity C_A and the transistor an input capacity C_T. These two capacities form a capacitive voltage divider and the signal voltage V_S between the input terminals 1 and 2 of the transistor is

$$V_T = \frac{E \cdot h_{eff}}{1 + \frac{C_T}{C_A}}$$

V_S is nearly independent on frequency and, therefore, the monopole with integrated fieldeffect-transistor gives an active antenna with extremely broad bandwidth even for electrically small monopoles. So, generally, bandwidth is no problem for active antennas, even not for very small monopoles, and monopole height can be chosen arbitrarily. In practice, the antenna may contain additional reactances for frequency selectivity, if wanted.

Output power is an unimportant quantity for active antennas because output power here is generated by amplification. Therefore, only signal-to-noise ratio is that main problem which governs active antennas. To get a simple survey, we assume that the active antenna has a sufficient amplification so that signal-to-noise ratio is determined by the input circuitry of fig.1 and not by the following receiver. The noise is a sum of external noise and internal noise. The external is received by the monopole together with the signal and a part of the monopole output. The internal noise in our case is the electronic noise of the transistor.

Fig.2 explains an important fact: V_S^2 is the square of the signal voltage between terminals 1 and 2 and represented by the arrow V_S^2 ; V_{NA}^2 is the square of the noise-voltage due to external noise and represented by the arrow V_{NA}^2 ; V_{NT}^2 is the square of the noise-voltage due to internal noise and mainly the equivalent transistor noise and represented by the arrow V_{NT}^2. If using the squares the equivalent total noise V_{Ntotal}^2 is the sum of V_{NA}^2 and V_{NT}^2 as shown in fig.2. The ratio of V_S^2 and V_{Ntotal}^2 is the signal-to-noise ratio of this ideal receiving system. Fig.2a, b and c show systems with different monopole heights. In Fig.2a the monopole has the longest monopole, fig.2b a shorter monopole and fig. 2c a still shorter monopole. V_S^2 and V_{NA}^2 are proportional to the square of monopole height, and the ratio of V_S^2 and V_{NA}^2 is independent of monopole height, while V_{NT}^2 has the same arrow length in all 3 cases independent of monopole height, if related to terminals 1 and 2.

In fig.2a the monopole height is chosen so that the transistor noise V_{NT}^2 is considerably smaller than the external noise V_{NA}^2 and the total noise is mainly determined by the external noise.

In fig.2c the monopole height is far smaller than in fig.2a and V_S^2 and V_{NA}^2 are smaller, consequently. In fig.2c the same transistor noise V_{NT}^2 adds to a smaller external noise V_{NA}^2 and, therefore, here the total noise is mainly determined by the transistor noise. Fig.2b shows the optimum case with a special monopole height h_{opt} in which the external and the internal noise have equal level ($V_{NA}^2 = V_{NT}^2$). The signal-to-noise ratio S/N depending on effective monopole height h_{eff} is for a given transistor noise shown in fig.3. For very long dipoles S/N approaches asymptotically an upper limit. This means that a monopole height far beyond h_{opt} gives no remarkable improvement of S/N, but an increasing expense. On the other hand, a monopole height far below h_{opt} gives a very bad noise situation. Therefore, there is an optimum monopole height as a good compromise between expenses and reception quality.

The external noise is increasing rapidly with decreasing frequency and, consequently, for given equivalent transistor noise brings up the unexpected fact that with decreasing frequency we can use shorter monopoles for active antennas in which the monopole is integrated with a fieldeffect transistor. In fig.4 we see a measured curve of h_{opt} depending on frequency based on very many measurements which we undertook in Germany and may also be true in USA. The thick horizontal lines in fig.4 indicate the monopole height of real commercial antennas which we developed together with industry in Germany.

A monopole antenna with transistor in practice must fulfill additional requirements, mainly linearity. We extended development work on electronic circuitry for active antennas to get low noise and linearity simultaneously. We succeeded to get linearity up to extreme

conditions, when the receiving antenna is near to a powerful transmitter station. We also investigated the stability of operation, especially phase stability of the output signal, under different environments and changing temperature. So we can offer reliable active antennas for direction finding and navigational aids. Another important point is to protect the transistor against electrical discharges of the atmotsphere, for example during a thunderstorm. Active antennas on ships have been tested on the oceans already for years. So we finally can offer now active antennas for many applications with improved quality. The improvement at lower frequencies concerning small antenna height is impressive, while at higher frequencies we do not tend to very small antennas but to better signal-to-noise ratio.

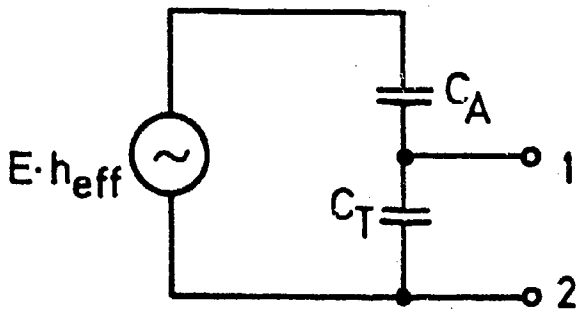
C_A
$E \cdot h_{eff}$
1
C_T
2

Fig. 1

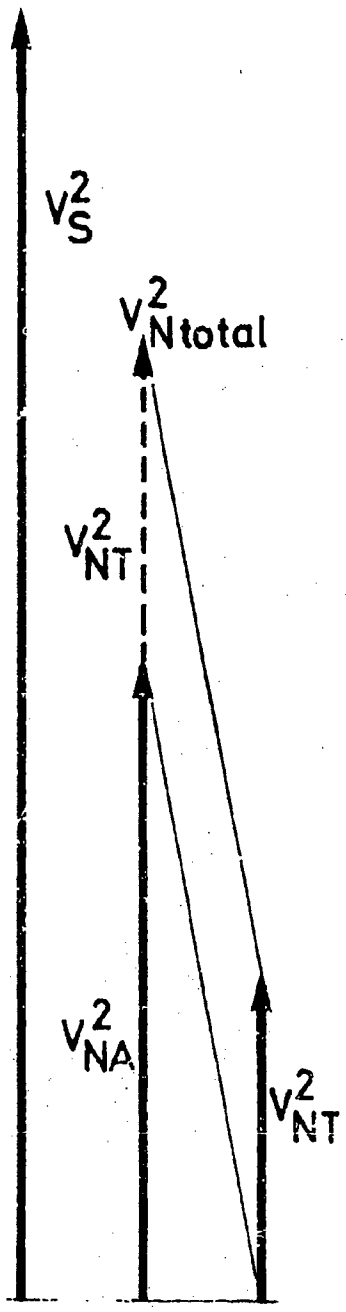
V_S^2
V_{Ntotal}^2
V_{NT}^2
V_{NA}^2
V_{NT}^2
a)

Fig. 2

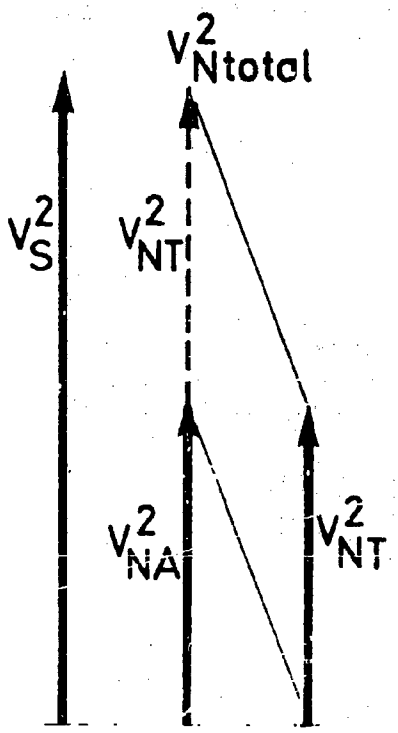
V_{Ntotal}^2
V_S^2
V_{NT}^2
V_{NA}^2
V_{NT}^2
b)

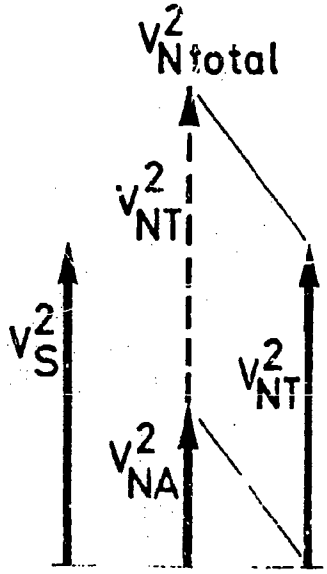
V_{Ntotal}^2
V_{NT}^2
V_S^2
V_{NT}^2
V_{NA}^2
c)

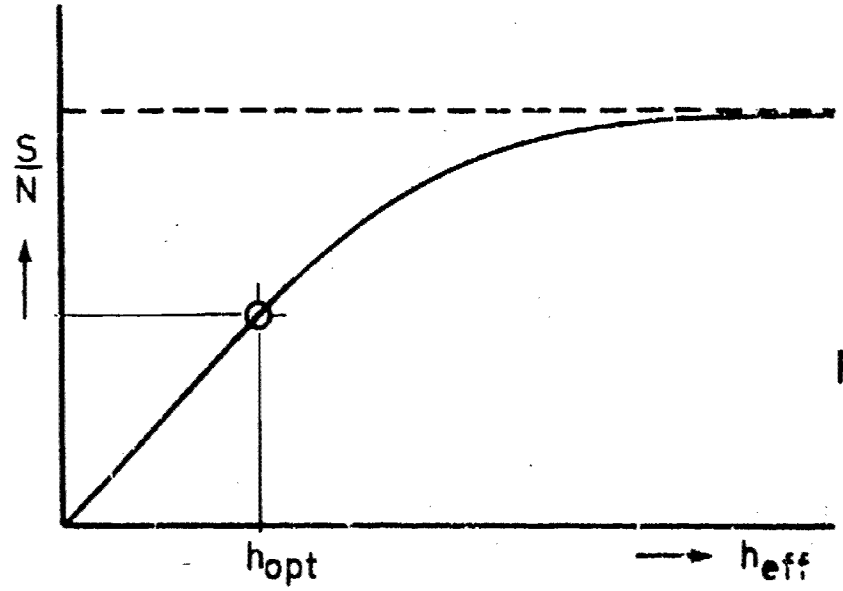
S/N
h_{opt}
h_{eff}

Fig. 3

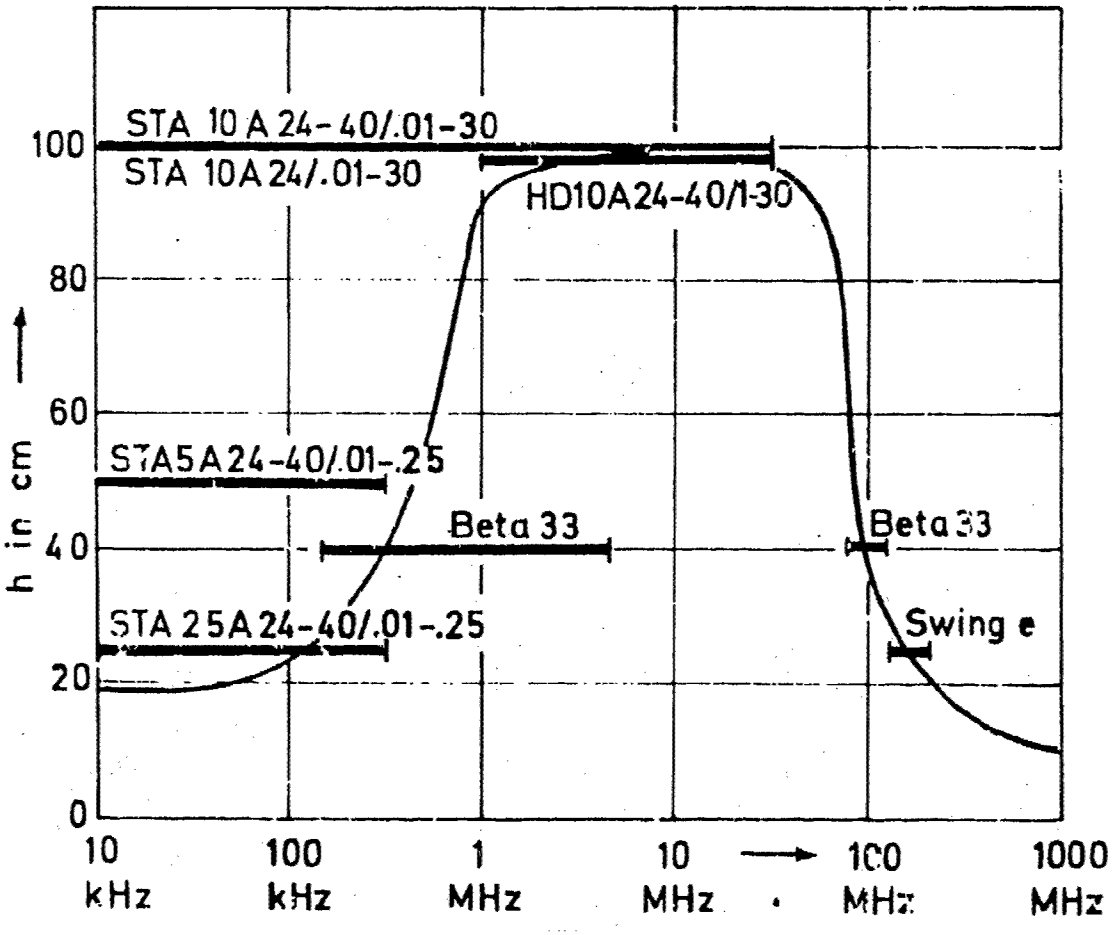
STA 10 A 24-40/.01-30
STA 10A 24/.01-30
HD10A24-40/1-30
STA5A24-40/.01-.25
Beta 33
Beta 33
STA 25A 24-40/.01-.25
Swing e
h in cm
100
80
60
40
20
0
10 kHz
100 kHz
1 MHz
10 MHz
100 MHz
1000 MHz

Fig. 4

AN ERROR ANALYSIS FOR THE WHEELER METHOD OF MEASURING THE RADIATING EFFICIENCY OF ELECTRICALLY SMALL ANTENNAS*

Glenn S. Smith
School of Electrical Engineering
Georgia Institute of Technology
Atlanta, Georgia 30332

A model problem was formulated to evaluate the accuracy of the Wheeler method for measuring the efficiency of electrically small antennas. The antenna in the model is a circular loop and the radiation shield is a spherical metal shell. Calculated values of the actual efficiency and the efficiency that would be measured using the Wheeler method are compared to determine the accuracy of the method.

The radiating efficiency of an antenna is defined as

$$\eta = \frac{P_R}{P_R + P_L} = \frac{R_R}{R_R + R_L} \tag{1}$$

where P_R is the power radiated and P_L the power lost in the antenna due to mechanisms such as ohmic heating. R_R and R_L are the series components of the terminal resistance of the antenna ($R = R_R + R_L$) which represent the power radiated and power lost. The radiating efficiency is an important parameter for characterizing electrically small antennas and a difficult one to measure. H. A. Wheeler suggested a simple method for measuring the efficiency using a "radiation shield" [1],[2]. Briefly, the procedure is to make two measurements of the resistance of the antenna, one measurement with the antenna isolated $R = R_R + R_L$ and a second measurement with the antenna completely enclosed in a highly conducting metal shield R'. Since the shield eliminates the radiation, the resistance R' is the result of the losses in the antenna and shield, $R' = R_L' + R_S$. An efficiency η_S can be calculated from the two measured resistances

$$\eta_S = \frac{R - R'}{R} = \frac{R_R + (R_L - R_L' - R_S)}{R_R + R_L} \tag{2}$$

*This work was supported in part by NASA under contract NAS5-22422 with the Engineering Experiment Station, Georgia Institute of Technology.

If the resistance attributed to the losses in the shield, R_S, is negligible and $R_L' \approx R_L$, the efficiency η_S is approximately the same as the actual efficiency of the antenna.

$$\eta_S \approx \frac{R_R}{R_R + R_L} \qquad (3)$$

For this approximation to be true

$$R_L = R_L' = R_S \ll R_R \qquad (4)$$

The accuracy of the method depends on how well this inequality is satisfied and is a function of the properties of the antenna, frequency and size of the shield.

To investigate the accuracy of the method, a model problem was formulated where the antenna is a thin-wire circular loop and the shield a concentric spherical shell, see Figure 1 for the details of the geometry. The current distribution in the loop can be obtained as a Fourier series.

$$I'(\varphi) = \sum_{m=-\infty}^{\infty} \exp(-jm\varphi) \frac{-jV_0}{\pi\zeta_0} \sum_{m=-\infty}^{\infty} (a_m + jb_m + d)^{-1} \exp(-jm\varphi) \qquad (5)$$

where the terms b_m are due to the presence of the shield and the terms a_m are due to the finite conductivity of the loop. The current in the isolated loop $I(\varphi)$ is given by (5) with $b_m = 0$. The details of computing the coefficients a_m, b_m are quite involved and will not be discussed here, but are similar to those used in previous analyses [3,4]. The four resistances R_R, R_L, R_L', and R_S can be determined once the current distributions $I(\varphi)$ and $I'(\varphi)$ are known. They can then be used with (1) and (2) to determine the actual radiation efficiency of the loop and the radiating efficiency that would be measured using the Wheeler method [5].

The two efficiencies were computed for various loop and shield sizes; typical results are given in Table 1. For this example the shield is a wavelength in circumference ($k_0 a = 1.0$ a radiansphere as suggested by Wheeler), both the wire and shield have the same loss tangent $\tau_W = \rho_S = 1.09 \times 10^{-10}$. This corresponds to copper at a frequency of 50 mHz. When the loop size is in the range $0.05 \le k_0 b \le 0.1$, $R_L' \approx R_L$ and the accuracy of the method is very good, $\eta_S \approx \eta_A$. Near the antiresonant size for the loop ($k_0 b \approx 0.2$) the difference between R_L' and R_L is large, and the assumption (4) is not

satisfied. The difference between R_l' and R_l is due to a change in the current distribution in the loop when the shield is added.

At the lower radio frequencies, for example in the HF band, a conventional method for measuring the efficiency, such as pattern integration, is difficult to use; the Wheeler method is an attractive alternative because of its simple measurement procedure. At these frequencies, a shield with $\beta_0 c = 1.0$ is often too large to be practical and an electrically smaller shield must be used. For the smaller shields the resistance due to the shield, R_S, can be comparable to the radiation resistance, R_R. In these cases (4) is not satisfied and the errors associated with the method can be large. This is illustrated in Figure 2 where the ratio η_S/η is shown as a function of the size of the shield, $\beta_0 c$, and loss tangent $p = P_W = P_S$. The size of the loop is $\beta_0 b = 0.64$, $a/b = 0.05$. Note that the ratio can be negative for the smaller values of $\beta_0 c$.

The results of the analysis for this model problem indicate that the Wheeler method for measuring the radiating efficiency can be quite accurate when the shield used has dimensions which are a substantial fraction of a wavelength and the antenna is not operated near a critical point like at antiresonance. For shields that are electrically smaller, the errors associated with the method can be large.

[1] H. A. Wheeler, Proc. IRE, pp. 1325-1331, Aug. 1959.

[2] E. H. Newman, P. Bohley, and C. H. Walter, Trans. IEEE Antennas Propagat., pp. 457-461, July 1975.

[3] G. S. Smith, Radio Science, pp. 711-725, July 1973.

[4] G. S. Smith, Radio Science, pp. 35-41, Jan. 1974.

TABLE I

$\beta_0 b$	$R_R(\Omega)$	$R_L(\Omega)$	$R'_L(\Omega)$	$R_S(\Omega)$	η	η_s	η_s/η
0.05	1.27×10^{-5}	1.89×10^{-2}	1.89×10^{-2}	6.83×10^{-8}	6.33%	6.33%	1.00
0.10	2.23×10^{-3}	4.02×10^{-2}	4.01×10^{-2}	1.17×10^{-5}	35.7	35.7	1.00
0.15	1.32×10^{-1}	6.69×10^{-2}	6.69×10^{-2}	6.71×10^{-6}	66.3	66.3	1.00
0.20	5.20×10^{-1}	1.05×10^{-1}	1.05×10^{-1}	2.54×10^{-5}	83.3	83.3	1.00
0.30	5.55	2.78×10^{-1}	2.75×10^{-1}	2.40×10^{-3}	95.2	95.3	1.00
0.40	8.59×10^{1}	1.47	1.37	3.07×10^{-2}	98.3	98.4	1.00
0.482	1.61×10^{4}	1.32×10^{2}	1.35×10^{6}	5.72×10^{3}	99.2	-82.90	-83.5
0.50	2.05×10^{3}	1.46×10^{1}	2.84×10^{1}	1.36×10^{-1}	99.3	98.6	0.993
0.60	1.69×10^{2}	6.07×10^{-1}	7.20×10^{-1}	6.36×10^{-3}	99.6	99.6	0.999
0.70	1.03×10^{2}	2.32×10^{-1}	2.61×10^{-1}	3.81×10^{-3}	99.8	99.7	1.00
0.80	9.38×10^{1}	1.60×10^{-1}	1.76×10^{-1}	4.17×10^{-3}	99.8	99.8	1.00
0.90	1.01×10^{2}	1.51×10^{-1}	1.64×10^{-1}	7.92×10^{-3}	99.9	99.8	1.00

Resistances and Efficiencies for Loop and Loop with Spherical Cap, $\beta_0 c = 1.0$, $a/c = 0.005$, $p_w = p_s = 2.1\times10^{10}$.

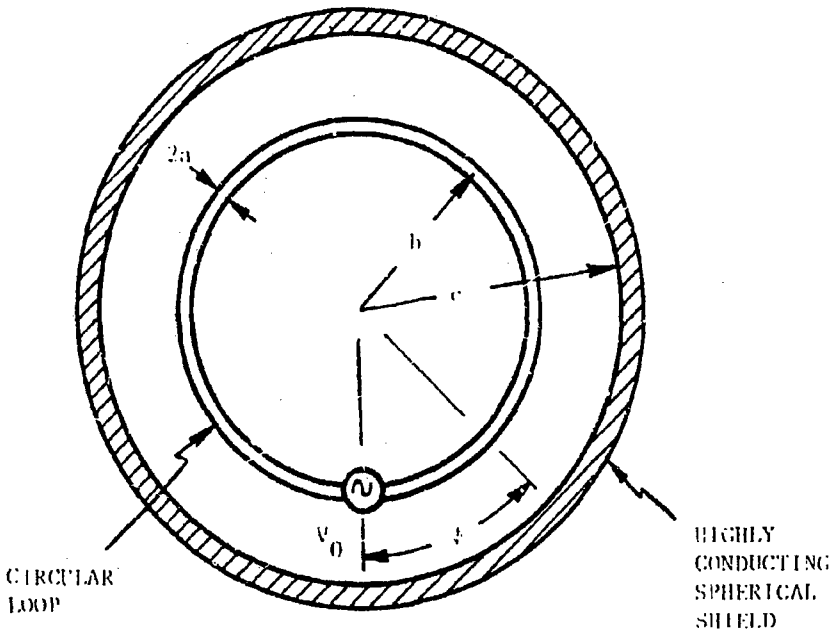

FIGURE 1. CIRCULAR-LOOP ANTENNA
WITH SPHERICAL RADIATION SHIELD.

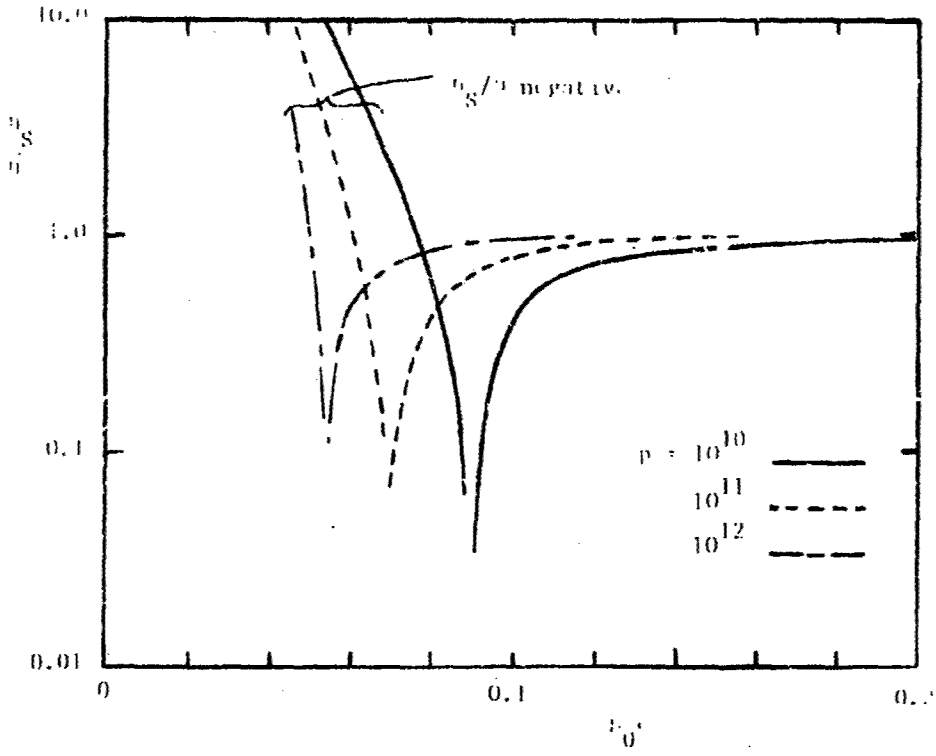

FIGURE 3. THE EFFICIENCY RATIO η_S/η AS A FUNCTION OF THE RADIUS OF THE SHIELD a^*. $F_0 b = 0.04$, $\alpha = 0.05$.

A REVIEW OF INDUCTIVELY LOADED ANTENNAS

by

R. C. HANSEN
Consulting Engineer
Tarzana, California 91356

ABSTRACT

A review of inductively loaded short whip antennas is given, starting with the 1944 measurements of Bulgerin and Walters. Several empirical and approximate theories will be described. The moment method solution for discrete loading will then be covered with a discussion of the tradeoff of input resistance versus efficiency, efficiency transition point, bandwidth, and cryogenics. Distributed loading and supergain effects will also be included.

A Review of Inductively Loaded Antennas

It has been known for some time that the efficiency is improved when the tuning coil is moved from the monopole base (feed point) and located in series with the monopole itself. The coil is then called a loading coil. One of the early papers is by Belrose [1], who analyzes the antenna as a transmission line. Although this analysis is only approximate, the trends are correct. Early experimental work was by Bulgerin and Walters [2] who measured a series of fat monopoles at 100 mhz. Gap problems at the loading coil position and relatively low Q coils have limited the usefulness of these data. Harrison [3]-[5] analyzed the loaded dipole using super-position of asymmetrically excited dipoles. Only a zero order solution is available for the asymmetrically excited dipole [6], and this becomes less accurate as the feed point moves toward the end. Harrison's results show a gradual increase in efficiency as the loading point moved closer to the dipole ends; his data essentially stopped at the 2/3 load point, i.e., the loading coil located 2/3 of the distance from feed to end. Czerwinski [7], [8] measured monopoles constructed of a helix of small diameter and tapered pitch. This distributed inductance is less advantageous than a discrete load for narrow-band operation. Lin, et al [9] showed that loading past resonance can produce current reversals along the antenna with modest directivity increase and sharper patterns. Along with this modest supergain as one would expect goes a decreased bandwidth.

The loading inductor functions by keeping the current distribution nearly constant from the feed to the load point, with a nearly linear decrease from the load to the end. Since a short monopole has a "triangular" current distribution, the loading increases the current moment, and the closer the load point to the end, the larger the increase in current moment. The transmitting parameter, radiation resistance, varies as current moment squared, and the receiving parameter, effective length, varies as current moment; so inductive loading is clearly advantageous. For a given monopole and load point, the value of loading reactance that most closely approximates the "constant plus linear" current distribution is not quite sufficient to produce input impedance resonance. The load value for resonance produces a modest current peak just beyond the load point; the current moment is increased over that of the "triangular" distribution by more than predicted by the "constant plus linear" model [10]. As the load point moves toward the monopole end, the resonant loading reactance value increases rapidly as the load point approaches the end. Since the radiation resistance is increasing more slowly, the efficiency must peak, unlike the calculated results of Harrison referred to earlier.

Ref. [10] gives an accurate solution to the inductive loading trade-off for thin antennas using moment methods. Results are also given for a flat wire ($\Omega = 50$) although the accuracy is marginal for that case. However, almost all practical antennas that could be loaded are thin.

The ratio of distance between feed and load point to whip length (or monopole length) is called γ. Data were calculated for loading points of 0.1, 0.2, 0.3, 0.4, and 0.5. Figs. 1 to 3 show the resistance components versus the variation of γ. From these figures it is clear that a significant part of the input resistance is due to loading coil losses, especially for very short monopoles. The input resistance is the sum of an enhanced radiation resistance over coil loss resistance. The latter is not exactly the coil resistance as the current at the load point is not exactly equal to the feed current. A radiation resistance improvement factor β is defined as the ratio of loaded to unloaded value, and is shown in Fig. 4.

Fig. 5 shows efficiency η versus load point γ. Since loading coil loss is usually very much larger than monopole heat loss, the infinite Q curves have efficiency of unity. Ferrite cores with permeabilities of the order of 15 allow coil Q's as high as 300 at VHF, while higher permeability cores typically allow Q's of 100-200 at HF. Monopole lengths above 0.15λ are seldom loaded as their radiation resistance and bandwidth are more tractable. Of course, the latter monopoles have higher efficiency as there is less antenna resistance to offset. Maximum efficiency occurs for a loading point between 0.3 and 0.4 from the feed, although the efficiency varies slowly with load point. There is no appreciable variation of the maximum point with Q or with monopole length. Note that when the coil is located at the feed, the efficiency is always lower. Thus for maximum efficiency the inductive load should be located at roughly 0.4. However, in most cases a small sacrifice in efficiency should be made to obtain a higher input resistance. Figs. 1-3 show the input resistance versus γ and the trade-off may be made between these figures and Fig. 5. Thus these figures allow the important tradeoff between efficiency and input resistance to be made. With a given type of impedance matching network with its losses, and for a specific monopole, there will be a value of γ which will maximize the overall efficiency.

When a lossless loading coil is used, the bandwidth is essentially undamped. This occurs even though the radiation resistance is substantially increased. Table I shows these parameters for a monopole of $h/\lambda = 0.1$, $h/a = 500$, and $\gamma = 2/3$. The fractional bandwidth then is approximately the inverse of overall Q. Using real loading coils of course introduces loss, and this loss will improve the bandwidth at the expense of efficiency. Table I also shows parameters for coil Q of 300 and 100. The fractional bandwidth with coil losses is approximately equal to the bandwidth without coil losses plus $1/Q_{coil}$. The interesting conclusion then is that bandwidth is improved by inductive loading only through the loading coil loss.

The effect of inductive loading on S/N has been investigated by Ramsdale [11].

The ratio of S/N with and without loading is:

$$\frac{S/N\ (\beta)}{S/N\ (\alpha)} \qquad \beta \frac{R_L + R_r T_r T_s}{\beta R_L + \alpha R_r T_r T_s}$$

where R_L and R_r are radiation and coil loss at the feed; T_s and T_r are sky temperature and coil loss, K. When $T_s \gg T_r$ the S/N is independent of loading. However, when $T_s \lesssim T_r$, the result becomes:

$$\frac{S/N\ (\beta)}{S/N\ (\alpha)} \qquad \frac{\beta}{\alpha}$$

This is shown in Fig. 6. Generally for frequencies below 100 mhz, $T_s > 290$ deg. K and so the S/N is not affected by loading.

Conclusions:

Maximum efficiency occurs essentially independent of dipole length and fatness at a load point roughly 0.4 from the feed. The efficiency varies slowly with load point. Radiation and input resistance both increase as the load point moves toward the monopole end. Current rises from the feed value to a modest peak at the load point and then decays, allowing radiation resistance improvement over an unloaded monopole by a factor as large as 4. A compromise load point may be chosen to give an input resistance closer to 50 Ω than the maximum efficiency loading would yield, at some loss in efficiency. Bandwidth with loading is essentially unchanged; loading coil loss increases bandwidth. S/N is generally not affected by loading.

TABLE I

Efficiency and Bandwidth versus Loading at Center Frequency
h/λ = 0.1, h/a = 500

		R	Bandwidth %
no load		3.91	.81
load, Q =	∞	10.85	.81
load, Q =	800	11.95	1.09
load, Q =	100	23.2	1.70

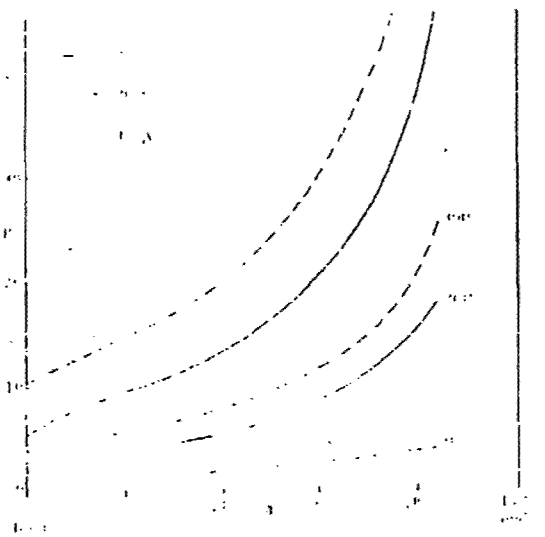

Fig. 1 Input resistance versus loading point.

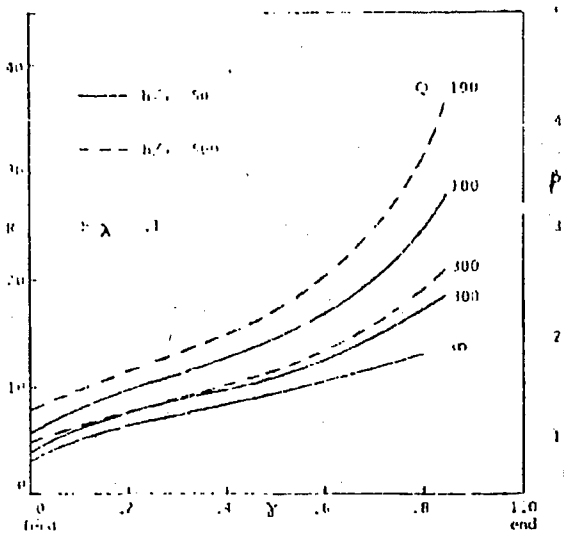

Fig 2. Input resistance versus loading point.

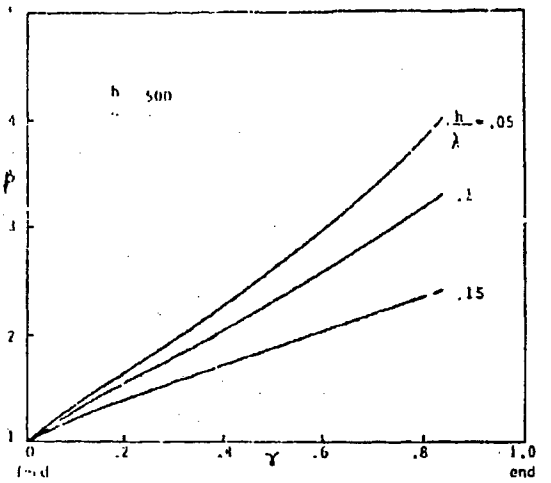

Fig. 4. Radiation resistance improvement factor.

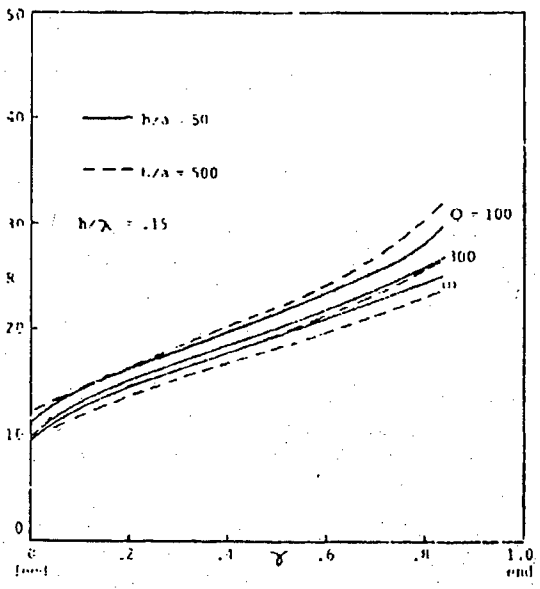

Fig. 3. Input resistance versus loading point.

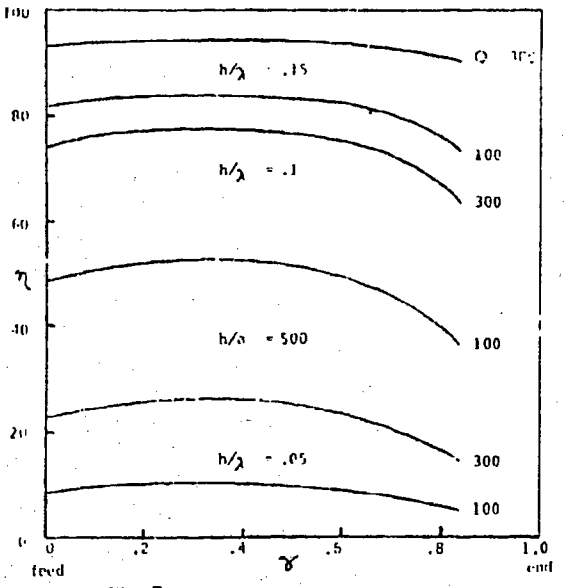

Fig. 5. Efficiency versus loading point.

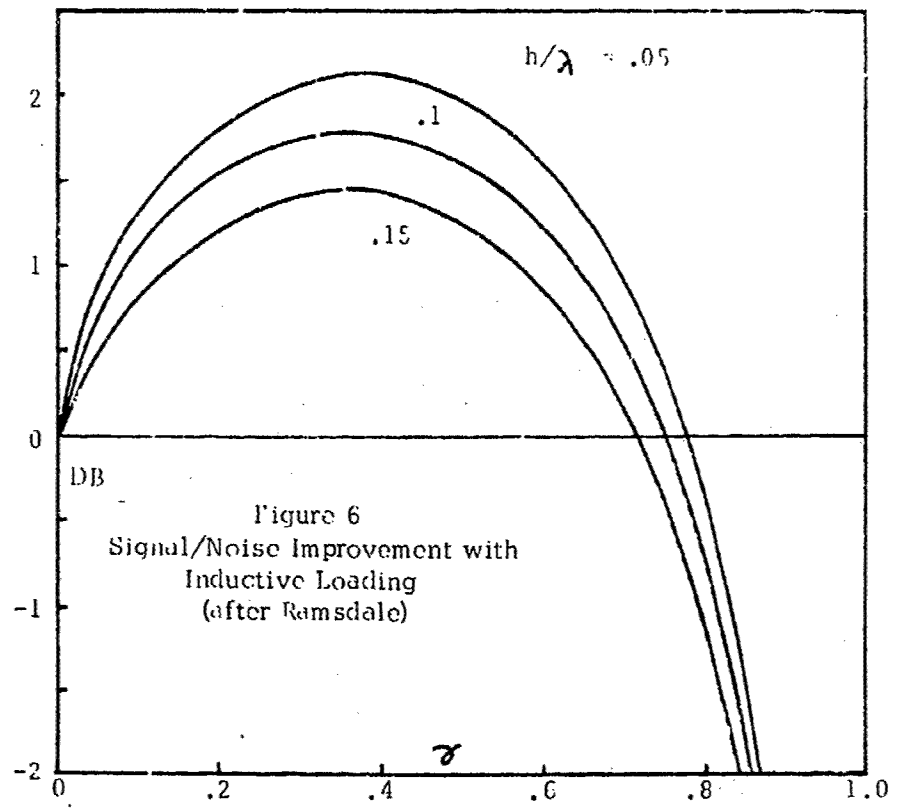

Figure 6
Signal/Noise Improvement with
Inductive Loading
(after Ramsdale)

References

[1] J. S. Belrose, "Short Antennas for Mobile Operation," QST, Sept. 1953, pp. 30-35, 108.

[2] M. A. Bulgerin and A. B. Walters, NOLC Rept. 154, pp. 67-83, 1954.

[3] C. W. Harrison, "Monopole with Inductive Loading," IEEE Trans., Vol. AP-11, pp. 394-400, July 1963.

[4] ———, "Monopole with Inductive Loading," Sandia Corp., Rept. SCR-590, Nov. 1962.

[5] K. Fujimoto, "A Loaded Antenna System Applied to VHF Portable Communication Equipment," IEEE Trans., Vol. VT-17, pp. 6-12, Oct. 1968.

[6] R.W.P. King, The Theory of Linear Antennas, Cambridge, Mass., Harvard Univ. Press, 1956, Chap. III, 29.

[7] W. P. Czerwinski, "On Optimizing Efficiency and Bandwidth of Inductively Loaded Antennas," IEEE Trans., Vol. AP-13, pp. 811-812, Sept. 1965.

[8] ———, "On a Foreshortened Center-Fed Whip Antenna," IEEE Trans., Vol. VC-15, pp. 33-39, Oct. 1966.

[9] C. J. Lin, D. P. Nyquist, and K. M. Chen, "Short Cylindrical Antennas with Enhanced Radiation or High Directivity," IEEE Trans., Vol. AP-18, pp. 576-580, July 1970.

[10] R. C. Hansen, "Efficiency and Matching Tradeoffs for Inductively Loaded Short Antennas," IEEE Trans., Vol. COM-23, pp. 430-435, Apr. 1975.

[11] P. A. Ramsdale, "Signal/Noise Ratio of Inductive-Loaded Antennas," Electr. Ltrs., Vol. 11, No. 24, Nov. 27, 1975, pp. 590-591.

A LOW PROFILE REMOTE-TUNED DIPOLE ANTENNA FOR THE 30 to 80 MHz RANGE

D. V. CAMPBELL
Communications/Automatic Data Processing Laboratory
U. S. Army Electronics Command, Fort Monmouth, New Jersey 07703

ABSTRACT

Tactical FM communications systems make extensive use of the VHF frequency range 30-80 MHz. Efficient VHF antennas for command posts and vehicles are of resonant length and, therefore, large. Low profile monopole VHF antennas fed against ground planes have been studied in the past. The antenna discussed here, in contrast, consists of a low profile center-fed dipole approximately one meter in length. This dipole requires no ground plane, and, in addition, achieves a high efficiency-to-size ratio.

1. INTRODUCTION

Tactical communications systems employ the VHF frequency range 30 to 80 MHz. Resonant length VHF antennas are large. The antenna discussed here is only one-tenth of a wavelength long. A high efficiency-to-size ratio has been achieved.

2. SHORT CENTER FED DIPOLE ANTENNA

Low profile monopole antennas have been studied extensively in the past [1], [2]. Monopoles require a large ground plane or vehicle body for their operation. The antenna investigated here consists, instead, of a short (0.1 wavelength) center-fed dipole and requires no ground plane. Because the bulky ground plane is eliminated, it can easily be deployed in difficult environments, for example, in trees.

A. Configuration of Antenna

The essential features of the dipole are shown in Fig. 1. The radiator is center-fed. The capacitive reactance of the dipole is cancelled by the combination of fixed inductance and variable capacitance connected in series with the feedpoint.

B. Antenna Tuner

A combined coarse- and fine-tuning system is employed to resonate the antenna. Fixed low loss inductors are switched into the antenna circuit in series with the variable (fine tuning) capacitor. With proper dimensioning of the inductors, overlapping frequency bands (sub-bands) are obtained. When the tuning capacitor is set at maximum, C_{max}, the resonance frequency is:

$$f_1 = \frac{1}{2\pi} \sqrt{\frac{1}{L}\left(\frac{1}{C_A} + \frac{1}{C_{max}}\right)}$$

and when the tuning capacitor is set at minimum, C_{min}, the resonance frequency is:

$$f_u = \frac{1}{2\pi} \sqrt{\frac{1}{L}\left(\frac{1}{C_A} + \frac{1}{C_{min}}\right)} ,$$

where L is the inductance and C_A the antenna "capacitance." For example, if C_A, C_{min}, and C_{max} are 5-, 8-, and 100-pF, respectively, then $f_u/f_l = 1.24$. If six sub-bands (N = 6) are used to tune the antenna from 30 to 80 MHz, the required range in each sub-band is:

$$f_u/f_l = (f_{max}/f_{min})^{1/N} = 1.177.$$

Thus the first band would extend from 30 to 35.33 MHz; the second band from 35.33 to 41.6 MHz, and so on.

C. Cable Choke

The feedline is connected to the lower end of the dipole through a cable choke [3], [4] consisting of coaxial cable formed into a coil or toroid. This cable choke provides a high impedance between the end of the dipole and the feedline. The internal transmission properties of the feedline are not affected by the cable choke.

Because the cable choke is directly connected to the end of the dipole, it significantly affects the current distribution and efficiency. Ideally, the cable choke should act as an insulator. Actually, the cable choke behaves more or less as a parallel LC tank circuit connected between the end of the dipole and the feedline.

3. THEORETICAL ANALYSIS

The theory presented here is based on Harrison [2], who analyzed the electrically short isolated center-driven dipole antenna with symmetric impedance loading, and its monopole equivalent. Although his analysis involves approximations, it is nevertheless very clear, and permits inductively loaded monopoles to be designed with engineering accuracy.

The antenna studied here is shown in Fig. 2A. Our case differs from Harrison's in that the feed- and loading points are interchanged. The figure shows the center-fed dipole with the cable choke at its base above an infinite, perfectly conducting ground plane. The equivalent isolated dipole is shown in Fig. 2B. The dipole is driven at two points located at $z = \pm h_2$, is loaded at its midpoint $z = 0$ by the cable choke (denoted by impedance $2Z_c$), and has the total length $2h_1$.

The structure shown in Fig. 2A approximates the case where the dipole is mounted on a ground plane or vehicle. This model is useful for efficiency considerations

The antennas of Fig. 2 can be analyzed by following a procedure similar to Harrison's. We find that the feedpoint impedance, Z, and the voltage across the cable choke, V_c, are respectively:

$$\frac{Z(G_1 + h_c) + Z(G_1 - h_c)}{\ldots}$$

$$1 + \ldots(G_1 + h_c, 2h_c) - Z(h_1, h_c) + (G_1 + h_c, n) \frac{\ldots}{Z_c + \ldots(h_1)}$$

$$\ldots =$$

$$\frac{V_c}{V} = \frac{Z(G_1 + h_c, h_c)}{\ldots} \cdot \frac{\ldots(G_1) \ldots}{\ldots}$$

$$\ldots(h_1 + \ldots) + Z(h_1 - h_c) \quad \ldots(h_1) + Z_c$$

The impedances $Z(\ )$ and the complex distribution functions $I(\ )$ are given in [2].

4. THEORETICAL EFFICIENCY OF THE VERTICAL DIPOLE ABOVE A GROUND PLANE

The formula given above and in [2] have been used to determine theoretically the efficiency of the low profile resonated dipole when installed above a ground plane. Calculations have been made using dimensions approximating the antenna when operating at ... MHz ($2h_1$ ... and H_c ...). In Table 1, the calculated results are given for several different cable lengths.

... efficiency, of course, is dependent on the electrical properties of the ... For example, the ... is ... higher (lower) when ... is capacitive (see, Table 1). This tendency can be understood by a circuit that the current may ... between the choke and the feedpoint when the choke is inductive.

The theoretical efficiency is believed to be somewhat ... of the approximations used in deriving the current distribution of the symmetrical dipole [2]. The actual efficiency is probably somewhat less than the theory predicts.

5. EXPERIMENTAL RESULTS

The experimental antenna incorporates a center-fed radiating element ... long; highly, resonating inductors; bandswitch; variable tuning capacitor; and broadband cable choke. Tuning and bandswitching are remotely controlled.

A. Tuning Characteristics

The antenna can be resonated between 30 and 80 MHz in seven overlapping subbands. At most frequencies, the voltage standing wave ratio (VSWR) is three or less when the antenna is resonated.

5. Relative Efficiency

The low profile dipole was been compared to the standard AS [illegible]/VRC centered whip antenna, which is approximately 5 meters long and is assumed to have nearly unity gain. The antennas were installed above a 2-meter square ground plane, fed equal power, and the field intensity measured. The measured relative efficiency was -6 dB, or approximately 25% at 50 MHz (see Fig. 5), which is smaller than the theoretical efficiency. The actual efficiency was probably at least 30%.

6. SUMMARY

An electrically short center-fed dipole antenna for 30 to 80 MHz has been discussed. The impedance and efficiency when mounted above a ground plane has been determined both theoretically and experimentally. The antenna is portable and can be easily deployed since a ground plane is not required.

REFERENCES

[1] J. [illegible]. Belrose, "Short antennas for mobile operation," *QST*, The American Radio Relay League, Inc., West Hartford, Connecticut, Sept. 1 [illegible].

[2] C. W. Harrison, Jr., "Monopole with inductive loading," *IEEE Transactions on Antennas and Propagation*, vol. AP-11, July 1963, pp. 394-400.

[3] [illegible]. T. Harper, "Broadband cable chokes," *IEEE Proc., Int'l. Electronics Conference*, pp. 144-151.

[4] Wesnow Smith, *Antenna Manual*, Santa Barbara, California: Editors and Engineers, LTD., 1948, p. 230.

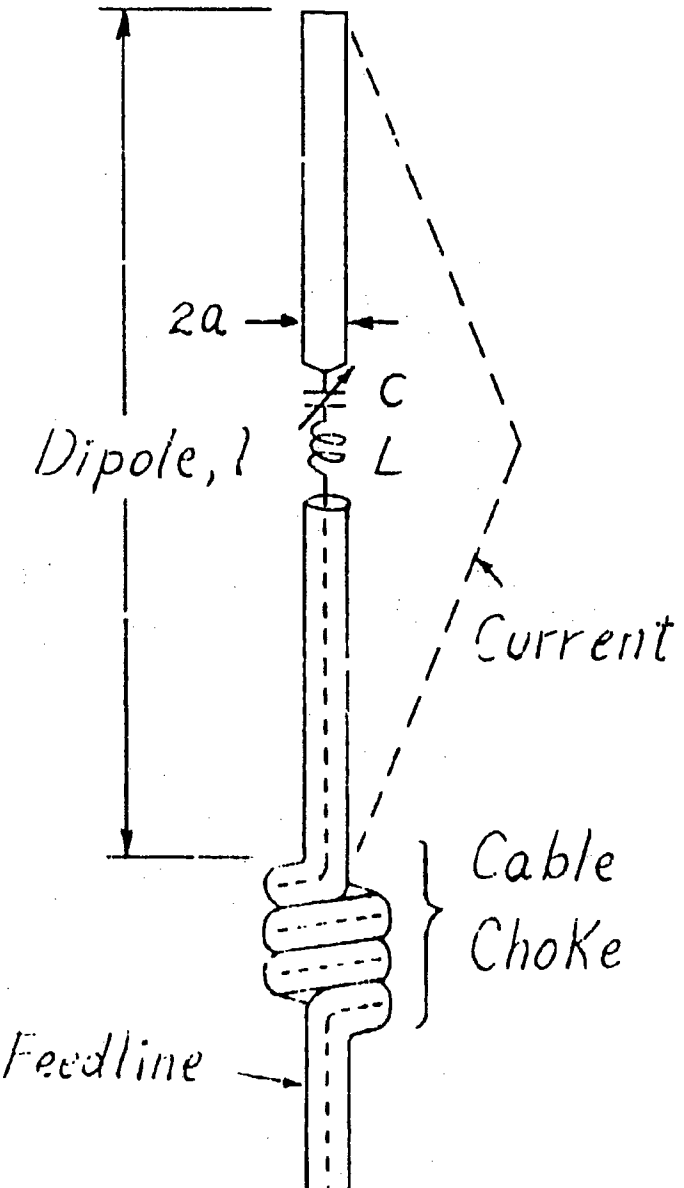

Fig. 1

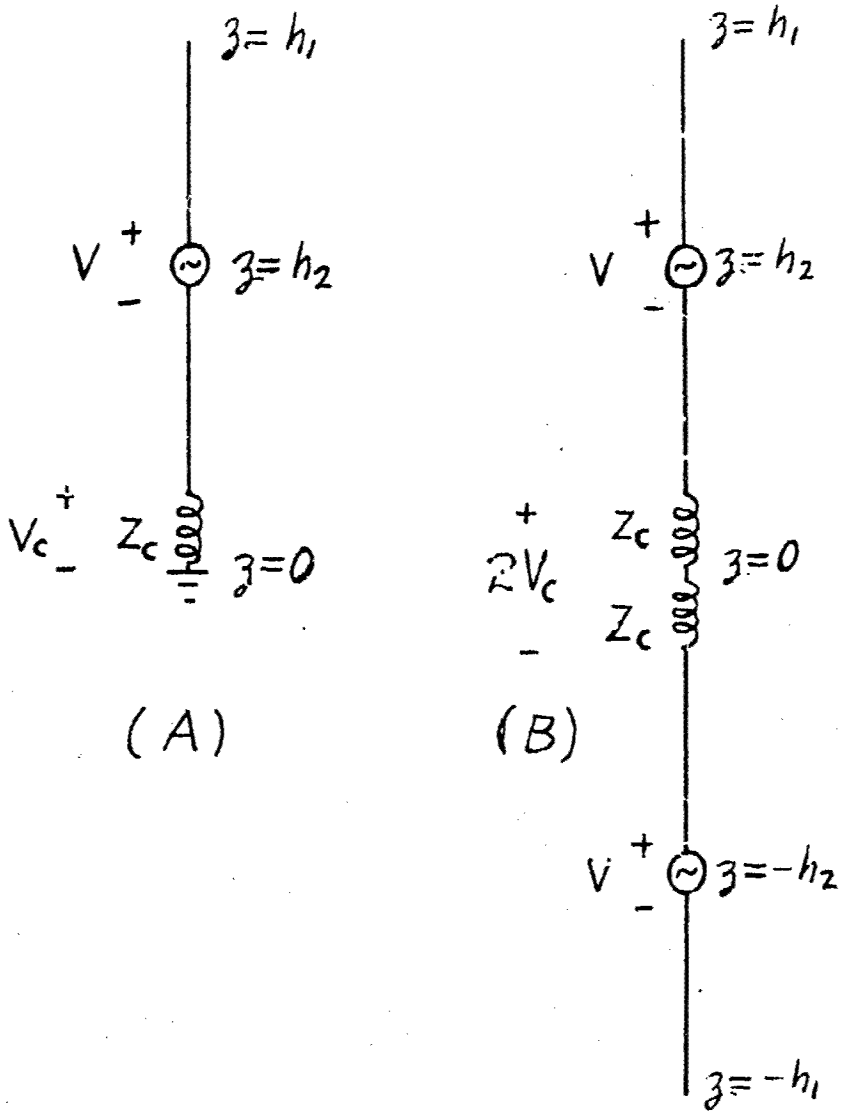

Fig. 2

TABLE 1.

(Data refers to antenna dimensions shown in figure below.)

Z_c (Ω)	Z (Ω)	$\lvert V_c/V \rvert$	Z_T (Ω)	R_{RAD} (Ω)	EFF. (%)
113.6 - j5302	10.48 - j1467	0.5505	4.89 + j1467	7.85	51
113.6 + j5302	11.8 - j1777	0.639	5.92 + j1777	6.59	37.3
0 - j5302	8.12 - j1467	--	4.87 + j1467	8.12	62.4
0 + j5302	7.13 - j1777	--	4.89 + j1777	7.13	59.3
∞	7.72 - j1596	--	5.32 + j1596	7.72	59.2
0 + j0	10.25 - j705	0	2.35 + j 705	10.25	61.3

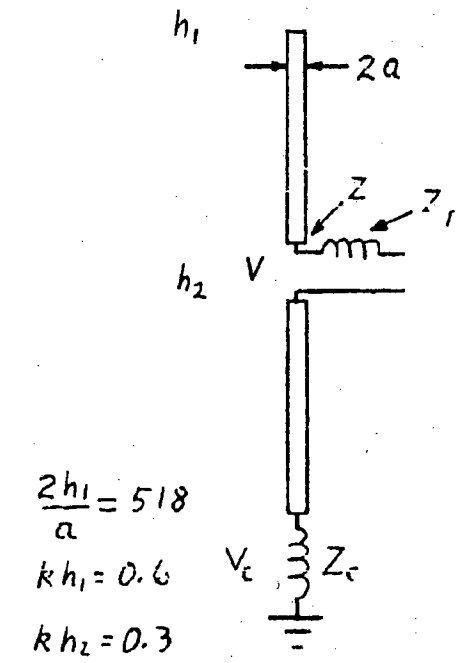

$\frac{2h_1}{a} = 518$

$kh_1 = 0.6$

$kh_2 = 0.3$

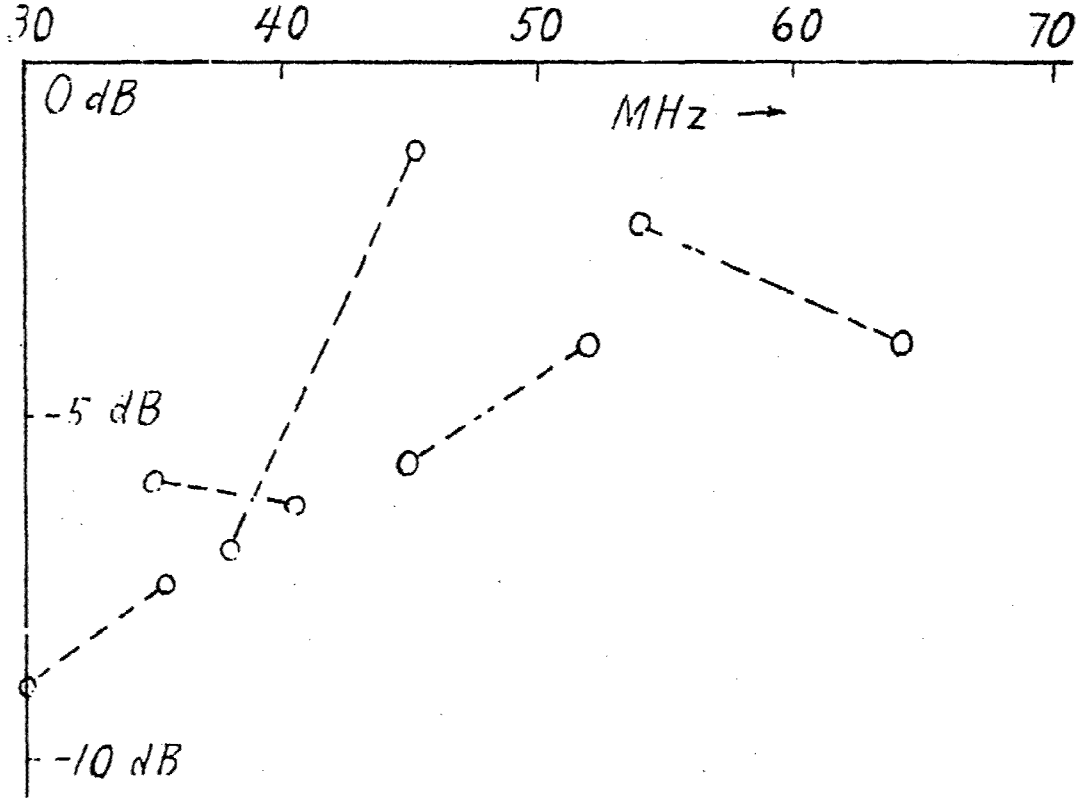

Fig. 3

MULTI-ELEMENT MONOPOLE ANTENNAS

G. GOUBAU

ABSTRACT

The antennas discussed in this paper are assemblies of closely spaced short monopoles with top capacitors and inductive interconnections. They radiate like ordinary monopole antennas, but can be designed to have bandwidths exceeding 1:2.

The antennas discussed in this paper can be derived from a short thick monopole with top capacitor as shown in Fig. 1. The thick conductor is replaced by a number of thin conductors, and the top capacitor divided into a corresponding number of segments, one connected to each of these conductors as illustrated in Fig. 2. In this manner one obtains an assembly of closely-spaced monopoles which are fed by a common source. If all these sub-monopoles are alike and symmetrically arranged, they can be interconnected at the top by inductances, as indicated by the loops in Fig. 2, without affecting the electric properties of the assembly. This means the structure of Fig. 2 behaves like the single monopole of Fig. 1.

Now assume that the interconnections of the sub-monopoles near the ground plane are removed, and all the sub-monopoles excited by individual sources of the same frequency as illustrated in Fig. 3. Then, the structure represents a radiating N-port network, where N is the number of sub-monopoles. The relation between the currents I_n in the sub-monopoles and the voltages V_n at the input terminals can be formulated by an admittance matrix:

$$I_n = \sum_{m=1}^{N} Y_{nm} V_m \; ; \qquad Y_{nm} = Y_{mn} \; . \qquad (1)$$

The coefficients Y_{nm} of this admittance matrix depend not only on the dimensions of the sub-monopoles and their spatial arrangement, but also on the interconnecting inductances.

The radiation along the ground plane is determined by the total current, i.e. the sum of the currents in the sub-monopoles:

$$I = \sum_{n=1}^{N} I_n = \sum_{n=1}^{N} \sum_{m=1}^{N} Y_{nm} V_m \; . \qquad (2)$$

If all the sub-monopoles are alike and arranged symmetrically, so that each sub-monopole behaves identically within the assembly

$$\sum_{n=1}^{N} Y_{nn} - \sum_{m=1}^{N} Y_{mn} = \text{const.} = Y_N \quad , \tag{3}$$

thus the total current

$$I = Y_N \sum_{m=1}^{N} V_m \quad . \tag{4}$$

If $\sum_{m=1}^{N} V_m = 0$, there is no radiation along the ground plane.

In the case where all sub-monopoles are interconnected at the base (Fig. 2), all voltages V_n are the same (V) and

$$I = NY_N V = YV \quad , \tag{5}$$

where Y is the input admittance of the assembly when operated as a single monopole.

We now consider the case where only one of the sub monopoles, say No. 1, is connected to the power source ($V_1 = V$), while all the others are grounded, as shown in Fig. 3. This state of excitation can be considered as the superposition of two excitations:

$$V_m = V'_m + V''_m,$$

$$\text{where: } V'_1 = V'_2 = \cdots = V'_N = V'$$

$$\text{and } \sum_{m=1}^{N} V''_m = 0.$$

Then,

$$V''_n = V' \quad \text{for} \quad n \neq 1 \quad , \tag{6}$$

$$V''_1 = V'' = V''_2 = \cdots = V''_N = (N-1)V' \quad , \tag{7}$$

$$V_1 = \quad + V_1'' \quad \ldots \quad (5)$$

The currents associated with these excitations are respectively I_m' and I_m''.

The currents I_m' are the same ($I_m' = I/2$) and independent of the coupling mode between the subassemblies. Using Eq. (5) with $V_1 = V_1'$ and eliminating V_1' with Eq. (6), one obtains

$$I_m' = I/2 \quad VV'/2 \quad VV/2^2 \quad . \quad (9)$$

The currents I_m'' differ and depend on the coupling mode chosen which is to be chosen[11] so that I_1'' is zero at one particular frequency. Then, for this frequency, the input current of the system is

$$I = VV/N^2 \quad . \quad (10)$$

Therefore the input impedance is N^2 times the input impedance of the system when all the subassemblies are interconnected at the base (Fig. 1). The effective radiation resistance is thus increased by the factor N^2 or the effective height of the antenna by the factor N.

Figure 5 shows the VSWR of such an antenna whose physical height is one-half of a free-space wavelength. A monopole of the same height would have a radiation resistance of about 8 ohms. Thus N = 5, and the antenna is matched by a factor of 25 to the 50-ohm coaxial feed cable.

The fact that the effective height of an antenna can be increased by using additional elements is, of course, not new. The most common use is the folded monopole, where antennas have two elements connected at the top and fed at the bottom. The present concept of the same height

One of the attractive features of the antenna described here is that it can be used for very wide frequency bands as a plane monopole. To suppress excitation of horizontal mode caused by the currents in the adjacent plates, the feed line could be a three-conductor transmission line with two conductors connected to adjacent plates and one with three conductors and shorts for adjacent plates. [illegible] of the monopole, the spacing between plates at the [illegible] is made smaller than a quarter wavelength at the highest frequency of operation. This antenna is not really [illegible] but it is [illegible] and, because it is [illegible] the [illegible] is made comparable [illegible]

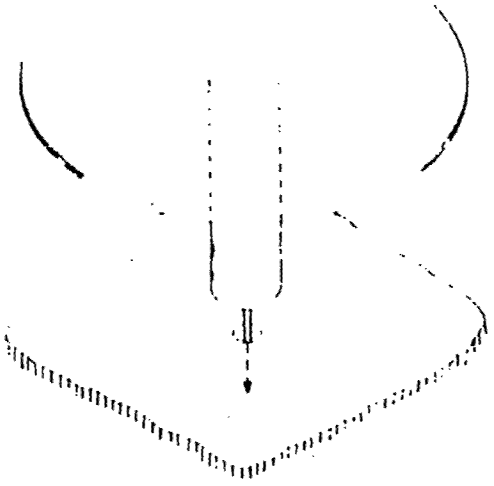

Fig. 1. Monopole with top capacitor.

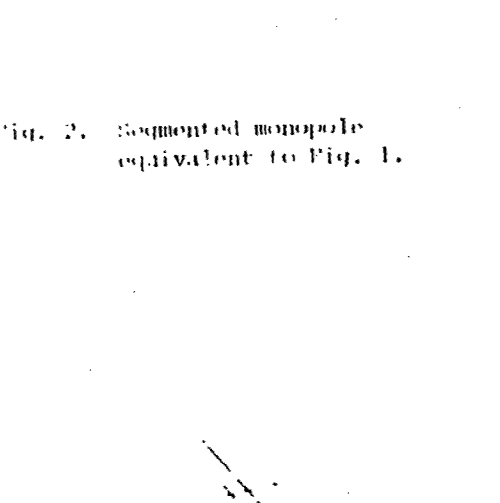

Fig. 2. Segmented monopole equivalent to Fig. 1.

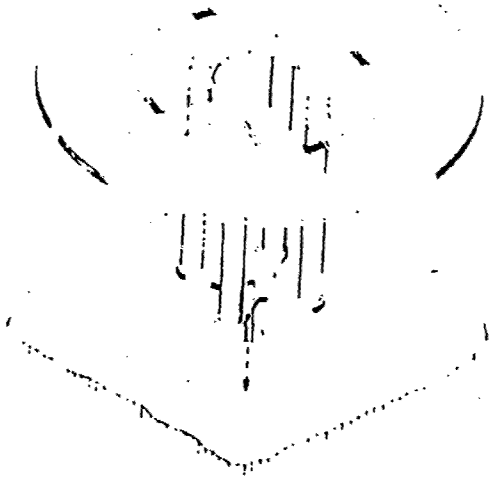

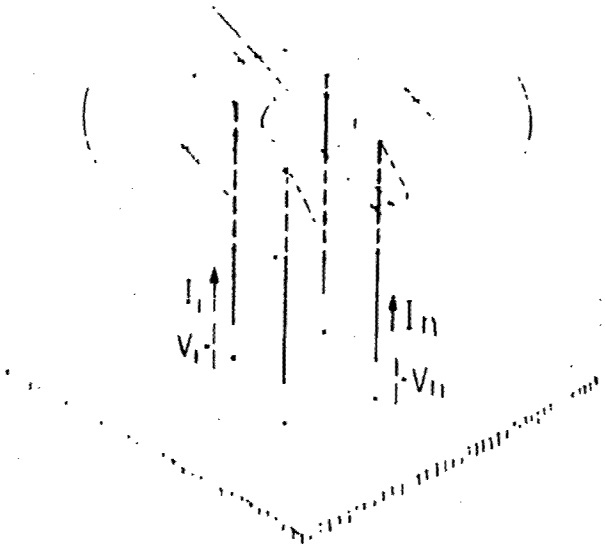

Fig. 3. Multi element monopole as an N port network.

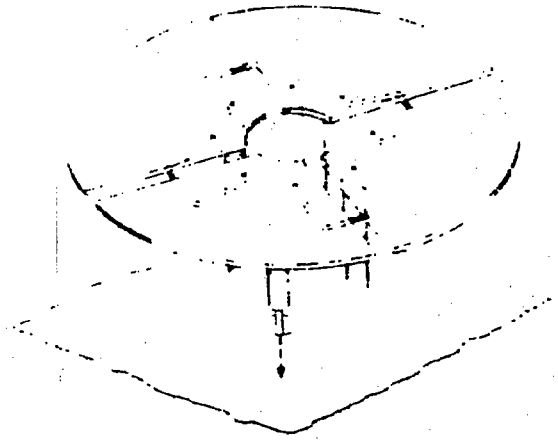

Fig. 4. Antenna with 4 identical symmetrically arranged sub-monopoles.

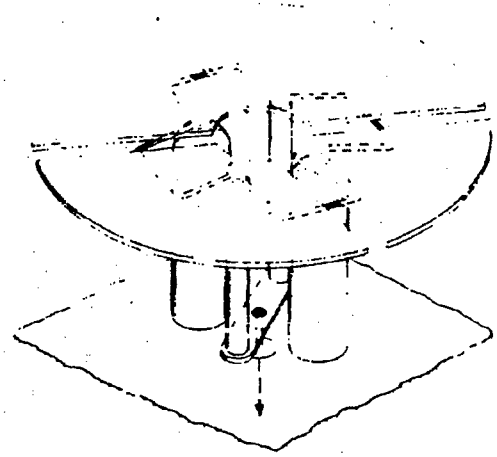

Fig. 6. Broad-band multi-element monopole antenna.

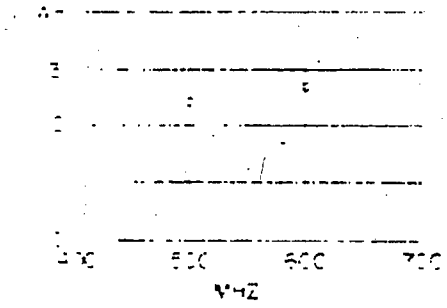

Fig. 5. Measured VSWR of an antenna of the kind of Fig. 4.

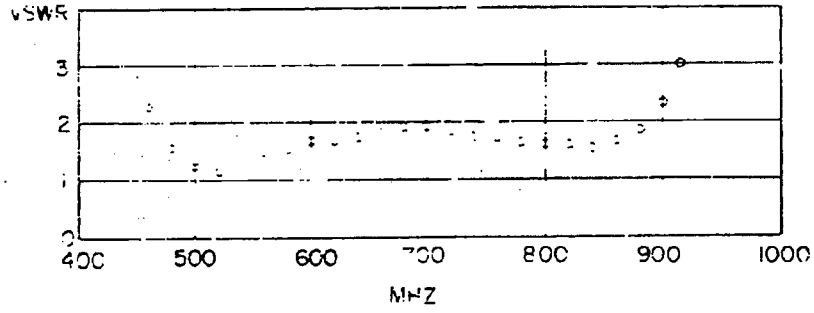

Fig. 7. Measured VSWR of the antenna of Fig. 6. Antenna height: 4.3 cm; diameter of capacitor plate: 12.3 cm.

AN EXPERIMENTAL AND THEORETICAL INVESTIGATION OF THE CIRCULAR DISC, PRINTED CIRCUIT ANTENNA

Stuart A. Long and Liang C. Shen
Department of Electrical Engineering
University of Houston
Houston, Texas 77004

Abstract

A circular conducting disc over a ground plane is investigated as a low-profile antenna. The input impedance and radiation pattern are measured as a function of frequency and the thickness of the antenna. An approximate theoretical solution is also derived.

Introduction

The broad class of printed circuit antennas consists of various shapes of flat radiators parallel to and very near a large ground plane. Most practical examples are etched on one side of a microwave printed circuit board and therefore a dielectric fills the region between the radiator and the ground plane. Such a structure can be made to radiate relatively efficiently in a direction normal to the ground plane while remaining quite thin with respect to a wavelength. This low-profile characteristic along with its ruggedness and ease of fabrication have resulted in an increasing application of these antennas to a wide variety of differing systems [1,2,3].

Circular Disc Radiator

One particular printed circuit antenna, the circular disc radiator, was chosen for a systematic and careful experimental investigation. (See figure 1.) Using standard photo-etching techniques common to all printed circuit fabrication the circular disc could be made quite accurately. The radiators were designed to be resonant at 2.9 GHz by choosing their radius "a" such that $ka = 1.84$. This corresponds to resonance of the lowest order mode as determined by an analysis of the circular disc resonator. The antennas were fabricated on teflon-fiberglass ($\epsilon_r = 2.56$) printed circuit boards of four different thicknesses varying from 0.13 to 1.52 mm (0.0053 inch to 0.0599 inch). The circular disc was driven at its edge from the underside of the ground plane using a panel mounted coaxial feed. The magnitude of each component of the far field, was then measured as a function of θ, for various constant values of ϕ. Radiation patterns were taken for each of the four different thicknesses of the printed circuit board. In addition the driving point impedance was measured as a function of frequency for each thickness of the dielectric using a network analyzer.

Experimental Results

The radiation fields in the two major planes, L_θ for $\phi = 0$, and L_ϕ for $\phi = 90^0$ are shown in figure 2 as a function of the polar angle. The pattern is seemingly not dependent on the thickness "d" to any appreciable degree and patterns for the other thicknesses not shown reflect this same behavior. At the design frequency the patterns are seen to be quite broad in both principal

planes with a 3dB beam width of approximately 115° for E_θ and 90° for E_ϕ. It should be noted that in the plane of the antenna ($\theta = 90°$) the fields are inherently different. E_ϕ has a deep null in the plane but E_θ has only been reduced 20dB from the maximum. Each pattern begins to degrade slightly as the frequency is changed from the designed 2.9 GHz. The most apparent change is a dip in field strength of 4 to 5 dB at $\theta = 0$ for a change in frequency to 3.1 GHz. This of course represents a serious degradation and emphasizes the frequency dependent nature of the antenna. The real and imaginary parts of the complex input impedance are shown as function of frequency for each of the four thicknesses in figures 3 and 4. Here, the effect of the thickness on the impedance of the antenna is shown quite graphically. The value of "d" is seen to effect both the frequency for which the impedance is totally real and the value of the resistance at this point. The maximum resistance varies from only 27 ohms for the case of d = 0.13 mm to more than 350 ohms for d = 1.52 mm. The frequency at which this maximum resistance occurs coincides very closely with the point that the reactance crosses the axis. This "experimental resonance" position is seen to vary considerably for differing values of the thickness, but in all cases remains within a range of 10% below the design value of 2.9 GHz.

Model of Circular Disc, Printed Circuit Antenna

To permit a more detailed study of the circuit properties of the radiating structure a model of the actual printed circuit antenna was made of a thin circular plate separated from a ground plane by a slab of styrofoam as shown in figure 5. The use of styrofoam ($\epsilon_r = 1.02$) as the dielectric permits the circuit properties to be measured without the discontinuous dielectric layer present, as if all the area surrounding the radiator were air. In addition the model also allows the antenna to be driven at several points along a radius from the center of the disc to the outer edge. In this fashion the functional dependence of the impedance on the position of the feed point may also be found. The entire procedure can also be repeated with a different thickness of styrofoam to investigate the behavior of the circuit properties as a function of the spacing between the disc and ground plane. Alternatively a dielectric slab of the same thickness might be used to measure the dependence of the impedance on the dielectric constant.

Currents and Fields for the Circular Disc Resonator

The circular disc structure shown in figure 1 is equivalent to the parallel plate antenna shown in figure 6 if the ground plane is sufficiently large so that image theory can be applied and if the permittivity of the dielectric is approximately the same as that of the surrounding medium. The fields inside the parallel plate region and the currents on the disc have previously been found using an analysis of the resonance conditions in circular disc structures [4]. These results can then be used to investigate the radiation properties of the structure. To retain the desirable low-profile characteristics the thickness of the antenna, which is the separation distance "d" of the disc from the ground plane, must remain small compared to a wavelength. For this reason field configurations between the plates having only circumferential and radial variations but no variation in the z direction have been investigated. This is a reasonable assumption so long as the restriction $d < \lambda$ is retained. The components of the fields between the plates can be expressed in terms of a z directed electric Hertz vector, and these fields may then be used to calculate the surface cur-

rents on the circular disc. The radial component of the surface current and hence H_ϕ must vanish, however, at the edge of the disc. Thus for each mode configuration a particular radius can be found for resonance corresponding to zeros of the derivative of the Bessel function. The mode corresponding to n = 1 and ka = 1.84 has, for any given frequency, the minimum diameter, and is therefore the dominant mode. The field components for this mode can be found from the more general expressions, and the surface currents calculated.

$$E_z = E_o J_1 (kr) \cos \phi$$

$$H_r = \frac{-j\omega\varepsilon}{k^2 r} E_o J_1 (kr) \sin \phi$$

$$H_\phi = \frac{-j\omega\varepsilon}{k} E_o J_1' (kr) \cos \phi$$

$$K_\phi = \frac{j\omega\varepsilon}{k^2 r} E_o J_1 (kr) \sin \phi$$

$$K_r = \frac{-j\omega\varepsilon}{k} E_o J_1' (kr) \cos \phi$$

Calculation of the Far Fields

To find the radiation fields of this structure the vector potential may be calculated for the distribution of surface currents that have been previously derived. Using image theory, the plate a distance d above an infinite ground plane is equivalent to two discs a distance 2d apart. An effective array factor can be calculated to account for the two discs and the total far fields can then be found for the n = 1 mode for the cavity filled with air. An alternate approach to find the radiation fields is also possible. Instead of using the currents as the source, the fields at the aperture between the disc and the ground plane may be represented by equivalent magnetic surface currents and the far fields calculated from them. The following fields are found for the n = 1 mode with the cavity filled with air.

$$E_\theta = -jL_o \frac{e^{-jk_o r}}{r} a\, k_o d \cos \phi\, J_1 (k_o a)\, J_1' (k_o a \sin \theta)$$

$$E_\phi = jL_o \frac{e^{-jk_o r}}{r} d \sin \phi \frac{\cos \theta}{\sin \theta} J_1 (k_o a)\, J_1 (k_o a \sin \theta)$$

For our previous assumption of $d \ll \lambda_o$ or $k_o d \ll 1$ the fields found using the two methods are essentially equal. With the knowledge of the radiation fields the total radiated power and the directive gain can be calculated. Using the previously found current distribution the losses due to the finite conductivity of the disc and thus the efficiency can also be found.

Far Fields with a Dielectric

An approximation to the far fields can be made for the more usual case when a dielectric with a permittivity different from the surrounding free space separates the disc from the ground plane. The fields can be calculated as before using the equivalent magnetic current model if the dielectric outside the cavity is neglected. The fields inside will change as will the size of the disc necessary for resonance in the n = 1 mode. The new fields for the dominant mode are as follows.

$$E_\theta = -jL_o \frac{e^{-jk_o r}}{r} k_o a' d\, J_1 (ka') \cos \phi\, J_1' (k_o a' \sin \theta)$$

$$E_\phi = jE_o \frac{e^{-jk_o r}}{r} d\, J_1(ka') \frac{\cos\theta}{\sin\theta} \sin\phi\, J_1(k_o a' \sin\theta)$$

Note that $ka' = 1.84$ and $a' = a/\sqrt{\epsilon_r}$ which means that the physical size of the disc has been reduced. Using the same techniques as before the total radiated power can be found. It can also be shown that the power losses due to the finite conductivity will be exactly the same and is thus not dependent on the value of ϵ_r. In this case, however, there does exist the possibility of additional losses if the dielectric is not ideal. These losses can be found from the fields in the cavity and the efficiency once again calculated.

References

[1] R. L. Munson, "Conformal Microstrip Antennas and Microstrip Phased Arrays," IEEE Tran. Antennas and Propagation, AP-22, pp. 74-78, Jan. 74.

[2] J. Q. Howell, "Microstrip Antennas," IEEE Tran. Antennas and Propagation, AP-23, pp. 90-93, Jan. 75.

[3] G. H. Schnetzer, "Characteristics and Applications of Rectangular Microstrip Antennas," Report No. SAND75-0339, Sandia Laboratories, July 75.

[4] J. Watkins, "Circular Resonant Structures in Microstrip," Electronic Letters, Vol. 5, No. 21, Oct. 16, 69.

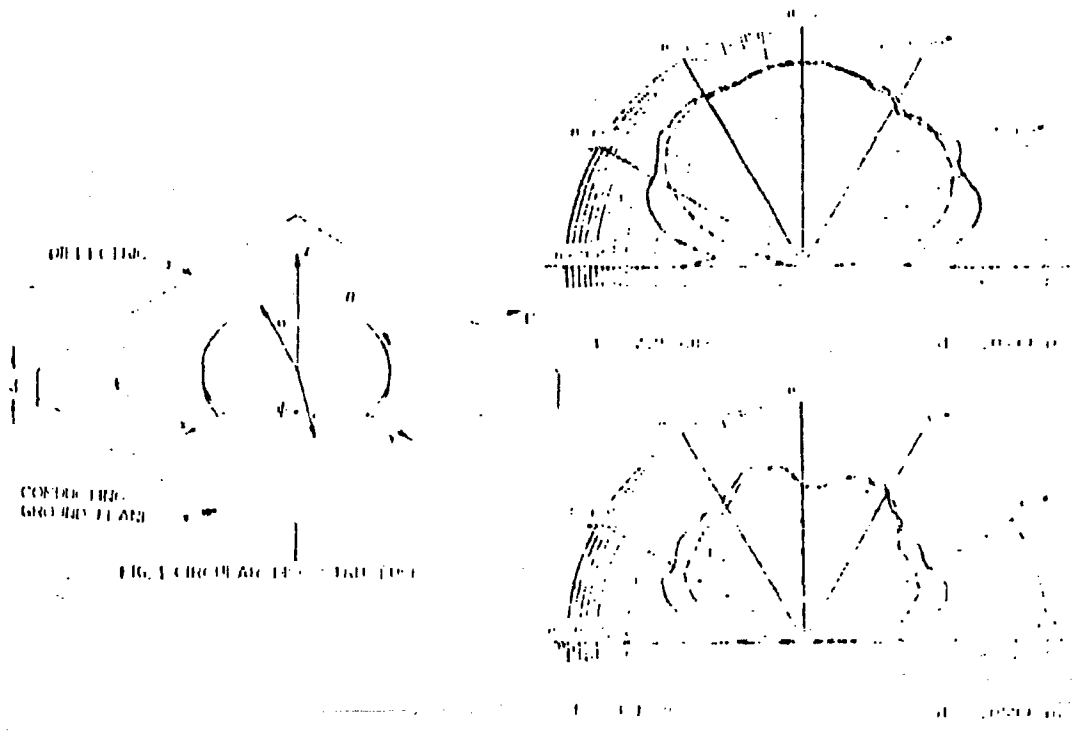

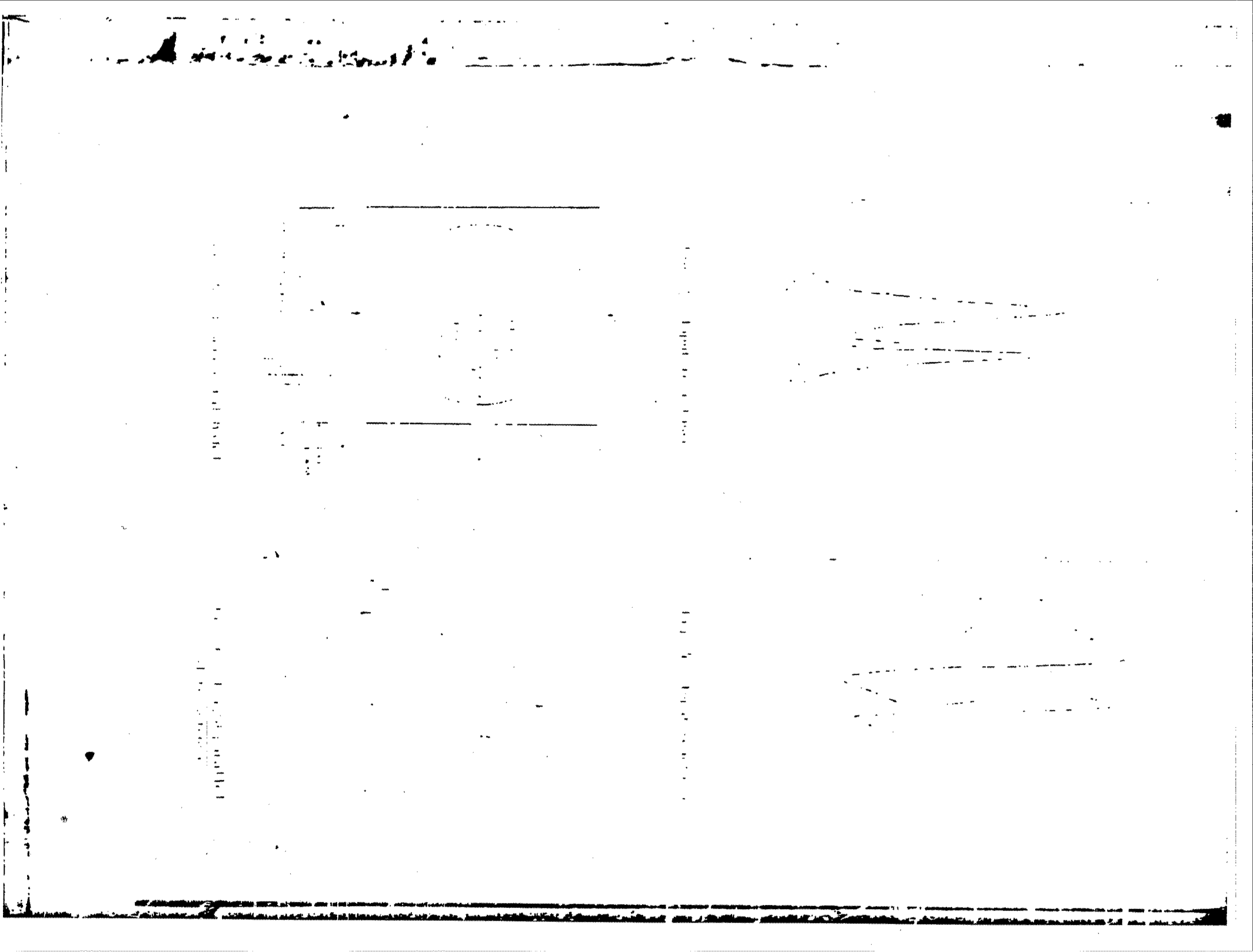

[illegible]

[illegible]
[illegible] Division
Applied [illegible] Laboratory
[illegible] Experiment Station
[illegible] Institute of Technology
Atlanta, Georgia [illegible]

[illegible] computer [illegible]. [illegible] theoretical pattern [illegible]

[illegible]

[illegible]

to achieve broad bandwidth with an aperture much smaller than the spirals. Figure 3 shows typical axial ratios for sum and difference patterns versus the angle off boresight. These pattern characteristics are generally good even when the antenna diameter is small. Figure 4 shows an interesting rippling effect of pattern axial ratio when the current ring is simulated by an array. Note the significant improvement of axial ratio one can obtain by increasing the number of array elements from 6 to 8.

Except for a lower radiation efficiency of the 3 mode, the decrease of the diameter of a current ring has not affect in theory the quality of the broadband monopulse RF patterns. However, the decrease of ring diameter imposes ever stringent tolerance requirements which are difficult to achieve at present. Figure 5 shows two conical patterns in the boresight region where serious rippling and nulling resulting from slight excitation errors of 2° can be observed. While this difficulty in physical realizability is a common phenomenon of electrically small antennas, the current ring antenna requires only geometrical and electrical symmetry instead of large and costly modulating currents. Therefore, it may be possible in the future to reduce the antenna diameter to about 0.02λ as long as a precision beam forming network can be fabricated. In addition, compensation for reduced radiation efficiency and interference of missile fuselage can be achieved by a processor with pre-stored memory of correction data. In this case the symmetry and simplicity of a missile obviously a great advantage for implementing a processor with memory, as compared with the complex structure such as that of a helicopter.

References:

1. A. J. Simila, "Reduced Size, Dual Mode Spiral for Two Plane Monopulse Direction Finding," NAVWEPS report 8757, U.S. Naval Ordnance Test Station, China Lake, California, May 1966.

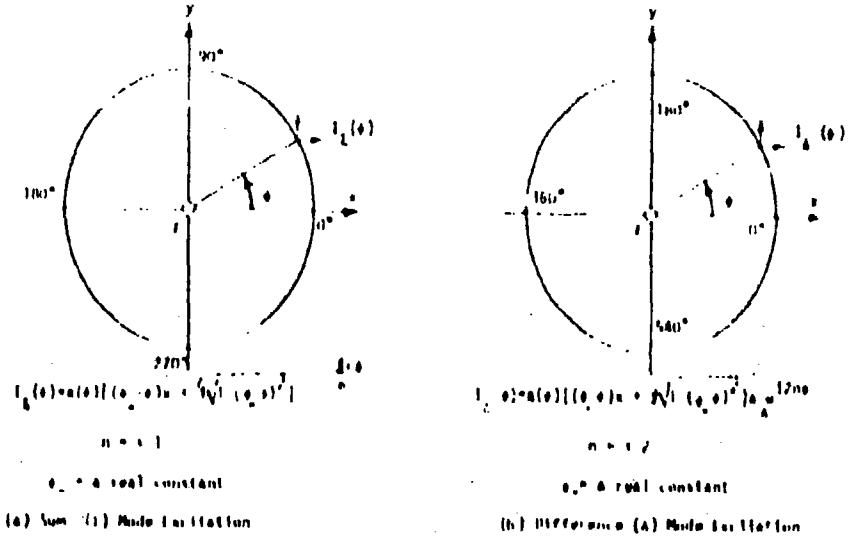

FIGURE 1.
EXCITATION OF SUM (Σ) AND DIFFERENCE (Δ)
MODES IN A CURRENT RING ANTENNA

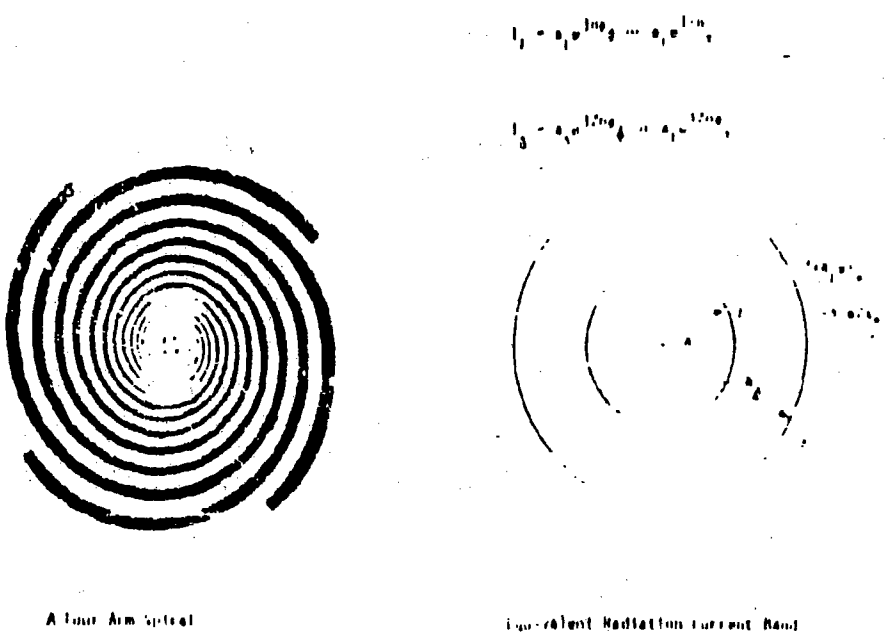

FIGURE 2.
EQUIVALENT CURRENT BAND THEORY FOR A MULTI ARM SPIRAL

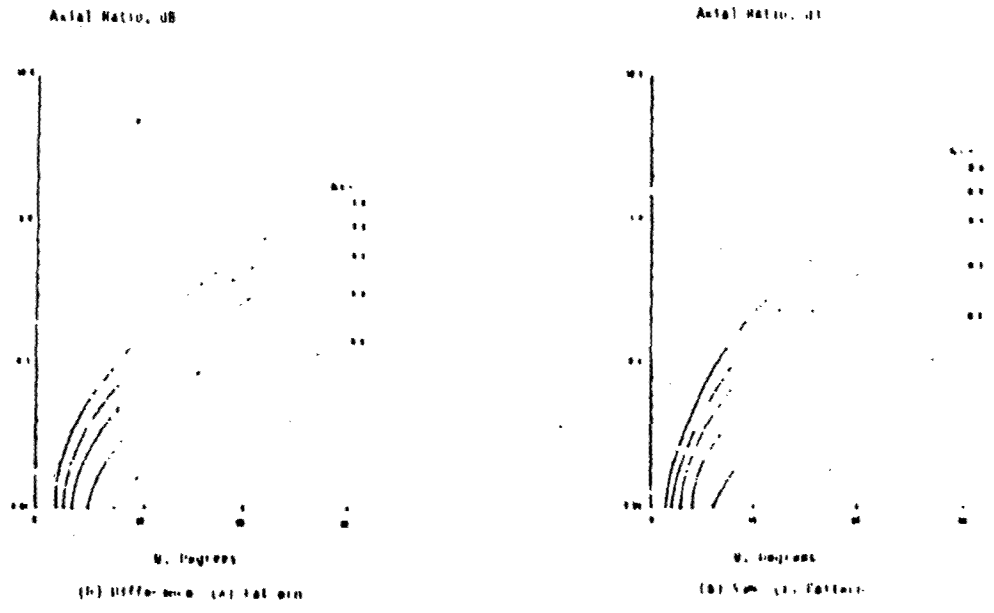

FIGURE 3.

AXIAL RATIO VS ANTENNA DIAMETER AND ANGLE OFF BORESIGHT, θ.

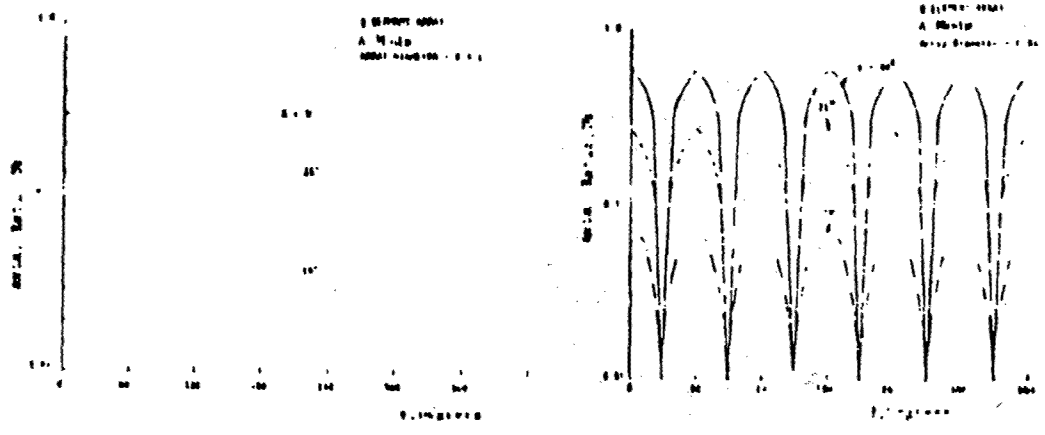

FIGURE 4.

COMPARISON OF AXIAL RATIO BETWEEN [illegible] AND [illegible] SIMULATIONS

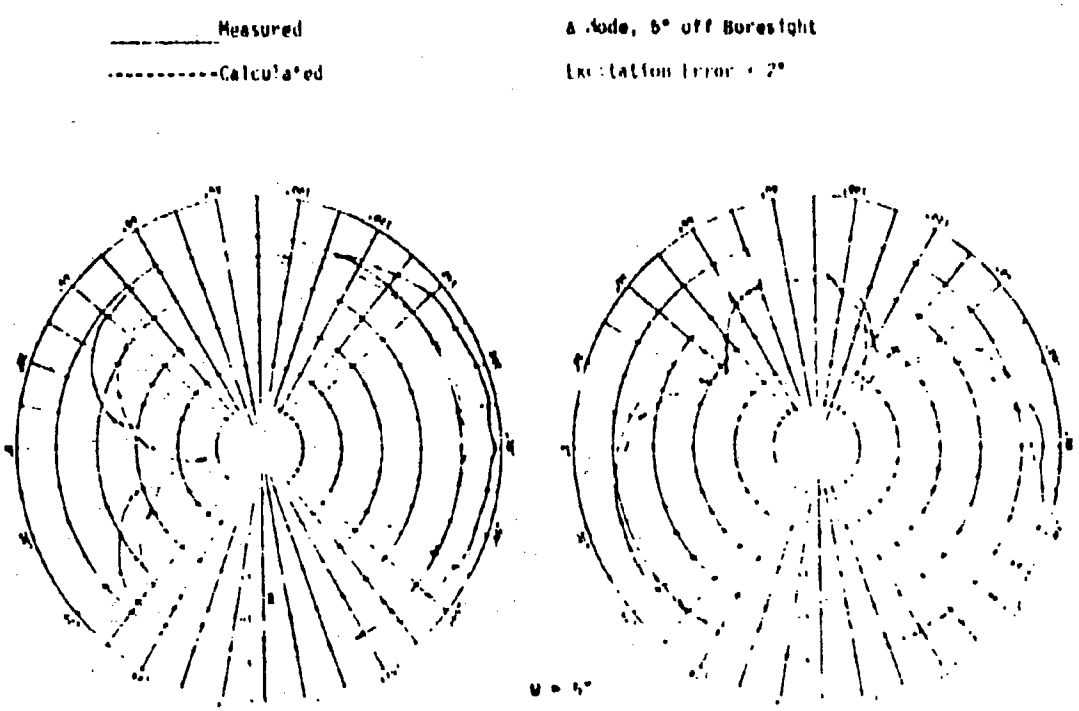

FIGURE 5.

OPTICAL CUTS AT TWO FREQUENCIES WHEN ANTENNA DIAMETER IS ABOUT 0.7λ.

2. P. D. Grant, "The Determination of Antenna Patterns of N Arm Antennas by Means of Bicomplex Functions," IEEE Trans. Ant. and Prop., Vol. AP 18, September 1970, pp. 686-689.

[illegible]

[illegible]

[illegible]

Abstract

[illegible] Performance [illegible] power efficiency for long-haul [illegible] Available designs are discussed which can be placed within [illegible]

I. INTRODUCTION

[illegible] past three decades and may provide the greatest advancement to [illegible] operations comparable with [illegible], approaching that of fixed plant installations. The demand [illegible] that it be transportable, easily erectable and highly directive at low elevation angles [illegible] must be resistant to [illegible] and have the ability of being used at heights as low [illegible] Past [illegible] have seriously hampered the development of suitable antennas to date. Without [illegible] of the field integral equations as used in conjunction with the reflection coefficient [illegible] performance of elevated long-wire antennas over imperfectly conducting [illegible] for evaluating the conduction losses in the ground plane is discussed. The [illegible] is applicable to the long-term high-frequency sky-wave prediction [illegible] for complete communications

II. BACKGROUND

[illegible] were mounted relatively close to the earth. However, these antennas exhibited [illegible] were thought to be effective as receive antennas.[1] Only in recent years has the [illegible] been realized.[2],[3] [illegible] VHF and UHF transmitting antennas.[2],[4] Early workers in the high-frequency, [illegible] efficiency rapidly increased with antenna size and height above [illegible].[4] In the UHF [illegible] antennas were tested on a trans-Atlantic ionospheric path [illegible] horizontal dipole, horizontal rhombic antenna at four heights.[5] Although theoretical work [illegible] was that very-angle directive [illegible] coupled to [illegible] at [illegible] [illegible] and [illegible] rather than a vertically polarized wave.[6] [illegible] [illegible] with [illegible] [illegible] the [illegible] began to lack from the UHF broadcast antenna [illegible] Lastly, [illegible] [illegible] techniques as the sky-wave [illegible] should be applied for [illegible] [illegible] leaving the 2 to 10 MHz band open for [illegible] operations.

[illegible] Newell optimized the vertical half-rhombic antenna for VHF applications.[7] Natali, although [illegible] [illegible] were made, the vertical half-rhombic was found to operate at frequencies [illegible] the design frequency.[8] Thereon [illegible] Di Matteo [illegible] except for the vertical half-rhombic [illegible] [illegible] proposed to be improved for radiation pattern control were not [illegible] [illegible] the U.S. Navy, Di Matteo selected the vertical half-rhombic as the most economical for [illegible] [illegible].[9] Further study by the U.S. Army indicated that the vertical half-rhombic model [illegible] that the stepped-up antenna commonly used with today's transportable [illegible]

[illegible]

[illegible] Navy [illegible] AMPO [illegible]

given by Burns [12]. The electrical parameters of the earth affect the current distribution on the wire segments in this manner as verified by Siegel [13]. However, when the wire segments are touching or within 0.1 wavelengths of a finitely conducting plane, NEC is found to improperly model conduction and induction losses in the ground plane. These losses should manifest themselves in the input impedance of an antenna in close proximity of the earth.

Induction losses associated with near field ground reflection can be assumed to affect the input resistance of the antenna, such that [15]

$$R_{in} = [1 + 1/2 (G_{pg} - G_{cg})] R_{ii} \quad (1)$$

Where:

R_{in} = input resistance of a base fed antenna over a finitely conducting ground plane

R_{ii} = radiation resistance of the antenna as determined from perfect earth calculations

G_{pg} = average gain of the antenna mounted on a perfectly conducting earth

G_{cg} = average gain of the antenna mounted over a finitely conducting earth having a loss current equal in magnitude and phase to the same antenna over perfect earth

The reflection coefficient approximation method based on the surface impedance of the ground plane adequately accounts for induction losses but does not consider conduction losses [10]. A semi-empirical approach for obtaining ground losses due to conduction current heating of the earth is given in ref. 14 and is reproduced here as Eq. (2).

$$R_{ij} = 0.046 \sqrt{f/\sigma} \quad (2)$$

Where:

R_{ij} = ground resistance as measured at the input of the antenna

f = frequency in MHz

σ = earth's conductivity in mhos/m

Thus the input resistance of the base fed antenna over a finitely conducting earth is given by

$$R_{in} = [1 + 1/2(G_{pg} - G_{cg}) + \frac{R_{ij}}{R_{ii}}] R_{ii} \quad (3)$$

With the exception of R_{ij}, the terms in Eq. (3) can be readily obtained from AMP. The resistance predicted by NEC can be directly compared with the radiation efficiency in order to compute the effect on the power gain of the antenna as given in Eq. (4).

$$\Delta G = 10 \log \left(\frac{R_{ii}}{R_{in}} \right) \quad (4)$$

As shown by comparison, Eq. (4) gives excellent agreement with measured data for vertical monopoles and inverted L antennas [14]. The computed values of input impedance and measured values obtained from a 40 foot

high inverted L having a base of 20 feet are shown in Fig. 1. The antenna employed only a 4 foot ground stake and was erected over poor soil (i.e., 0.001 mho/m and dielectric constant of 4). The agreement shown indicates that the relative change in gain, as given by Eq. (4), due to resistance changes, should give a reasonable estimate of the true radiated power. The reactance values shown in Fig. 1 also show excellent agreement even though the X values were computed for poor earth conditions using AMP.

4. PERFORMANCE ANALYSIS

The classic vertical half rhombic design given by Laport[6] and shown in Fig. 2 is modified using AMP modified by Eqs. (3) and (4). The two wire system effect is obtained from Schelkunoff's[17] equivalent radius formulation and use of tapered wire segments in AMP. Two basic configurations are investigated: (1) a base station antenna having L = 400 feet, H = 50 feet, H_2 = H_1 = 15 feet and terminating resistance = 500 ohms, and (2) a field station antenna having L = 100 feet, H = 15 feet, H_2 = H_1 = 5 feet, and terminating resistance = 500 ohms. Computed values of the maximum power gain in the plane of the antenna for both configurations are shown in Fig. 3. The gain is computed for poor ground conditions using Eq. (4) and letting the ground conduction loss equal to $(2 \cdot 1/2)(i_{g_1}^2 R_{g_1})$ to account for the two ground terminals of the antenna design and the improvement due to increased efficiency at the terminated end.

In that the smaller of the two vertical half rhombic antennas is approaching a wave antenna design, a third design is analyzed for the case of a horizontal wire 1000 feet long and 5 feet above the earth. The wave antenna is terminated in a 500 ohm load. The maximum gain values are plotted in Fig. 3. As is well known, the wave antenna requires poor earth in order to obtain the wave tilt needed to form a directive beam. To determine the effect of soil conductivity on the power gain, a second analysis is performed on the three antenna configurations with σ = 0.01 for a good ground. The resulting power gains are also shown in Fig. 3.

5. DISCUSSION

From the comparison of gain, the somewhat startling result is shown that the horizontal long wire mounted 5 feet above poor ground is superior to either the tilted long wire or the short vertical half rhombic. Theoretically, this is possible since the full advantage of beam formation is not realized with the vertical half rhombic design having a reduced electrical height. A comparison of power efficiency shows a different picture, as may be seen in Fig. 4. In this comparison the vertical half rhombic having a height of 50 feet shows a consistently better capability of radiating the input power. From a practical viewpoint this is very important in that less power must be dissipated in the terminating load. Also, the high voltage standing wave ratio effect that occurs when the antenna is inadequately grounded at the terminated end is less pronounced for the antenna having a greater radiation efficiency.

6. CONCLUSIONS

A method utilizing a recommended, available numerical technique for antenna modeling is described in conjunction with design and performance analysis of long wire antennas mounted electrically close to the earth. For long haul sky-wave application the vertical half rhombic and the wave antenna are shown to provide sufficient low angle directivity to overcome efficiency losses even in the lower portion of the HF band at electrical heights of 0.01H wavelengths (i.e., 5 feet at 3 MHz) above poor ground. The horizontal wave antenna is acceptable for receive and low power transmit applications over poor earth. Raising the center of the wave antenna to form a vertical half rhombic improves the power handling capability by reducing the current at the terminated end of the antenna and reduces the dependency of the antenna performance on ground conductivity.

REFERENCES

1. Beverage, H. H., Rice, C. W., and Kellog, E. W., "The Wave Antenna, A New Type of Highly Directive Antenna," Transactions of AIEE, Vol. 42, pp. 215-266, 1923.

2. Seeley, L. W., and R. D. Smith, "Radiation Efficiency of Variable-Wave-Velocity Horizontal Antenna Near the Earth", Naval Ordnance Laboratory Corona Report 730, pp. 19, Aug 67. AD 668397.

3 Seeley, L. W., and W. K. Moisan, "Horizontal End-Loaded VLF Transmitting Antenna", Naval Weapons Center Corona Laboratories Technical Publication 702, pp. 49, June 1968. AD 839107.

4 Carter, P. S., Hansell, C. W., and Lindenblad, N. E., "Development of Directive Transmitting Antennas", Proc. of IRE, Vol. 19, No. 10, pp. 1773-1842, Oct 31.

5 Bruce, E., "Developments in Short Wave Directive Antennas", Bell Systems Technical Journal, Vol. 10, pp. 593-683, 1931.

6. Lamont, L., Radio Antenna Engineering, published by Mei Ya Publications (Taiwan), pp. 378-379, 1967.

7 Newell, N. G., "The Inverted-V Antenna for Ground to Ground VHF Communication", Signals Research and Development Establishment Report No. 67011, pg. 12, Sep 67. AD 679483.

8 Ma, M. T., Theory and Application of Antenna Arrays, published by Wiley Interscience (New York), pp. 397-403, 1974.

9 Ma, M. T., and Tveten, L. H., "A Broadband Antenna Array for Scatter Measurements", Office of Telecommunications (Dept of Commerce, Boulder, CO), Report 78-141, pp. 57, April 1978.

10 Lane, G., "Feasibility of Using a Simple Antenna Structure at Fort Hueneme for Skywave Communications With the East Coast", USACEEIA Technical Report EME-78-19, pp. 71, December 1978.

11. Antenna Modeling Program Engineering Manual Prepared by Information Systems Division of MB Associates (under ONR Contract No. N00014-77-C-0187), 1977.

12 Baños, A. Jr., Dipole Radiation in the Presence of a Conducting Half-Space, Published by Pergamon Press, New York (1966).

13 Nagel, M., "The Electromagnetic Fields of Dipoles, Antennas and Arrays in a Dissipative Half Space", Ph. D Dissertation, Harvard University (Cambridge, MA), 1970.

14 Lane, G., and C. Mason, "Ground Resistance for MF/HF Design Analysis of Grounded Antenna Systems", USAEEIA Technical Report EME-78-7, pp. 31, April 1978.

15 Lane, G., "A Modeling Technique for Antenna Performance Over Lossy Earth", USAEEIA Technical Report EME-78-1, pp. 18, January 1978.

16 Wait, James R., Characteristics of Antennas over Lossy Earth, Chapter 23 in Antenna Theory Part 2, Edited by Collin and Zucker, Published by McGraw-Hill Book Co., New York (1969).

17 Schelkunoff, S. A. and H. T. Friis, Antennas Theory and Practice, Published by John Wiley & Sons, Inc., (New York, NY), p. 110, 1952.

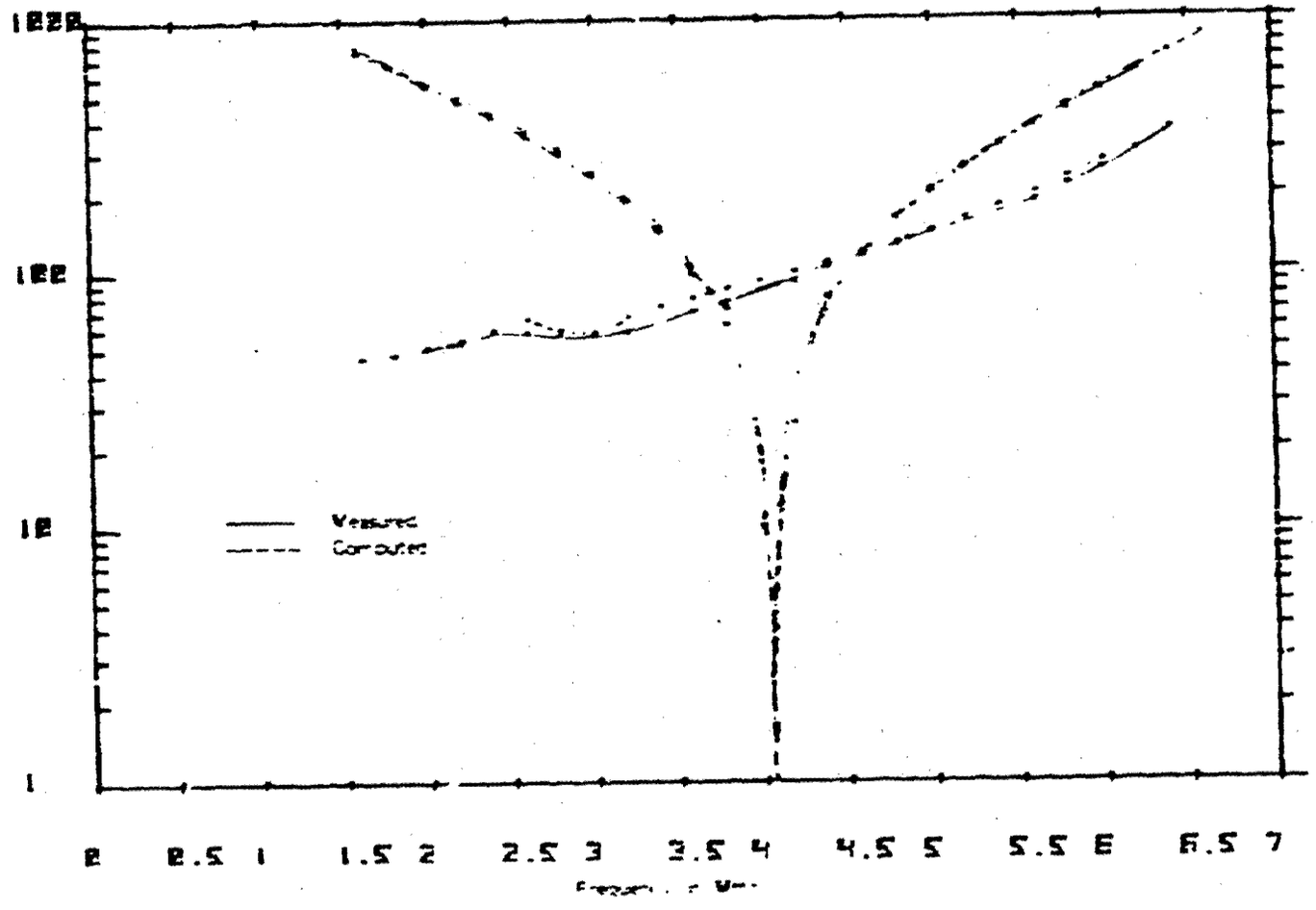
1000
100
10
1
Measured
Computed
8
8.5
1
1.5
2
2.5
3
3.5
4
4.5
5
5.5
6
6.5
7

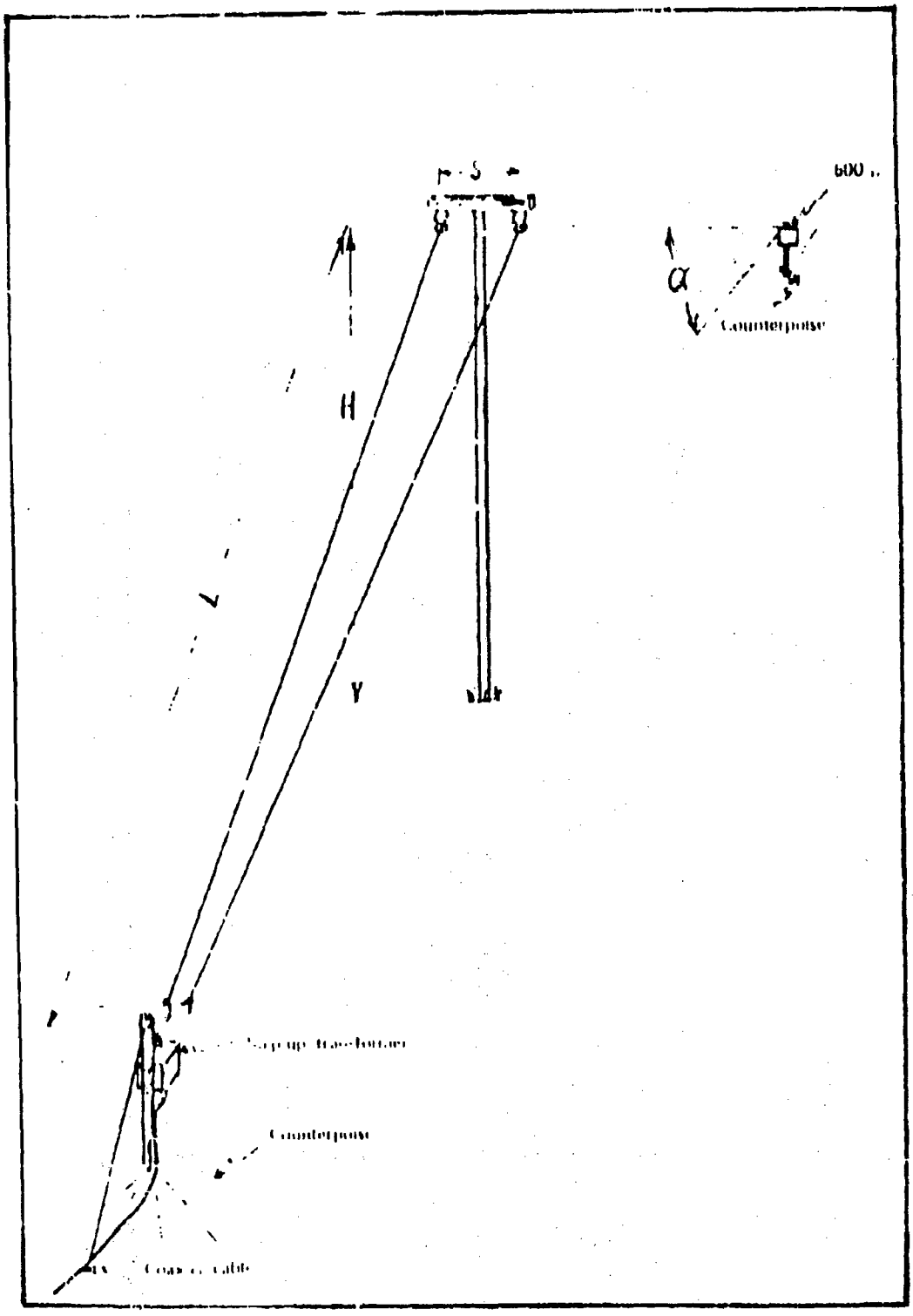

Figure 2 Vertical half-wave antenna

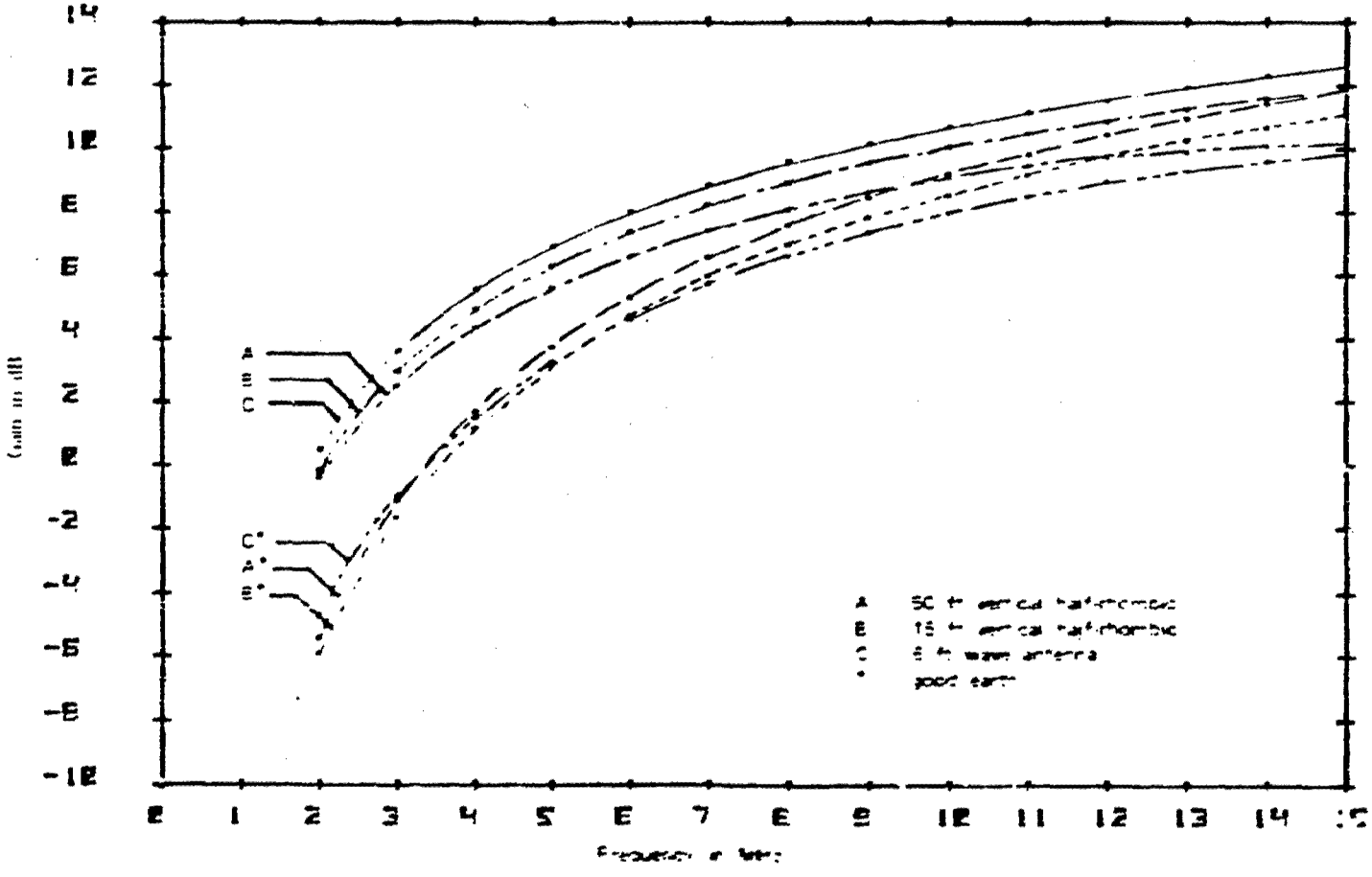

Figure 3 Effective power gain versus frequency for various 1000 ft. long wire antennas at different heights above poor earth and good earth *

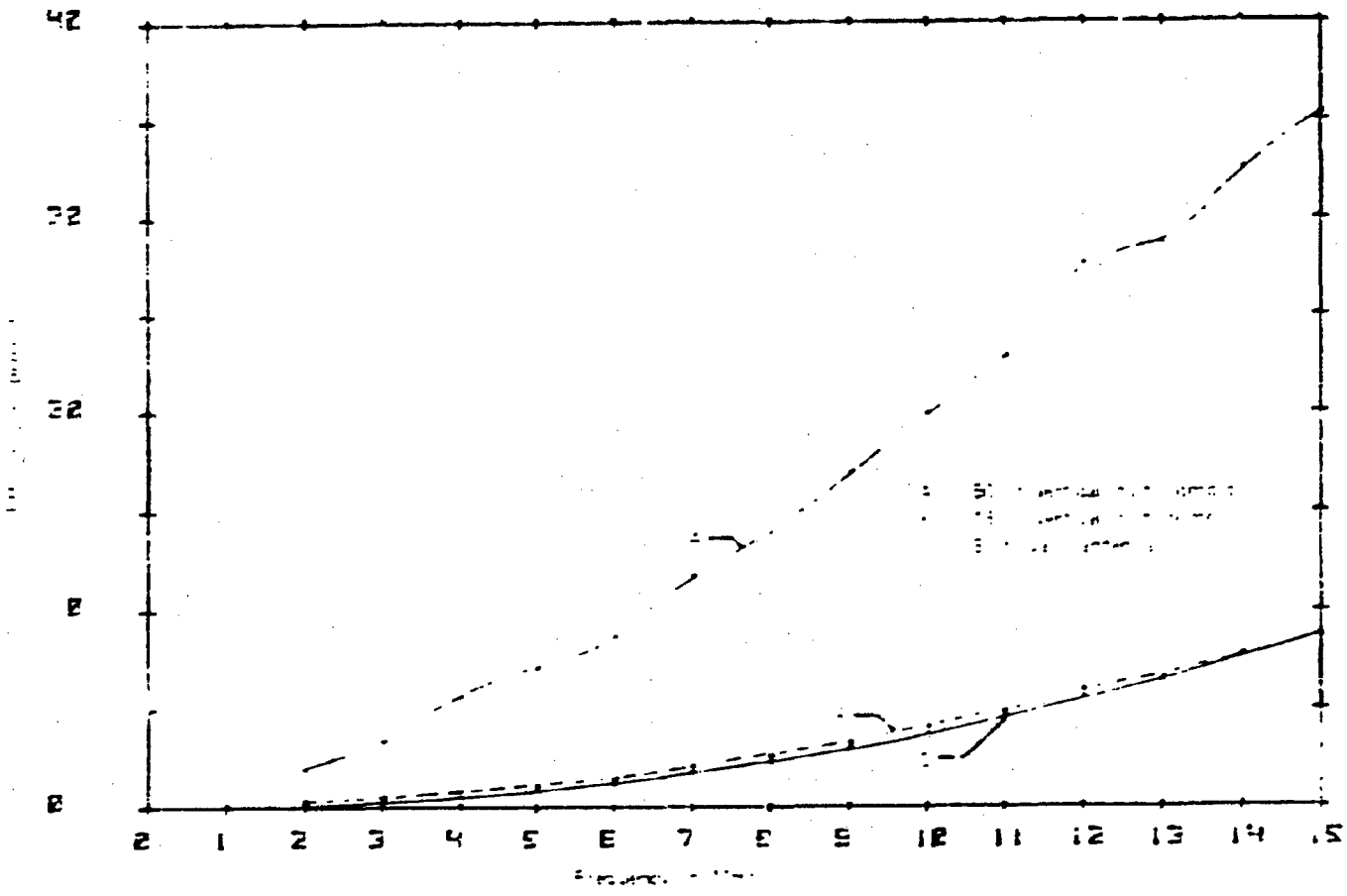

AIR FORCE VLF COMMUNICATION ANTENNAS

Peter R. Franchi
Deputy for Electronic Technology(RADC)
Hanscom AFB, MA 01731

Abstract

The VLF antennas described in this talk provide stable, long range communication for the Airborne Element of Emergency Communication Network by using the excellent propagation characteristics of the ionosphere and earth at these frequencies. These antennas are used by the Advanced Airborne Command Post and consist of one or two long, very thin, trailing wires. During flight the wires are unreeled from the rear of the aircraft. After the message has been transmitted, the wires are reeled back into the aircraft.

There have been four major efforts with this type of antenna. The first was called Power Box and was at a higher range of frequencies. The ARC-90 of the Air Force and the TACAN-T/P of the Navy followed. These systems were basically in the VLF range. The Air Force tried to make a major improvement with the multiwire antenna system but the effort on this system had to be curtailed because of a higher total weight and unexpected manufacturing complexity. Currently, work is proceeding on a modified [illegible] type antenna.

There are five major antenna concerns for this type of antenna. These are vertical polarization efficiency, bandwidth, power handling capability, antenna weight and antenna size or structural reliability. Lesser concerns are reeling time, EMP protection, and radiation pattern changes due to aircraft flight changes.

AIR FORCE VLF COMMUNICATION ANTENNAS

Peter R. Franchi
Deputy for Electronic Technology (RADC)
Hanscom AFB, MA 01731

I. Introduction

Why is the Air Force interested in VLF propagation? There are three principle advantages; these are 1) propagation is less affected by ionospheric disturbances than HF propagation 2) there is a relatively slow fading rate at VLF and 3) communication with submerged antennas is possible to some extent. There are also problems. The principle ones are very large antennas physically, low bandwidths, and high atmospheric noise levels. It is primarily the increased reliability that advances the use of VLF to the Air Force for an Airborne Command Post. The efforts of the Air Force in VLF airborne communication is reviewed from the initial work sixteen years ago to the present operating system (and possible future ones) with consideration of the major technical problems.

II. Power Box

In 1960 and 1961, Boeing conducted a series of tests for the Air Force on an LF trailing wire system called Power Box. These tests had three objectives; 1) to determine the feasibility of radiating LF from an aircraft 2) to measure field intensities at various distances, and 3) to determine the practicality of trailing a long wire from a jet aircraft. These tests ranged in frequency from 60KHz to 300KHz. The test aircraft was flown over Wisconsin with eighteen receiving sites scattered around North America.

The antenna for this series of measurements was a long wire (up to 3000 feet), reeled out from the lower bottom of the aircraft and towing a aerodynamic body to lower the trailing end of the wire. The wire was fed against the aircraft. Since the aircraft was so small electrically, the antenna is basically an end-fed dipole. Airspeed and weight of the aerodynamic body control the average trailing angle of the wire from horizontal. Although the TE wave mode propagates with less attenuation at LF and VLF, it is more difficult to receive horizontal polarization close to the ground. For this reason and since the vertical component of these tilted dipoles radiate uniformly in azimuth, the vertical E field radiation was and still is the desired radiation polarization. For this program, ranges of greater than 1000 nautical miles were reasonable for transmitter power on the order of 2.5KW. The principle problems for these tests were corona discharge and wire breakage.

III. ARC-96 and TACAMO IVB

After considerable study, the Air Force developed a practical VLF airborne system modeled after the Power Box LF antenna. There were just two significant changes in the antenna. First, it was increased in length to provide for the lower frequencies and a stabilizing drogue replaced the aero-

dynamic weight. This change resulted in a smaller vertical component, hence less power was radiated into the desired vertical polarization. The transmitter power was increased but breakdown due to end feeding limited the increase. The strength and reliability of the wire were also increased leading to less breakage problems. This system was designated the ARC-96. A somewhat similar system, TACAMO IVB, was developed by the Navy. In the VLF system, the airplane trailed two wires, one with a drogue and one with a weight. For transmitting periods the plane flew in a specified circular pattern, allowing the end of the longer weighted line to drop vertically. This greatly increased the vertical component of radiated power. The stationary location of the aircraft for the critical transmit periods is not an acceptable concept to the Air Force. Apparently, the stationary location of the TACAMO IVB and the low efficiency for the vertically polarized energy coupled with a larger aircraft induced the Air Force to examine a more advanced system.

IV. Multiwire Antenna

The advanced antenna consisted basically of three trailing wires and is called the multiwire system. An upper wire with its own reel trailed at a close to horizontal angle. A second shorter wire, streamlined and attached to a streamlined weight, trailed at an angle much closer to vertical. This wire increased the vertical radiated component by greater than an order of magnitude over the range of operating frequencies. The third wire was unreeled from the streamlined weight on command from the airplane. This wire also trailed close to horizontal. The deployed antenna appearance is that of a letter U on its side. At the junction of the upper wire and the near vertical streamlined wire is the feed point. (As was the case for the ARC-96 antenna, the final ten or fifteen percent of the horizontal trailing wires droop a little toward vertical).

This U-shaped antenna has two important advantages over the ARC-96 antenna: first, the vertical efficiency is about an order of magnitude better because of the greater vertical extension, second, the antenna is fed closer to the center enabling a much higher transmitting power to be used. In addition, the shorter sections of wire decrease the possibility of breakage. More importantly, the combination of higher vertical efficiency and increased power handling increase the effective range significantly.

With these great advantages, there were also several important disadvantages. This antenna was far more complex requiring three separate reels, one of which was in the streamlined weight. The streamlined cable required a fabrication procedure of very close tolerance to prevent aerodynamic instability. Generally, the complexity of the system increased the antenna-transmitter system weight. Finally, the change in location of the feed point to a more central position sharply reduced the system bandwidth. Primarily because of the greater complexity and weight, the Air Force moved from the multiwire antenna to a more modest system.

V. Modified Trailing Wire

The present proposed system consists of two wires, one upper shorter length of wire terminated with a drogue and a longer section terminated with an aerodynamic body. Neither wire would be streamlined. The total length for this system is approximately the same as the multi-wire system or the ARC-96 antenna (i.e., a resonant length). One can then see that the effective radiation resistance would be smaller for this antenna than the other two and the vertical projection would be less giving somewhat less vertically radiated power. Because this antenna is fed closer to the center, a larger transmitted power is possible than the ARC-96. This system is not exceedingly complex. It is close to the present TACAMO IVB in system components. As a compromise antenna, it is a very good practical choice, but other antennas are likely based on the current problem and new research.

VI. Possible Antennas

What type antennas are likely to emerge? Two possibilities are obvious. One would be another attempt to increase the vertical component of the antenna again by the use of streamlined cables and weights. Additional research and development work based on reducing the system weight and complexity of a multiwire antenna might yield more feasible techniques.

The other possibility is using the antenna at ELF frequencies. The current ELF ground based transmitter is extremely inefficient because of the size and close coupling to the lossy ground. An airborne ELF antenna would be smaller but better in terms of ground loss. Such an antenna would be an electrically small antenna although very large physically. The major advantage of these frequencies is that communication with submarines is much more feasible because of the decreased wave attenuation in the water. In addition, air propagation losses are also lower and there is great difficulty locating ground sites for ELF transmitters because of high ground conductivity and objections of environmentalists.

In summary, there has been a fairly rapid evolution of airborne antennas in the LF-VLF range. These antennas provide stable, reliable, long range communication, all very important features to the Air Force. There are still many problems. The ARC-96 antenna has poor power handling applicability and vertical radiation efficiency. The multiwire antenna is too heavy and complex and the new system may suffer bandwidth and vertical radiation efficiency problems. Because the need is there, an ELF electrically small antenna may be a future possibility. Such an antenna would have many technical problems to overcome.

THE UMBRELLA TOP-LOADED VERTICAL RADIATOR FOR USE AT MEDIUM FREQUENCIES

John S. Belrose
Radio Communications Laboratory
Communications Research Centre
Department of Communications
Ottawa, Canada

ABSTRACT

If the physical height of a vertical antenna is short compared with a quarter wavelength some form of capacitive top loading must be employed to reduce the capacitive reactance of the antenna and to increase its radiation efficiency. At VLF/LF two or more towers are usually employed to support some form of extensive top loading, and an antenna tower or a central insulated tower is employed for the radiator. A single grounded tower radiator is a more practical antenna, particularly for use at MF. The base insulator can be dispensed with by feeding the tower as an open circuited transmission line, terminated in the reactance of the top loading (a method that does not seem to be mentioned in published articles on ground plane vertical antennas). Umbrella top loading of the vertical radiator is the most gainful way to improve the radiation efficiency of a single tower antenna. The radiation efficiency of an umbrella top loaded antenna exceeds that for a T- or L-type antenna employing two towers each half the height of the single tower radiator (i.e. antennas that utilize the same number of tower sections).

The umbrella top loading consists of a number of wires strung obliquely to the ground from the top of the radiator, and insulated from the ground (with or without a skirt). This antenna was first used by Smith and Johnston at broadcast frequencies in 1947, and later by Belrose et al. at LF. Since the current on the umbrella wires has a vertical component that is oppositely directed to the current on the tower, the radiation from the umbrella wires in part cancels the radiation from the top part of the tower. Thus as the length of the umbrella wires are increased, the radiation resistance increases and then decreases, whereas the antenna reactance decreases continuously for increase in length of the umbrella wires for operation on frequencies below the fundamental frequency of the antenna.

The dependence of the antenna reactance and radiation resistance on antenna parameters (length and number of umbrella radials) was obtained by model measurements for short umbrella antennas (employing model frequencies in the range 2-100 MHz) and measurements of radiated field strength were measured at

7785 kHz. The results are summarized in a very compact way, by plotting the data as ratios of the height of the antenna to the wavelength and as ratios of operating frequency to the fundamental frequency of the antenna, which can be readily used to design umbrella top loaded antennas for any frequency. Design data, as an example, for resonant and non-resonant antennas for operation on 160 M are discussed.

REFERENCES

Belrose, J.S., W.L. Hatton, C.A. McKerrow and R.S. Thain, The Engineering of Communication Systems for Low Frequencies, Proc. IRE, 47, 661-680, 1959.

Smith C.E. and E.M. Johnson, Performance of Short Antennas, Proc. IRE, 35, 1026-1038, 1947.

ELECTRICALLY SMALL ANTENNAS: THEORY AND EXPERIMENT

John S. Belrose
Radio Communications Laboratory
Communications Research Centre
Department of Communications
Ottawa, Canada

ABSTRACT

The difficulties with electrically small antennas are well understood, and are:

1. the loss resistance for the antenna is greater than the radiation resistance and hence the radiation efficiency is low;

2. since the antenna is non-resonant a tuning network must be employed to match the reactive impedance of the antenna to the 50 ohm impedance required by most transceivers; and

3. since the antenna is highly reactive the bandwidth is small.

The need for an antenna matching network results in additional loss. While the expected performance for electrically small antennas is closely predictable, the claimed radiation efficiencies for particular antennas is sometimes greater than is practically realizeable. Specifically, the radiation efficiency for short centre loaded vertical whip antennas has been claimed to be as much as 14 dB greater than for a base loaded antenna of the same physical height (Spilsbury, 1973), yet theoretically (backed by experimental measurement) one should expect only a few decibels difference (Belrose, 1953).

Rather impossible efficiencies have also been claimed for the low profile directly driven ring radiator (DDRR) which is an antenna that is particularly misunderstood (Belrose, 1975). The efficiency of small loop antennas seems also to have been exagerated (Patterson, 1967; McCoy, 1968), since even if the loss resistances could be reduced sufficiently to achieve the claimed radiation efficiencies, the bandwidth of the antenna would be excessively narrow.

The purpose of this paper is to review the fundamental limitations of small and low profile antennas, and to compare

theoretical with experimental radiation efficiencies. While the remarks to be made are not new or state-of-the-art ideas, there seems to be miscomprehension and controversy over the practical performance that can be achieved with small antennas.

REFERENCES

Belrose, J.S., Short Antennas for Mobile Operation, QST, 30, September, 1953.

Belrose, J.S., Transmission-Line Low Profile Antennas, QST, 19, December, 1975.

McCoy, L.G., The Army Loop in Ham Communications, QST, 17, March 1968.

Patterson, K.H., Down-to-Earth Army Antenna, Electronics, 111, August 21, 1967.

Spilsbury, A.J., A Single MF-HF-VHF Marine Antenna, paper presented at the Seattle RTCM Assembly Meeting, Radio Technical Commission for Marine Services, Washington, D.C., 1973.

ELECTRICALLY SMALL COMPLEMENTARY PAIR ANTENNAS AND SCATTERERS

K. G. Schroeder
The Aerospace Corporation
El Segundo, California 90245

ABSTRACT

Electrically small (reduced size) antennas are inherently narrowband, or inefficient, or both. A summary is presented of prior work on electrically small antennas using capacitive tuning to optimize the impedance match and efficiency of such structures. The design of electrically small complementary pairs is described, and preliminary measurement results are shown for monopoles. These measurements indicate a substantial improvement in gain-bandwidth product as compared to conventional matching techniques for electrically small antennas.

DISCUSSION

Whenever available installation height is limited, the antenna can be foreshortened so as to fit into the limited space. This causes the antenna impedance to become very reactive. Past practice was to tune out the capacitive reactance by means of an inductor, or to transform the reactance and use a variable capacitor for tuning (Fig. 1). This renders such an "electrically small" antenna narrowband, and its efficiency is reduced by losses occurring in the tuning circuits. This problem becomes substantial for radiator lengths of less than $\lambda/8$.

An alternate approach for tuning a short dipole or monopole consists of using two of the antennas, which are mutually coupled, and matching the input reactance of one with the reactance of the other after it has gone through an inversion circuit. This inversion circuit is realizable in the form of an externally complementarized hybrid feed circuit similar to the one described previously for resonant-height antennas [2]. Mutual coupling between the two elements in the pair can be adjusted in a constrained design volume by varying (a) the length-to-diameter ratio of the elements, and (b) the element spacing and feed cable length differential for phasing.

A monopole configuration of the ESCP (Electrically Small Complementary Pair) was described in [3]. The monopoles were of small length-to-diameter ratio (Fig. 2) and their combined input impedance is shown in Fig. 3. The total matching loss for this pair is depicted in Fig. 4, which includes the loss incurred if the residual mismatch at the hybrid sum port is totally converted into loss of power. In the case of a scatterer, one can visualize a matching circuit, which partially reclaims this mismatch loss by transferring the impedance at the lower frequencies only; this is now feasible since only a relatively small reactance is involved. For this case, the equivalent radar cross section (RCS) can be approximated as shown in Fig. 5. This is plotted as the top curve in Fig. 6. If one makes allowance for 2.5 dB additional one-way matching loss (e.g., due to the above mentioned tuning device,

cable losses, ohmic losses in the radiators etc), the lower RCS curve in Fig. 6 results, i.e., a plot 5 dB below the previous one. (This is obviously conservative.)

Finally, a reflection type amplifier could be employed to shape the response curve as given in Fig. 7, for conservative gain of 3 dB in the amplifier. A comparison was now made between this ESCP scatterer, and other possible techniques. The best alternate solution presented in the past consisted of dual arrays of crossed shorted dipoles, tightly coupled in the endfire dimension. Since the dipoles were thin, they were narrowband, and the double-tuned curve showed a large dip in between the two peaks (Fig. 8). Neglecting this dip, a total bandwidth Δf in percentage can be assigned, and, multiplied with the measured peak efficiency of 50%, yields a gain/bandwidth product $G/G_o \times \Delta f\ \% = 0.1$. The same factor for the passive ESCP antenna, with a conservative 2.5 dB additional loss, is 0.2. It should be pointed out that the comparison is in favor of the dipole arrays, since they can only be used as scatterers, and no feed point is available to drive them as an antenna.

A number of other electrically small antenna types were analyzed, and were all found to have < 0.1 gain/bandwidth product. Since some of the approaches require DC power to drive matching networks and/or amplifiers, direct comparison with passively matched antennas and scatterers is very difficult. Some new standards are required regarding efficiency, bandwidth and physical dimensions of electrically small antennas before accurate evaluation of relative merit can be made. In gross terms, however, it appears that the ESCP provides the potential of considerable improvement in gain/bandwidth product.

REFERENCES

1. J. A. Seeger, R. L. Hamson, A. W. Walters, "Antenna Miniaturization," Electronic Design, pp. 64-69, March 4, 1959.

2. K. G. Schroeder, "The Complementary Pair - A Broadband Element Group for Phased Arrays," PTGAP International Symposium Record, pp. 128-133, 1964.

3. K. G. Schroeder and K. M. Sco Hoo, "Electrically Small Complementary Point (ESCP) with Inter-Element Coupling", Transactions on Antennas and Propagation, Vol. AP-24, No. 4, July 1976.

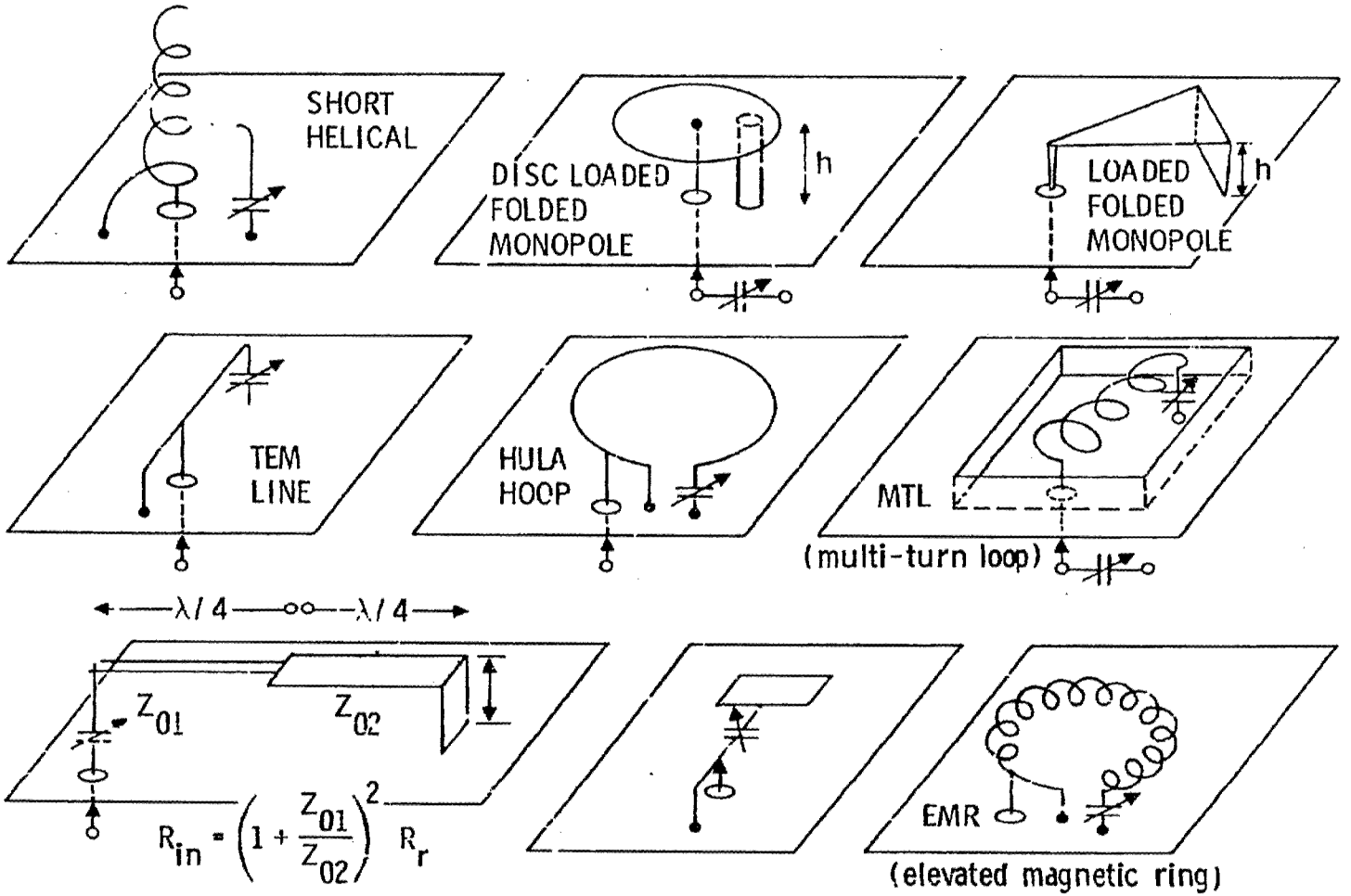

Figure 1. Capacitive Matching Techniques for High-Efficiency Electrically Small Monopoles

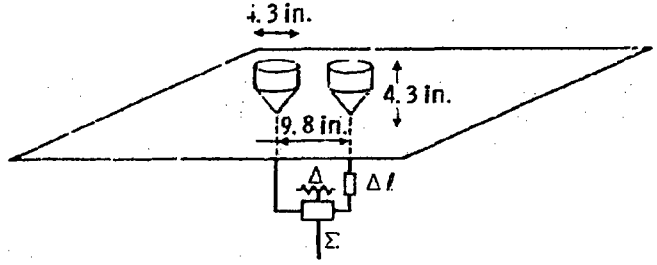

Figure 2. Electrically Small Complementary Pair Preliminary Test Configuration

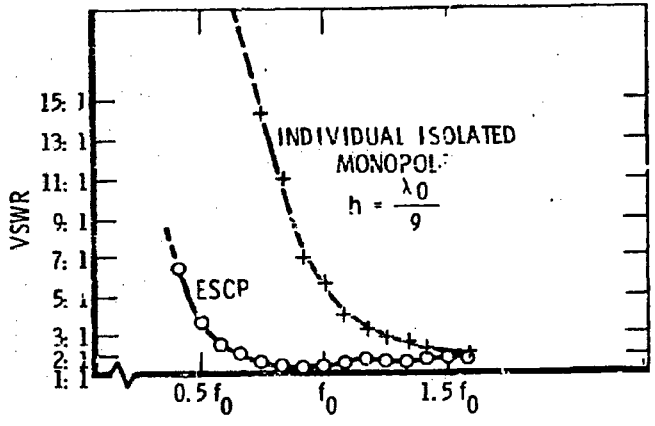

Figure 3. ESCP Input Impedance Match

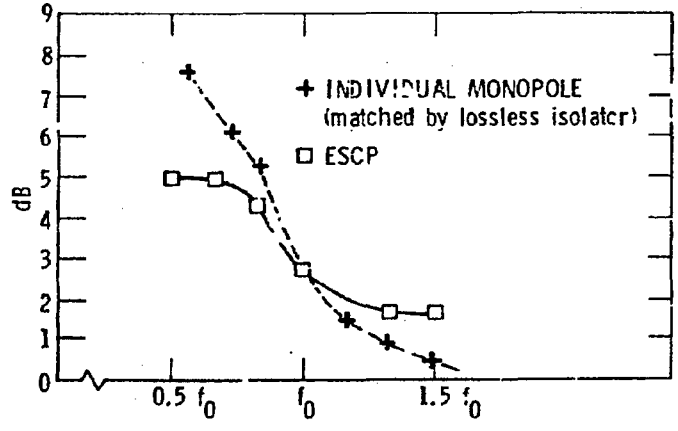

Figure 4. ESCP Matching Loss

	$0.5 f_0$	f_0	$1.5 f_0$
	150	300	450
G_D	1.75	1.75	2.2
G_{ARRAY}	1	3	3+
$G_D + G_A$	2.75	4.75	5.2
LOSS (mismatch tuned at 150)	-4.50 dB	-2.50	-2
G_{NET}	-1.75	+2.25	+3.2
G^2	-3.5 dB	+4.5 dB	+6.4 dB
λ	2m	1m	2m / 3
λ^2	$4m^2$	$1m^2$	$4m^2$
λ^2 dBsm	6 dBsm	0	-3.5
$G^2 \lambda^2$	+2.5	+4.5	+2.9
$\sigma_{MAX} = \frac{G^2 \lambda^2}{\pi}$	-2.5 dBsm	-0.5*	-3.1*
σ_{MAX}*	-2.5	-3	-5.6
σ_{MIN} (2.5 dB additional loss)	-7.5 dBsm	-8 dBsm	-10.6 dBsm
σ_{MIN} (3 dB amp between 150 and 300)	-4.5	-5	-10 dBsm**

* Matching at 1/2 f_0 will cause ~3:1 mismatch at f_0 and 1.5 f_0, with potential loss increase of ~1.25 dB, and RCS reduction of ~2.5 dB.

** Can be lower depending on frequency characteristic of amplifier.

Figure 5. RCS vs Frequency, L ≈ 8.6-in. Scatterer Length

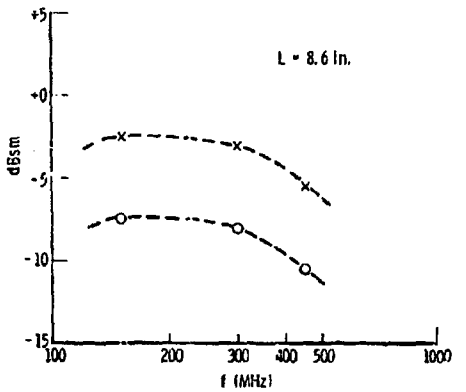

Figure 6. Estimated ESCP RCS

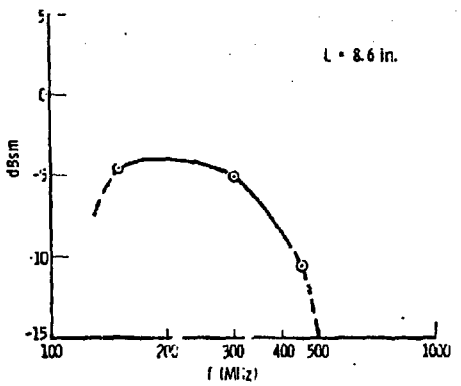

Figure 7. Estimated ESCP RCS 3-dB Gain Reflection Amplifier

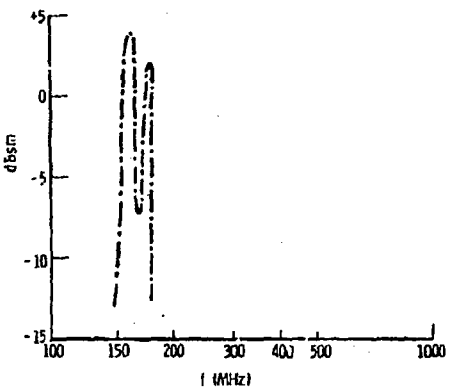

Figure 8. Typical Narrowband Scatterer (Double-Tuned)

SOME EXAMPLES OF SMALL, LOW-NOISE,HIGHLY LINEAR ACTIVE ANTENNAS PRODUCED IN QUANTITY FOR VARIOUS APPLICATIONS

by

H. K. LINDENMEIER AND F. M. LANDSTORFER

Technical University
Munich, Germany

ABSTRACT

Various types of low-noise active receiving antennas are introduced and their technical data explained:

(1) A highly linear broadband (10 kHz to 30 MHz) rod antenna of 1-meter height and wide linearity range.

(2) A 0.25-meter high broadband antenna for OMEGA-, DECCA, and LORAN-C navigation.

(3) A diversity antenna, consisting of two crossed horizontal active dipoles for 1 MHz to 30 MHz and a vertical active monopole from 10 kHz to 30 MHz. The length of all elements is 1 meter.

(4) An active antenna of 2-meter height for direction finding from 0.25 to 30 MHz for application in a mobile Adcock system.

(5) Receiving antenna for guided waves for 47 to 68 MHz used for optimum reception of signals radiated from a slotted coaxial cable.

SOME EXAMPLES OF SMALL, LOW NOISE AND HIGH LINEAR ACTIVE ANTENNAS PRODUCED IN QUANTITY FOR VARIOUS APPLICATIONS.

1. Broadband antenna from 10 kHz to 30 MHz with high linearity range and 1m height.

The annexed illustration shows the active rod antenna into the base-insolator of which the antenna amplifier is inserted. The dc-power is supplied to the amplifier from the power supply via the inner and outer conductors of the coaxial antenna cable. This antenna replaces the common conventional 6 m high passive whip antenna. In spite of the considerable smaller height of the active antenna the signal-to-noise-ratio at the low end of the band is even 25 dB superior to the snr of the conventional antenna with receiver if both antennas are mounted upon a conductive ground plane. At the high end of the band the snr of both systems is approximately equivalent. With many applications, as for example on ships, a nearby installed transmitting antenna impresses a strong electromagnetic field at the location of the receiving antenna. Therefore special efforts have been made to obtain an antenna amplifier causing very low non-linear effects within an extreme wide voltage range. Precautionary measures protect the amplifier against damage by electrostatic discharge. Tests have shown that the active antenna withstands the atomic e.m.p. In the following the most important data of the active antenna are listed.

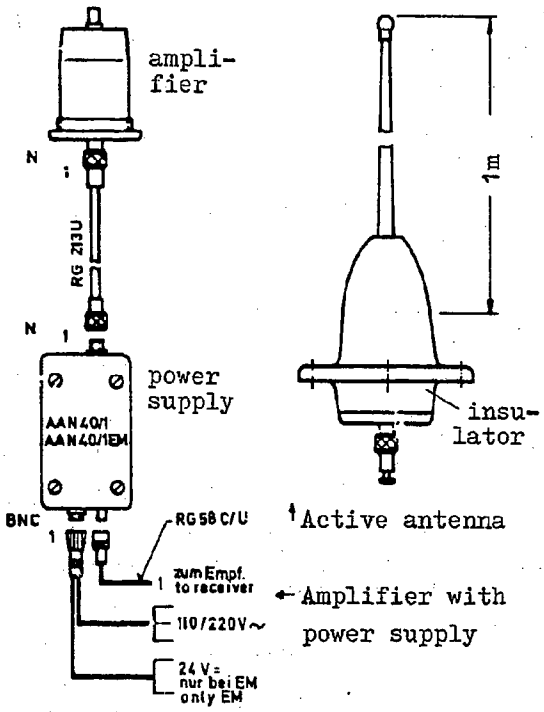

At the output terminals the active antenna may be described as an emf, produced by the fieldstrength E, with the output impedance in series.

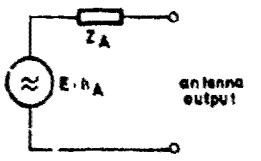

Equivalent circuit.

Z_A: Output impedance = 50 ohms.
VSWR = 1.1 (within the above cited frequency range)
h_A : Effective height of active antenna with reference to the output terminals. E = vertical component of electric field strength (antenna vertically mounted on ground plane).
h_A = 21 cm. (constant within a tolerance of $\pm$ 1 dB).

The equivalent noise field strength due to amplifier noise $E_N/\sqrt{B}$ is that rms-value of a sinusoidal signal field strength per $\sqrt{\text{bandwidth}}$ necessary to achieve snr = 1 (≙0 dB) at the antenna output.

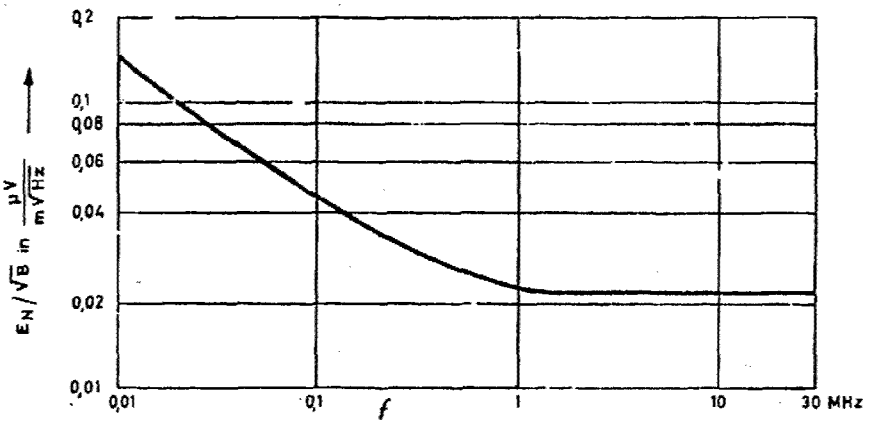

Diagram of equivalent noise field strength/ $\sqrt{\text{bandwidth}}$ versus frequency with antenna on ground plane and received ground wave.

The maximum tolerable (rms-value of sinusoidal) field strength E_t, that causes 1 dB reduction of amplification due to nonlinearity, is shown in the following diagram (antenna on ground plane and with ground wave).

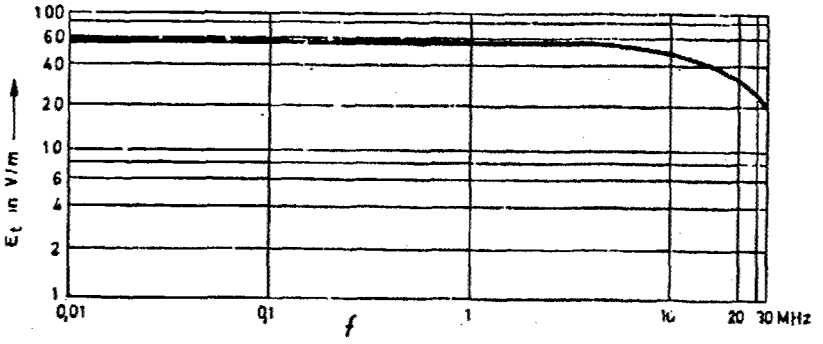

With two sinusoidal signal field strengths of different frequencies f_1 and f_2 but of same rms-value $E_1=E_2=E=100$ mV/m the distortion at the antenna output due to second order intermodulation at lower frequencies

is 80 dB and at higher frequencies is 70 dB below the output signals at f_1 and f_2. The suppression of third order intermodulation products at low frequencies is better than 120 dB and at higher frequencies better than 105 dB. With practical operation the distortion by these kinds of nonlinear effects is rather unlikely since it only occurs if there are several strong signals and if the frequency of the received signal by coincidence equals the frequency of one of the intermodulation products. With most cases in practice the receiving-system is more endangered by distortions caused by cross modulation from a nearby located transmitter. In this case the tolerable rms-value E_u of an unwanted amplitude modulated signal (modulation factor is 30%) at the frequency f_u causing a modulation factor of 3% of the wanted signal at the frequency f_S is important. E_u has been optimized with the present antenna and is plotted versus f_u for various values of f_S in the following diagram.

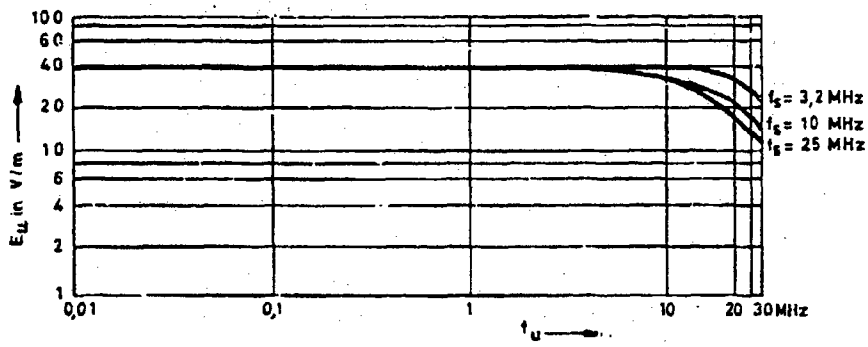

2. Navigational antenna for OMEGA, DECCA and LORAN-C.

The antenna has the same shape as the one in ch.1. The frequency range reaches from 8 kHz to 130 kHz. Unwanted signals above 140 kHz are suppressed by means of a Cauer-lowpass-filter within the antenna amplifier in order to protect the subsequent navigational receivers from nonlinear distortions due to overload conditions. The suppresion of unwanted signals in the range from 400 kHz to 30 MHz is better than 60 dB. Phase delay distortion is guaranteed less than 3 degrees, which limits DECCA-navigational errors to 30m. The diagram next page shows the tolerable unwanted fieldstrength for 0.1=3%/30% cross modulation as defined in ch.1

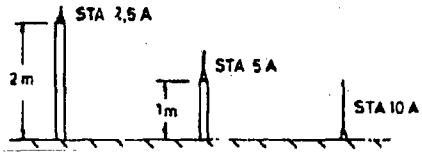

In case of mounting the antenna on a 2m high mast, the length of the rod may be reduced to 25cm in order to obtain roughly identical data as with 1m rod on ground.

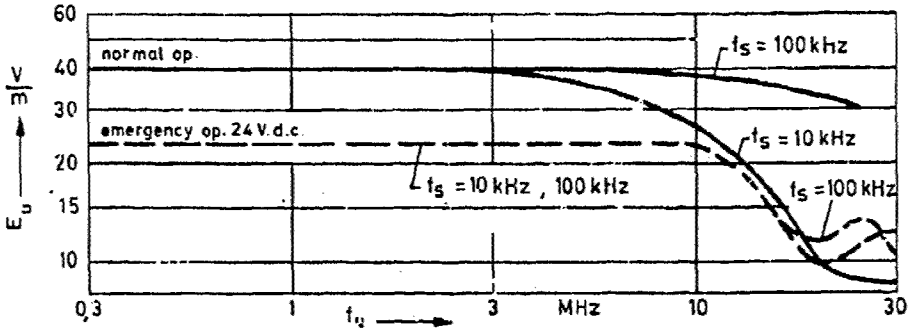

3. Active diversity antenna.

As shown in the illustration the antenna consists of two crossed horizontal dipoles, each driving an amplifier with balanced input and unbalanced output, and a vertical active monopole, as described in ch.1. The length of all rods is 1m. All amplifiers are located within a screening case inside of a fibreglass reinforced polyester insulator and have seperate output terminals which are to be connected via cables to an antenna selector system. Usually this antenna is mounted on top of a 3-6m high mast. Thus as far as the vertical field components are concerned the equivalent noise fieldstrength and the different values of tolerable fieldstrengths of the active monopole as described in ch.1 are reduced. Since the sky wave is only received at frequencies above 1 MHz the horizontal dipoles are designed for 1 MHz to 30 MHz with an output voltage at the load impedance (50 ohms) of 0.6V per 1V/m horizontal fieldstrength E_h (tolerance $\pm$ 1.5 dB). The equivalent noise fieldstrength of the horizontal dipoles is $E_{Nh}/\sqrt{B} = 0.015\ \mu V/(m\sqrt{Hz})$. Nonlinear distortions caused by horizontal field components and due to second and third order intermodulation are equal to that of the active monopole Since the antenna is mounted on a mast cross modulation with the horizontal dipoles may occur not only caused by the push-pull voltage but also by a push-push voltage at the input terminals of the antenna amplifier. The push-pull voltage originates from a horizontal field component E_{uh} while the push-push voltage is produced by a vertical field component E_{uv}. The tolerable horizontal component for a cross modulation of 3%/30% = 0.1 (s. ch.1) is E_{uh} = 7V/m. For the example of a 3m high mast and frequencies f_u below the quarter wave-resonance of the mast E_{uv} = 5V/m.

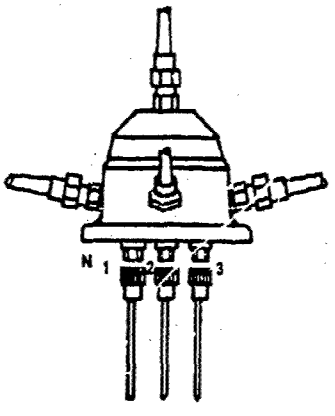

4. Active antenna for direction-finder from 0.25 to 30 MHz.

The photograph shows an adcock direction-finder system consisting of eight single active antennas, the total height of each is 2m. The antenna amplifier is built into the top end of a 1m high tube mast, whereon a 1m long plug-in whip antenna is mounted. The special designed amplifier meets very hard requirements as to a tolerable spread in phase of less than 1 degree and a tolerable spread in gain of less than 0.1 dB between units. The passive antenna parts between the low end of the whip and the high end of the mast are loaded with the small input capacitance of the high impedance amplifier. Therefore the currents on the antenna parts are very small and prevent the antennas from radiation coupling. The antenna mast forms a counterbalance to the whip. Therefore with a very simple ground network extreme small direction finding errors are obtained even with sky wave bearings. The equivalent noise fieldstrength $E_N / \sqrt{B} \leq 3$ nV/(m $\sqrt{Hz}$). Suppression of intermodulation products is better than 100 dB with two signals of E = 10mV/m each. The antenna replaces a 6 m high passive whip antenna and makes it now feasible to mount the adcock system very easily in the field.

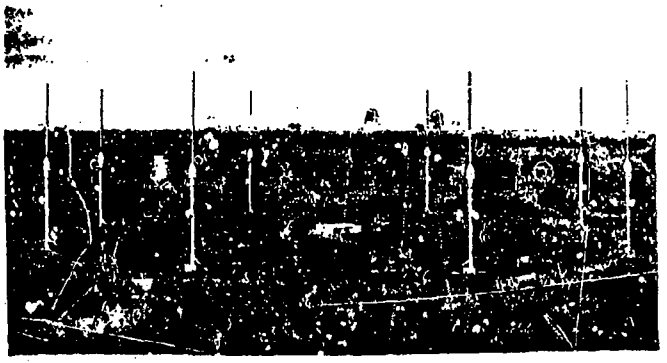

Direction-finder system with active antennas.

Antenna amplifier

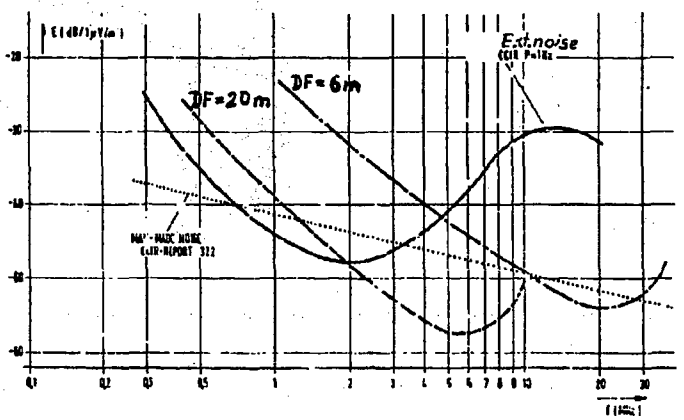

Equivalent noise fieldstrength of df-system with B = 1Hz

5. Receiving Antenna for Guided Waves

The active antenna K 50238 is designed for optimum reception of signals radiated from a slotted coaxial cable. It operates in the lower VHF-band and couples to the magnetic TEM-field of the slotted line.
In order to meet official requirements as to the tolerable interference fieldstrength outside the installations, the active circuit of the antenna is optimized for maximum signal-to-noise ratio S/N at its output, with low levels of transmitted power. Typical values are S/N≤ 40 dB at 20 cm clear distance between cable and antenna, and transmitter power adjusted to a level which gives less than 30 µV/m interference fieldstrength at 30 m distance from the cable.
Applications are found wherever a signal has to be transmitted from a fixed station to a movable object following a predetermined track along which the slotted cable can be mounted, such as a railway car or a big rail-bound crane. At the moment these antennas are in use with the rapid-railway systems of Vienna, Munich and Paris. There 2 or 3 TV-pictures of the railway platform are transmitted simultaneously to monitors within the locomotive in order to give the engine driver a good survey of the platform and help him with clearing in and out of the station.

Further data

Frequency range:
47 - 68 MHz
Characteristic impedance of output: 75 Ω (unbalanced, VSWR < 2)
Bias: 12 V/ 5 mAmps
Material: stainless steel and fibre glass
Weight: 8 kg

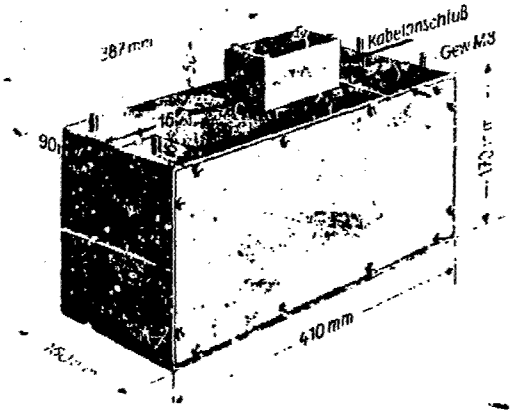

Sections 1 to 4 are by H.K.Lindenmeier, section 5 is by F.M.Landstorfer.

TRADE-OFFS IN THE DESIGN OF A SMALL ACTIVE ANTENNA FOR TELEVISION RECEPTION

by

J. J. GIBSON

RCA Laboratories, Princeton, N. J.

ABSTRACT

The development of the "Mini-State" antenna, a small, active, rotatable, directional antenna for television reception is discussed with particular emphasis on basic principles, criteria of performance, and trade-offs between size, signal-to-noise ratio, bandwidth, directional characteristics, distortion and cost.

TRADE-OFFS IN THE DESIGN OF A SMALL ACTIVE ANTENNA FOR TELEVISION RECEPTION

by

J. J. Gibson, RCA Laboratories, Princeton, N. J.

SUMMARY

The "Mini-State"[1] is a small active TV antenna designed for suburban and metropolitan reception areas where a small size indoor-outdoor antenna is very desirable, and where multipath and man-made noise is more of a problem than random noise generated in the reception system. Small size, large bandwidth, and a directional radiation pattern are achieved at the expense of signal-to-noise ratio. The signal to noise ratio (S/N) relative to signal to the noise ratio (S_o/N_o) of a dipole with a system temperature of $T_o = 290^oK$ is introduced as a practical, meaningful, and measurable figure of merit:

$$M = (S/N)/(S_o/N_o) = (S/S_o)/(N/N_o) = (D/T)\ T_o$$

where (S/S_o) is the antenna gain relative to a dipole, (N/N_o) is the excess noise which can be measured in a screen room, D is the directivity, and T is the actual system temperature. While the variation in directivity is small between various designs of small antennas, the system temperature is critically dependent on a large number of factors such as: the noise figure and the gain of the amplifier, which are both dependent on the antenna impedance; antenna losses; receiver noise figure; cable losses; noise temperature of the field. These trade-offs will be discussed in some detail.

It is shown that if it is assumed that the noise temperature of the field and of all passive components in the system is T_o, the figure of merit is

$$M = DK/F$$

where K is the antenna efficiency (radiation resistance/total resistance) and F is the system noise figure. It is possible to design a lossy antenna with a good noise figure (and large bandwidth) with about the same figure of merit as a low-loss antenna with a poor noise figure. The final choice for the VHF antenna (54-216 MHz) was a terminated two-port loop, which is a lossy broadband antenna with a cardioid type pattern and with nulls towards the back. The diameter of the loop is 18 inches, which is one-tenth of the longest wavelength used for broadcast television (Channel 2). A low characteristic impedance of the structure, which is beneficial for the efficiency "K", is achieved by making the loop out of a 2-inch wide strip. A broadband match to the terminating resistance is obtained with slots cut out of the loop. The figure of merit of the system, including the TV receiver, ranges from -21 dB at channel 2 to -10 dB at channel 13. Good rejection is obtained over a 100° angle in the horizontal plane towards the back. Two deep nulls in the pattern provide for excellent single "ghost" rejection. A UHF antenna (407-806 MHz), a yagi with a 2.5 dB gain, is inserted inside the VHF antenna. Slotted UHF stubs in the front part of the VHF loop minimize the interaction between the antennas. An amplifying device is required close to the input of the VHF antenna, partly to improve the figure of merit and partly to maintain good radiation patterns, which otherwise might be destroyed due to direct pick-up by the cable and the receiver.

Since the antenna must also operate in strong signal areas, considerable attention has been given to intermodulation distortion in the broadband amplifier. Dynamic range, noise performance, bandwidth, stability and costs of amplifiers with bipolar and MOS transistors were extensively studied both experimentally and theoretically.

The design trade-offs are discussed in the context of the system environment, i.e. the electromagnetic field at one end and the receiver at the other, the performance requirements, which depend on subjective effects of various disturbances and the need to provide good quality reception at a large number of locations, and cost.

1) "The Mini-State - a Small Television Antenna" by J. J. Gibson and R. M. Wilson, to be published shortly in IEEE Transactions on Consumer Electronics.

VHF MANPACK LOG PERIODIC ANTENNA

J. C. DAVIS, DHV, INC.

ABSTRACT

A lightweight VHF manpack antenna is described which operates over the frequency range of 26 to 88 MHz, has 4 dbi of gain, has a VSWR of 2:1, radiates 100 watts of RF power and can be erected by two men in 10 minutes. It has a unique configuration for minimizing the array size and for ease of erection. Also, due to the broadband properties, it can be used with frequency hopping and spread spectrum systems.

SUMMARY

A lightweight, quick erect VHF manpack log periodic antenna has been developed which operates over the frequency band of 26 to 88 MHz. The erected equipment is shown in figure 1. The array size is reduced by utilizing swept forward elements of the "V" type at the lower frequencies. As the element length decreases along the LP structure, the angle of the elements increases so that at the higher frequencies the elements are regular dipole elements. A plan view of the array is shown in figure 2.

The antenna weighs 30 pounds, is packaged in a canvas bag, and can be erected by two men in 10 minutes. A key design factor in realizing the quick erection is storage of the LP array on a nylon template using velcro straps. This prevents the phospher bronze elements and feeders from becoming tangled when rolled into a lightweight compact package.

The antenna is supported by a fiberglass quadrapod structure which is mounted on a tubular mast. The fiberglass quadrapod is sectionalized for compact stowage. The fiberglass members are connected with shock cord for easy installation.

Briefly the installation consists of:

a) Unrolling the nylon template containing the LP array.
b) Assembling the quadrapod.
c) Placing quadrapod on nylon template and attaching LP array to quadrapod at four places.
d) Removing nylon template from LP array and connecting coaxial input cable.
e) Assembling mast and connecting quadrapod to top of mast.
f) Erecting antenna and attaching guys.

The gain of the antenna is 4 dbi at the low end of the frequency range increasing to approximately 5.5 dbi at mid band. The front to back ratio increases from 4 db at the low end to 10 db at mid band. Representative measured radiation patterns are shown in figure 3. Input impedance of the antenna is fifty ohms with a VSWR less than 2:1. The antenna is capable of operating with 100 watts of input power. A key feature of this antenna is that it can be used in systems employing frequency hopping or spread spectrum due to the broad bandwidth.

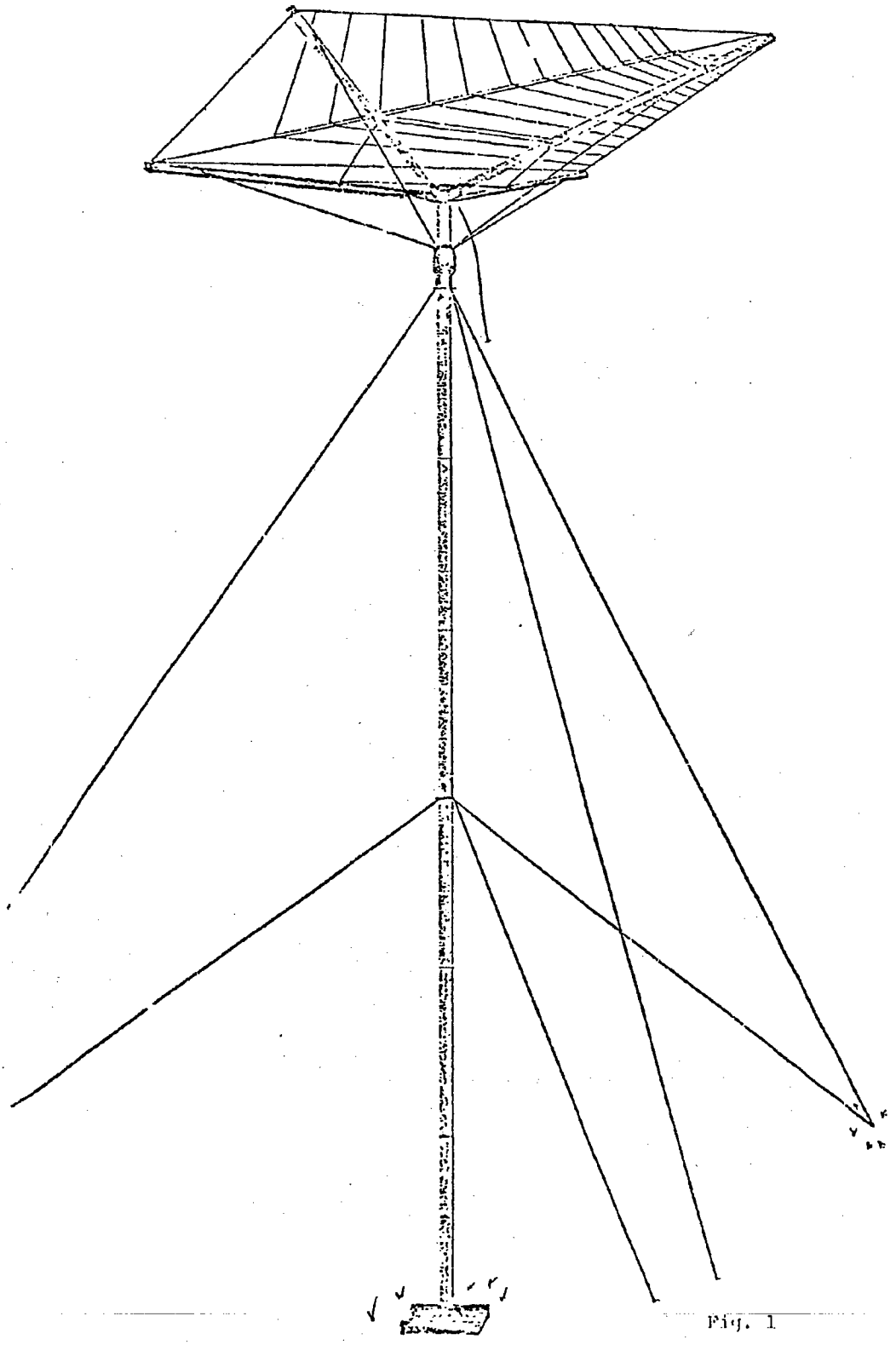

Fig. 1

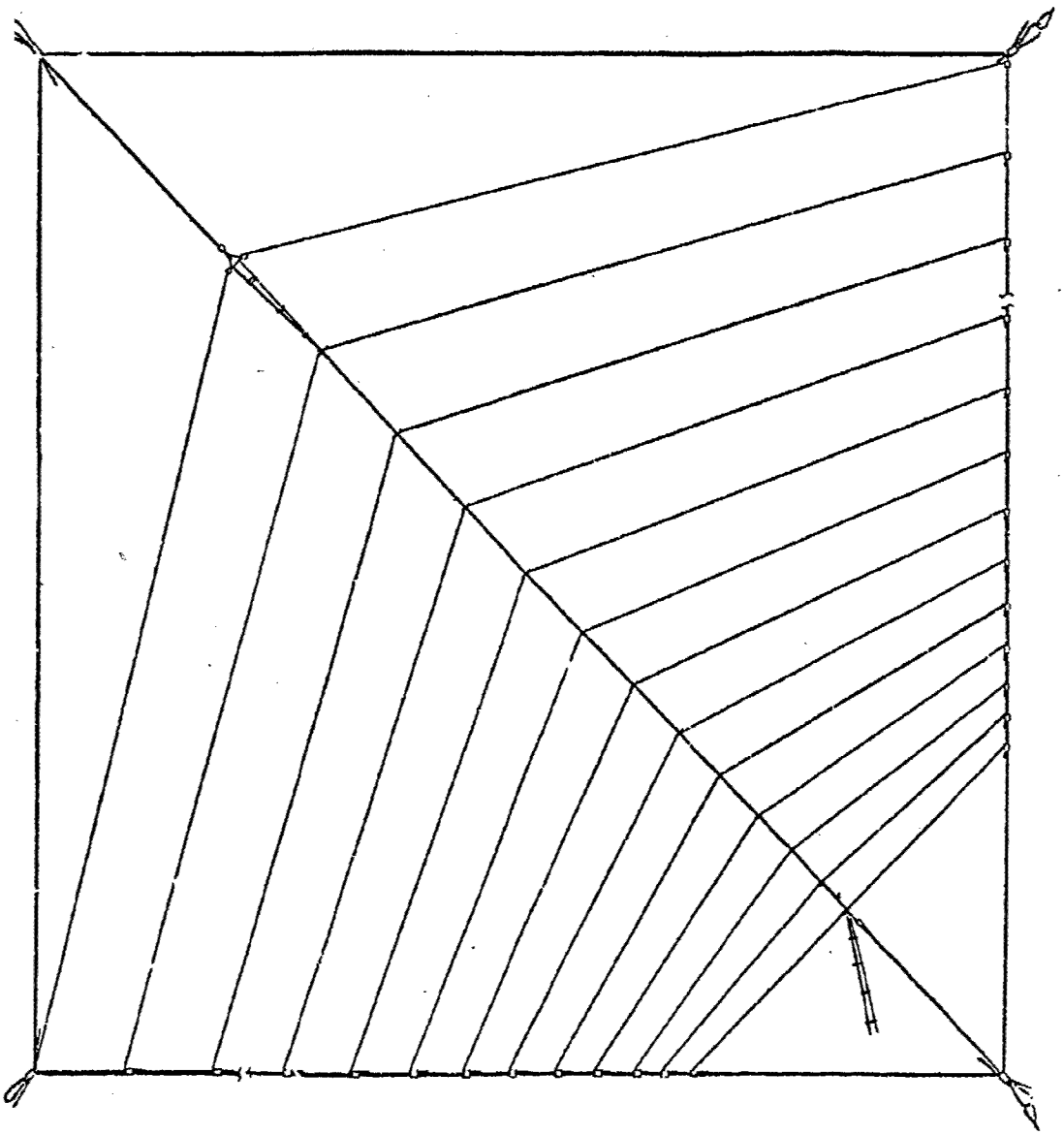

Figure 2

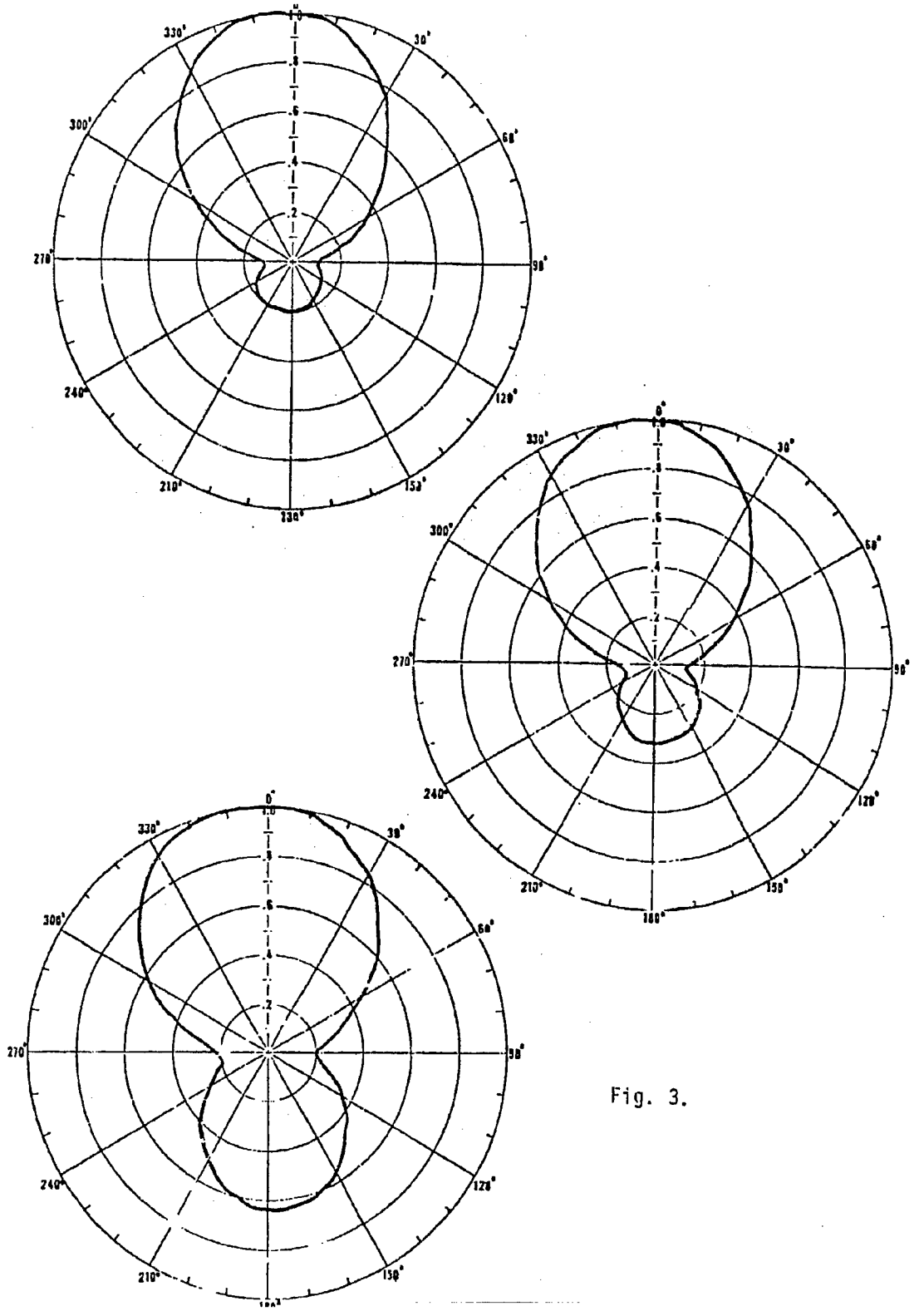

Fig. 3.

A TECHNIQUE FOR CALCULATING THE RADIATION AND IMPEDANCE CHARACTERISTICS OF ANTENNAS MOUNTED ON A FINITE GROUND PLANE OR OTHER STRUCTURES

by

R. Mittra, Y. Rahmat-Samii and P. Parhami

Electromagnetics Laboratory, Department of Electrical Engineering
University of Illinois, Urbana, Illinois 61801

ABSTRACT

In this paper we consider some aspects of determining the characteristics of antennas mounted on a finite ground plane or other platforms. We begin by briefly reviewing three available techniques, viz., wire grid modeling, combination of E and H equations; combination of Moment Method and GTD. Next we present an alternate method based on the finite-difference technique and the use of numerical Green's function. The latter approach is not only conveniently applied to the problem under consideration, but is also extendable to large size ground planes through the use of the spectral theory of diffraction.

ANTENNAS ON COMPLEX STRUCTURES

Raj Mittra
Electromagnetics Laboratory
Department of Electrical Engineering
University of Illinois
Urbana, Illinois 61801

SUMMARY

One of the most challenging problems facing the numerical and analytical electromagneticist today is the design of antennas to be mounted on complex structures, such as automobiles, ships and aircrafts. The problem is complicated for at least two reasons. First, the modeling of complex structures is in itself a difficult problem. Second, and perhaps the more important from the user's point of view, is the choice of the type of formulation best suited for the particular geometry under consideration.

Basically, two different types of integral equations may be employed to characterize the electromagnetic radiation properties of a given antenna configuration [1]. These equations take the form

$$\hat{n} \times \bar{E}^{inc}(\bar{r}) = \frac{1}{4\pi j\omega\varepsilon}\, \hat{n} \times \int (-\omega^2 \mu \bar{J}_s \phi + \nabla'_s \cdot \bar{J}_s \nabla'\phi) ds'$$

$$\bar{J}_s(\bar{r}) = 2\hat{n} \times \bar{H}^{inc}(\bar{r}) + \frac{1}{2\pi}\, \hat{n} \times \int \bar{J}_s \times \nabla'\phi \, ds' \qquad \bar{r} \in S \tag{1}$$

where $\bar{J}_s$ is the induced surface current, $\bar{E}^{inc}$, $\bar{H}^{inc}$ are the incident electric and magnetic fields, ϕ is the scalar Green's function given by

$$\phi = e^{-jk|\bar{r}-\bar{r}'|}/|\bar{r}-\bar{r}'|, \tag{2}$$

and the symbol $\int$ implies that the integral is a principal-value type.

It is well-known that the H-integral equation is fraught with numerical difficulties when applied to electrically thin structures such as wires or shells. Perhaps less well-known is the cause of the difficulty, which stems from the fact that in the formulation of the H-integral equation the boundary condition, viz. $\hat{n} \times \bar{E} = 0$ on the surface of the body, is not imposed directly but follows as a consequence of the fact that $\hat{n} \times \bar{H} = \bar{J}_s$ implies $\hat{n} \times \bar{E} = 0$ only if the surface is closed [2].

The chief advantage of the H-equation can be noted by referring to (1) wherein we observe that the kernel of the H-equation is simpler than the E-equation due to the absence of a derivative on the induced surface

current $\bar{J}_s$. Even more important is the fact that for relatively smooth surfaces the self-patch integral, for which the kernel is the most singular, is negligibly small, thus making this equation numerically attractive. In contrast, the self-patch integral in the E-equation has a substantial contribution and must be evaluated very carefully because of the presence of the singularities of the kernel.

This advantageous feature of the H-equation is absent, however, when appendages such as antennas are present in otherwise smooth structures. The H-field varies rapidly near the base of the antenna, and the self-patch principal value integral is no longer negligibly small or well-behaved. In any event, one is forced to use the E-integral equation for the wire and, consequently, it becomes necessary to employ a hybrid system comprising the H-equation for the surface and the E-equation for the wire. Of course, one may choose to use the E-equation throughout, either for a combination of surface and wire models or for a thin-wire model of the entire structure in which the surface portion is replaced by a wire mesh. Considerable work has been done in the direction of modeling a complex structure with thin wires [3]. Although convenient for many applications, this type of modeling is not necessarily the most efficient from a numerical point of view when judged on the basis of number of unknowns required to achieve a given accuracy of the solution. Also, the wire-grid modeling sometimes introduces fictitious circulating currents, and the results derived from the use of such models often show a shift in the predicted resonances from the true ones for the actual surface.

Nevertheless, many of the antenna modeling programs typically use the thin-wire codes, perhaps due to their availability and versatility. There exists a great need, however, for developing hybrid programs that handle the surface portion of a structure directly, rather than in terms of a thin-wire model, when there are wire appendages to the structure.

Although many different approaches to this problem are possible, we describe below a procedure which has been under development recently at the University of Illinois [4]. The method is based on a finite difference approximation to the differential operator appearing in the E-integral equation and the use of the concept of the numerical Green's function. For simplicity of illustration, we consider the problem of a vertical monopole antenna located on a finite ground plane (see Fig. 1). We construct the numerical Green's function by considering a single *elemental* dipole located at a finite height above the ground plane (see Fig. 2). The surface currents induced on the plate may be expressed in terms of the equation

$$\begin{Bmatrix} J_x \\ J_y \end{Bmatrix} = [Y_p] \begin{Bmatrix} E_x^i \\ E_y^i \end{Bmatrix} \tag{3}$$

where E_x^i, E_y^i are the electric field components on the plate produced by the elemental dipole radiating in free space and the matrix $[Y_p]$ is given by

$$[Y_p] = \frac{-j8\pi^2}{\eta} \begin{bmatrix} \left(k^2 + \frac{\partial^2}{\partial x^2}\right) \bar{\bar{M}} & \frac{\partial^2}{\partial x \partial y} \bar{\bar{M}} \\ \frac{\partial^2}{\partial x \partial y} \bar{\bar{M}} & \left(k^2 + \frac{\partial^2}{\partial y^2}\right) \bar{\bar{M}} \end{bmatrix} \tag{4}$$

where $M_{ij} = \int_{S_j} \phi(\rho_i, \rho')ds'$

$S = j^{th}$ surface patch

ρ_i = location of the i^{th} observation patch (5)

In the finite difference approach, the derivatives on $\bar{\bar{M}}$ appearing in (4) are computed by the conventional finite difference methods. We have found in connection with our previous work on wire junctions that the numerical differencing for the purpose of computing derivatives must be done properly, otherwise, the results will be erroneous. The critical parameter is the width of the interval used to compute the finite differences. Taking a cue from the wire-junction problem, we choose the interval to be one-half the patch size and process (4) numerically using a finite-difference form. We may use a similar numerical procedure to convert the integral representation for the wire and the wire-plate interaction and write these in matrix form as

$$\text{WIRE} \ldots \{E_z\} = [Z_w]\{J_z\} \tag{6}$$

$$\text{WIRE} + \text{PLATE} \ldots \begin{Bmatrix} E_x^i \\ E_y^i \end{Bmatrix} = [Z_{wp}]\{J_z\} \tag{7}$$

$$\text{PLATE} \ldots \{E_z\} = [Z_{pw}] \begin{Bmatrix} J_x \\ J_y \end{Bmatrix} \tag{8}$$

where J_z is the current on the wire.

Combining (3), (6), (7) and (8), we may derive a composite matrix equation which reads

$$-\left\{E_z^{inc}\right\} = \left[[Z_w] + [Z_{pw}][Y_p][Z_{wp}]\right]\{J_z\} \tag{9}$$

where E_z^{inc} is the incident field due to the given source. Inverting the matrix in large square brackets appearing in (9), we obtain a solution for the current in the wire. The currents on the plate can be derived subsequently via (6) - (8) that relate J_z and J_x, J_y. Although not shown here, extensive numerical calculations have been carried out for the above geometry--both for the antenna located at the center and near the corner of the plate, and for the antenna in a radiating or scattering mode. The results have been checked against other available data and satisfactory agreement has been observed. A somewhat more sophisticated and accurate approach based on the incorporation of the edge condition has also been developed and tested. One additional feature of the method worthy of mention here is that it shows promise for extension by a newly developed spectral domain method [5,6] for handling problems of this type to base structures that are large compared to the wavelength, even when the antenna being investigated is half-wavelength or less.

ACKNOWLEDGEMENT

The work reported in this paper was supported in part by the Army Research Office, Durham, North Carolina, under Grant DAHC04-74-G-0113.

REFERENCES

[1] A. J. Poggio and E. K. Miller, "Integral Equation Solution of Three-Dimensional Scattering Problems," Ch. 4, Computer Techniques for Electromagnetics, R. Mittra (Ed.) Pergamon Press, 1973.

[2] R. Mittra, Y. Rahmat-Samii, D. V. Jamnejad and W. A. Davis, "A New Look at the Thin-Plate Scattering Problem," Radio Science, vol. 8, no. 10, pp. 869-75, October 1973.

[3] E. K. Miller and F. J. Deadrick, "Some Computational Aspects of Thin-Wire Modeling," Ch. 4, Numerical and Asymptotic Techniques in Electromagnetics, R. Mittra (Ed.) Springer-Verlag, 1975.

[4] P. Parhami, Y. Rahmat-Samii and R. Mittra, "Antennas over Finite Ground Planes," (to be published).

[5] R. Mittra, Y. Rahmat-Samii and W. L. Ko, "Spectral Theory of Diffraction, Applied Physics, vol. 10, pp. 1-13, 1976.

[6] W. L. Ko and R. Mittra, "A Method for Combining Integral Equation and Asymptotic Techniques for Solving Electromagnetic Scattering Problems," Electromagnetics Laboratory Report 76-6, University of Illinois at Urbana-Champaign, May 1976.

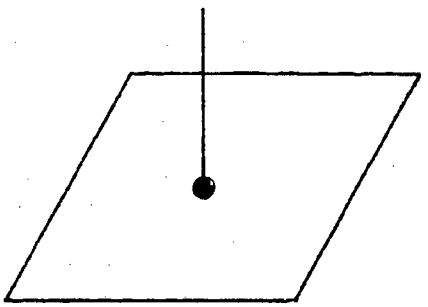

Fig. 1. Antenna on a finite ground plane.

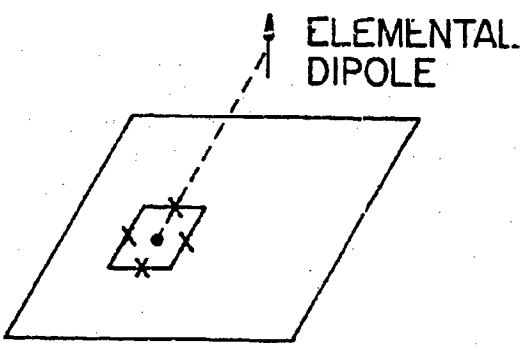

Fig. 2. Elemental dipole.

RF TRANLINE ANTENNA FOR VEHICLES

J.E. Brunner, J.R. Gruber

Cincinnati Electronics Corporation

ABSTRACT

The paper describes an electrically small antenna for helicopters and ground vehicles in the range of 2 to 30 MHz. Typical length of the radiator is 10 feet, $\lambda/50$ at 2 MHz. The radiator is mounted parallel to the vehicle surface and resembles a shorted transmission line. The antenna system includes an automatic coupler designed to achieve high radiation efficiency for Nap-of-the-Earth communications in excess of 60 miles.

SUMMARY

An efficient antenna and automatic coupler has been developed for use on small helicopters and ground vehicles in the range of 2 to 30 MHz. The low-profile radiator, with nominal length of 10 feet, is mounted parallel to the vehicle surface (spaced about 8 inches away) and resembles a transmission line shorted at the far end. A primary application is to provide Nap-of-the-Earth communications in excess of 60 miles, under all terrain conditions, for low-flying helicopters and ground vehicles. This entails use of the Near-Vertical-Incidence mode of ionospheric propagation and frequencies in the range of 2 to 8 MHz.

Typical helicopter installation is on the upper or lower surface of the tail boom, both locations giving good radiation patterns for communications via sky-wave or ground wave. Figure 1 shows a fiberglass shrouded Tranline Antenna installed on the UH-1 type helicopter. A 1-inch O.D. aluminum tube has also been utilized as the radiator on the UH-1 and OH-58 helicopters. Above 10 MHz the electrical length of the antenna is shortened by use of a vacuum switch, which permits efficient impedance matching at the higher frequencies.

Impedances presented by the Tranline Antenna are quite low at the lower frequencies. Figure 2 is a plot of both the resistive and reactive components of impedance when the antenna is mounted on two different helicopters, the UH-1 and OH-58. These data indicate that care must be taken to design the coupler for the antenna environment since the ground-plane system affects the real component of the impedance and, therefore, determines the voltage and current stress in the matching components.

The automatic coupler is located as near to the radiator feedpoint as possible to maximize overall efficiency. An objective of the coupler design has been to provide the required impedance transformation across the frequency range while maintaining the highest possible efficiency. Efficiency in excess of 90 percent is achieved even at the low end of the range where antenna Q is very high. The coupler network contains no inductors, only low-loss ceramic capacitors to accomplish the desired transformation.

Two different matching network configurations have been developed for the Tranline — both incorporate RF sensors which provide automatic tuning. One configuration is a digitally controlled L-network of binarily related, switchable, fixed capacitors. The other utilizes coded frequency information from the radio set to achieve coarse tune of the L-network with final matching accomplished by a closed-loop, tunable variable capacitor. Tuning time is 1 second for the first configuration and less than 2.5 seconds for the second.

Radiation patterns (normalized) at 6.2 MHz, measured on a 1/20 scale helicopter, are given in Figure 3. The roll plane pattern results primarily from the electric dipole mode of excitation and the yaw plane pattern results from magnetic dipole mode of excitation. These patterns do not change appreciably over the 2 to 12 MHz range although the relative RF power radiated in each mode changes considerably. Radiation pattern measurements reveal that the two modes are approximately equal in power radiated at 2 MHz, but the electric dipole mode (from currents in the fuselage) quickly dominates at higher frequencies. The electric dipole mode is about 6 db higher at 6 MHz and 10 db higher at 9 MHz. A good discussion of modal analysis applied to HF antennas in small aircraft is contained in Reference 1.

Estimates of Tranline effective gain, operating on a small helicopter such as the OH-58, have been made. The effective gain, including coupler losses, varies as follows: about - 11.5 dBi at 2 MHz, -3 dBi at 3.6 MHz, to-1 dBi at 5 MHz. Measurements made both by Cincinnati Electronics and other activities have provided confirmatory data. The gain rises very rapidly with frequency because the radiation resistance associated with the electric dipole mode is proportional to the sixth (6th) power of frequency. Attractiveness of the Tranline for HF communications results largely from its ability to excite the airframe in the dipole mode, thereby achieving much higher efficiency than would be expected from a radiator length of $\lambda/50$ at 2 MHz.

REFERENCE

1. Pavey N.A.D., "Radiation Characteristics of HF Notch Aerials Installed in Small Aircraft". Advisory Group for Aerospace Research & Development of NATO; Conference Pre-Print No. 139 on Antennas for Avionics.

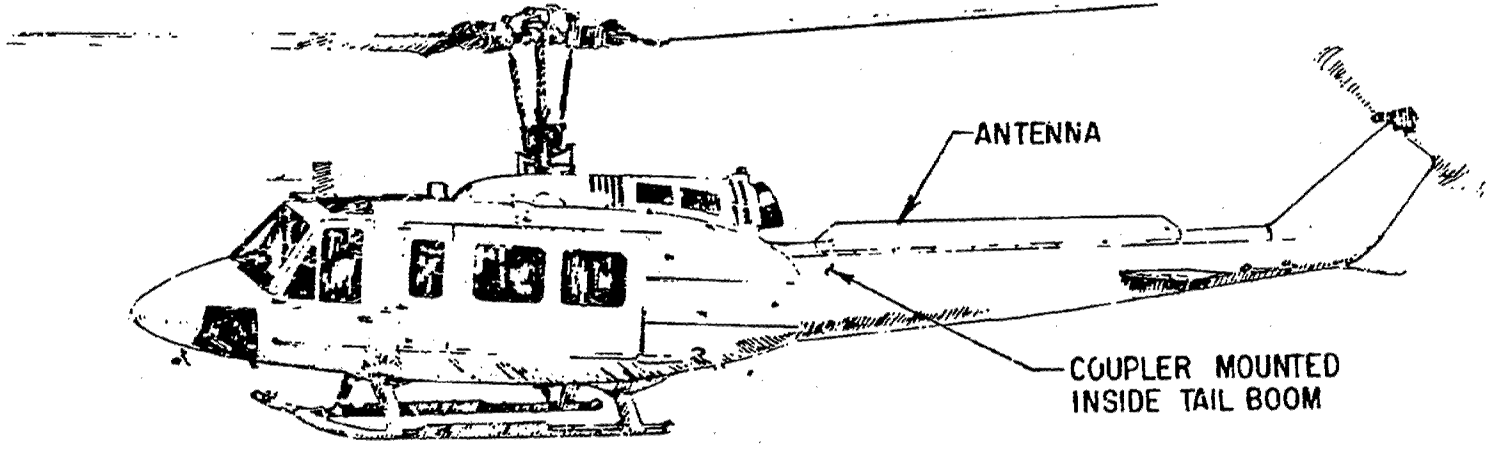

Figure 1 -HF Antenna Mounted on Helicopter (Pictorial View)

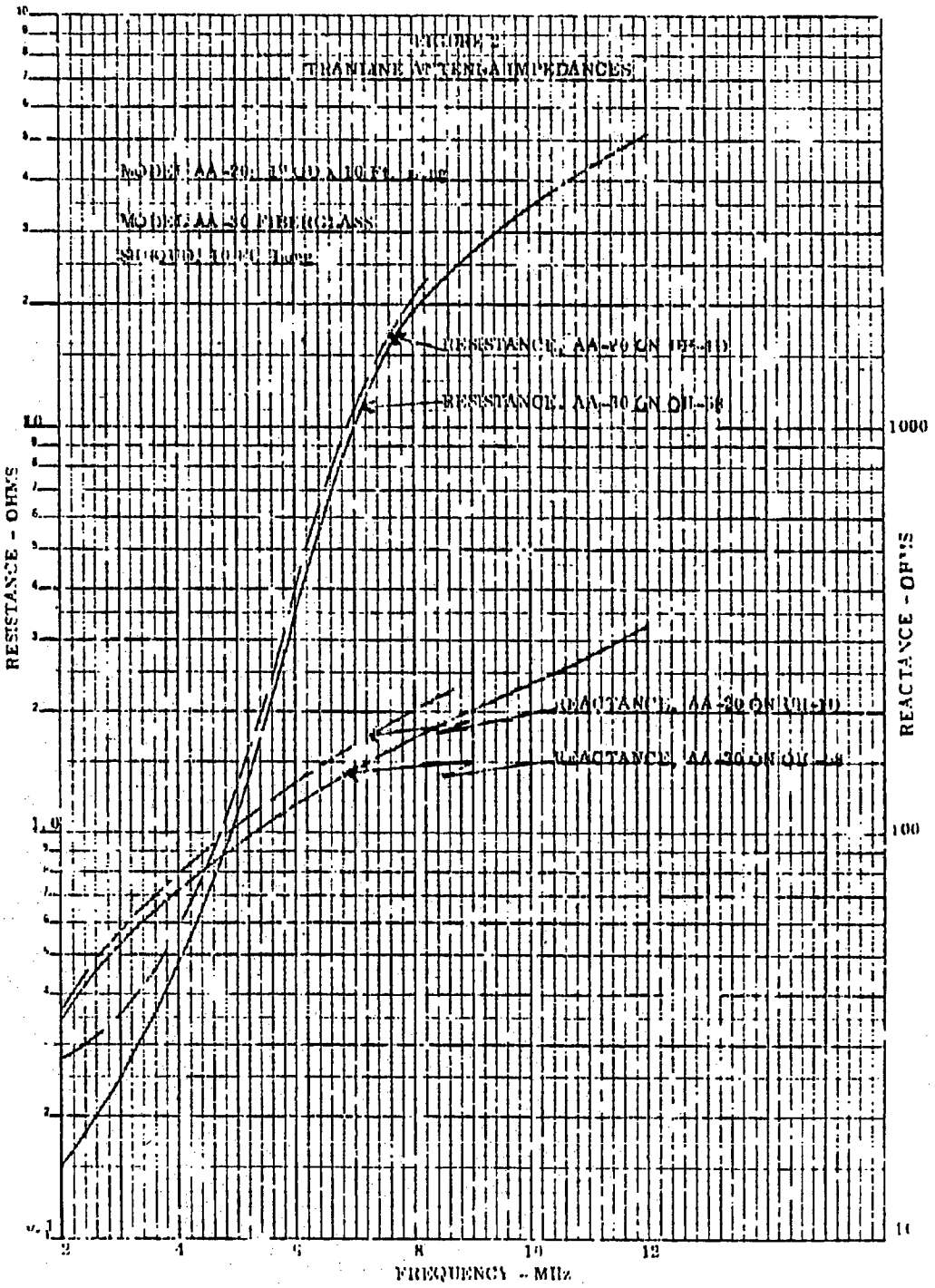
TRANLINE W TENGA IMPEDANCES
MODEL AA-20: 3" OD x 10 Ft. Long
MODEL AA-30 FIBERGLASS
RESISTANCE, AA-20 ON 195-10
RESISTANCE, AA-30 ON 011-58
REACTANCE, AA-20 ON 011-10
REACTANCE, AA-30 ON 011-58
RESISTANCE - OHMS
REACTANCE - OHMS
FREQUENCY - MHz
10
1.0
.1
1000
100
10
2
4
6
8
10
12

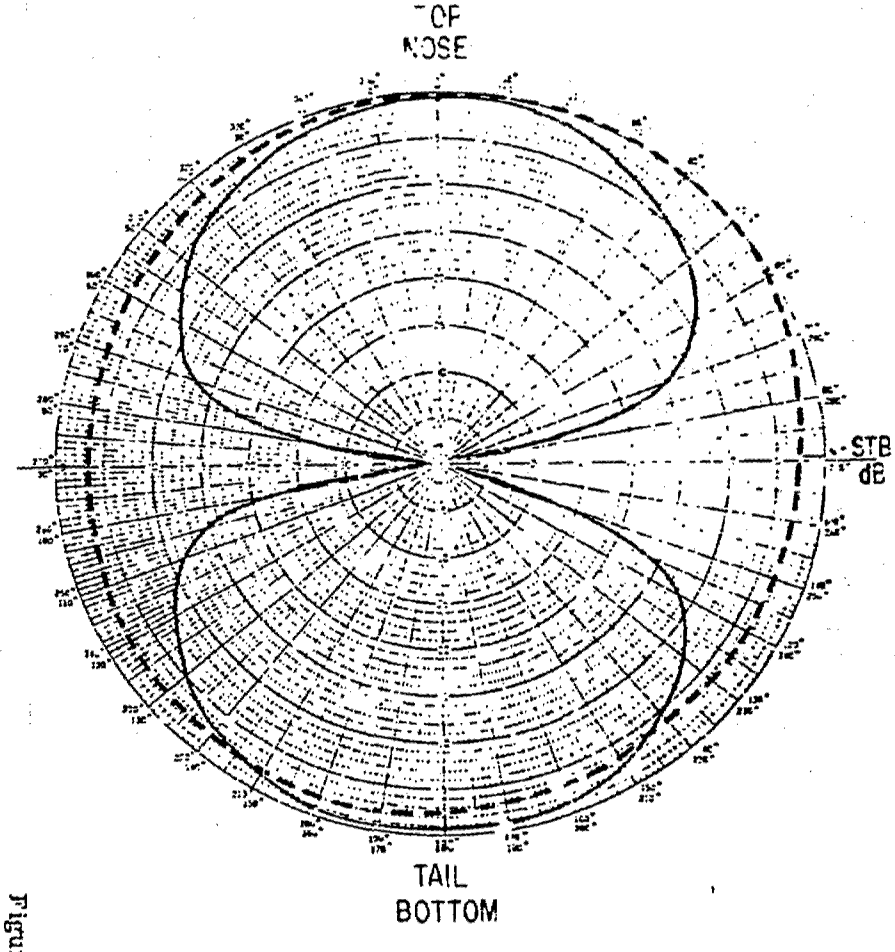

RADIATION PATTERNS - 6.2MHz

– – – ROLL PLANE (HORIZONTAL POL.)

——— YAW PLANE (VERTICAL POL.)

CINCINNATI ELECTRONICS

Figure 3

PREDICTION AND MEASUREMENT OF HF ANTENNA RADIATION PATTERNS OF HELICOPTERS*

L. N. Medgyesi-Mitschang
McDonnell Douglas Research Laboratories
St. Louis, MO

J. B. Brune
U.S. Army Electronics Command
Ft. Monmouth, N.J.

Abstract

An analytical technique for predicting radiation patterns of HF antennas on helicopters, based on the method of moments (MM) and implemented by a computer algorithm, is presented. The antennas treated by this formulation are electrically small but may extend over a considerable portion of the aircraft fuselage. Effects of lossy ground planes in the vicinity of these radiating systems are considered. An experimental test program, conducted at ECOM in conjunction with this analysis, is described.

Extended Summary

In the case of HF antennas mounted on aircraft, the interaction with the adjacent fuselage skin, the shape of the aircraft, and the positioning of the antenna can significantly affect the radiation pattern. It can be shown that an analytical technique based on the method of moments (MM) theory provides an effective approach for predicting the radiation patterns of HF antennas on helicopters.

The general approach for treating EM radiation and scattering problems using MM techniques is discussed at length in References 1-3. The formulation presented will be specialized to helicopters with off-fuselage HF radiators. An electric field integral equation (EFIE) for both the aircraft body and the off-surface radiation is used. In this analysis the helicopter fuselage is represented by a perfectly conducting body of revolution having a surface area at each longitudinal body station approximating that of the actual vehicle. The unknown currents on the body are expressed in a modal expansion.[2] The antenna is represented as an interconnected sequence of wire segments for which a MM wire representation is used.[4] The coupling between the surface currents and the antenna currents is given by a coupling matrix that includes all the interaction terms. The resulting matrix equations are solved for the unknown currents, and the power gain is computed for horizontal and vertical polarizations in the principal radiation planes.

In the MM approach, each element on the body surface and each element on the antenna is identified with a surface or wire current. In the presence of the Earth, these currents are modified. If the whole radiating system is above a perfectly conducting surface, the system can be represented by image currents. In the presence of an imperfectly conducting surface, the image currents are modified by the appropriate reflection coefficients.[5] In the case of plane wave reflections, these reflection coefficients are the Fresnel coefficients. The coefficients can be generalized to include higher order effects (such as surface waves, near-field effects, including induction and static terms) as in Norton's formulation.[6] The effect of image currents can be incorporated approximately into the radiation transfer matrices, corresponding to the fuselage surface and the wire radiator (off-surface antenna), respectively. The analytical expressions for these matrices for free-space radiation are given in References 2 and 7. In the presence of the Earth, the transfer matrices are modified with the applicable expressions, given in Reference 8.

*Research supported by the U.S. Army Electronics Command (Ft Monmouth, NJ) under Contract DAAB07-75-0907.

A computer algorithm was developed to implement this analysis. Using this algorithm, the radiation patterns were computed in free-space and in the presence of the Earth for the OH-58 and the UH-1D (Huey) helicopters over a broad frequency range (2-24 MHz). Both aircraft were equipped with a 3.04 m (10 ft) long shorted loop antenna located at various positions and with various off-sets on the rear boom.

An experimental test program using a full-scale UH-1D helicopter, equipped with a bottom-mounted loop antenna was conducted at the ECOM antenna range.[9] The UH-1D aircraft (without rotors) was mounted on a 9.1 m (30 ft) high tunnable platform. Two receiving antenna configurations were used. A horizontal dipole (resonant at 4 MHz) situated 9.1 m (30 ft) above ground and 1644 m (5408 ft) from the helicopter was utilized to receive a predominantly horizontal polarization. A 6.08 m (20 ft) vertical whip antenna was employed for receiving the vertical polarization. Details of the experimental techniques used in this range validation are given in Reference 9. The skywave contributions were monitored. The horizontal radiation patterns in both vertical and horizontal polarizations were measured by rotating the helicopter. These results were compared with the predicted patterns from the NOE-modified MM analysis over the entire HF band. Representative examples of this validation effort are shown in Figure 1. The horizontally polarized patterns for the shorted loop, rotated 20° from the bottom of the rear boom are shown in Figure 2. The computed patterns for both horizontal and vertical (θ) polarizations correlate well with the measured results for a broad frequency range.

References

1. R. Mittra, Computer Techniques for Electromagnetics (Pergamon Press, Oxford, 1973).
2. J. R. Mautz and R. F. Harrington, Radiation and Scattering from Bodies of Revolution, Appl. Sci. Res. 20, 405 (1969).
3. J. R. Mautz, Scattering from Loaded Wire Objects Near a Loaded Surface of Revolution, SURC TN74-030, Syracuse University, N.Y., January 1974.
4. J. R. Mautz and R. F. Harrington, Computer Programs for Characteristic Modes of Wire Objects, Scientific Repor No. 11, AFCRL-71-0174, March 1971.
5. E. C. Jordan, Electromagnetic Waves and Radiating Systems, (Prentice-Hall Inc., Englewood Cliffs, N.J. 1950), Chapter 1 .
6. D. L. Lager and R. J. Lytle, Fortran Subroutines for the Numerical Evaluation of Sommerfeld Integrals, UCRL-51821, Lawrence Livermore Laboratory, May 1975.
7. L. N. Medgyesi-Mitschang and J. H. Mullen, Radiation and Scattering from Asymmetrically Excited Bodies of Revolution, IEEE Trans. Antenna and Propagat. AP-24, 90, January 1976.
8. L. N. Medgyesi-Mitschang, Prediction of HF Antenna Radiation Patterns, ECOM Report 907-3, 30 April 1976.
9. J. F. Brune and J. E. Reilly, Compact HF Antenna (with Propagation Studies), ECOM Report 4366, November 1975.

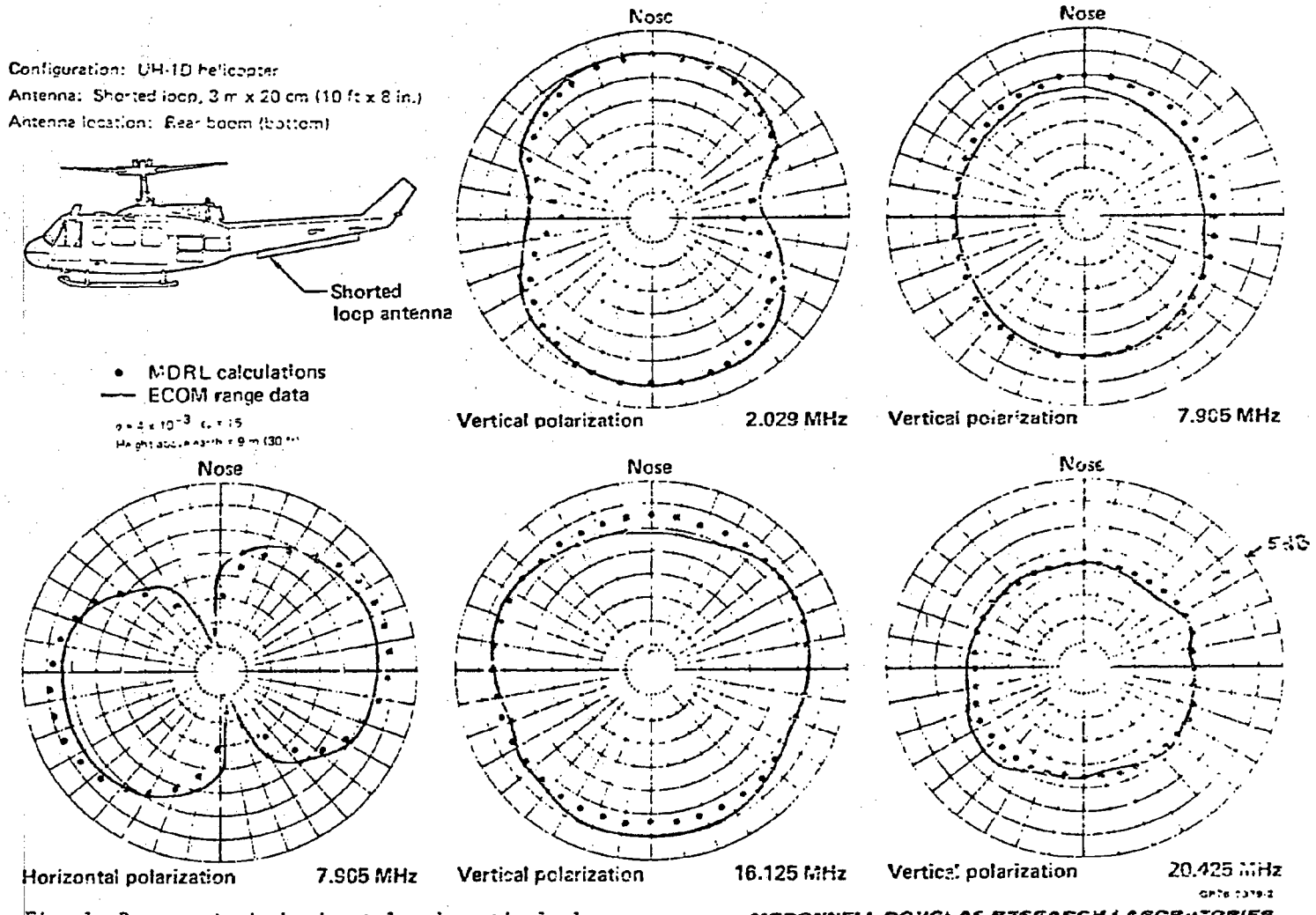

Fig. 1 Power gain in horizontal and vertical planes with NOE effects for UH-1D (bottom-mounted antenna)

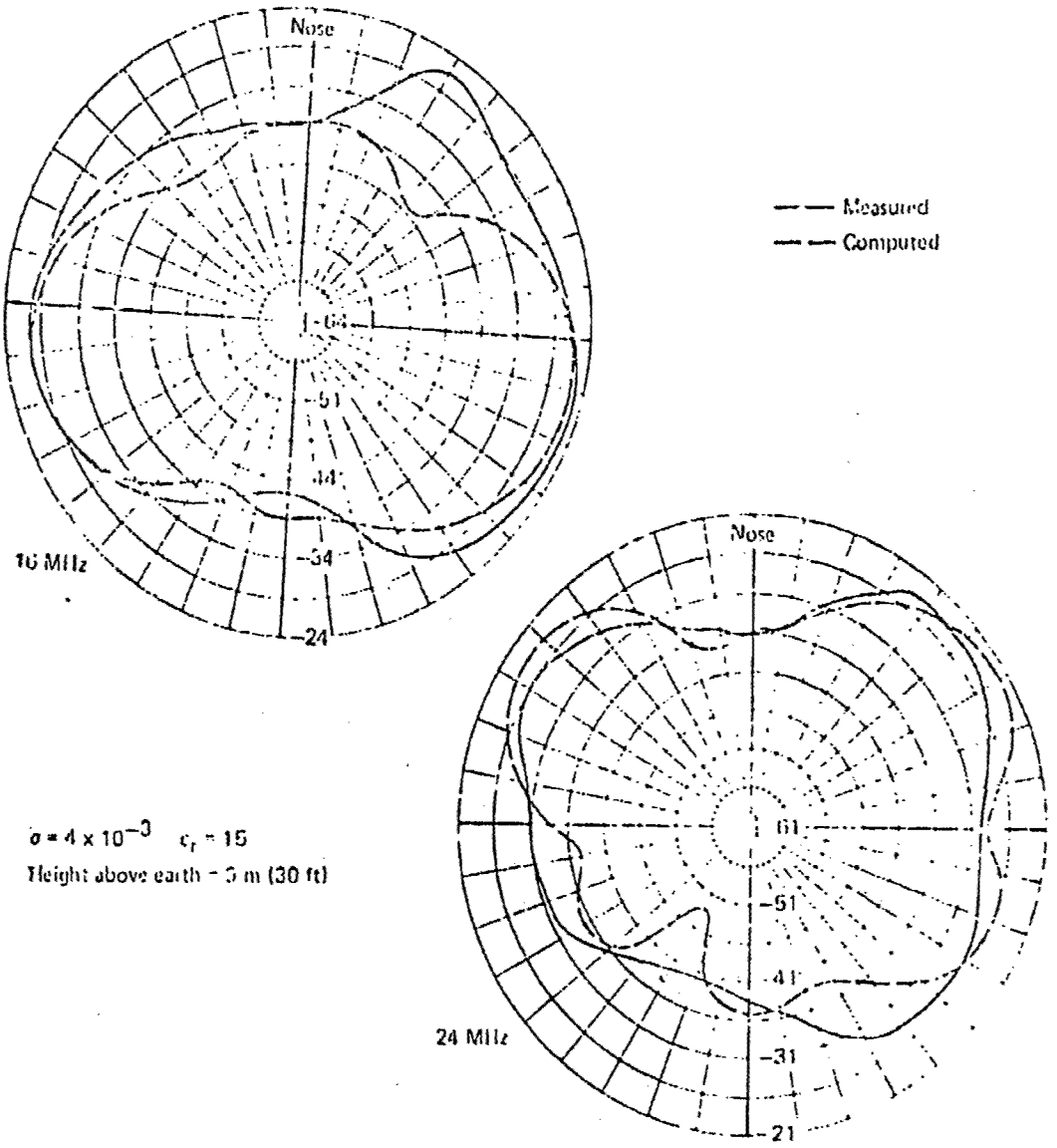

$\sigma = 4 \times 10^{-3}$ $\epsilon_r = 15$

Height above earth = 9 m (30 ft)

Configuration: UH-1D helicopter

Antenna: Shorted loop 3 m x [illegible] m (10 ft x 8 in.)

Antenna location: Rear boom (20° offset from bottom)

Polarization: horizontal

Fig. 2 Power gain in horizontal plane with NOE effects for UH-1D (antenna offset 20° from bottom)

SCALE MODEL TEST RESULTS FOR AN ELECTRICALLY-SMALL LOOP ON A UH-1D AIRCRAFT

by

H. H. Jenkins and B. J. Wilson
Engineering Experiment Station
Georgia Institute of Technology
Atlanta, Georgia 30332

and

L. Scott
U.S. Army Electronics Command
Ft. Monmouth, New Jersey 07703

ABSTRACT

Radiation pattern measurements were performed on an electrically-small loop antenna on a 40:1 model of a UH-1D airframe. Various loop feed methods were used, and the effects on radiation characteristics noted.

Major implications are that (1) unbalanced and grounded feed modes create considerable airframe reradiation, and (2) a balanced/isolated mode produces patterns comparable to free-space patterns indicating minimization of airframe reradiation effects.

Background

A feasibility study of electrically-small loops as HF (2-12 MHz) transmitting antennas for the UH-1D aircraft is underway*. One design goal is to obtain vertical polarization directivity to port and starboard; another is that the antenna should have negligible effects on flight characteristics.

Experimental investigations are being performed on a single-turn vertical loop which is (1) wrapped around the airframe perpendicular to the centerline of the aircraft, and (2) conformal in that the loop follows the airframe contour and is closely spaced to the airframe.

A 40:1 scale model is being used. Figure 1 shows the dimensions of the scale model and the location of the loop antenna. The major "resonant" features of the UH-1D are the rotor and the airframe length at the high end of the band. The specific candidate loop configuration has a circumference-to-wavelength ratio of 0.4λ at 12 MHz and is located approximately 3m from the nose of the UH-1D on the full-scale model.

An antenna configuration of the type described above could exhibit considerable electrical coupling to the airframe with attendant radiation pattern distortion. Since an electrically-small loop has inherently low efficiency, the desired radiation from the loop could be significantly altered by undesired airframe reradiation. The following reports on methods for "decoupling" the loop from the airframe in order to acquire radiation characteristics similar to free-space conditions.

---

*Work performed under Contract DAAB07-75-C-1948 with the U.S. Army Electronics Command.

Theoretical, free-space patterns were calculated in order to provide a reference point for the experimental data. Derivations given in King [1] were used with the coordinate configuration shown in Figure .. Consider a loop lying in the XY-plane with its center at the origin of the rectangular coordinates X, Y, and Z. The loop radius is b, and the drive voltage source is V_o which creates a current $I(\phi)$ in the loop element. The current distribution is given by

$$I(\phi) = \frac{-jV_o}{\pi\zeta} \sum_{-\infty}^{+\infty} \frac{e^{jn\phi}}{A_n} \qquad (1)$$

where

ζ = the characteristic impedance of the loop,

A_n = a constant representation of the nth order current mode, and

n = an integer which is the order of the current mode under consideration.

The postulated current distribution assumes that higher-order dipole modes exist in addition to the n=0 circulating magnetic mode that is normally used to calculate the far-field patterns for electrically-small loops. When the loop circumference-to-wavelength ratio is <1, the most significant modes are n=0 and n=1; the modes for n>2 can be ignored. In this case the resultant far-field E-field consists of an E_ϕ component varying as sin θ and an E_θ component varying as cos θ. The E_ϕ component is the classical loop figure-eight pattern due to the n=0 mode. E_θ is created by the higher-order dipole modes and is a major function of the loop electrical size. For the candidate UH-1D loop, theory predicts the E_θ and E_ϕ maxima are of comparable amplitude at the upper end of the 2-12 MHz band.

The loop/airframe may be viewed as an H-field element (loop) enclosing a conducting cylinder (airframe). It is known that, if equal and opposite RF currents can be induced on a conducting cylinder, reradiation effects can be minimized. The loop is physically balanced, i.e., symmetrical about the UH-1D centerline axis; therefore, it was postulated that some degree of airframe reradiation reduction might be obtained by driving the loop with an electrically balanced feed.

The concept that an antenna system that is physically and electrically balanced will produce less airframe reradiation has been previously proven to be a very successful technique for E-field elements (dipoles) mounted

---

[1] King, R. W. P. and C. W. Harrison, Antennas and Waves: A Modern Approach, MIT Press, 1969, Sections 9.4 and 9.5.

perpendicular to flat airframe structures such as wings. For example, Carter [2] demonstrated that in the HF region a dipole can be mounted with elements over and under the wing of an aircraft and coupling to the airframe minimized. Bolljahn and Reese [3] conducted similar investigations.

What is postulated is that the UH-1D loop with a balanced feed is, in essence, an H-field equivalent of the dipole/wing situation. Rather than a balanced dipole (E-field element) mounted over and under a conductor, we have a balanced loop (H-field element) enclosing a conductor. In a way, the two configurations are analogous and electrical duals.

Three loop antenna feed configurations were investigated: (1) an unbalanced mode with one side of the loop driven and one side grounded to the airframe, (2) an unbalanced mode with the feedpoints isolated from the airframe, and (3) a balanced mode with feedpoints isolated from the airframe.

Experimental Investigations

Tests were performed on the 40:1 scale model in an anechoic chamber at 400 MHz (10 MHz full-scale). Figure 2 shows the pattern measurement coordinate system. Azimuth and transverse plane patterns were obtained for both E_θ and E_ϕ field components.

Test Results

Figures 3 and 4 illustrate the feed effects on the azimuth plane characteristics. The unbalanced mode (Figure 3) creates relatively large symmetrical E_θ components with maxima port and starboard. The E_ϕ component is relatively small and highly asymmetrical. The same characteristics were evident for the balanced/grounded feed configuration. A comparison of Figures 3 and 4 demonstrate the significant change in radiation characteristics when the balanced/isolated feed is used; the Figure 4 patterns correspond very closely to the theoretical, free-space patterns. Both E_θ and E_ϕ are symmetrical, spatially orthogonal, and with maxima oriented in the proper azimuthal directions. It was also observed that the E_θ level increased considerably when the balanced/isolated mode was used.

Transverse plane patterns show that both the E_θ and E_ϕ components are essentially omnidirectional. For the unbalanced and grounded feed modes, the E_θ levels exceed the E_ϕ levels from 2 to 13 dB; however, for the balanced/isolated mode the E_ϕ level exceeds the E_θ level by about 6-9 dB - a situation that more closely approaches free-space characteristics.

Tests were also conducted on an 80:1 scale model at 400 MHz (5 MHz full-scale) and similar results obtained.

---

[2] Carter, P. S., "Study of the Feasibility of Airborne HF/DF Antenna Systems," IRE Trans. Aero. and Nav. Elec., March 1957, pp. 19-23.

[3] Bolljahn, J. T. and R. F. Reese, "Electrically-Small Antennas and the LF Aircraft Antenna Problem," IRE Trans. Antennas and Propagation, Oct. 1957, pp. 46-54.

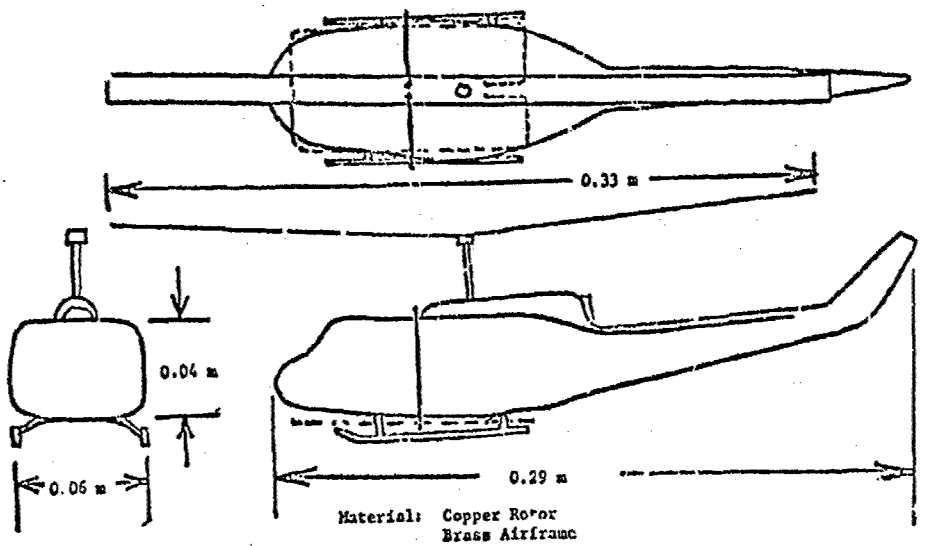

Fig. 1 Dimensions of the 40:1 UH-1D Scale Model Showing Locations of Vertical Loop (Solid Line) and Horizontal Loop (Dashed Line).

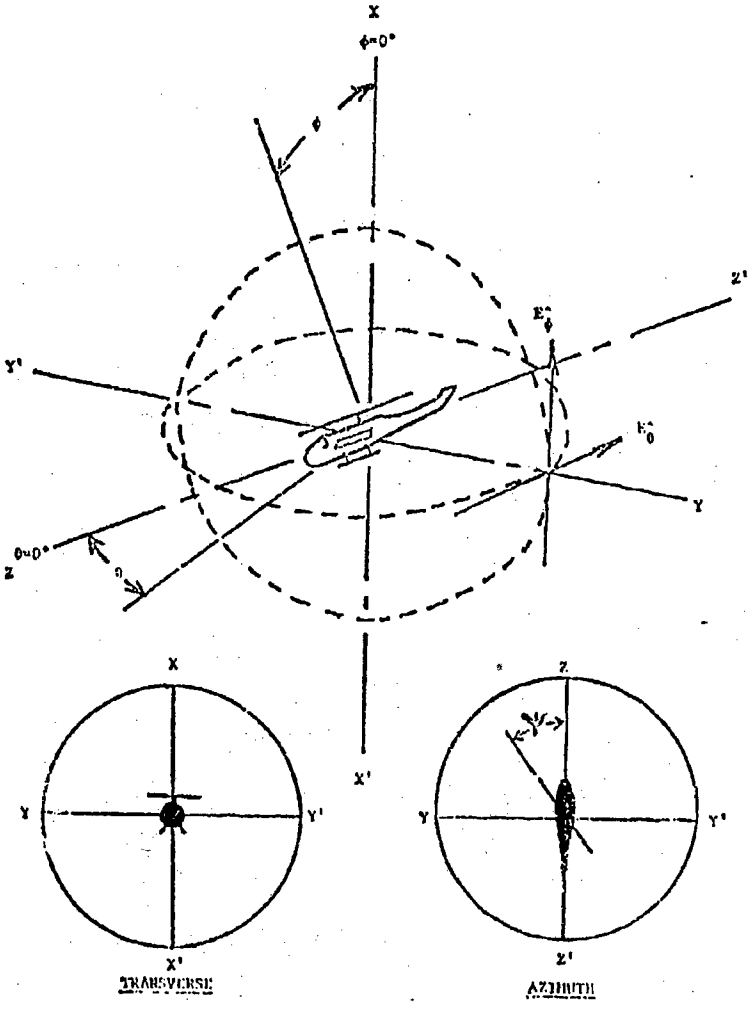

Figure 2. Pattern Measurement Coordinate System

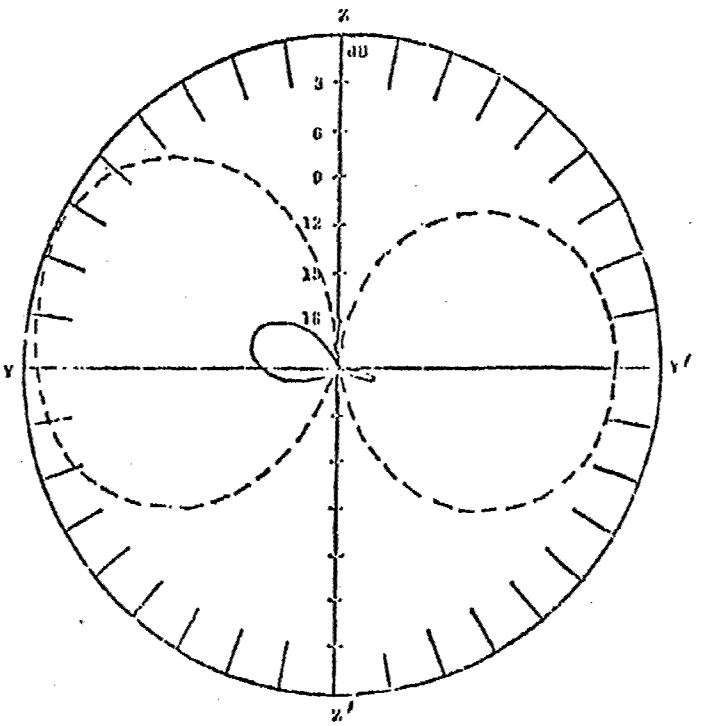

LOOP ANTENNA: VERTICAL
MODEL: 40:1
FULL SCALE FREQ.: 10 MHz
ϕ: NH

FEED: UNBAL./ISO.
RESP. PLANE: AZI.
E_θ: - - - - -
E_ϕ: ·

FIGURE 7. AZIMUTH PLANE PATTERNS, VERTICAL LOOP, 40:1 MODEL, 10 MHz, UNBALANCED FEED.

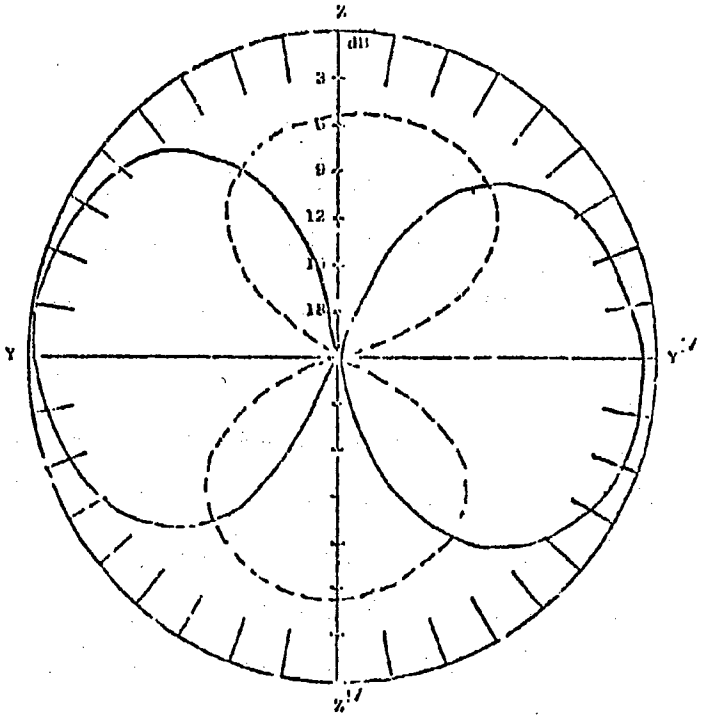

LOOP ANTENNA: VERTICAL
MODEL: 40:1
FULL-SCALE FREQ.: 10 MHz
ψ: NR

FEED: BAL./UNB.
RESP. PLANE: AZI.
E_θ: - - - - - -
E_ϕ: · · ——

FIGURE 4. AZIMUTH PLANE PATTERNS, VERTICAL LOOP, 40:1 MODEL, 10 MHz, BALANCED FEED.

COMPUTER MODELING OF SMALL ANTENNAS ON AIRCRAFT*

Johnson J. H. Wang
Electromagnetic Effectiveness Division
Applied Engineering Laboratory
Engineering Experiment Station
Georgia Institute of Technology
Atlanta, Georgia 30332

Abstract: The method of moment computational technique was employed for the analysis, design, and optimization of instrument-pod-mounted wire antennas on an aircraft. The aircraft was simulated with a wire-grid model and satisfactory numerical convergence, even for the impedance, was achieved. An anomaly, however, exists for the case of a folded dipole with ends terminated on the pod.

Summary: Galerkin's method and wire-grid modelling [1] was employed to perform a comprehensive analysis of the pattern and impedance of instrument-pod-mounted wire antennas on an aircraft. The frequencies of interest are such that the aircraft is several wavelengths long with its computer-printed top-view geometry shown in Figure 1. Each asterisk represents a junction or end point of the wire-grid structure and the wire antenna mounted on it.

Excellent convergence of the numerical solution for the radiation patterns was observed as shown in the typical example of Figure 2. Fair convergence was also achieved for the impedance calculations as shown in examples of Figure . Up to 260 segments were used for the wire-grid model and 2 to 5 minutes CPU time was needed for each calculation of the impedance and pattern. This relatively fine wire-grid structure resulted in good

*This research was supported by A. F. Contract No F33615-75-C-1223.

numerical convergence. Such fine wire gridding is required to obtain good results for complex configurations [2]. During the study, several alternate wire-grid configurations employing from 120 to 260 wire segments were examined. Although the impedance calculations required use of the maximum number of segments to establish convergence of the solution, the radiation pattern solution exhibits convergence with a fewer number of segments. Thus both reliable impedance and pattern data can be obtained using a reasonable number of wire segments in the model.

An anomaly of the computational technique was observed when it was applied to a folded dipole terminated on the instrument pod as shown in Figure 4. Rapid and large changes in impedance accompanied each variation of the segmentation scheme, and extremely poor convergence behavior was noted. However, when the folded dipole was isolated from the pod instead of being terminated on it, good convergence behavior was observed, as shown in Figure 5.

An extensive study was made to examine this anomaly. Various wire-grid configurations which were finer and more detailed than the one shown in Figure 5 were employed and they invariably led to erratic impedance data. However, reasonable and consistent pattern data were generated in all cases examined.

The erratic behavior of the impedance for the pod-terminated folded dipole is attributed to two effects. First the antenna current is directly coupled to the pod wire-grid model, thus producing strong interior coupling between the wire segments which model the pod. This coupling produces a significant interior resonance effect. Second, the wires which model the pod tend to simulate a multi-element folded dipole which tends to increase the impedance proportional to the number of grid segments.

It can be concluded that wire-grid modelling is a reliable approximation in scattering problems but should be used with caution in antenna problems. The use of a surface-type integral-equation should circumvent the numerical difficulties which have been discussed for antennas which are directly terminated on the surface.

References:

1. J. H. Richmond, "A Wire-Grid Model for Scattering by Conducting Bodies," IEEE Trans. Antenna Propagat., AP-14, November 1966, pp. 782-786.

2. Y. T. Lin and J. H. Richmond, "EM Modelling of Aircraft at Low Frequencies," IEEE Trans. Ant. Propagation, AP-23, January 1975, pp. 53-56.

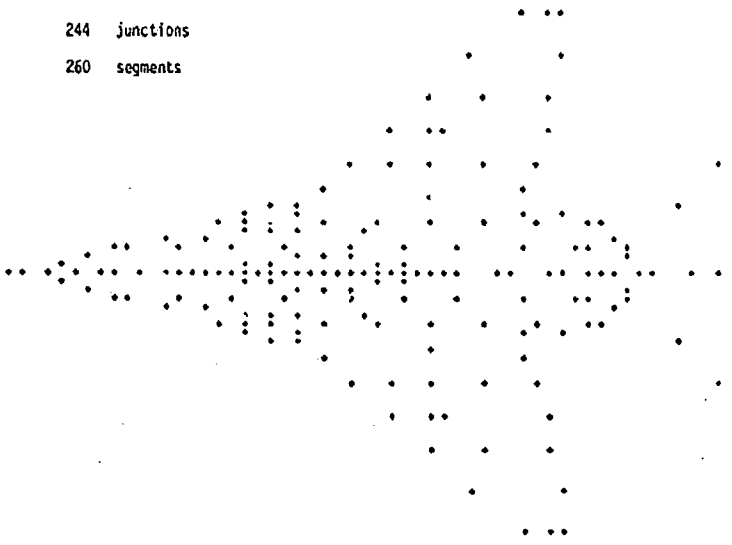

FIGURE 1.
COMPUTER PRINT-OUT OF THE TOP VIEW OF THE WIRE-GRID MODEL OF AN AIRCRAFT

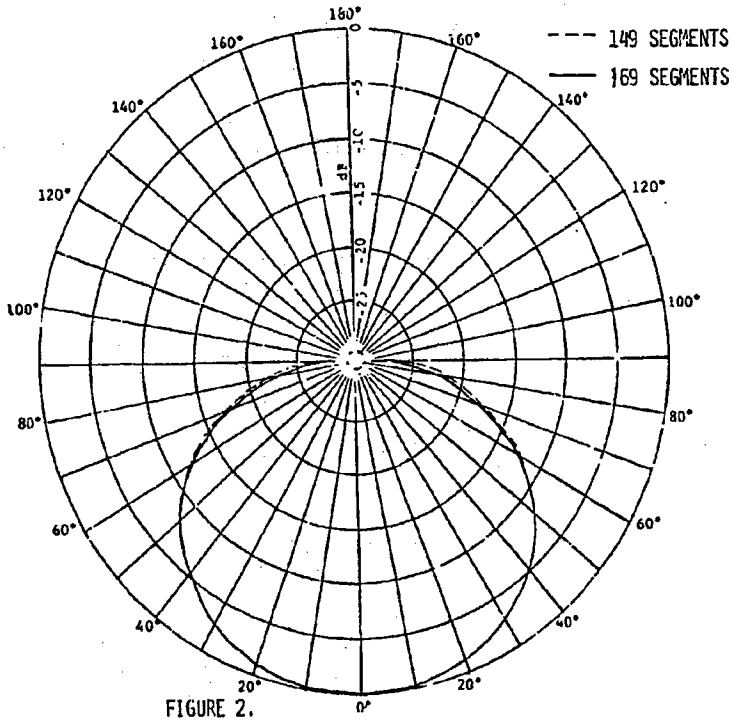

FIGURE 2.
CONVERGENCE TEST FOR PATTERN OF DIPOLE UNDER AIRCRAFT

EXAMPLES OF CONVERGENCE TESTS

	NO. POINTS	NO. SEGMENTS	IMPEDANCE (OHMS)
CASE I: FOLDED DIPOLE NEAR POD	78	84	29.36+j146.91
	96	102	29.93+j154.65
CASE II: SINGLE DIPOLE UNDER AIRCRAFT	133	149	10.38+j1.06
	153	169	12.33+j5.34

FIGURE 3.

EXAMPLE OF CONVERGENCE TESTS ON IMPEDANCE

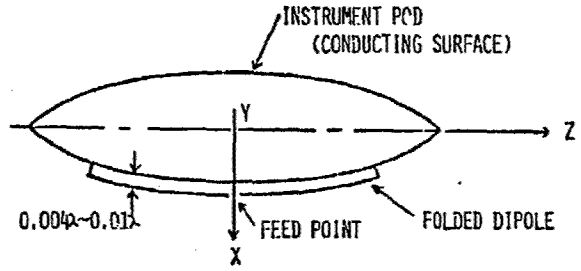

FIGURE 4. A FOLDED-DIPOLE INTEGRATED INTO THE INSTRUMENT POD

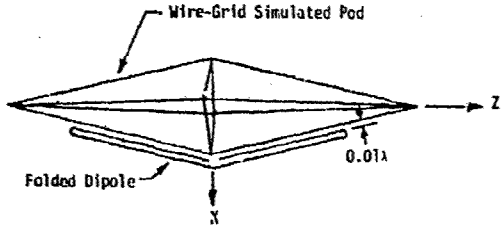

	IMPEDANCE (OHMS)	NO. OF SEGMENTS
Case I	29.4 + j146.9	84
Case II	29.9 + j154.7	102

FIGURE 5

A FOLDED DIPOLE IN CLOSE PROXIMITY TO A CONDUCTING POD

LOW PROFILE VHF ANTENNA FOR ARMOR

J.E. Brunner, G. Seward

Cincinnati Electronics Corporation

ABSTRACT

A low-profile hardened antenna has been designed for 30 to 80 MHz communications on armored vehicles. The low antenna height makes it relatively inconspicuous and yet its radiation efficiency will be adequate for most tactical needs. Its 6-inch height is less than $\lambda/60$ at 30 MHz. Use of armor plate and fiberglass-epoxy construction results in very low vulnerability to blast and shell fragments. Automatic tuning is also included.

SUMMARY

The electrically small antenna configuration herein described, is designed to provide the physical properties required for operation on tactical armored-vehicles under battle field condition. These properties include minimal visual detectability and the capability to withstand high-intensity shock blasts and shell fragments. Also, it is desired that the antenna provide a reasonable communication range (approx. 5 miles) when operated in conjunction with standard VHF military radios such as the VRC-12 and PRC-77. A further consideration is ability to mount the subject antenna using the existing mounting holes employed by the AS-1729 10-foot whip antenna.

As illustrated in figure 1, the subject antenna is basically a short monopole which is heavily top-loaded by a disc formed of armor-plate material. The disc is supported above the surface of the vehicle (tank hull, etc.) by a layer of dense dielectric material, such as fiberglass, to reduce vulnerability to damage by shell fragments and shock blast.

The disc is spaced approximately 6-inches above the vehicle surface and is 18-inches in diameter. The design is somewhat flexible in that the disc can be shaped to conform to the vehicle surface and spacing can be somewhat altered as necessary.

The heavily top-loaded monopole configuration was chosen in order to provide maximum radiation resistance, by virtue of near uniform current distribution, while maintaining minimum height to satisfy the operational constraints. For a height of 6-inches, the top-loaded configuration provides a radiation resistance of 0.36 ohm to 2.6 ohms over the 30 to 80 MHz frequency range. The antenna is matched by a series inductor and shunt capacitor which are housed in the antenna coupler unit shown in figure 1. For a minimum inductor Q of 200, the composite antenna efficiency varies from 11% at 30 MHz to 70% at 80 MHz. Matching to a 50 ohm source is accomplished as shown in the Smith Chart plot of figure 2.

Over the frequency range of interest, it has been shown that the antenna can be matched to within a 2:1 VSWR by varying the shunt capacitance in direct proportion to the series inductance. In other words, the antenna can be matched by rotation of a single shaft which drives a gear train designed to provide the necessary linear proportionality between capacitance and inductance values. The above approach is possible by virtue of the fact that the shunt capacitance value is not extremely critical even though the very short antenna represents a rather high-Q structure. For example, a 4:1 variation of the antenna resistive component (inductor loss resistance plus radiation resistance) can be matched within a VSWR of 2:1 with a given value of shunt capacity. The single shaft tuning capability, combined with control signals derived by sensing the magnitude of input RF current, current through the shunt capacitor and antenna current, has resulted in an automatic matching system which allows matching at any frequency within the 30-80 MHz band.

Communication Range

Predictions of communication range, based upon ground-to-ground VHF propagation, have been made for the Low-profile, hardened antenna. These predictions have been made for two types of radio equipment, the AN/VRC-12 and AN/PRC-77, deployed in combinations tabulated below, Table 1.

For combinations (a) and (b) Low-profile Antenna (LPA) is employed at one end of the link and the AS-1729 vehicular whip is used at the other end of the link. Combinations (c) and (d) use an LPA at both ends of the communication link.

TABLE 1 - COMMUNICATION LINKS

Antenna Types	Radio Type	Transmitter Power (Watts)
(a) AS-1729 to LPA	AN/VRC-12	40
(b) AS-1729 to LPA	AN/PRC-77	2
(c) LPA to LPA	AN/VRC-12	40
(d) LPA to LPA	AN/PRC-77	2

For each combination, the antennas are considered to be at ground level and the signal level at the 50-ohm receiver input is assumed to be one microvolt (-107 dBm). This level corresponds to a receiver input signal to noise ratio of ten dB and is equivalent to approximately 25-dB S/N ratio at the receiver audio output for the radio equipment under consideration, provided the equipment is in good operating condition.

Computations are based upon propagation over a smooth earth with the following soil constants.

	Relative Dielectric Constant	Conductivity (mhos/meter)
Poor Soil	4	0.001
Good Soil	30	0.02

Propagation curves, originally prepared by K. Bullington of Bell Laboratories, were utilized in the range computations.

Results of the range predictions are given in Table 2 for the various antenna and radio combinations listed in Table 1. Analysis of the data shows that, for a fixed set of parameters, good soil gives more than twice the range obtained over poor soil. Also, using a 40-watt radio gives about twice the range provided by a two-watt radio under the same conditions.

It is significant that the six-inch, Low profile Antenna (LPA) at each end of a tactical link will give reliable range of five miles or greater over any type soil with the 40-watt radio. Using the lower power two-watt radio two low profile antennas, Condition (d), will yield a five-mile range over good soil. Even the worst case (condition (d) over poor soil at 30 MHz) will provide adequate coverage within typical operational areas of a tank or mechanized infantry company.

TABLE 2. COMMUNICATION RANGE-STATUTE MILES

	h = 6" (Good Soil)		h = 6" (Poor Soil)	
Condition	30	60	30	60
(a) AS-1729-LPA* (40W)	19	13	8.0	5.7
(b) AS-1729-LPA* (2W)	9.4	6.4	4.0	2.8
(c) LPA-LPA* (40W)	11.0	11.0	4.6	5.0
(d) LPA-LPA (2W)	5.4	5.4	2.2	2.3

*Low-profile Antenna

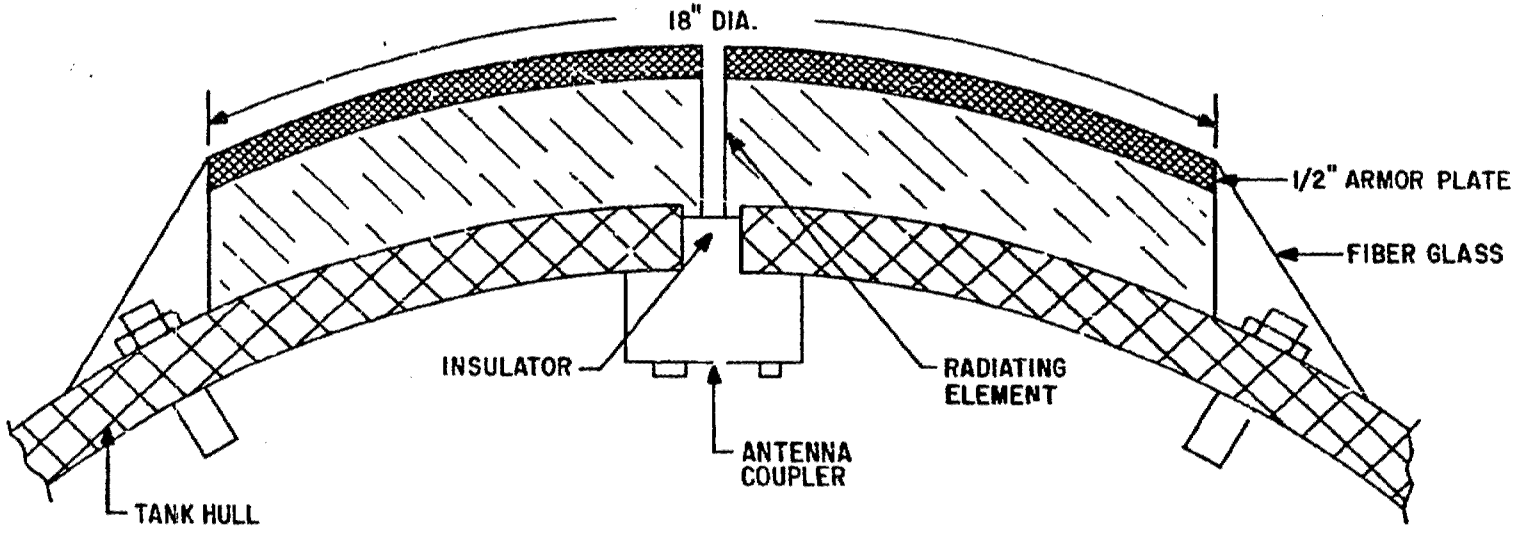

Figure 1. Low-Profile VHF Antenna

TYPICAL TUNING PATH OF LOW-PROFILE ANTENNA

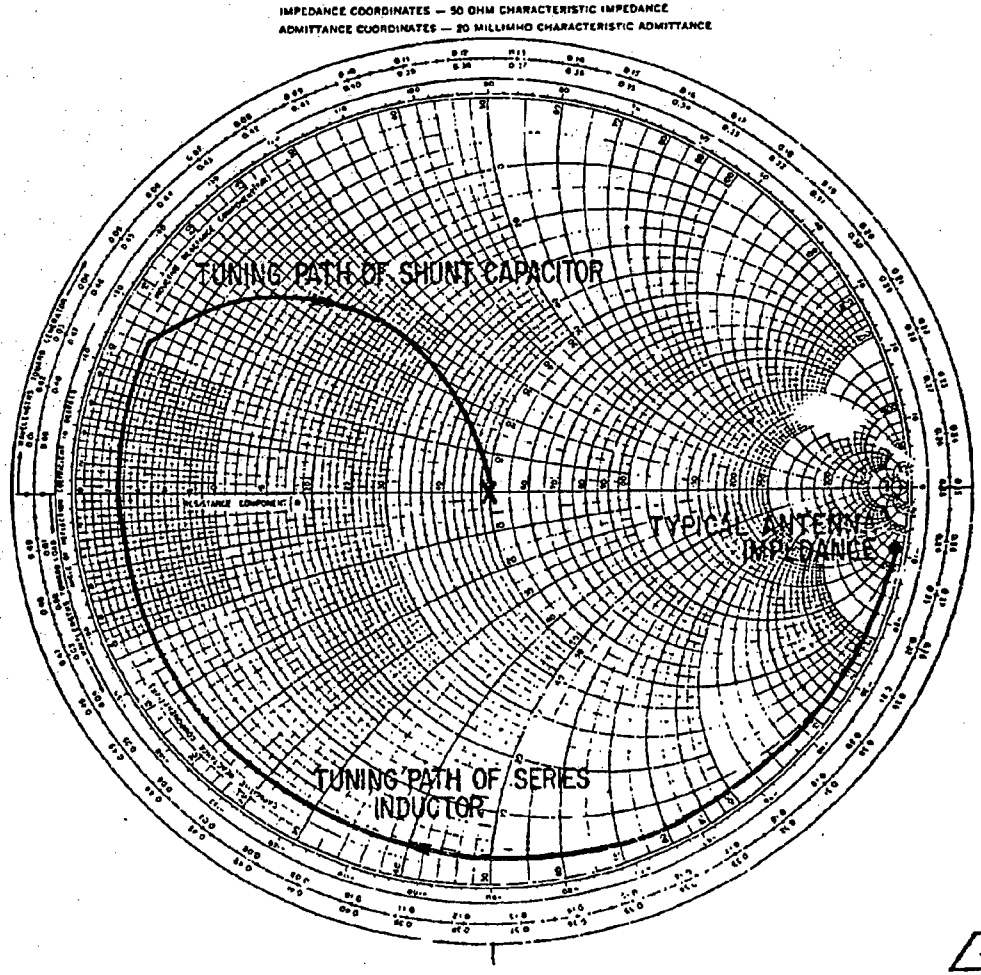

Figure 2

CINCINNATI ELECTRONICS

SLOT-ANTENNAS FOR VEHICULAR COMMUNICATION IN THE VHF RANGE

Kurt Ikrath
Communications/Automatic Data Processing Laboratory
U. S. Army Electronics Command, Fort Monmouth, New Jersey 07703

ABSTRACT

A test series was conducted establishing that long slots in the metal skin of vehicles can be used as inconspicuous but efficient antennas. The following configurations were studied: a. A "doorslot antenna" provided by a slightly opened door of a truck-carried shelter; b. A U-shaped "roof-slot antenna" in the moderately raised (false) roof of a similar truck-carried shelter; c. A "hood-slot antenna" provided by electrically isolating the motor hood of a jeep from the main body of the vehicle; and, d. A "dual-slot antenna" obtained by replacing the bustle rack on the turret of a tank by a sheet metal contraption bent around the back part of the turret.

1. INTRODUCTION

When one considers the mechanical and electromagnetic relations between idealized versions of whip and of slot antennas [1], it is evident that vehicular whip antennas can be replaced by slot antennas. In practice, however, an ideal whip antenna can be approached more closely than can an ideal slot antenna, which is flush with the surface of a vehicle.

The impedance and radiation characteristics of a vehicular slot antenna are greatly influenced by the structure of the vehicle, particularly at VHF where the vehicle dimensions are comparable to the wavelength. In this case, the metal body of the vehicle, rather than the slot, acts as an antenna coupled by means of the slot to the radio set inside the vehicle. This utilization of trucks, jeeps, and tanks as antennas by means of slots is part of a larger effort to exploit diverse stationary and mobile structures of urban environments as inconspicuous camouflaged radio antennas [2], [3].

2. JEEP HOOD-SLOT

2.1. Construction. The existing slot between the body and hood of a jeep (Fig. 1) was used to operate the jeep as an inconspicuous VHF antenna.

2.2. Impedance Matching. Principally, two methods were used to match the impedance at a chosen feed point along the hood slot to the 50-ohms transceiver impedance: (1) The slot feed point impedance was tuned to 50 ohms by reactive loading of the slot at chosen tuning points, and (2) A matching circuit in the feed cable was used to match the impedance at a chosen slot feed point to the 50-ohms feed cable. Combinations of both methods were also used in conjunction with radiation pattern control experiments.

2.3. Radiation Pattern Control. The shapes of radiation patterns were varied by changing the slot configuration, i.e., the locations of feed- and tuning points along the slot, and by unbalancing the reactive loading at symmetrically-located tuning points. This reactive loading included short- and open-load conditions as limiting cases. Figure 2 shows the different types of radiation patterns which were obtained with different configurations of slot feed loading circuits.

2.4. Communications Range. Using 30 to 40 watts of RF power and operating on 49.9 MHz, a communications range of 15 miles was achieved between the hood-slot-coupled jeep and a fixed base station employing a standard whip antenna.

3. ROOF-SLOT ANTENNA

3.1. Construction. A false roof was installed 20 cm above the actual roof of a vehicular shelter. A U-shaped slot was cut along the edges of the false roof (Fig. 3).

3.2. Impedance Matching. The same type of impedance matching as described in Section 2.2 was used.

3.3. Radiation Pattern Control. The shapes of the radiation patterns were controlled by reactive loading and interchanges of slot feed- and tuning-points, as in the case of the jeep. Typical patterns are shown in Fig. 4 relative to the pattern from a standard vehicular whip mounted on the same vehicle.

3.4. Communications Range. Using 30 to 40 watts RF power and operating on 30.7 and 49.9 MHz, a communications range of up to 18 miles was achieved with the roof-slot-coupled truck and fixed base station employing a standard whip.

4.1. Construction. A dual-slot-structure was devised to excite the tank as an antenna. Two slots (10 to 30 cm in width) were formed by the gaps between the wall of the turret and a heavy metal sheet 2.5 mm thick, 50 cm wide, and 2 x 194 cm long, which was bent around the back half of the turret. This metal sheet also served as the support for a bustle rack (Fig. 5).

4.2. Impedance Matching. The slot impedance was matched to the 50-ohms feed cable by means of a matching circuit mounted on the turret at the center of the upper slot.

4.3. Radiation Patterns. Radiation patterns obtained under symmetrical feed- and load-conditions of the dual-slot-structure on the tank are given in Fig. 6 relative to the pattern of a standard whip on the tank.

4.4. Communications Range. Employing 30- to 50-watts RF power and operating on 30.1 and 49.9 MHz, a 15-to 18-mile communications range between the dual-slot-coupled tank, the false-roof slot-coupled truck, and the hood-slot-coupled jeep was achieved.

REFERENCES

[1] H. G. Booker, "Slot aerials and their relations to complementary wire aerials (Babinet's Principle), "Journal Inst. Electrical Engrs., vol. IIIA, 1946, pp. 620-626.

[2] K. Ikrath, K. J. Murphy and W. Kennebeck, "Utilization as RF-antennas of live and of lifeless structures in natural and in man made jungles," Res. & Dev. Technical Report ECOM-4133, US Army Electronics Command, Fort Monmouth, NJ, June 1973 (AD 763 887).

[3] News Item entitled, "Need an invisible VHF antenna in a vehicle? Open the door a bit." Electronic Design, no. 8, April 12, 1975, p. 32.

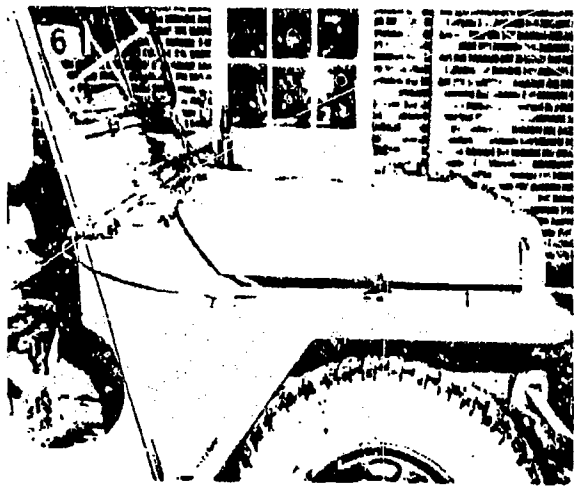

Fig. 1. Hood-slot antenna on jeep.

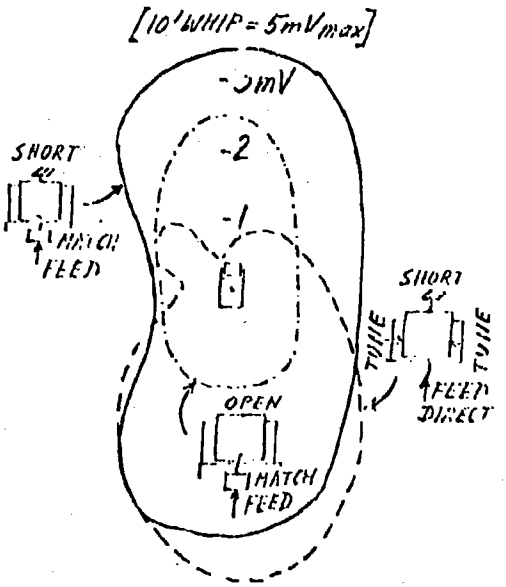

Fig. 2. Linear radiation patterns, 49.9 MHz, from hood-slot of jeep for different feed- and tuning configurations.

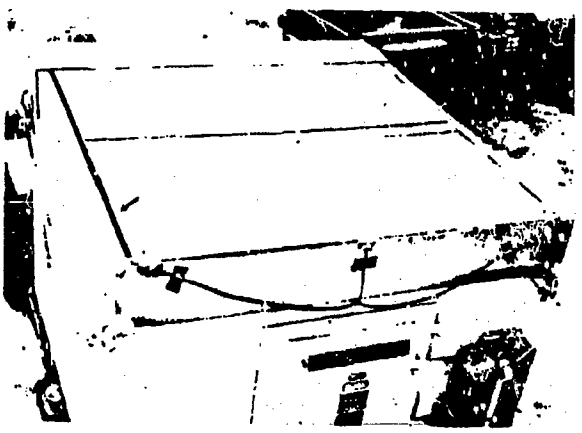

Fig. 3. Roof-slot antenna for vehicular shelter.

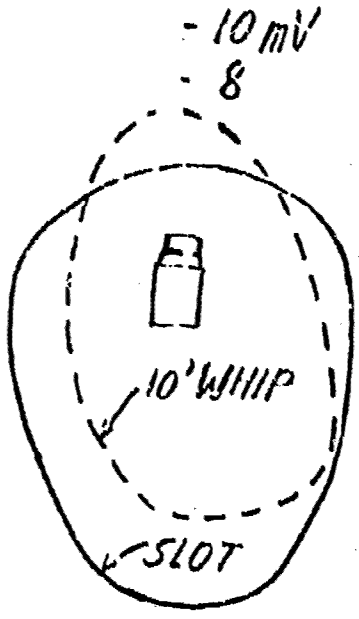

Fig. 4. Linear radiation patterns, 38 Mlz, for roof-slot-coupled truck.

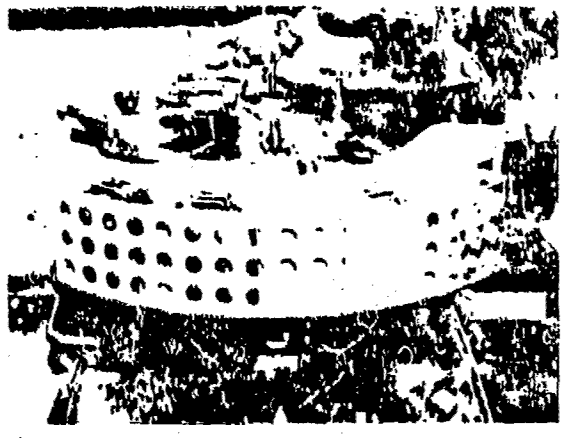

Fig. 5. Dual-slot-coupled M-60 Tank.

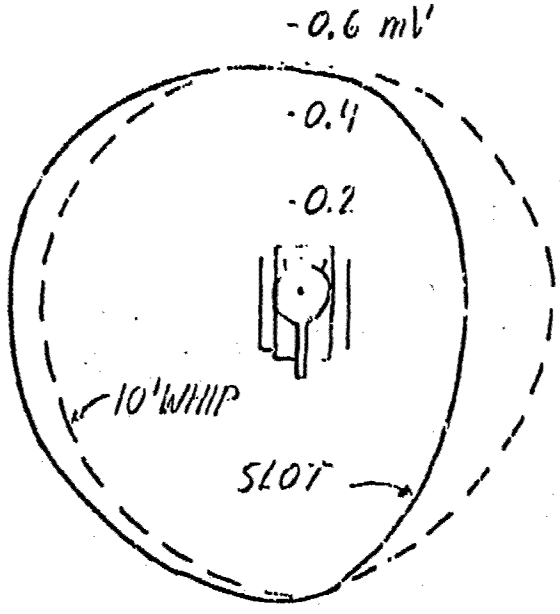

Fig. 6. Linear radiation patterns, 49.9 Mlz, from dual-slot and from 10 foot whip on M-60 Tank.

WIRE ANTENNAS IN THE PRESENCE OF MATERIAL BODIES*

E. H. Newman

The Ohio State University ElectroScience Laboratory
Department of Electrical Engineering
Columbus, Ohio 43212
23 April 1976

ABSTRACT

A moment method solution for thin wire antennas in the presence of lossy and inhomogeneous dielectric and/or ferrite bodies is presented.

I. INTRODUCTION

A theory and computer program have been developed to treat thin wire antennas in the presence of dielectric and/or ferrite inhomogeneities. These techniques are relevant to small antennas since many small antennas (i.e., loops, dipoles, etc.) are thin wire structures. Also many small antennas radiate in the presence of dielectric or ferrite inhomogeneities. Common examples are the man pack antenna and a ferrite loaded loop. It is well known that the inhomogeneity can significantly modify the far-field pattern, impedance, resonant length, efficiency, bandwidth, etc. of the antenna The theory is sufficiently general to treat lossy and inhomogeneous dielectric and ferrites, and when fully developed, the computer program will be capable of showing the effects of the inhomogeneity on the above quantities. It is important to note that the computer program will be capable of making parameter studies which would be cumbersome to do experimentally, such as showing the effects on the efficiency of varying the inhomogeneity loss tangent.

In Section II, the theory upon which the computer program is based will be outlined. The analysis is a moment method solution where the dielectric and/or ferrite is represented by equivalent volume polarization currents. The solution is accurate, but is in practice limited to electrically small inhomogeneities.

In Section III some initial results for the admittance of dielectric loaded loops are compared with experiment. Theory and experiment are in good agreement.

II. THEORY

In this section the moment method solution to thin wire antennas in the presence of a dielectric and/or ferrite inhomogeneity will be outlined.

The basic problem is illustrated in Figure 1a. Let S denote the surface of the wire structure, and let V denote the interior volume occupied by the inhomogeneity. The impressed sources $(\underline{J}_i, \underline{M}_i)$ are considered to be time harmonic

*The work reported in this paper was supported in part by Contract DAAG 29-76-G-0067 between U. S. Army Research Office, and The Ohio State University Research Foundation.

and the $e^{j\omega t}$ time dependence will be suppressed. The ambient medium (external to S and V) is free space and has parameters (μ_0,ϵ_0). The medium internal to V has parameters (μ,ϵ) which can be complex functions of position. Thus, the inhomogeneity can be inhomogeneous and lossy. In the presence of the wire and the inhomogeneity, the sources $(\underline{J}_i,\underline{M}_i)$ generate the field $(\underline{E},\underline{H})$. In free space, these sources generate the incident field $(\underline{E}^i,\underline{H}^i)$. Thus, we have known sources, $(\underline{J}_i,\underline{M}_i)$, radiating an unknown field, $(\underline{E},\underline{H})$, in the presence of two distinct inhomogeneities, which are the wire and dielectric/ferrite.

The first step in the solution is to replace the two inhomogeneities by equivalent sources. Specifically, the wire can be replaced by free space if the following surface current densities

$$\underline{J}_s = \hat{n} \times \underline{H} \tag{1}$$

$$\underline{M}_s = \underline{E} \times \hat{n} \tag{2}$$

are introduced on the surface S. The unit vector $\hat{n}$ is directed outward on S. Also, the dielectric/ferrite inhomogeneity can be replaced by free space if the volume polarization currents

$$\underline{J} = j\omega(\epsilon-\epsilon_0)\underline{E} \tag{3}$$

$$\underline{M} = j\omega(\mu-\mu_0)\underline{H} \tag{4}$$

are introduced in the volume V. The equivalent problem is shown in Figure 1b where the sources $(\underline{J}_i,\underline{M}_i)$, $(\underline{J}_s,\underline{M}_s)$ and $(\underline{J},\underline{E})$ radiate the field $(\underline{E},\underline{H})$ in the free space medium (μ_0,ϵ_0). It is important to emphasize that in the equivalent problem the sources radiate in free space. $(\underline{J}_s,\underline{M}_s)$ and $(\underline{J},\underline{M})$ are unknown currents since the field $(\underline{E},\underline{H})$ is unknown. However, they are evaluated in the course of the moment method solution.

Below we employ the following notation:

$(\underline{E}^S,\underline{H}^S)$ = fields radiated by $(\underline{J}_s,\underline{M}_s)$ in free space (5a)

$(\underline{E}^J,\underline{H}^J)$ = fields radiated by $(\underline{J},\underline{M})$ in free space (5b)

The unknown currents are expanded or approximated by a finite series of basis functions as follows:

$$\underline{J}_s = \sum_{n=1}^{N} I_n \underline{F}_n \tag{6}$$

$$\underline{J} = \sum_{n=N+1}^{N+M} I_n \underline{G}_n \tag{7}$$

$$\underline{M} = \sum_{n=N+M+1}^{N+M+P} I_n \underline{Q}_n. \tag{8}$$

$\underline{M}_S$ requires no separate expansion since it is related to $\underline{J}_S$ by

$$\underline{M}_S = Z_S \underline{J}_S \times \hat{n} \tag{9}$$

where Z_S is the wire surface impedance for exterior excitation. Note that $\underline{J}_S$, $\underline{J}$ and $\underline{M}$ are expanded in terms of N, M, and P basis functions, respectively. The unknown coefficient I_n, n=1,2,$\cdots$N+M+P, are evaluated by enforcing in some approximate sense the following three conditions:

$$\underline{E}^i + \underline{E}^s + \underline{E}^J = 0 \quad \text{interior to S} \tag{10}$$

$$\underline{E}^i + \underline{E}^s + \underline{E}^J = \underline{E} \quad \text{in V} \tag{11}$$

$$\underline{H}^i + \underline{H}^s + \underline{H}^J = \underline{H} \quad \text{in V.} \tag{12}$$

Without going through the details, enforcing Equations (10-12) leads to the following system of simultaneous linear equations

$$[Z]I = V \tag{13}$$

which can be solved for the vector I containing the unknown coefficients from Equations (6-8).

The advantage of the above solution is that no assumptions are necessary concerning the magnitude of the currents on the wire or in the dielectric/ferrite inhomogeneity. Thus, the solution can approach the exact solution as the number of unknowns is increased. All mutual interactions and surface waves are automatically included. Further, provided subsectional basis functions are used, the method is applicable to fairly arbitrary wire and inhomogeneous dielectric/ferrite geometries.

In the next section a comparison between computed and measured admittance for a dielectric loaded square loop will be given.

III. NUMERICAL RESULTS

In this section numerical data will be presented for the admittance of a dielectric loaded loop antenna. The computations are made using the techniques described in the previous section. Referring to Equations (6-8), piecewise sinusoidal modes are employed to expand the wire current, and constant current rectangular parallelpiped cells are used to expand the volume polarization currents. Piecewise sinusoidal test on weighting functions are used on the wire, while delta functions are used in the dielectric.

The geometry for the dielectric loaded square loop is shown in Figure 2. The dielectric is centered in the square loop. The loop has side lengths s, and thus the loop circumference is L=4s. The inhomogeneity has dimensions d_1 by d_2 by d_3 and a relative dielectric constant $\epsilon_r=\epsilon/\epsilon_0$. For the data to be present here s = 3 in., d_1 = 2.36 in., d_2 = 2.60 in., and d_3 = 1.02 in. The loop is constructed from tin coated copper wire of radius 0.016 in. Figures 3 and 4 show the measured and calculated loop conductance versus L in wavelengths, and for ϵ_r=2.1 and 10, respectively. Although the susceptance is not shown here, the agreement is equally good.

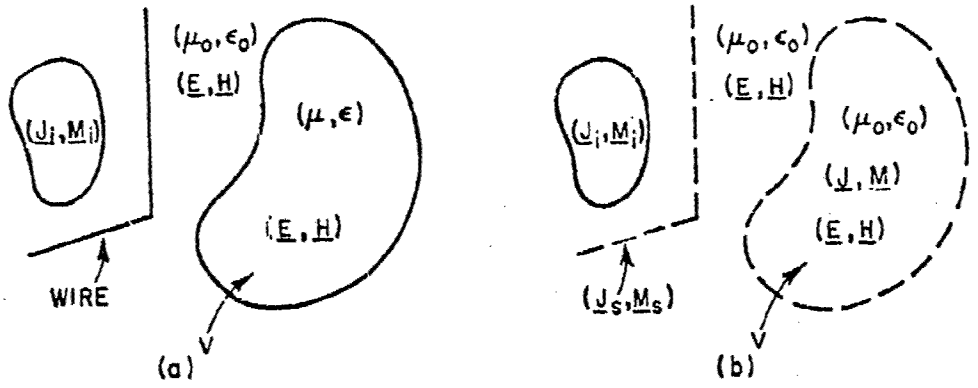

Figure 1a. The original problem. Figure 1b. The equivalent problem.

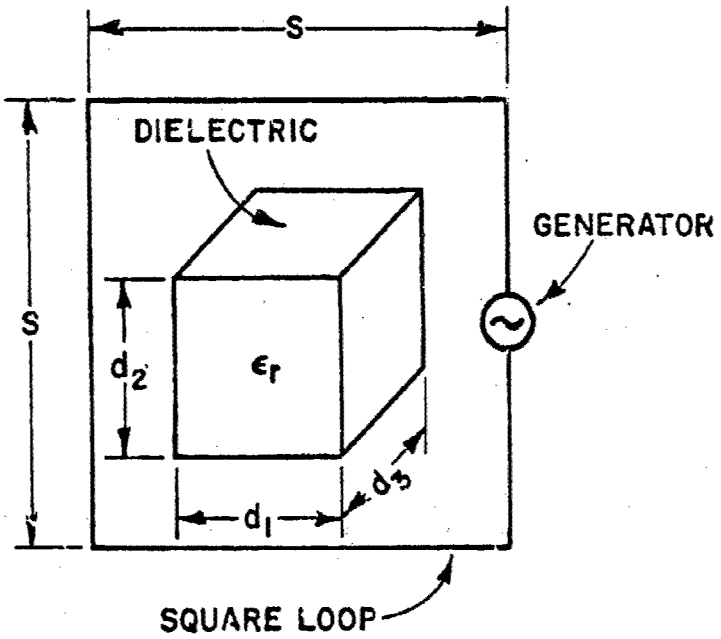

Figure 2. Geometry for dielectric loaded square loop.

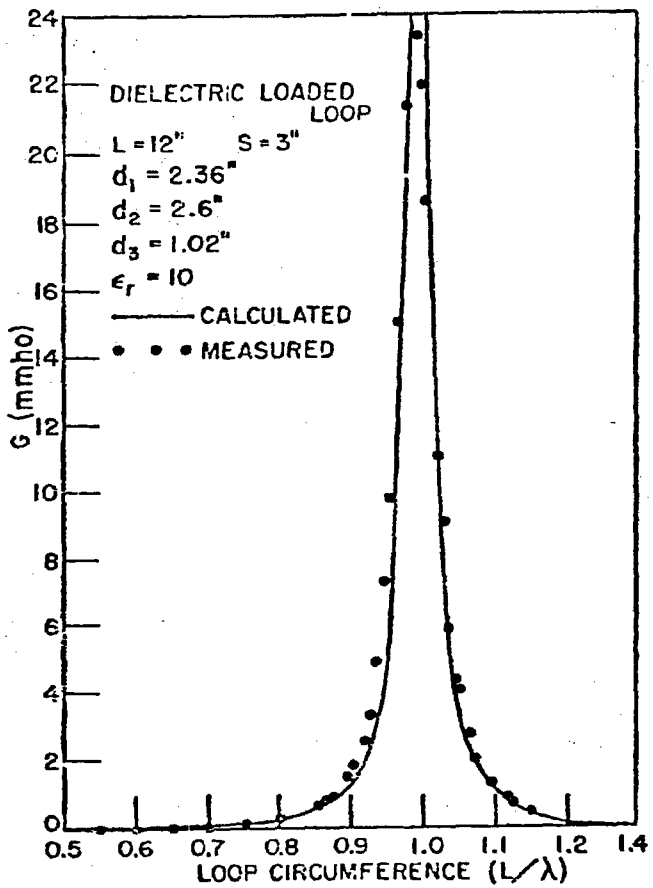

Figure 3. Dielectric loaded loop conductance with ϵ_r = 2.1.

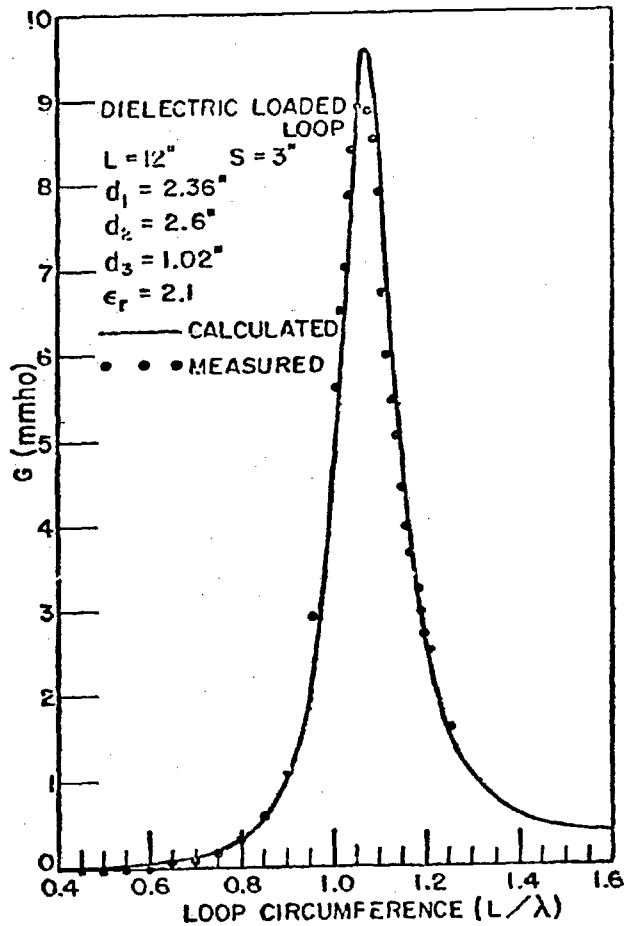

Figure 4. Dielectric loaded loop conductance with ϵ_r = 10.

COUPLING OF SMALL ANTENNAS WITH HUMAN BODY*

Kun-Mu Chen and Dennis P. Nyquist

Department of Electrical Engineering and Systems Science
Michigan State University
East Lansing, Michigan 48824

ABSTRACT:

The problem of the coupling between the near-zone EM fields of an electrically-small (whip) antenna and the body of a radio operator is studied. The impedance characteristics of the antenna and the EM fields induced inside the operator's body are determined. The EM radiation from the combined antenna-body structure is studied.

SUMMARY:

When an electrically-small (whip) antenna is carried on the back of a radio operator, two important questions which arise are: (1) what are the effects of the human body on the performance of the antenna? and (2) what are the EM fields induced in the operator's body and their possible biological effects? An investigation of the currents and EM fields in a radiating system consisting of the small antenna coupled with a biological body is necessary to answer these questions.

Consider a thin-wire antenna of radius "a" located in free space adjacent to a conducting biological body having conductivity σ and permittivity $\epsilon = \epsilon_r \epsilon_0$ as indicated in Figure 1. The antenna is excited at frequency ω by a slice generator of voltage V_0. This excitation maintains a current $\vec{I}(\vec{r})$ in the in the antenna and an induced internal electric field $\vec{E}(\vec{r})$ in the body. $\vec{I}(\vec{r})$ and $\vec{E}(\vec{r})$ are coupled to one another.

The induced field $\vec{E}^i$ maintained by $\vec{I}(\vec{r})$ in the antenna can be expressed as

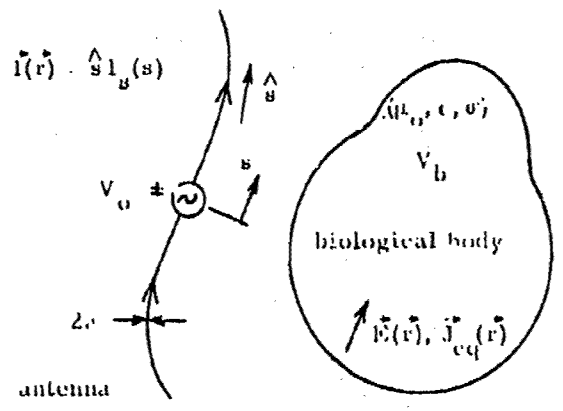

Figure 1. Geometrical arrangement of thin-wire antenna coupled to conducting biological body.

*This research was supported by the Army Office of Research under Grant DAAG29-76-G-0201.

$$\vec{E}^i(\vec{r}) = \int_{ant} \vec{I}(\vec{r}') \cdot \overleftrightarrow{G}(\vec{r}, \vec{r}')\, ds' = \text{induced field maintained by } \vec{I} \qquad (1)$$

while the scattered field $\vec{E}^s$ maintained by induced conduction and polarization currents $\vec{J}_{eq}(\vec{r}) = [\sigma + j\omega(\epsilon - \epsilon_0)]\vec{E}(\vec{r}) = \tau \vec{E}(\vec{r})$ in the biological body (τ equivalent complex conductivity) is given, as indicated by Van Bladel [1], by

$$\vec{E}^s(\vec{r}) = \int_{V_b} \vec{J}_{eq}(\vec{r}') \cdot \left[\text{P. V.}\, \overleftrightarrow{G}(\vec{r}, \vec{r}') - \frac{\overleftrightarrow{I}\delta(\vec{r} - \vec{r}')}{j3\omega\epsilon_0}\right] dv' = \text{scattered field maintained by } \vec{J}_{eq} \qquad (2)$$

where P. V. denotes the principal value and $\overleftrightarrow{G}(\vec{r}, \vec{r}')$ is the free-space tensor Green's function

$$\overleftrightarrow{G}(\vec{r}, \vec{r}') = -j\omega\mu_0\left[\overleftrightarrow{I} + \frac{\nabla\nabla}{k_0^2}\right] G_0(\vec{r}, \vec{r}')$$

and $G_0(\vec{r}, \vec{r}') = e^{-jk_0R}/4\pi R$ is the scalar free-space Green's function with $k_0 = \omega\sqrt{\mu_0\epsilon_0}$ and $R = |\vec{r} - \vec{r}'|$. In the biological body, the total field is

$$\vec{E}^i + \vec{E}^s = \vec{E} \quad \ldots \text{ at points in the body,} \qquad (3)$$

while the boundary condition at the surface of the antenna requires

$$\hat{s} \cdot (\vec{E}^i + \vec{E}^s) = -V_0\delta(s) \quad \ldots \text{ at points on antenna surface.} \qquad (4)$$

Substituting appropriate forms for $\vec{E}^i$ and $\vec{E}^s$ from equations (1) and (2) into equations (3) and (4) leads to the following pair of coupled integral equations for $\vec{I} = \hat{s}I_s$ and $\vec{E}$:

$$\left[1 + \frac{\tau(\vec{r})}{j3\omega\epsilon_0}\right]\vec{E}(\vec{r}) - \text{P. V.} \int_{V_b} \tau(\vec{r}')\vec{E}(\vec{r}') \cdot \overleftrightarrow{G}(\vec{r}, \vec{r}')\, dV'$$

$$\int_{ant} I_s(s')\hat{s}' \cdot \overleftrightarrow{G}(\vec{r}, \vec{r}')ds' \quad \ldots \text{ for } \vec{r} \text{ in } V_b \qquad (5)$$

$$\hat{s} \cdot \int_{ant} I_s(s')\hat{s}' \cdot \overleftrightarrow{G}(\vec{r}, \vec{r}')ds' + \hat{s} \cdot \int_{V_b} \tau(\vec{r}')\vec{E}(\vec{r}') \cdot \overleftrightarrow{G}(\vec{r}, \vec{r}')\, dV'$$

$$= -V_0\delta(s) \quad \ldots \text{ for } \vec{r} \text{ on antenna surface.} \qquad (6)$$

Equations (5) and (6) can be solved numerically by the method of moments, following the method described by Livesay and Chen [2], to determine the antenna current $I_s(s)$ and the internal field $\vec{E}$ induced in the body.

Based on $I_s(s)$ the input impedance to the antenna can be determined. From the value of $\vec{E}$, possible biological effects can be evaluated. Using $\vec{I} = \hat{s}I_s$ and $\vec{J}_{eq} = \tau\vec{E}$ (induced current in the body), the EM field radiated by the composite antenna-body system can be determined.

Numerical results are obtained for a dipole antenna adjacent to a biological body with a rectangular-cylindrical shape as indicated in Figure 2. The short dipole of half-length $h = 0.1\ \lambda_o$ is excited at a frequency of $f = 50$ MHz (free-space wavelength $\lambda_o = 6$ m) by an input current $I_o = 1.0$ A. At this frequency, $\sigma = 0.75$ mhos and $\epsilon_r = 89.0$ in the biological body. All dimensions (selected to model a human radio operator) are given in the figure. If the dipole current is approximated by the sinusoidal distribution $I_x(x) = (I_o/\sin k_o h) \sin k_o(h-|x|)$, then equation (5) can be solved independently for $\vec{E}$ since its right-hand side becomes a known impressed field. The magnitude $|\vec{E}|$ of the induced field in each of the 28 body partitions used to obtain the numerical solution is indicated in the figure. The input power to the antenna is $P_{in} = 5.2$ W while the power dissipated in the biological body is $P_d = 0.282$ W.

For reference, the magnitude $|\vec{E}|$ of the field induced in the same body by a plane wave, propagating in the z-direction and polarized in the x-direction as shown, of power density $S_o = 10$ mW/cm^2 is indicated in Figure 3. The dissipated power is $P_d = 12.9$ W in this case. Comparison of Figures 2 and 3 shows that the electric field induced in the body by the short dipole might reach hazardous levels if the input power to the dipole were increased.

The dipole impedance can be calculated in terms of the assumed sinusoidal current and the total field $E_x = E_x^i + E_x^s$ at its surface by the variational formula (based on equation (4))

$$Z_{in} = Z_o + Z_p = -\frac{1}{I_o^2}\int_{-h}^{h} I_x(x)\, E_x(x)\, dx$$

$$Z_o = -\frac{1}{I_o^2}\int_{-h}^{h} I_x(x)\, E_x^i(x)\, dx\,, \qquad Z_p = -\frac{1}{I_o^2}\int_{-h}^{h} I_x(x)\, E_x^s(x)\, dx$$

where Z_o is the impedance of an isolated dipole (when $E_x^s = 0$) and Z_p is the perturbation to the dipole impedance due to its coupling with the biological body (when $E_x^s \neq 0$). Tables 1 and 2 indicate the values of Z_p = perturbation impedance, Z_{in} = input impedance, P_{in} = input power, P_d = power dissipated in body, P_r = radiated power, and the power ratios P_d/P_r and P_d/P_{in} for a dipole of half-length $h = 0.1\ \lambda_o$ located with various values of x_o and z_o. It is found that both Z_p and P_d/P_{in} depend strongly on x_o while they steadily decrease for increasing z_o. Table 3 indicates the dependence of the same quantities upon location x_o ($z_o = 0.2$ m - fixed) for a dipole of near-resonant length $h = 0.25\ \lambda_o$; it is evident that Z_p and P_d/P_{in} are relatively insensitive to changes in x_o compared with the corresponding variations for a short dipole.

REFERENCES:

1. J. Van Bladel, "Some remarks on Green's dyadic for infinite space," IRE Trans. Antennas and Prop., vol. AP-9, pp. 563-566, Nov. 1961.

2. D. Livesay and K. M. Chen, "Electromagnetic fields induced inside arbitrarily-shaped biological bodies," IEEE Trans. Microwave Theory and Tech., vol. MTT-22, pp. 1273-1280, Dec. 1974.

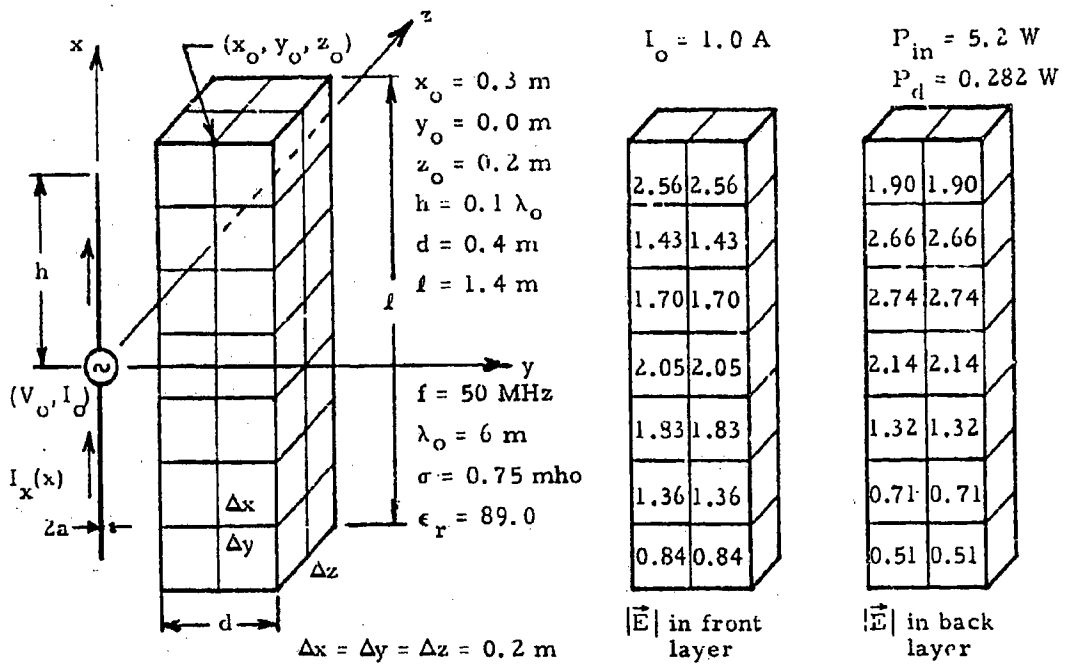

Figure 2. Electric field (magnitude in V/m) excited in biological body by short-dipole antenna (h = 0.1 λ_o, h/a = 100, Z_{in} = 10.4 - j662.1 ohms, I_o = 1.0 A, P_{in} = 5.2 W).

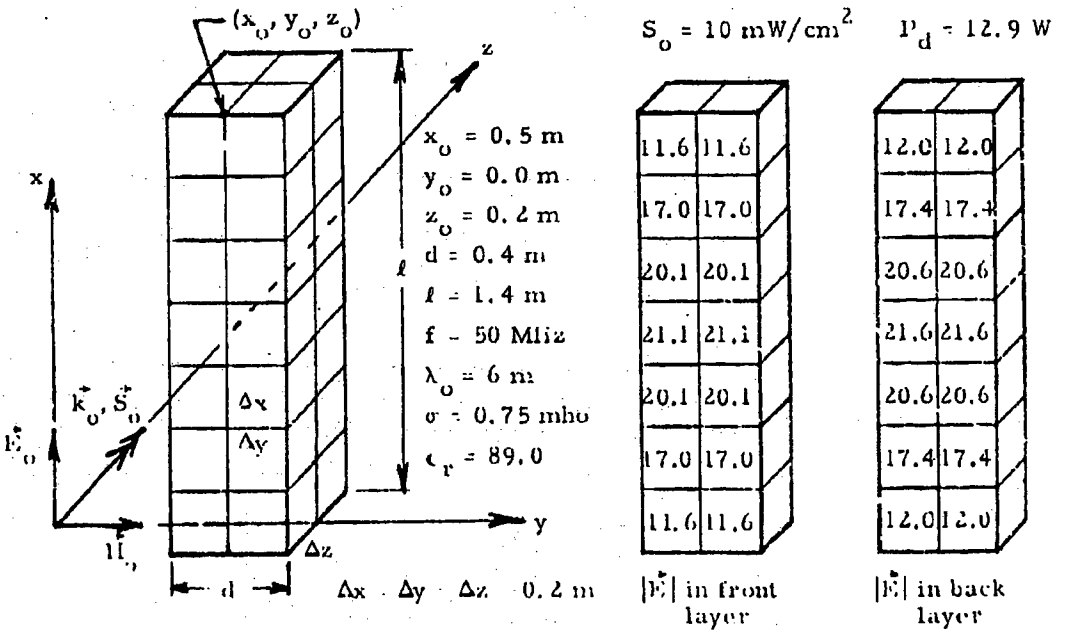

Figure 3. Electric field (magnitude in V/m) excited in biological body by impressed plane wave (with maximal power density S_o = 10 mW/cm^2).

z_o(m)	Z_p (ohms)	Z_{in} (ohms)	P_{in}(W)	P_d(W)	P_r(W)	P_d/P_r	P_d/P_{in}
0.1	2.36 - j61.4	10.7 - j700.7	5.35	0.565	4.79	0.118	0.106
0.2	2.07 - j22.7	10.4 - j662.1	5.20	0.282	4.92	0.057	0.054
0.3	1.72 - j9.10	10.1 - j648.5	5.03	0.167	4.86	0.034	0.033
0.5	1.28 - j1.53	9.62 - j640.9	4.81	0.089	4.72	0.019	0.019
1.0	0.990+j0.128	9.32 - j639.2	4.66	0.045	4.62	0.010	0.010

Table 1. Dependence of impedances and dissipated and radiated powers upon dipole location z_o ($h = 0.1\ \lambda_o$, $h/a = 100$, $x_o = 0.3$ m, $y_o = 0$, $Z_o = 8.33 - j639.4$ ohms).

x_o(m)	Z_p (ohms)	Z_{in} (ohms)	P_{in}(W)	P_d(W)	P_r(W)	P_d/P_r	P_d/P_{in}
0.0	-4.71 - j13.9	3.62 - j653.2	1.81	0.218	1.59	0.137	0.120
0.1	-2.06 - j15.1	6.27 - j654.4	3.14	0.181	2.96	0.061	0.058
0.2	0.29 - j18.3	8.62 - j657.7	4.31	0.204	4.11	0.050	0.047
0.3	2.07 - j22.7	10.4 - j662.1	5.20	0.282	4.92	0.057	0.054
0.7	4.22 - j33.1	12.6 - j672.4	6.28	0.623	5.66	0.110	0.099

Table 2. Dependence of impedances and dissipated and radiated powers upon dipole location x_o ($h = 0.1\ \lambda_o$, $h/a = 100$, $y_o = 0$, $z_o = 0.2$ m, $Z_o = 8.33 - j639.4$ ohms).

x_o(m)	Z_p (ohms)	Z_{in} (ohms)	P_{in}(W)	P_d(W)	P_r(W)	P_d/P_r	P_d/P_{in}
-0.3	-20.1 - j7.30	53.0 + j1.87	26.5	0.948	25.6	0.037	0.036
0.0	-9.75 - j2.37	63.4 + j6.80	31.7	0.964	30.7	0.031	0.030
0.3	-2.29 + j1.32	70.8 + j10.5	35.4	1.04	34.4	0.030	0.030

Table 3. Dependence of impedances and dissipated and radiated powers upon dipole location x_o ($h = 0.25\ \lambda_o$, $h/a = 100$, $y_o = 0$, $z_o = 0.2$ m, $Z_o = 73.1 + j9.17$ ohms).

EXPERIMENTAL INVESTIGATION OF MANPACK WHIP ANTENNAS: ANTENNA CHARACTERISTICS AND PROXIMITY EFFECTS

J. W. MINK
COMMUNICATIONS/AUTOMATIC DATA PROCESSING LABORATORY
U. S. ARMY ELECTRONICS COMMAND, FORT MONMOUTH, NEW JERSEY 07703

ABSTRACT

Techniques were evaluated to determine the effects of an operator's proximity on the performance of VHF manpack antennas. An impedance bridge of manpack size that can be remotely operated without metallic leads was constructed and calibrated. The impedance variations due to proximity effects were systematically investigated throughout the 30 to 80 MHz band for various antenna configurations. This investigation showed that impedance variations are substantially reduced by exciting the antenna near its center.

DISCUSSION

The objective of this study is to develop a method for reducing proximity effects of manpack whip antennas in the VHF band. To achieve this objective, an experimental investigation of antenna impedance variations under realistic operating conditions must be performed, since, in general, the radiating system is very complex due to coupling between the antenna and surrounding objects. The impedance measuring system must satisfy the following requirements:

a. Measuring equipment must have the same geometrical size and configuration as the manpack set.

b. Remote operation must be possible without metallic leads, since they become part of the radiating system and affect impedance measurements.

A compact, battery operated VHF impedance meter was not commercially available; therefore, a measuring system had to be developed. It was determined that a resonant-bridge impedance meter was best suited for the measurements undertaken in this investigation. An impedance meter which included a crystal controlled signal source and battery was constructed in manpack size (9.5 × 12.7 × 19 cm). Measurements were made on all adjustable bridge components in terms of dial readings. From these measurements, empirical equations with minimum square error were obtained for each component. Equations for calibration of the bridge and the empirical equations for the bridge components were programmed into a computing calculator. (This technique enables one to quickly and accurately tranform dial settings into actual impedance values. One can also program the computer to take into account any transmission line between the terminals of the impedance meter and the antenna excitation point.)

A test stand that places the impedance meter at a typical operating height above ground was constructed entirely of dielectric materials. Remote tuning of the impedance meter was accomplished by means of dial strings from

the impedance meter shafts to parallel shafts at ground level, then by means of fiberglass rods along the ground to the operator's position. With this setup, it was found that the operator could null the impedance meter at distances of up to 20 feet without the aid of a telescope for observation of the bridge indicator. At 20 feet, movements of the equipment operator could not be detected from the antenna impedance measurements.

Various whip-type antenna configurations that may be used for manpack applications are shown in Fig. 1. Figure 1a shows the conventional base-fed whip, along with a typical current distribution. Due to a current maximum at its base, this antenna system is very sensitive to any change in surroundings near the packset or to any wires, such as the handset attached to the packset. Such changes cause large variations in the input impedance of the antenna. High currents on the packset are strongly coupled to the operator's body which acts mainly as an absorbing element and reduces the radiated power from the antenna system [1].

Figure 1b shows the configuration of a center-fed whip that has been isolated from the manpack by means of a parallel resonant circuit. This approach is widely used on vehicular antennas, e.g., the AS-1729/VRC center-fed whip. For manpack applications, it has the advantage of maximum antenna current at the center of the whip (away from the operator) and a minimum current at the packset. The position of the operator then has little effect on the antenna system, since coupling to the surrounding objects will be through the electromagnetic fields only. The major problem with this approach is its complexity, and therefore the cost of the tuning unit at the antenna base. To isolate the antenna from the packset, the resonant circuit at the antenna base must have a relatively high Q; hence, it must be tuned for each operating frequency, which requires an adjustable tuning element or the switching of fixed tuning elements.

Figure 1c shows an antenna configuration that represents a compromise between the base-fed and the center-fed whip. This compromise antenna has the advantage that no additional tuning elements are required to isolate the antenna from the packset. The excitation point of this antenna is moved upwards toward the center of the whip, and the packset is used as part of an asymmetrically fed dipole. The current maximum is moved away from the operator, as shown by the current distribution (Fig. 1c), and the currents on the packset are reduced. In this way, a reduction in impedance variations due to proximity effects is achieved.

The excitation point impedance of this antenna and proximity effects were systematically investigated as a function of the position of the excitation point, see Fig. 1c. For testing purposes, the whip was constructed of RG-58 C/U Coaxial Cable and had an overall length of four feet, with the shield removed from the upper portion. The asymmetric dipole was formed by attaching the shield of the cable to the shell of the packset; the excitation point was determined by the distance the shield extended above the packset. Using a coaxial cable enables one to determine the excitation point impedance from measurements at the antenna terminals by a transformation through a known length of transmission line.

The following set of measurements were performed at each frequency:

a. The excitation point was moved in increments of two inches from the base to the midpoint of the whip,

b. For each excitation point and frequency, the proximity effects were determined by the following set of measurements:

1. Antenna and packset freestanding
2. Packset freestanding, with handset extended from the packset
3. Packset on back of man, with and without handset
4. Packset on back of man,with a second man holding the handset.

This set of measurements was chosen because it represents realistic operating conditions.

A typical set of excitation point impedance measurements normalized to 50 ohms is shown in Fig. 2. In this figure, each curve represents the excitation point impedance of the antenna system for the stated operating conditions as the point of excitation is moved up the whip. The area of the Smith chart containing all the points for one excitation is minimized when the point of excitation is $\sim$20 inches from the antenna base. This, then, is the optimum excitation point in terms of reducing proximity effects. As can be seen from Fig. 2, the maximum impedance variations occur for the base-fed whip. A summary for all frequencies with the excitation point at 20 inches is shown in Fig. 3. Here each area represents the range of impedance due to proximity effects for that frequency. It was determined with this data that a 50-ohm transmission line was about optimum for transformation of the excitation point impedance.

Current distribution measurements verified the current distribution shown in Fig. 1c for the freestanding manpack. Figure 4 shows the measured current and theoretical current distribution obtained using the "Antenna Modeling Program" developed by MBA Associates and a wire grid model of the manpack set.

The input impedance (Terminals of the antenna system) for the final (Fig. 1c) antenna configuration measured with the packset on a man's back and operator holding the handset is shown in Fig. 5. This antenna was 48 inches long and was fed 20 inches up the whip from the packset. A 50-ohms coaxial cable was used as the transforming element. As can be seen from this curve (Fig. 5), the impedance of the antenna system was well behaved and one should be able to match over the frequency band of 30-80 MHz in a few sub-bands.

CONCLUSIONS

Impedance variations due to proximity effects were systematically investigated throughout the frequency band from 30 to 80 MHz for various antenna configurations. This investigation showed that the impedance variations are substantially reduced by exciting the antenna near its center.

REFERENCE

[1] Z. Krupka, "The Effect of the Human Body on Radiation Properties of Small-Sized Communication Systems," IEEE Trans. Antennas & Propagation, vol. AP-16, March 1968, pp. 154-163.

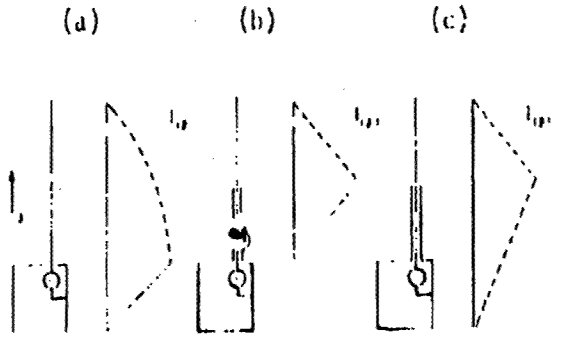

Characteristic features:

FIG. 1

Measurement Conditions:

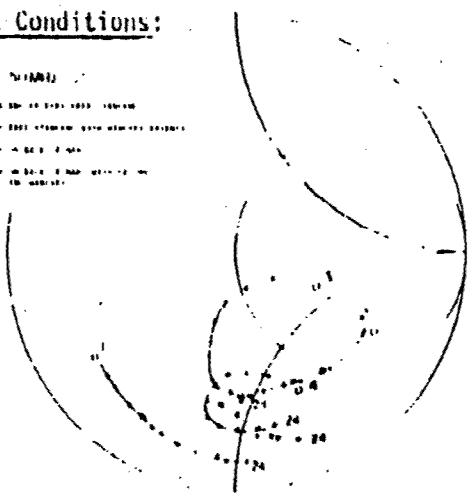

FIG. 2

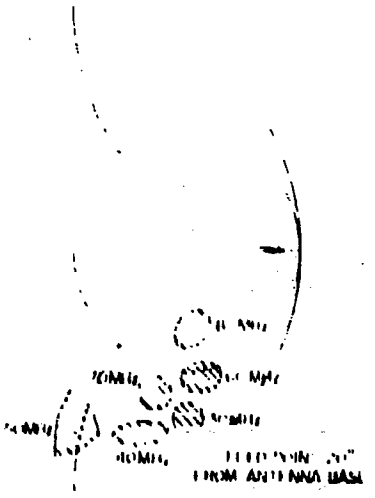

FIG.3

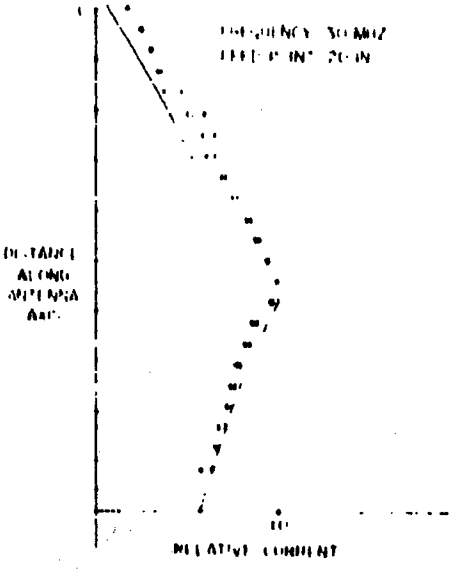

FIG. 4

FIG. 5

A SUPERCONDUCTIVE H-FIELD ANTENNA SYSTEM

Nancy K. Welker
Fernand D. Bedard
Laboratory for Physical Sciences
College Park, Maryland

ABSTRACT

A superconductive antenna/preamplifier system has been built which possesses three particularly desirable features: it is inherently broad band; the pick-up loop can be very small without giving up sensitivity due to the extremely low noise front end; and it is, therefore, ideally suited for use in compact arrays.

Ultra high sensitivity superconducting magnetometers for use near dc have been developed in recent years. Their performance suggested that they might be adaptable for use as H-field antennas in the rf region. The attractions for such systems appeared to be twofold: the pick-up loop can be made very small (~ several centimeters in diameter) with adequate sensitivity due to the extremely low noise front end; and this pick-up loop which is small relative to the wavelength of interest can provide an inherently broadband response. These antenna/preamplifier systems depend on the phenomenon of Josephson tunneling for their performance.

A Josephson junction is shown in Figure 1a consisting of a thin film superconductor, a thin insulating film and another thin superconducting film. If we put a voltmeter across the junction and attempt to transport current through the junction, we will obtain the highly non linear curve (1) of Figure 1b when the insulating layer is on the order of 100A thick. This results from single electron tunneling when the voltage exceeds the energy gap in the density of states, typically several millivolts. When the insulating layer is much thinner (10 20A), conduction is by correlated pairs of electrons, and no potential is developed across the junction as shown in curve (2) as long as we do not exceed I_{max} for that particular junction. This is known as Josephson or superconductive tunneling. When I_{max} is exceeded, the junction switches rapidly to curve (1). The barrier layer appears to the superelectrons to be an area of weakened superconductivity, not insulation. There are other ways to "weaken" superconductivity, one of which is shown in Figure 1c and is known as a weak link. It is simply a thin film superconductor which has been narrowed at one point to form the weak link. The I-V curve for such a device is somewhat different from that of a barrier Josephson junction and is shown in Figure 1d. When a Josephson junction is closed by a superconducting loop, it

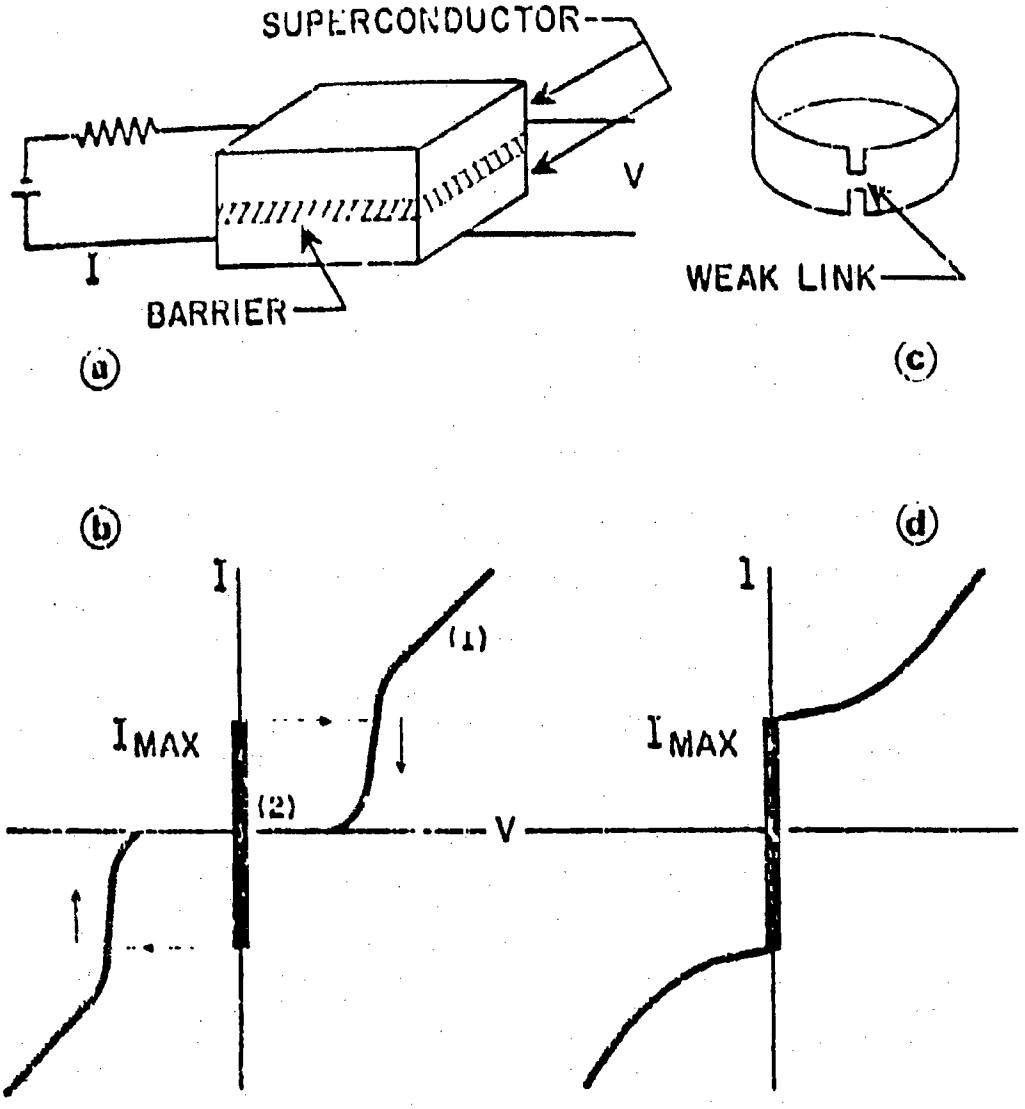

FIGURE 1

(a) Josephson Junction
(b) I-V curve for Josephson Junction
(c) Weak LINK
(d) I-V curve for Weak LINK

is known as a SQUID or Superconducting Quantum Interference Device. It is such a device that is used in our antenna/preamplifier system. The SQUID acts as a mixer between pump and signal frequencies and provides parametric amplification.

We chose as a first goal for our RF system a sensitivity of 1nV/meter corresponding to 4.1×10^{-11} gauss (4.1×10^{-15} tesla). This meant that the system would be atmospheric noise limited only over the low end of the HF band but even so required an improvement over commercial magnetometers which had a sensitivity on the order of 10^{-4} gauss. There are two ways to increase the sensitivity of a SQUID magnetometer system over and above just building more sensitive SQUID's. Most SQUID magnetometers are driven at a pump frequency of 30 MHz. Since the energy sensitivity is proportional to the pump frequency, we have gone to a pump frequency of 10 GHz giving a theoretical improvement in field sensitivity of 18. Another way to improve sensitivity is to increase the size of the pick up loop thus increasing the energy capture. For this reason the SQUID loop itself (1.0 mm diameter) is not used for signal pick-up but is fed by a 10 cm diameter superconducting loop which is inductively coupled to the SQUID. With the a two adjustable parameters--pump frequency and pick up loop size a sensitivity of better than 1nV/meter can be attained.

The next problem to be dealt with is dynamic range. If we start with the smallest signal that can be detected, for example 1nV/meter, what is the largest signal that can be accepted without overloading the system? We specified 80 dB or 10 mV/meter which is a fairly easily attainable goal. However, we must consider what is the useable dynamic range, i.e., how bad is the intermodulation distortion. We specified that, from a noise level, two signals each 30 dB above that level would produce intermodulation products no worse than the noise level. Even at that, this became the most difficult goal to attain due to the highly nonlinear character of the device. Its behavior is described by a product of Bessel functions

$$I/I_c = \sum_{m} \sum_{n} J_m\left(\frac{2\pi\Phi}{\Phi_0}\right) J_n\left(\frac{2\pi\Phi_s}{\Phi_0}\right) \sin(\omega_p + n\omega_s)t$$

where I_c is the maximum critical current, Φ_p and Φ_s are the fluxes due to the pump and the signal and Φ_0 is a constant which arises from the theory of superconductivity and has a value of 2×10^{-15} webers. Linearity is achieved through feedback using room temperature electronics, but this introduces noise to the SQUID from the first stage amplifier (T_n 600°K), thus limiting the useable bandwidth to several megahertz. This problem, of course, can be solved by going to lower noise temperature electronics, ideally totally superconductive.

The circuit for the antenna/preamplifier system is shown in Figure 3. The design and construction of the system was done by Develco, Inc., Mountain View, CA. The SQUID is pumped by a 10 GHz Gunn oscillator with pump power in the milliwatts range attenuated (~ 40 dB) by an adjustable PIN diode at room temperature and ~ 40 dB pad in liquid helium, and the pump power is coupled to the SQUID through a cooled circulator. The cooled attenuator and

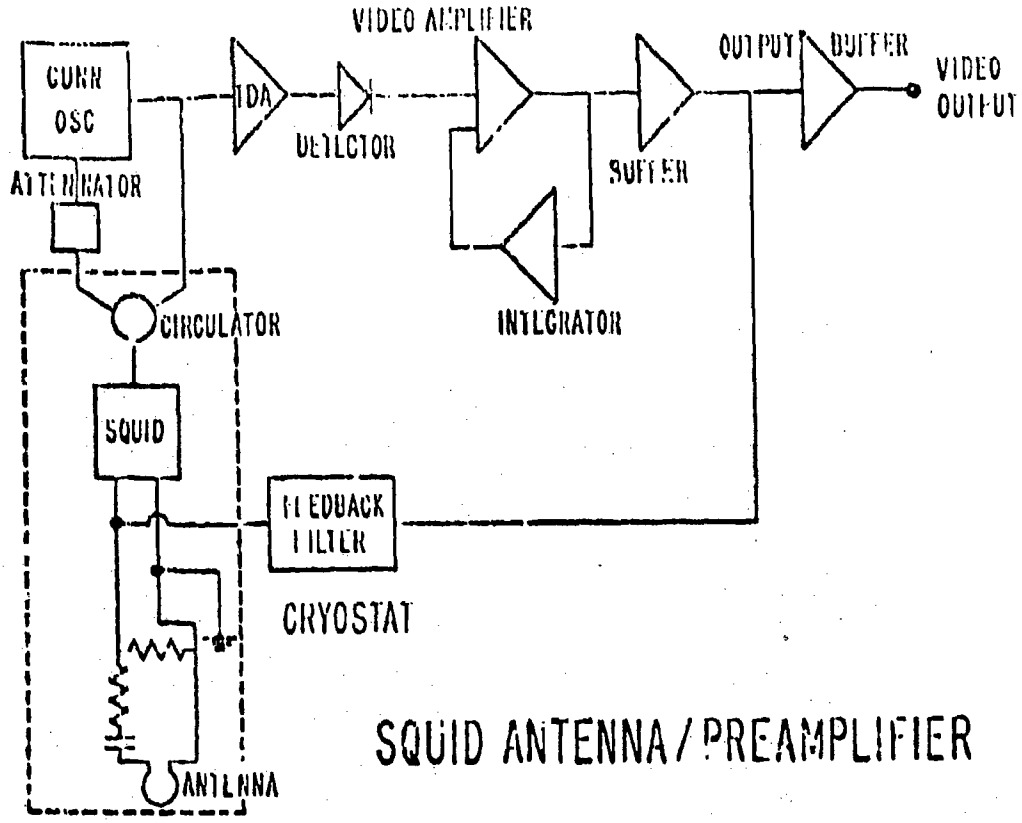

FIGURE 2

circulator reduce the temperature of the environment facing the SQUID to near 4K, thus reducing the noise power reaching the SQUID. The signal frequency is inductively coupled to the SQUID from a superconducting pick up loop. The reflected microwave power, modulated by the signal, goes to a tunnel diode amplifier and is detected by a tunnel diode to provide the video output. The feedback loop is used to linearize the system.

The cryostat used in this system has some unique features. It consists of a standard 30 liter superinsulated dewar topped by what is referred to as the "radome". The pick-up loop consisting of a 10 cm diameter two turn half loop of Nb ribbon over a 30 cm Nb ground plane is located in the radome and is kept in the superconducting state not by immersion in liquid but by vapor cooling. The temperature in the radome is maintained at 4.5K by the boil-off from the liquid helium below. The entire radome is insulated by 55 layers of double sided aluminized Mylar which would normally be excellent shielding against RF radiation. To get around this problem the metallization was meshed into small patches using a laser scribing technique in which the patch size was determined by considering the trade-offs between the RF

properties and the thermodynamic considerations. This formed an RC filter which was designed to roll off at 100 MHz.

Unfortunately, a complete set of performance characteristics are not available. The SQUID which was initially installed in the system had an energy sensitivity of 10^{-29} J in a one hertz bandwidth. With the 10 cm pick-up loop, this produces a calculated sensitivity of 8×10^{-12} G/$\sqrt{Hz}$ or .24 pV/m/$\sqrt{Hz}$, quite an adequate value. Because of the noise generated in the feedback electronics which is fed back to the SQUID, the output can be linearized over only a several megahertz band rather than the full RF band. This would be satisfactory for a number of applications. Total system tests have not been performed at the present time due to a gradual degradation in the SQUIDs which we have been using in the laboratory tests. The system will be completed in the near future. Nevertheless, even at this stage we believe that the feasibility of such a system has been demonstrated and the critical improvements identified.

There are several attractive applications for such a unit. The obvious one is the situation in which a low profile, broadband system is required. The radiation resistance of a 10 cm loop at 1 MHz is 2×10^{-6} Ω whereas its reactance is 10^{-1} Ω. Consequently, matching would be impossible and would also provide an intolerable Q. Since our antenna is operated in the pure reactive mode, it is broadbanded and highly inefficient. We can tolerate this inefficiency because of the very low noise temperature of the SQUID preamplifier. A second and perhaps more important application area is that of compact arrays. For frequencies at the lower end of the HF band and below the system should be atmospheric noise limited, by several orders of magnitude in the LF VLF range. Some of this excess sensitivity can be forfeited in the interest of increased directivity in compact array of antennas. We expect that in compact arrays one must reduce the size of the individual elements in order to reduce mutual interactions which, in general, cause a loss in sensitivity. Fortunately, in the superconductive system the elements are already small with the necessary sensitivity.

In conclusion, a SQUID antenna/preamplifier system has been demonstrated to operate as predicted. It is clear that to outclip the full benefit of its inherent broadband behavior, lower temperature feedback electronics, preferably superconducting, will have to be employed. When this has been done, such systems should be ideally suited for compact array applications.

AN APPROACH TO SHIPBOARD HF RECEIVING SYSTEMS

Richard K. Royce
Naval Research Laboratory
Code 5410
Washington, DC 20375

ABSTRACT

Antennas which are physically small relative to wavelength are analyzed for application to shipboard HF broadband receiving systems. Results show that these antennas can provide acceptable receiving system noise factors. Also, interference from collocated HF transmitting antennas is reduced to levels amenable to suppression by filter or signal cancellation techniques.

SUMMARY

In Navy fleet communications today, the shipboard HF receiving system is normally operated simultaneously with the ship's HF transmitting system. A ship's limited platform size, and a need for broadband multiple receiver operation from a single antenna are factors which suggest that physically small antennas offer a possible approach to providing more versatile and reliable shipboard HF receiving systems[1]. A number of advantages are available in this approach:

(1) An increased degree of freedom in placement of the antenna in the shipboard environment is available,

(2) Coupling to local transmitting antennas is reduced,

(3) Broadband operation in the sense that tuning, matching, or band switching over the 2 to 30 MHz frequency band is not required of the communicator.

The physically small miniature antenna under consideration here is a monopole as depicted in Figure 1. The monopole is approximately 1/8 wavelength or less in height. A coupling network designated "N" is located at the feed point and contains, among other components, an HF amplifier. The HF receiver itself may be located up to several hundred feet away from the antenna installation.

In order to use this antenna system in a shipboard environment, two factors must be considered as follows:

(1) The antenna system noise factor must not significantly degrade the operating noise factor,

(2) The distortion products generated in the coupling network "N" must not exceed acceptable levels.

First, consider the system noise factor. Figure 2 shows the measured system noise factor on a monopole which is 3 feet in height, 0.375 inches in diameter, and which has a 3-foot diameter top-loading disc. The feed point termination circuit "T" is a 1200-ohm to 50-ohm transformer which drives a 50-ohm input impedance rf amplifier. This receiving system noise factor varies from about 32 dB at 2 MHz to 22 dB at 30 MHz.

Figure 3 shows the quasi-minimum atmospheric noise levels expected to be encountered in typical Navy ship operations; and also, typical ship hull generated interference, in a 3 kHz bandwidth [2], [3]. Atmospheric noise varies from about 52 dB at 2 MHz to 20 dB at 30 MHz relative to KT_oB; and hull generated interference levels on a relatively clean ship are seen to be about 62 dB relative to KT_oB. It is noted that the noise factor obtained with the 3-foot disc top-loaded monopole (see Figure 2) is about equal to the expected atmospheric noise at all frequencies over the 2 - 30 MHz band. By appropriate selection of termination resistance and antenna design constants, the system sensitivity has been adjusted to be uniform with respect to atmospheric noise levels. The calculated degradation in operating noise factor, then is about 3 dB over the 2 - 30 MHz band. Relative to typical ship hull generated interference levels, degradation in operating noise factor is less than 1.0 dB from 2 - 30 MHz.

In consideration of these results, it appears possible to design a physically small monopole receiving system to have adequate sensitivity relative to expected ambient noise conditions in the shipboard environment.

Next, the presence in the receiving system of energy from colocated shipboard transmitting antennas was investigated relative to the generation of distortion products in that system. Figure 4 shows calculated and measured coupled voltages existing at the amplifier input of the termination network "T" for the 3-foot monopole receiving system described previously, except that the top loading disc is not included. The colocated transmitting antenna source is a 75-foot whip radiating 1 kilowatt of CW power. The 75 foot whip is located a distance of 100 feet from the short monopole. The dotted curve represents calculated data, and the solid curve is the measured result. The measured maximum coupled voltage is about 0.6 volts. Measured data on this receiving system, but with the 3 foot diameter top loading disc added to the short monopole element, showed approximately the same shape curve, but the maximum coupled voltage had increased to about 1.1 volts at the 100 foot spacing. At a spacing of 75 feet, the maximum coupled-in voltage would be the order of about 6 volts. The results in Figure 4 are relative to an average earth condition over which it was possible to make the measurements. Under perfect earth conditions, these voltages would not increase significantly.

Consideration of these coupled voltages in the physically small top loaded antenna receiving system relative to amplifiers [4] which are available today, indicates that the system would probably be marginal at the 100-foot separation; and it would not be usable at closer separations without application of techniques to further suppress the locally generated inter-

ference. However, it should be remembered that CW power is a worst case, and probably would not be encountered aboard ship. Also, the ship environment will affect the coupled voltage amplitude, increasing or decreasing it relative to the above values.

The power levels associated with these voltages at any of the antenna separations indicated are now of a reasonable magnitude, wherein techniques may be readily employed to provide additional rejection of the coupled-in energy from colocated transmitting systems. This rejection would be inserted between the antenna element feed point and the active terminating network in the physically small antenna receiving system. A possible rejection would be to use notch filters in the receiving system as given in Figure 5. The filter is tuned as part of the transmitter tuning procedure, providing the communicator with a broadband receiving system requiring receiver tuning only. A disadvantage of this technique is that the insertion loss of the filter must be offset by increased antenna size in order to maintain a given system noise factor. However, it can be readily implemented without introducing distortion products into the receiving system.

A second method of interference rejection would be to use signal cancellation techniques as suggested in Figure 6. A sample of the interfering signal is taken from the transmitter output, appropriately adjusted in amplitude and phase, and injected into the receiving system between the antenna feed point and the amplifier in the antenna termination. The amplitude and phase of the transmitter sample is adjusted such that a sample of incoming energy in the receiving system tends to be reduced to zero. The advantages of such a technique are numerous:

(1) As much as 20 to 40 dB or more of interfering signal cancellation can probably be achieved readily. It is estimated that 20 dB of cancellation would be adequate for many situations encountered aboard ship; and that up to 40 dB cancellation could be achieved without great difficulty.

(2) Negligible insertion loss can be realized and is projected to be about 1 dB.

(3) Full automation can be achieved; that is, no operator attention whatever is required.

(4) The signal cancellation circuit can be small, inexpensive, and highly reliable.

(5) The control unit can be small, relatively inexpensive, and located in the radio room to facilitate maintenance and enhance reliability.

(6) There is no apparent limitation to the number of interfering signals which can be cancelled in a given receiving system. Each additional frequency to be cancelled, beyond the first frequency, would require only partial duplication of components in the signal cancellation circuit and the control unit.

The signal cancellation circuit must be designed and operated so as not to introduce distortion products into the receiving system, and this fact is probably the ultimate challenge to implementation of the physically small antenna approach.

To summarize, it has been shown that the physically small antenna approach to HF shipboard receiving systems offers adequate sensitivity and increased isolation to local interference with appropriate design, facilitates circuit rejection of interference from the colocated transmitting antenna systems, and permits broadband multiple receiver operation for shipboard HF communications.

REFERENCES

[1] R. E. Royce, "Broadband, Miniature, Active-Type, HF, Receiving Antenna System", Report 7014, Naval Research Laboratory, Washington, DC, October 16, 1970.

[2] W. L. Gustafson and W. M. Chase, "Shipboard HF Receiving Antenna System Design Criteria", SECI/TR 1712, June 1970.

[3] S. E. Parker, "Cost-Effectiveness Comparison of Two Multicoupling Approaches to HF Transmitting System Engineering", NELC/TR 1537, February 1968.

[4] Adams-Russel Technical Bulletin No. M104, Adams-Russel Co., Waltham, Mass., June 1971.

MINIATURE ACTIVE-TYPE RECEIVING ANTENNA

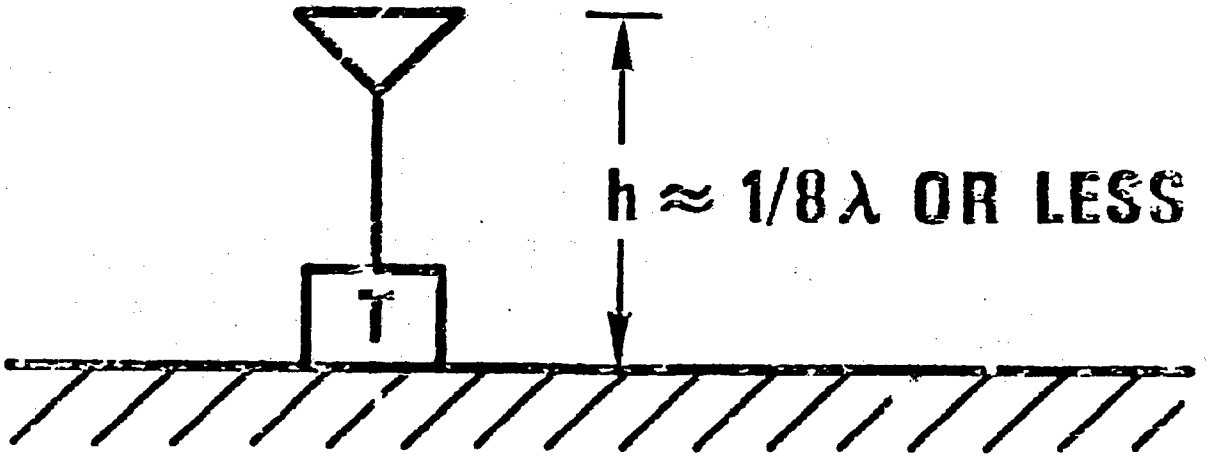

Figure 1. Miniature receiving antenna system.

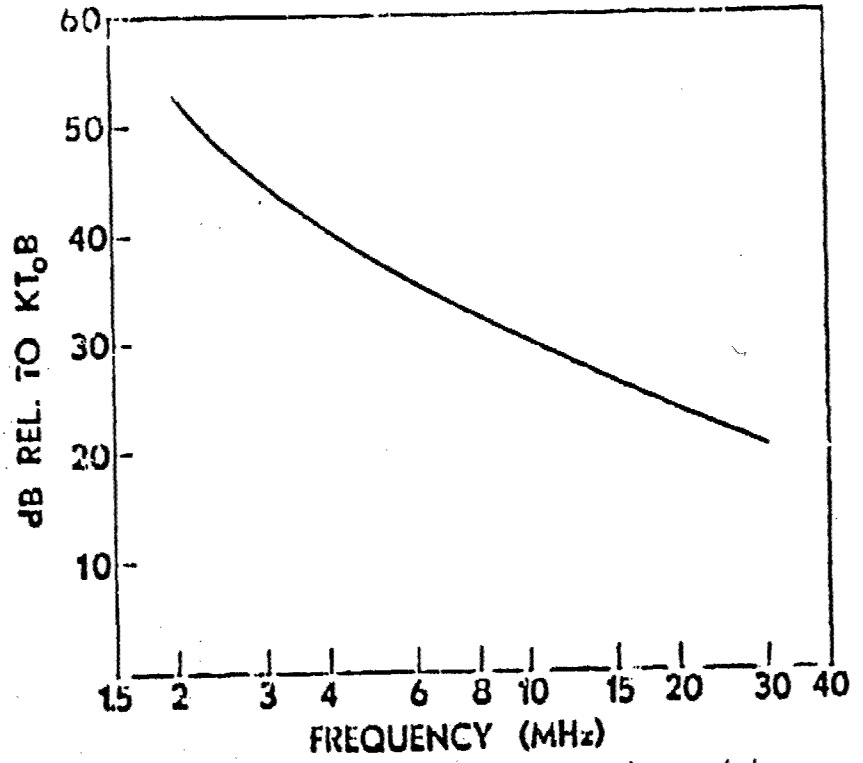

Figure 2. Top-loaded 3-foot monopole receiving antenna system noise factor.

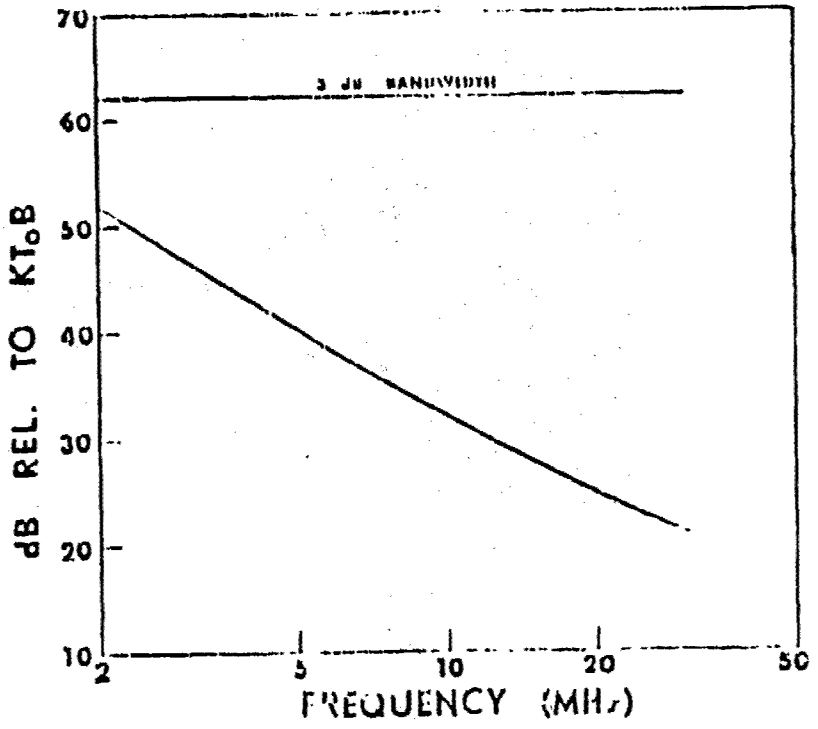

Figure 3. Typical expected shipboard ambient noise levels.

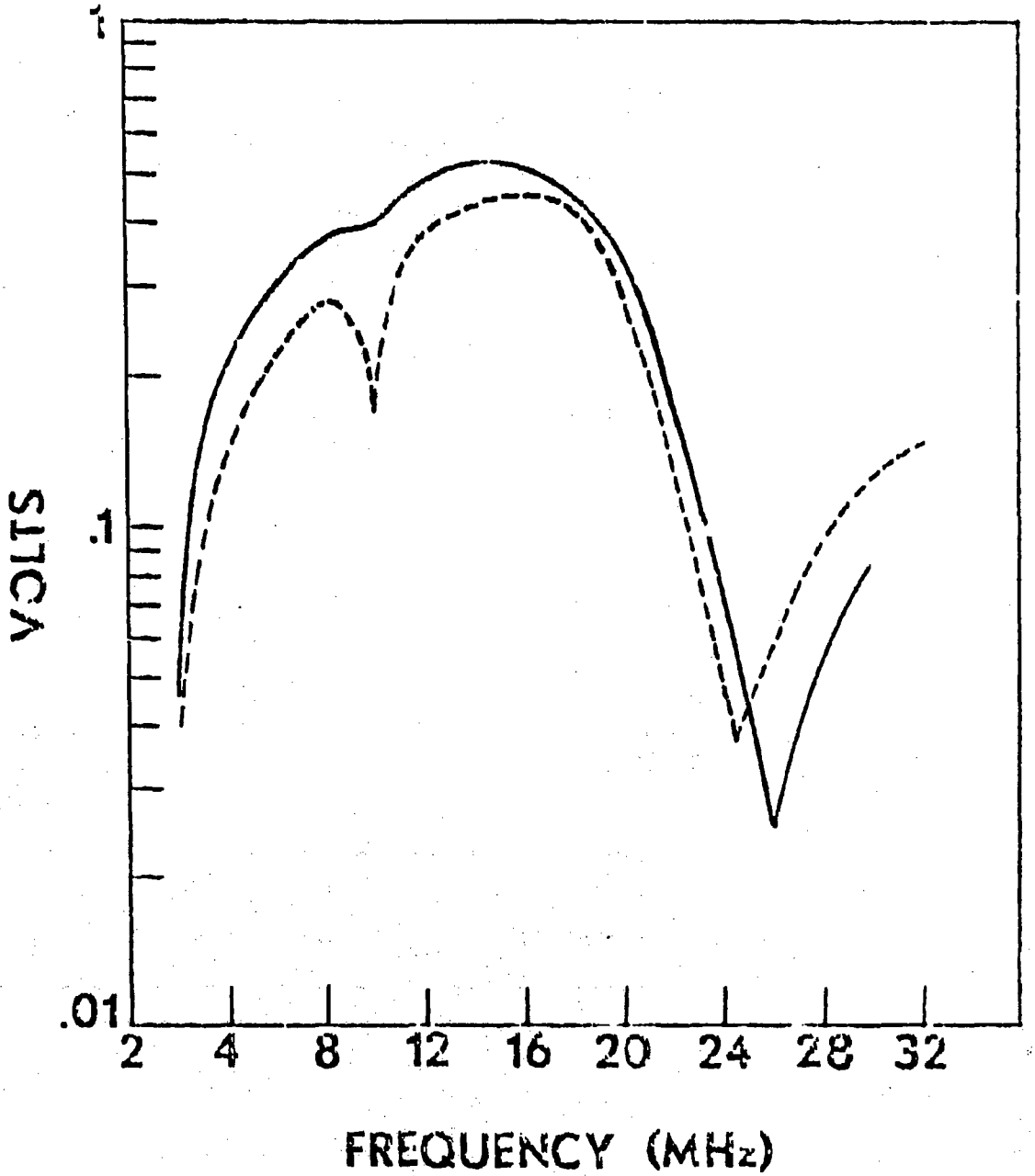

Figure 4. Voltage levels induced in the 3-foot monopole receiving antenna system by colocated transmitting antennas.

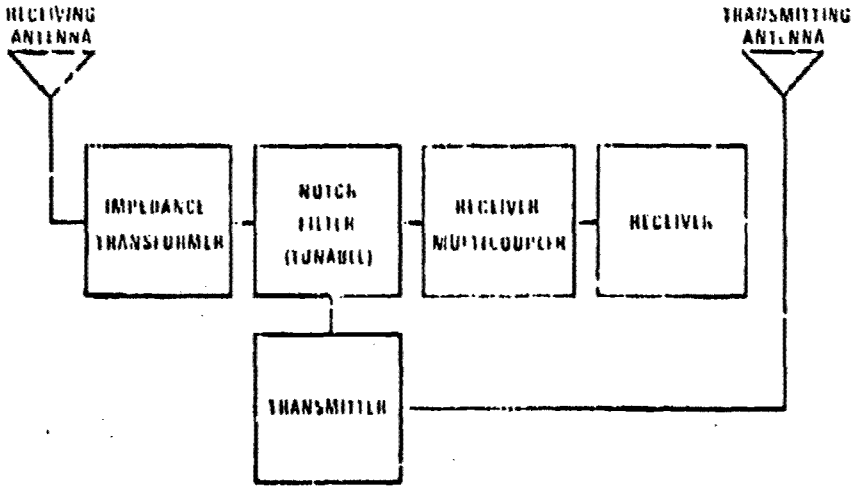

Figure 5. Notch filter technique for local interfering signal suppression.

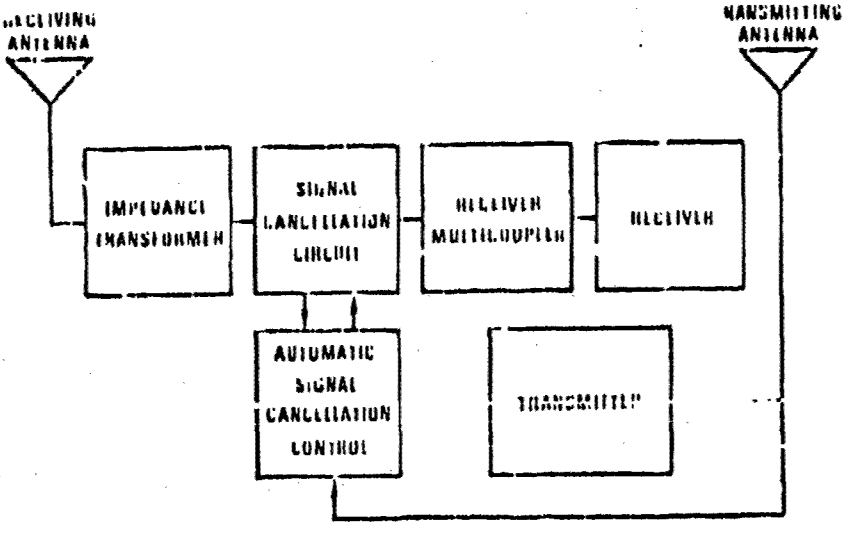

Figure 6. Signal cancellation technique for local interfering signal suppression.

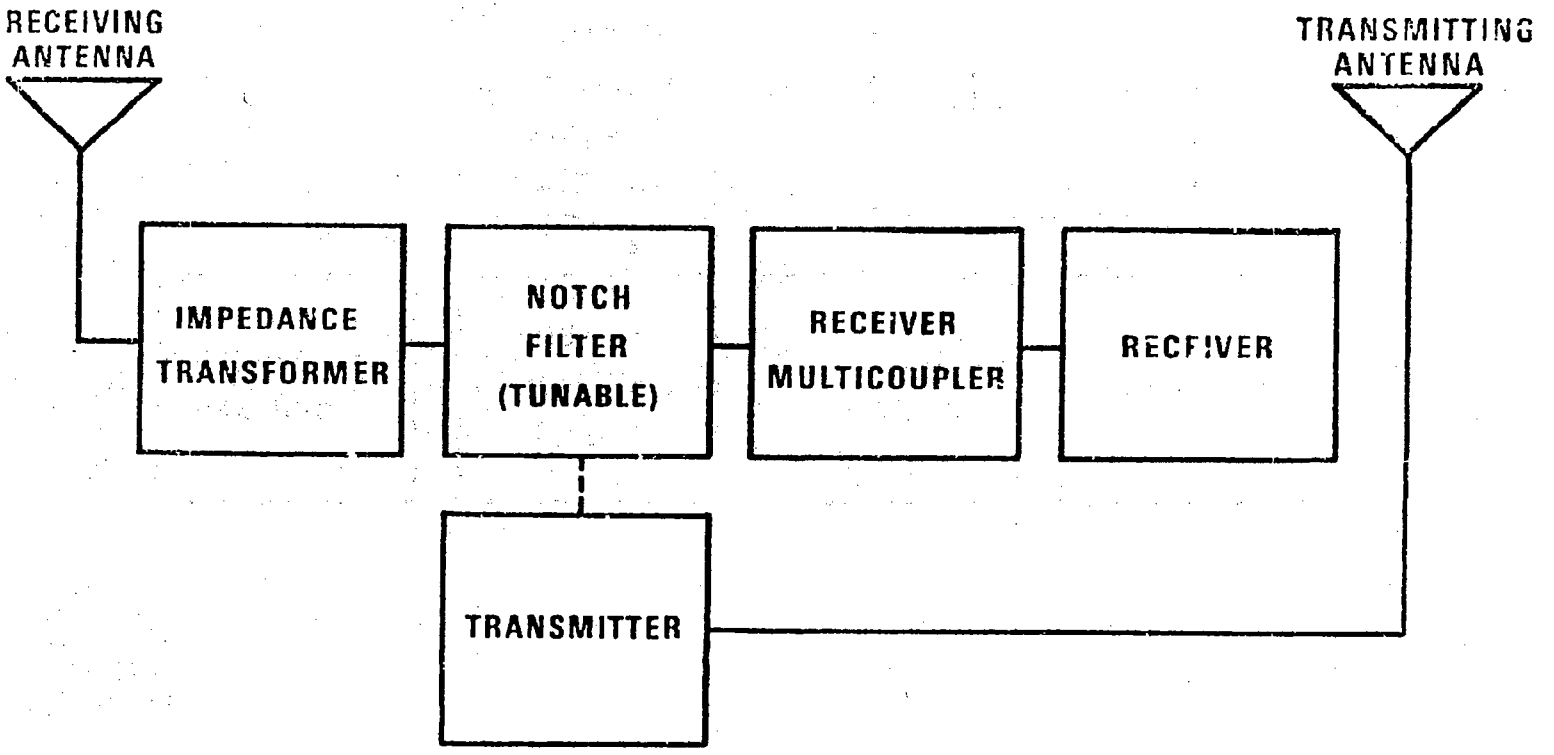

Figure 5. Notch filter technique for local interfering signal suppression.

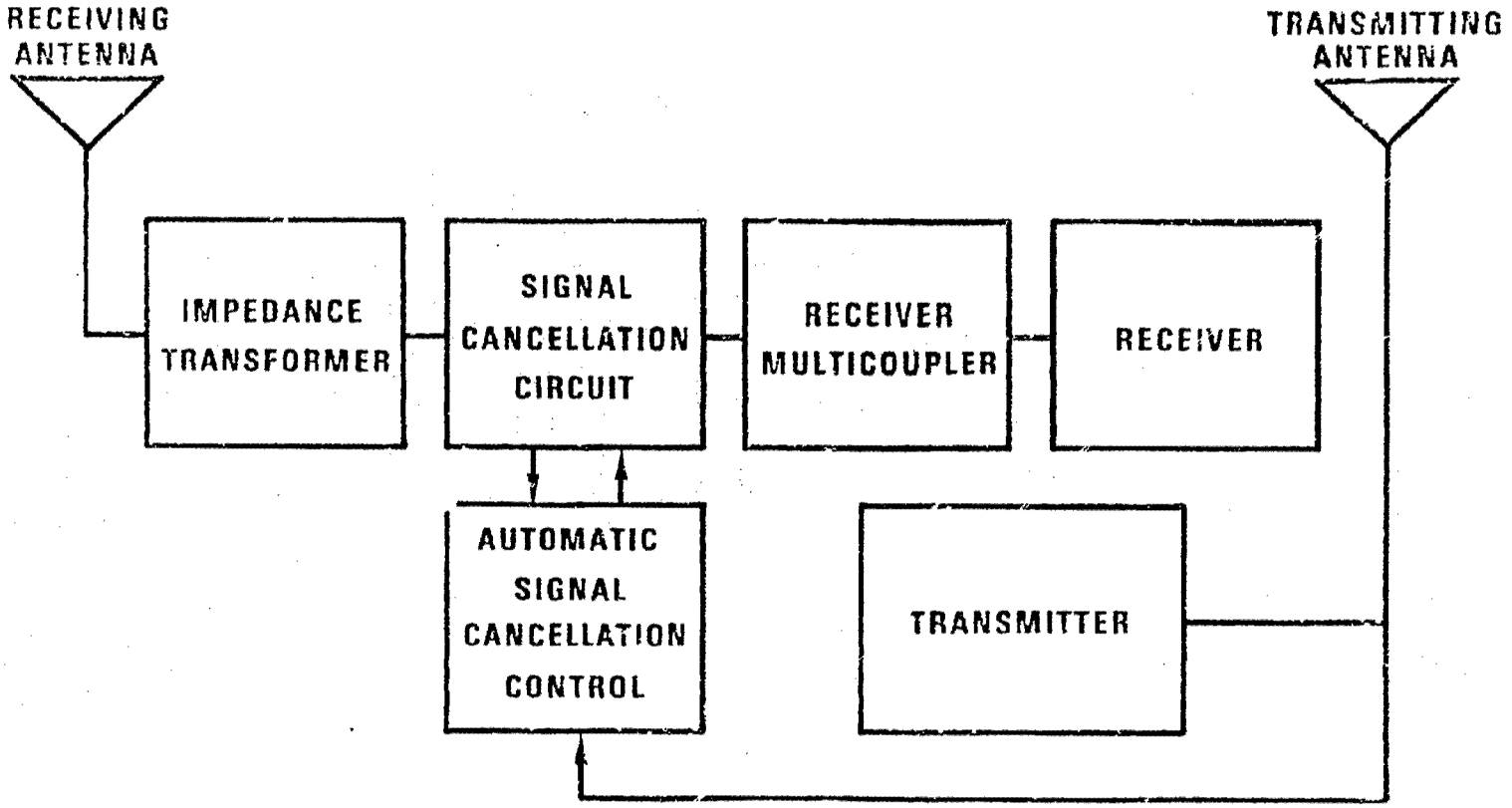

Figure 6. Signal cancellation technique for local interfering signal suppression.

APPLICATION OF ACTIVE-IMPEDANCE MATCHING TO ELECTRICALLY SMALL RECEIVING ANTENNAS*

A. J. Bahr

Remote Measurements Laboratory
Stanford Research Institute
Menlo Park, California 94025

ABSTRACT

The noise performance of an active receiving-antenna system consisting of antenna, active two-port network, and preamplifier is discussed. The design of the active two-port makes use of contours of constant noise temperature superimposed on a Smith chart. Experimental results are presented for a simple active antenna composed of a short monopole and a negative-impedance converter.

SUMMARY

For a passive small-antenna system, Wheeler has shown that the efficiency and/or bandwidth of the system is ultimately limited by the size of the antenna.[1] However, the performance limitations of a small antenna are modified if active circuits are introduced into the loading or matching networks associated with the antenna. The most common active-antenna arrangement consists of an amplifier integrated into an antenna. This arrangement was used as long ago as 1928[1] and has been studied extensively in more recent times by Meinke and his co-workers.[2,3] Most known methods of obtaining electronic amplification have been tried in this connection, including the use of tunnel diodes[4,5] and parametric amplifiers.[6] In many cases, one of the more important features of the amplifier (besides providing gain) is its ability to transform (or isolate) the impedance of the antenna. This feature can be used to obtain very large operating bandwidths with a small antenna.[7]

In this paper we focus on the impedance-transforming properties of the active network. We assume that the addition of active circuitry to the antenna does not alter such intrinsic properties of the antenna as field pattern or gain. In this situation the active network can be thought of as a matching network and/or amplifier that connects the antenna to the remainder of the receiver system. The design of the active antenna then reduces to finding the linear, active, two-port network that, when inserted between the antenna and RF preamplifier, minimizes the system noise figure over some prescribed bandwidth.

A schematic diagram of the system we wish to analyze is shown in Figure 1. The antenna is represented by its Thevenin equivalent circuit

* This work was supported by the Department of the Army, U.S. Army Research Office, under Contract DAHC04-75-C-0023.

composed of voltage source, V_S, and output (or radiation) impedance $R_S + jX_S$. The effective antenna noise temperature is T_S. In general, all of these quantities vary with frequency. The active matching network can be viewed as the combination of an arbitrary linear network having an effective input noise temperature, T_N, and any series reactances, X_S and X_L, that are part of the antenna output impedance and preamplifier input impedance, respectively. The real part of the preamplifier input impedance is denoted by R_L, and the output impedance of the active matching network is Z_{TS}, which, in effect, is a transformed source impedance.

By definition, the noise figure for this system is (assuming a high gain for the preamplifier)

$$F = 1 + \frac{T_N + (T_L)_{eff}}{T_S} \tag{1}$$

where $(T_L)_{eff}$ is the effective noise temperature at the input (terminals 1-1). As a result of our analysis, we find that

$$(T_L)_{eff} = Q_n[(T_L)_{min}/G_t] \cdot [\,|\Gamma_L - \Gamma_n|^2 + P_n] \tag{2}$$

where

$$\Gamma_L = \frac{Z_{TS} + R_L}{Z_{TS} + R_L} \tag{3}$$

and Q_n, P_n, and Γ_n are noise parameters for the preamplifier, and $(T_L)_{min}$ is its minimum noise temperature (i.e., for noise match). The quantity G_t is the transducer gain of the active network and is given by

$$G_t = \frac{K^2 R_S}{R_L} |1 - \Gamma_L|^2 \tag{4}$$

where K is the ratio of the magnitude of the open-circuit output voltage of the network (at terminals 2-2) to the magnitude of the open-circuit output voltage at the source (at terminals 1-1).

For purposes of design, it is convenient to use Eq. (2) to plot loci of constant

$$B = \frac{(R_{TS})_{opt}}{K^2 R_S} \frac{(T_L)_{min}}{(T_L)_{eff}} \tag{5}$$

in the Γ_L-plane, where $(R_{TS})_{opt}$ is the source resistance for noise match of the preamplifier. These loci are shown in Figure 2, which is an expanded Smith chart for Z_{TS}.

We can now use these loci to design an active matching network for a short monopole antenna (1/16-wavelength long at 30 MHz). If we assume that $T_N \ll T_S$, $(R_{TS})_{opt} = R_L = 50\ \Omega$, and $(T_L)_{min} = 0.5\ T_O$, we can satisfy the condition

$$(T_L)_{eff} \leq T_S = (3 \times 10^{16}/f^2)\ T_O \qquad (6)$$

if

$$B \geq 0.5/K^2 . \qquad (7)$$

In Eq. (6) f is the frequency in hertz and T_O is the reference temperature 288°K. This equation defines a 3-dB signal-to-noise bandwidth where $F \leq 2$. Now, we further assume that the active network can be represented as a pure series impedance so that $K = 1$. Hence, according to Eq. (7), the design locus must lie to the left of $B = 0.5$ circle in Figure 2. A suitable, but arbitrary, choice for this design locus is a portion of the circle $|1 - \Gamma_L|^2 = 4$.

We attempted to realize the desired design locus by using a negative-impedance converter (NIC) circuit of the type shown in Figure 3 to synthesize the required active series impedance. We designed a suitable amplifier and measured its input and output impedances and current gain as functions of frequency. From these data we were able to calculate the required NIC feedback impedance, Z_{FB}. However, we found that Z_{FB} can only be approximated by a passive circuit. Using the approximate Z_{FB}, we calculated that $Z_{TS} = Z_S + Z_{NIC}$ should follow the dashed curve shown in Figure 4.

For comparison, our experimental results are shown by the solid curve in Figure 4. The discrepancy between theory and experiment at low frequencies is probably due to inaccuracies in our theoretical antenna model at these frequencies (e.g., stray capacitance). Both theory and experiment agree well at high frequencies, but, because Z_{FB} is not correct at these frequencies, we have $B < 0.5$.

Using the experimental data shown in Figure 4, we can use Eq. (2) to calculate $(T_L)_{eff}$. These "experimental" values of $(T_L)_{eff}$ are compared with T_S in Figure 5. As predicted, we see that $(T_L)_{eff} < T_S$ at the lower frequencies, and vice versa at the higher frequencies. The noise temperature without matching, $(T_L)'_{eff}$, is also shown in the figure for comparison. This comparison indicates that active matching should improve the system noise figure over the whole operating band. However, experimentally, improvement was only obtained in the lower half of the band. It is not possible to pinpoint the source of this discrepancy because of the uncertainties concerning the true values of T_S, T_N, and the antenna impedance.

Hence, we have shown that transformation of a passive antenna impedance into an active impedance promises the realization of very

broad signal-to-noise bandwidths in a receiving system that uses an electrically small antenna. The limitations of this technique will involve questions of the noise contributed by the active network and of stability. Our future work will be aimed at incorporating stability and noise parameters directly in the design procedure, evaluating various active-matching networks, and developing computer-optimized design procedures.

REFERENCES

1. H. A. Wheeler, "Small Antennas," IEEE Trans. on Antennas and Propagation, Vol. AP-23, pp. 462-469 (July 1975).

2. H. H. Meinke, "Active Antennas," Nachrichtentechnische Zeitschrift, Vol. 19, pp. 697-705 (December 1966).

3. G. Flachenecker, et al., "Active Receiving Antennas," De Ingenieur, Vol. 84, pp. 74-80 (June 1972).

4. M. E. Pedinoff, "The Negative-Conductance Slot Amplifier," IRE Trans. on Microwave Theory and Techniques, Vol. MTT-9, pp. 557-566 (November 1961).

5. H. H. Meinke, "Tunnel Diodes Integrated with Microwave Antenna Systems," The Radio and Electrical Engineer, Vol. 31, pp. 76-80 (February 1966).

6. A. D. Frost, "Parametric-Amplifier Antenna," Proc. IRE, Vol. 48, pp. 1163-1164 (June 1960).

7. J. P. Daniel, G. Dubost, and J. Rospars, "Transistor-Fed Thick Folded Dipole with Large Bandwidth at Reception," Electronics Letters, Vol. 11, pp. 90-92 (February 1975).

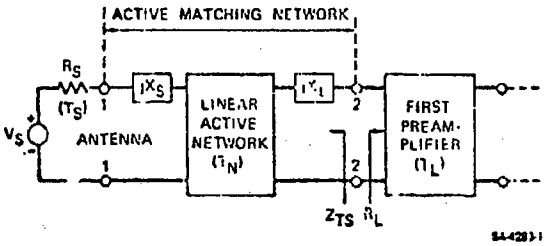

Fig. 1 Schematic diagram of receiving system.

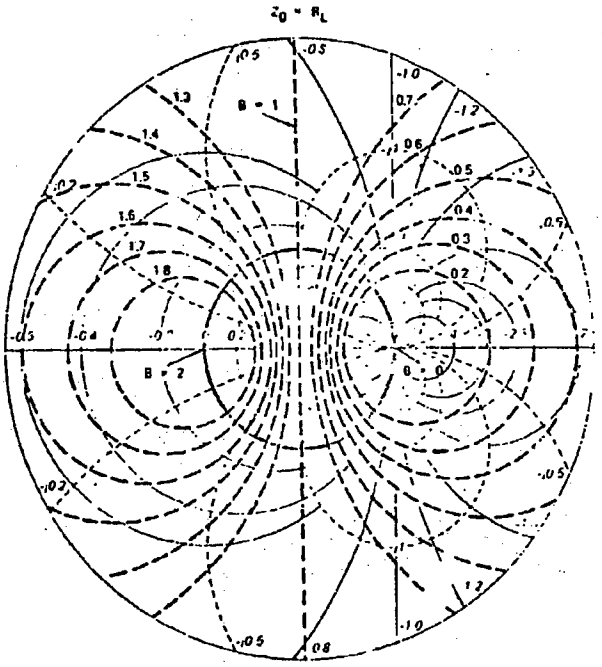

Fig. 2 Constant-B loci in the Γ_L-plane (Smith chart) for the case $R_L = (R_{TS})_{opt}$ and $Z_{cor} = 0$

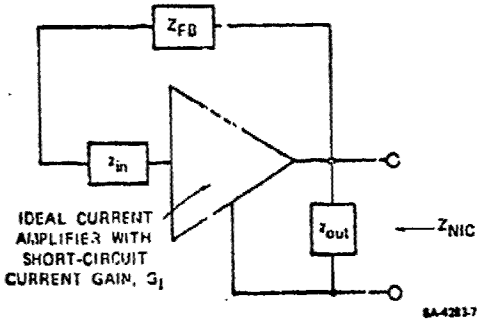

Fig. 3 Schematic diagram of a current-inverting NIC.

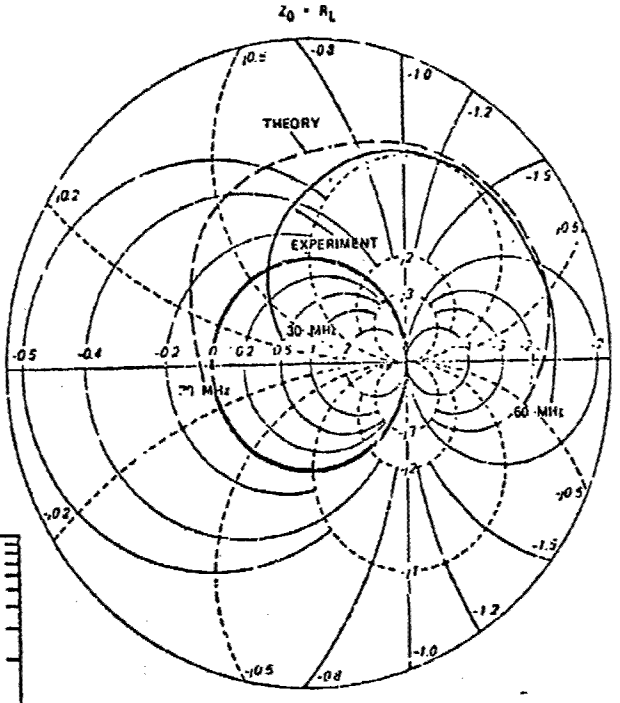

Fig. 4

Output impedance of an actively matched, short monopole as a function of frequency.

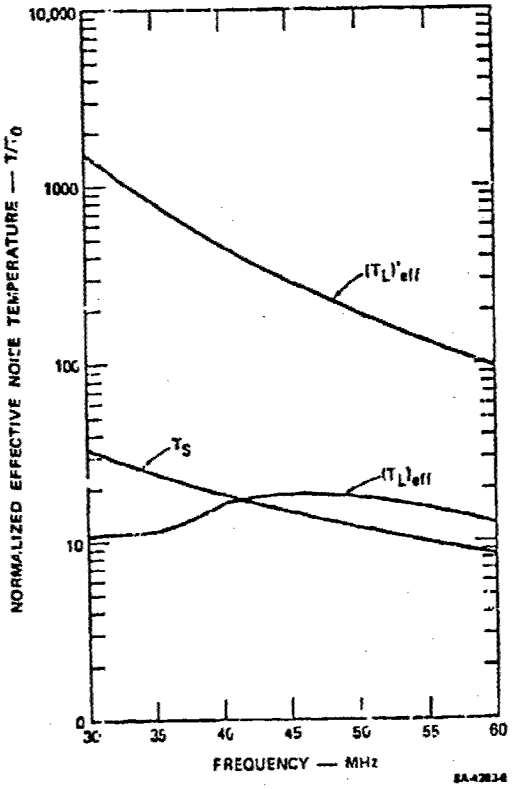

Fig. 5 Effective normalized noise temperature vs frequency.

ELECTRICALLY SMALL ANTENNAS WITH LOADING MATERIALS AND WITH ACTIVE ELEMENTS

John A. M. Lyon and Ralph E. Hiatt
The Radiation Laboratory
Department of Electrical and Computer Engineering
The University of Michigan

Abstract. This paper reviews work done at the University of Michigan on electrically small antennas. Ferrite and dielectric loadings of rectangular slot radiators are discussed. Results on the loading of spirals are also given. Electronic tuning of monopoles and folded monopoles over a ground plane utilizing active devices is also presented.

I. Introduction

This paper constitutes a survey of work done over several years. Initially dielectrics and ferrites were used as loading for slots, helices and spirals. The improvements and limitations obtained with loading were observed. Later, studies were made on equivalent circuits and models for monopole and folded monopole antennas. Electronic tuning was used with these antennas to permit operation at reduced size for a given frequency.

Any reduced size antenna suffers from the basic limitations (1) and (2). However, some loaded antennas provide a tolerable compromise between size, bandwidth, efficiency requirements and radiation patterns. Loaded slot antennas are discussed followed by a discussion of spiral antennas and then by electrically tuned folded monopoles.

II. Loaded Slot Antennas

Slot antennas have been used to meet a variety of applications where flush mounting is required. The slot antennas we have studied were backed by a cavity and our objective was to reduce the size of the cavity by dielectric or ferrite loading. Any such reduction is, of course, accompanied by decreased bandwidth and/or efficiency. For several applications, however, the size reduction advantages appear to outweigh the cost.

In an early study (3) a detailed analysis was made of the aperture admittance of rectangular cavity antennas taking into account material loading and the effect of higher order modes. The geometry involved is shown in Fig. 1. Aperture admittance data was calculated; this provided the information to calculate bandwidth, efficiency and resonant frequency. Using the simplified equivalent circuit of Fig. 2, it was found that the bandwidth of the loaded slots could be calculated with an accuracy that agreed with experimental results within 20 percent. The equivalent circuit models a ferrite loaded cavity backed by a short circuit, fed by a coaxial probe and radiating through the open aperture. The subscripts of Fig. 2, p and A, refer to the probe and the aperture. The

efficiency was calculated using the basic variational data. Predictions of efficiency based on calculations agreed within 10 percent with measured results.

It is interesting to compare the results of dielectric filled slots and ferrite filled slots. In our work on ferrite filled slots, material loading having a magnetic Q of approximately 35 has been used*. Many workers in the field have made use of dielectric filled slots where the dielectric has an electric Q of 200 or more. In either case, the material loading tends to reduce the size of the slot antenna. We found, however, that for a respectable efficiency, the magnetic Q of the ferrite can be considerably lower than the electric Q of the dielectric. This corresponds to saying that there is a much better impedance match at the aperture of the ferrite filled slot antenna than there is at the aperture of the dielectric filled slot antenna. The efficient radiation of energy from a dielectric filled slot antenna requires a relatively high electric Q.

A number of rectangular cavity slot antennas have been constructed and experimental data have been obtained with ferrite powder, solid ferrite and solid dielectric material. Some typical results are given in Table I.

TABLE I

PERFORMANCE COMPARISON OF RECTANGULAR CAVITY SLOT ANTENNAS

Loading	Air	Ferrite Powder	Ferrite Solid	Dielectric
Size (inches)	30 by $7\frac{1}{2}$ by 10	12 by 3 by 4	5 by 2 by $1\frac{1}{2}$	12 by 3 by 5
Volume (cubic inches)	2250	144	15	180
Bandwidth				
at VSWR = 3		22 MHz	19 MHz	10 MHz
at VSWR = 6		50 MHz	34 MHz	18 MHz
Efficiency	90 percent	65 percent	30 percent	85 percent
Directivity	5.8 db	5 db	5 db	5 db
Weight (pounds)	$25\frac{3}{4}$	$16\frac{3}{4}$	3.6	14.5
Frequency (MHz)	300	320	35.2	316

Slots loaded with dielectric material are now being used in a novel and important application (4); in the March 1976 issue of Microwaves there is a report on the successful use of such slots with a microwave thermograph to detect and locate hot spots below human body skin. The hot spots are indicative of the possible presence of cancer cells. The thermograph is similar to a sensitive radio astronomy receiver; it can detect

* We have defined magnetic Q as μ'/μ'' and electric Q as ϵ'/ϵ''.

signals with a sensitivity of 0.1°K. The tests have been made at S band (3.3 GHz) using X band waveguide slots (0.4x0.9") loaded with a dielectric. The antennas used are almost identical to those used by Lyon and Ibrahim (5) in their study of miniaturized slot elements in an array.

It was interesting to note that for some of the ferrite used the relative permeability decreased with increasing frequency. (See Fig. 3.) This offers the possibility of achieving more bandwidth than expected of materials with constant permeability.

III. Loaded Helical and Spiral Antennas

We studied the loading of helices, log conical spirals, Archimedean spirals and equiangular spirals. A major part of this work was experimental. We were concerned entirely with operation in the 1 λ or endfire mode. For cylindrical helices we found that ferrite loading reduced the efficiency by a factor of 1/2. However, the necessary diameter for endfire was also reduced by about the same factor. We were never able to reduce the radii of any helical antenna by a multiplicative factor smaller than 1/2 no matter how high we went with μ' or ϵ' .

In one experimental study of log conical spiral antennas two log conical spiral antennas were designed for the same frequency coverage. Bifilar feeds were used. One of these was unloaded. The second loaded with ferrite had a diameter at the base one-half of that of the air-filled one. The axial height of the loaded one was about half that of the unloaded or air-filled one. The loaded one had nine turns whereas the unloaded one had five turns. The small antenna contained powdered ferrite which was inserted within the conical structure. The powdered ferrite material was retained by putting a thin sheet of polyethylene plastic over the smaller log conical spiral. The ferrite powder completely filled all space inside the spiraled conducting elements. Ferrite extends just outside of the conducting elements since the supporting structure extends approximately 1/8" beyond the metal conducting elements. This ferrite-loaded antenna operated with VSWR characteristics as shown in Fig. 4 which also shows the VSWR for the same antenna without loading.

The efficiency of the larger log conical antenna without ferrite was compared with that of the small ferrite-filled log conical antenna. The small ferrite-filled log conical antenna had an efficiency of 23 percent at 400 Mc compared to an efficiency of 92 percent for the large log conical antenna at the same frequency. This decrease in efficiency is accompanied by a decrease in lineal antenna dimensions of approximately a factor of two and a volume decrease of about a factor of 7. This means that a much smaller antenna of the log conical type can be made at the sacrifice of approximately 6 db in efficiency. The radiation patterns show that otherwise the operating performance is as good as that of the corresponding air-filled log conical antenna.

The VSWR of a cavity-backed bifilar equiangular spiral was measured both with and without ferrite loading. The feed was of the "infinite balun" type. The VSWR for various conditions is shown in Fig. 5. The cavity was fully loaded with the ferrite powder. A thin layer of ferrite powder was also placed on top of the spiral. The fully

loaded case produced a reduction of the lower cutoff frequency by a factor of approximately 2. The introduction of the ferrite powder introduced a narrowbanding effect due to the fact that the magnetic Q becomes small above 700 MHz. It is expected that with the development of wideband, high Q ferrites, moderate widebanding of the spiral antenna could be achieved. With presently available materials, a 2 to 1 size reduction is possible. With such a reduction good axial radiation patterns have been maintained.

IV. Voltage Tunable Antennas

The tunable feature when applied to a small antenna will, in many cases, provide an adequate substitute for a broadband antenna. The frequency filtering of a narrow band but tunable antenna can reduce noise and in this way frequency filtering may be made to compensate for the loss of spatial filtering; electrically small antennas are, of necessity, not highly directive. Studies were made of the impedance characteristics offered by electric monopoles as well as folded monopoles over a wide frequency range. Impedance information gained was then used to synthesize an adequate circuit model of a particular antenna. The circuit model is then used in conjunction with a voltage controlled tuning unit in order to meet a prescribed frequency bandwidth. It is possible to use voltage tuning by active elements on a small antenna for some frequencies without any substantial degradation of the signal-to-noise ratio.

The small antennas studied herein were simple or folded electric monopoles. Calculations and measurements of impedances were made. The impedance characteristics were helpful in selecting an adequate circuit model. Some of the antennas became capacitive as the frequency applied was made lower, whereas others became inductive as the frequency became lower. Equivalent circuits for short antennas may at times be useful in considering techniques that may improve the performance. At any one frequency, the equivalent circuit for a short antenna can be represented by resistance and either capacitance or inductance. If one wishes such a simple equivalent circuit over a band of frequencies, both parameters would have to be properly frequency dependent. It is possible to devise an equivalent circuit using only frequency independent circuit elements if more elements are used. Fig. 6 shows the measured impedance of a folded monopole over a large ground plane. Below 100 MHz, it is seen that the impedance is largely inductive.

An electronic tuning unit as shown in Fig. 7 was assembled and used to tune a folded monopole. Fig. 8 shows the results of tuning this folded dipole. Also a folded monopole was used for dual frequency use; this had separate channels at each end.

V. Conclusions

Physically small antennas can be designed for successful operation. In general loading restricts the bandwidth although spirals and similar types continue to be reasonably broadbanded. Active element antennas have been developed which are essentially narrow banded. However, since these are tunable they are adaptable to wideband usage. The filter characteristic of such antennas is also useful from noise considerations.

References

1. H.A. Wheeler, "Fundamental limitations of small antennas", Proc. I R.E., Vol. 35, December 1947, pp. 1479-1484.

2. R.F. Harrington, Time harmonic electromagnetic fields, Mc-Graw-Hill Book Company, New York, 1961.

3. A.T. Adams, "Flush mounted rectangular cavity slot antennas - theory and design", IEEE Trans. AP, Vol. AP-15, No. 3, May 1967, pp. 342-351.

4. H.J. Hindin, "Microwave probe for cancer cells", Microwaves, Vol. 15, No. 3, March 1976, pp. 10, 14.

5. J.A.M. Lyon and M.A.H. Ibrahim, "Arrays using physically small slot antenna elements", URSI/IEEE Symposium, Austin, Texas, December 8 - 11, 1969.

6. A.T. Adams and J.A.M. Lyon. "Ferrite loaded antennas for aerospace applications", IEEE Trans. Aerospace, June 1965, pp. 489-494.

7. J.A.M. Lyon et al., "Electronically tuned small antennas for HF to UHF frequency bands", Twenty-first Annual Symposium USAF Antenna Research and Development, Monticello, Illinois, October 12 - 14, 1971.

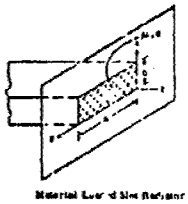

Fig. 1

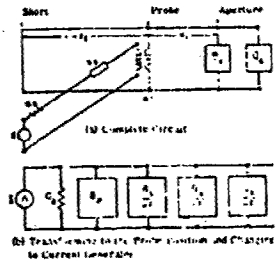

Fig. 2

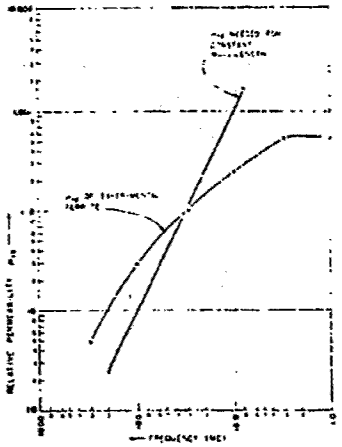

Dispersive characteristics of ferrite material

Fig. 3

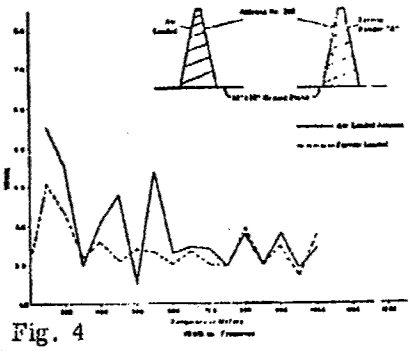

Fig. 4

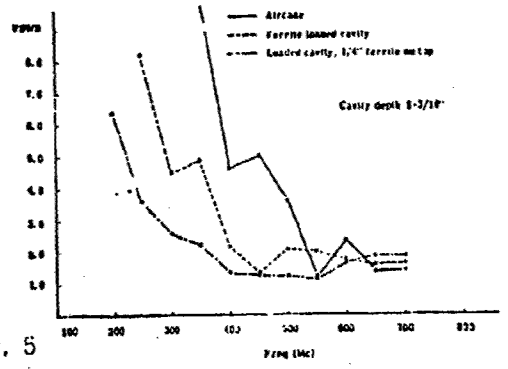

Fig. 5

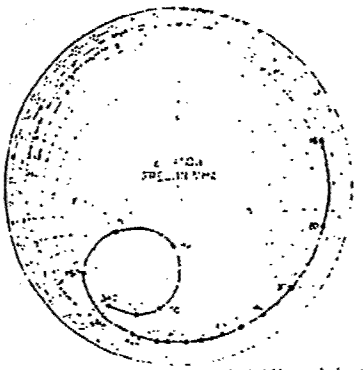

Fig. 6 Measured Impedance of [illegible] Folded Monopole Resonant at Approximately [illegible] Mc

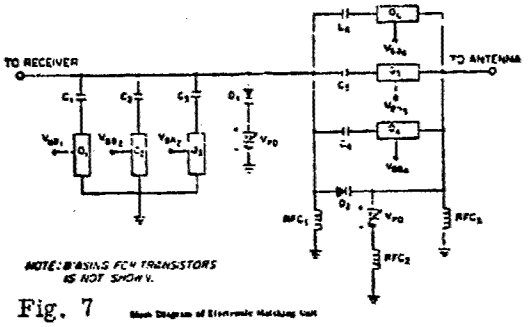

Fig. 7 Block Diagram of Electronic Matching Unit

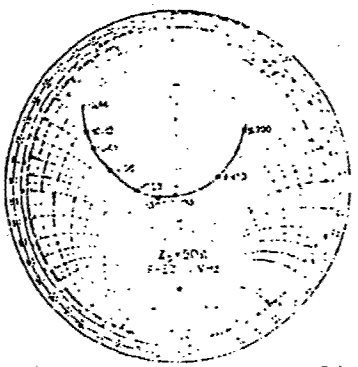

Fig. 8 Measured Impedance of Folded Monopole When Fed from Low Frequency End.

SHORT, ACTIVE, HIGH-FREQUENCY ANTENNA AS AN E-FIELD PROBE*

Edwin F. Laine
Lawrence Livermore Laboratory, University of California
Livermore, California 94550

ABSTRACT

The Lawrence Livermore Laboratory has developed a short, active, high-frequency antenna for use in subsurface geophysical exploration. The antenna, which uses dual-gate metallic-oxide field-effect transistors (MOSFETs), is used essentially as an E-field probe. Using sophisticated data-analysis techniques, information provided by the antenna system can be used to examine the characteristics of subsurface geological media.

SUMMARY

The short, active antenna described here was designed for use in underground geophysical investigations. The antenna system is used to measure the power received from an adjoining hole transmitting a high-frequency continuous-wave or swept-frequency signal transmitted through the earth. By measuring the received power and its relative phase shift (using the transmitted power as the reference), the conductivity and relative dielectric of the earth in a path between the two holes can be calculated. Sophisticated data-analysis methods, adopted from the medical profession, can then be used to reconstruct the characteristics of the media between the two holes.

The receiving antenna is electrically short (0.25 m) for the highest frequency used (typically 0.5 to 50 MHz); therefore, radiation resistance is very low and the short antenna looks capacitive (i.e., its capacitive reactance is very high). To obtain the almost open circuit voltage of the

*This work was performed under the auspices of the U.S. Energy Research and Development Administration under contract #W-7506-Eng-48.

antenna, it is necessary to have a low-capacity input amplifier that exhibits a very high reactive impedance for the highest frequency used. This is accomplished by using dual-gate metallic-oxide field-effect transistors (MOSFETs). A schematic diagram of the antenna system is shown in Fig. 1. The newer dual-gate models have a very low reverse-transfer capacity (0.05 pF) and a low gate-to-source capacity (3.0 pF). The transistor selected (3N200) has back-to-back diodes to protect the gates from damage. The antenna is a 25-cm-long wire-probe capacity coupled to gate 1 of Q1, which is an impedance converter, or source follower. Feedback from the source to gate 1 bootstraps the input impedance to a high level by reducing the input capacity. Q2 is a conventional, moderate-gain, wide-band amplifier. It is followed by amplifiers Q3 and Q4 interconnected to form a Darlington pair to drive a 50-Ω output cable. The dc operating voltage is fed down the output signal cable. The radio-frequency choke, L1 and C10, form a filter to eliminate signal feedback into the supply voltage at the amplifier. The signal and dc voltage are similarly decoupled and separated at the other end of the cable.

Active circuitry is constructed on a printed circuit board and housed in a water-tight brass casing. The wire antenna is housed in a tubular nylon container along with a small top-loading disc of copper (Fig. 2). A lifting handle is provided so a dacron messenger cable can be used to relieve strain on the signal cable when the antenna is used in deep holes. The entire 22-in.-long unit was made a uniform diameter (2 in.) to prevent snagging along rough sides of uncased drill holes. It was also made heavy enough to sink easily in water-filled holes. The coaxial connecting cable is threaded through randomly spaced ferrite beads for the first 50 ft. to suppress shield currents.

Each antenna probe is calibrated in a parallel-plate transmission line using a network analyzer. One channel records parallel-plate voltage versus frequency while the other channel does the same for antenna output. Typical probe-calibration curves are shown in Figs. 3 and 4.

This first model is an engineering prototype model. Newer more simplified models are currently being tested. The active circuitry has less components and the frequency response has been extended to 50 MHz.

In all these models the noise levels of the antenna circuitry are only a few db above the noise level of the test instruments; Network Analyzer (-90 dbm) or -100 dbm for a Spectrum Analyzer with a 1 KHz bandwidth.

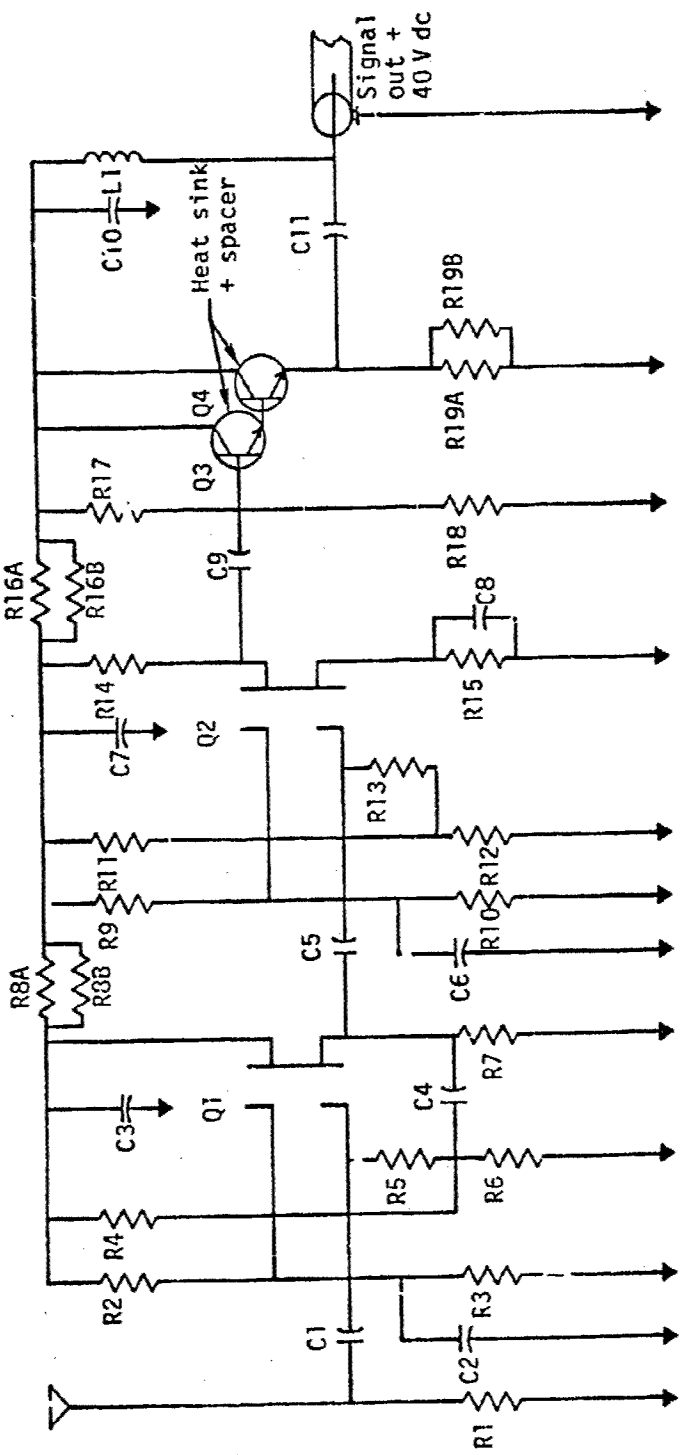

Fig. 1. Schematic of antenna system.

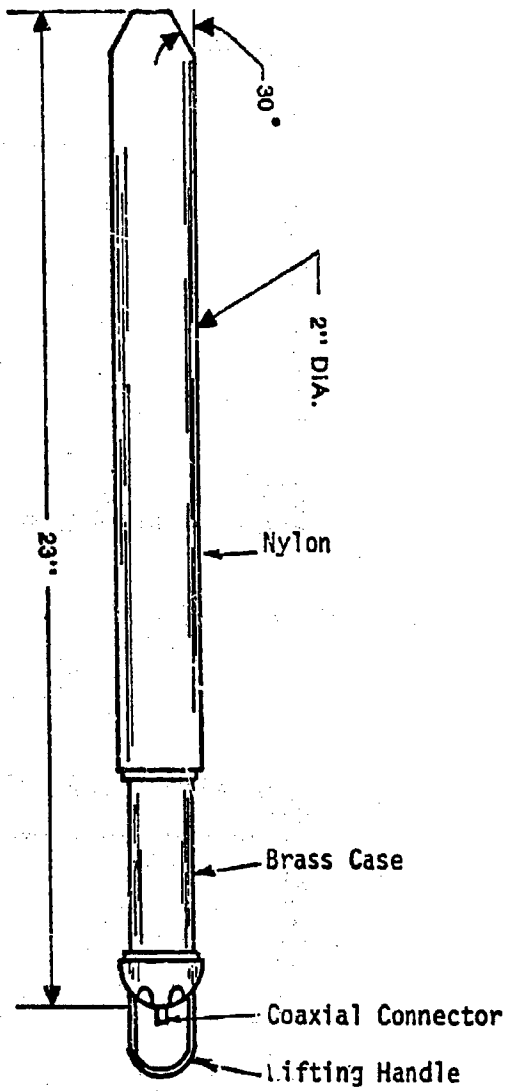

Fig. 2 - Assembled Antenna

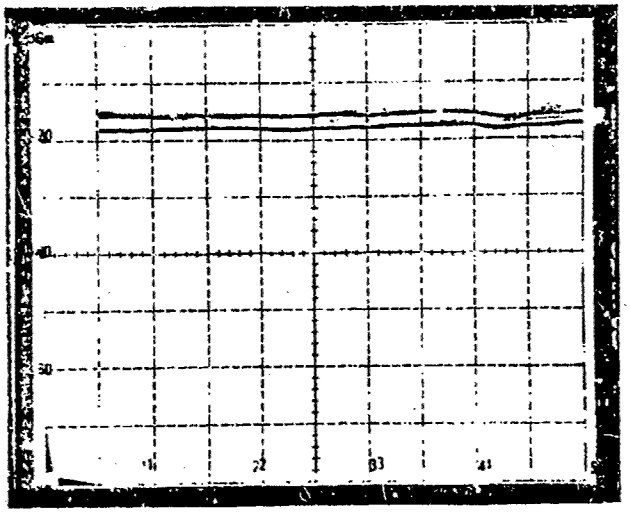

Fig. 3 - Upper Trace - Parallel Plate Voltage
Lower Trace - Antenna Output Voltage
Horiz. - 0.5 to 5 MHz
Vert. - 10 Decibels/Div.

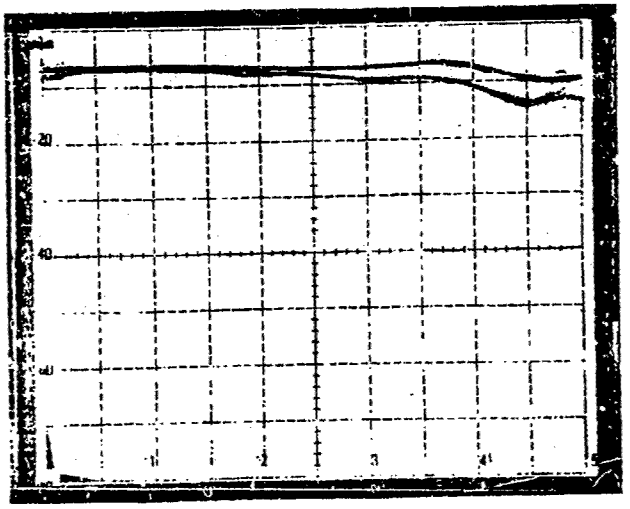

Fig. 4 - Upper Trace - Parallel Plate Voltage
Lower Trace - Antenna Output Voltage
Horiz. - 5.0 to 25 MHz
Vert. - 10 Decibels/Div.

EXCERPTS FROM THE DISCUSSIONS

The following excerpts from the technical discussions conducted during the Workshop are based on tape recordings. For coherency, they have been ordered according to subjects, rather than in the sequence in which the discussions took place. When possible, contributors are identified. The editors apologize for any omissions or incorrect quotations. Comments by the editors which are not excerpts of the discussions are marked by (E).

VEHICULAR ANTENNAS FOR HF SKY-WAVE TRANSMISSION

HF sky-wave transmission is of potential importance for ground-to-air communication with helicopters flying at very low altitudes (nap-of-the-earth flights), and for ground-to-ground communication in mountainous terrain (E).

A frequency band about 2 MHz wide is usually available for HF sky-wave communication within the 2 to 8 MHz range. The location of this "window" depends on the ionospheric conditions, and in general, can be predicted rather reliably from ionospheric observations (Brune).

Question (Lane): Which antenna configuration for vehicular applications should be selected to provide efficient high angle sky-wave radiation?

Comments:

——For helicopter applications, a vertical loop antenna, the so-called Tranline antenna, was recommended (Brune). (This antenna is described in the papers by Brunner and Gruber, p. 129, and by Medgyesi-Mitschang and Brune, p. 135. These papers had not yet been presented when the question was raised.)

——A vertical single-turn loop antenna for jeeps is presently under development at ECOM. This so-called roll-bar antenna consists of a rigid metal rod, having the shape of an inverted U, which extends from the rear bumper over the top of the jeep to the front bumper, where the feed point of the antenna is located. The loop is closed underneath the jeep by the outer conductor of a coaxial cable, which connects the feed point of the antenna with the transceiver set located in the rear of the jeep. The coaxial cable section provides an impedance transformation, which facilitates the matching of the antenna to the transceiver. The roll-bar antenna has shown a substantial improvement in sky-wave transmission over that provided by a standard 15' Army whip antenna. This improvement was obtained even though this new antenna could not be completely matched to the GRC-106 Radio Set used in the experiments (Czerwinski).

——Patterson antennas (which are vertical loop antennas) provide good sky-wave communication, but because of their size are more suitable for base stations than for vehicular applications. These antennas are described in detail in the August 1967 issue of *Electronics* (comment by Belrose). The effectiveness of a Patterson antenna in yielding reliable high angle sky-wave transmission has also been observed at Georgia Tech, where an antenna of this type provided consistently better communication over a 22 km ground distance than a resonated monopole antenna (Jenkins).

——Measurements with horizontal loop HF antennas installed on the roofs of cars have shown that the performance of such antennas is superior to that of commercially-available center-loaded whips (see for example, W. S. Bridges, *QST*, July 1968) (Belrose). Since horizontal loops do not radiate in the vertical direction, the improved performance is probably due to low internal antenna losses (high Q) (E).

INTERACTION OF ANTENNAS WITH THEIR PLATFORMS

Army antennas are usually operated under conditions where their electrical properties (current distribution, impedance characteristic, radiation pattern, and efficiency) are strongly affected by their platform environments, i.e., the structures on which the antennas are mounted, such as tanks, helicopters, and shelters. The presently used center-fed VHF whip antenna AS-1729/VRC was designed to have minimum interaction with its platform. With the trend toward smaller and smaller antennas, the decoupling of antennas from their platforms is no longer feasible. Small antennas have strong near fields, and when the near field region is close to the platform, interaction with the antenna increases accordingly. In the limiting case, the antenna degenerates to a coupling element between the transceiver and the platform which functions as the actual antenna. The conditions then become similar to those described in the paper by Ikrath, p. 159 (E).

Due to the structural complexity of typical Army platforms, any analytic-numerical study of the interaction between antenna and platform has to rely, to a large extent, on computer modeling. A number of comments concerned computer modeling codes and their underlying analytic approaches (E).

The wire grid model allows efficient handling of structures which can be modeled by up to ~250 elements, assuming the storage capacity of modern computers. If symmetry relations can be utilized, the upper bound on the number of elements can be increased correspondingly. The number of 250 elements is not a limit in principle, but rather a practical limit. If more elements are required, data storage discs or tapes may be employed. However, the transfer into and out of discs or tapes is time consuming, i.e., expensive, and in addition, may lead to errors (Mittra, Hansen, Medgyesi-Mitschang).

In applying the method of moments, the cell size should be chosen to provide at least 5 to 6 elements per wavelength. Empirically, this appears to be the absolute minimum to obtain acceptable accuracy when conventional basis functions are used. Special techniques allow a reduction in the number of elements in certain cases. Also, the use of variable cell size (i.e., adjusting the cell size over a given structure in accordance with local accuracy requirements) would be acceptable and would presumably make the program less expensive to run; but a program based on non-uniform cell size is more difficult to write (Mittra).

In general, a wire grid structure of 250 elements will not be sufficient to model Army platforms such as tanks or helicopters with acceptable accuracy. A problem with wire grid models is that--if the loop size is not small compared to the wavelength--the model tends to predetermine the direction of the current distribution. Moreover, the loops may produce fictitious resonances. Far field data, as for example scatter characteristics of helicopters or radiation patterns of tank antennas, may be obtained with acceptable accuracy. But the

computation of quantities strongly influenced by the near field, such as the input impedance or current distribution of antennas in close proximity to a structurally complex metal body, must be treated with a great deal of caution (Mittra, Hansen, Goubau, Schwering; see also paper by Wang, p. 147).

Obviously, very good results can be expected in the case of structures which are composed of linear conductors such as whips, loops, wire grid counterpoises, etc. (E).

For modeling structures with extended conducting surfaces, the patch model approach should be considered. This technique requires the same input; should be more accurate; is just as easy to apply, and at least as efficient as the wire grid model. At present, general computer codes for patch modeling are not available. Development of such codes was recommended (Harrington). Codes for wire grid modeling, on the other hand, are already in existence and have been widely tested and used. Examples include the MBA program, the codes developed at Ohio State and Syracuse Universities, the Lawrence Livermore programs, and others (E).

A patch model approach has in effect been used in the numerical method developed by Harrington for computing the fields of bodies of revolution. This method uses a Fourier expansion for the azimuthal field distribution and thus reduces the computational problem by one dimension. The method should give very accurate results at reasonable cost (Mittra). In the study described in the paper by Medgyesi-Mitschang and Brune, p. 135, this method has been employed to model helicopters. It was pointed out that, in addition to numerical efficiency, the method facilitates determination of ground effects (reflection coefficient method) and their dependence on flight altitude, since certain integrals can be evaluated in closed form. For details, see the paper cited above (Medgyesi-Mitschang).

INTERACTION OF HUMAN BODY WITH MANPACK ANTENNAS

In the two theoretical papers which apply to this subject, Newman p. 165 and Chen & Nyquist, p. 171, the human body is modeled by dielectric and moderately conducting bodies. In both papers, the interaction is formulated in terms of volume currents in the body. The question was raised (Mittra) whether formulation in terms of electric and magnetic surface currents had been considered (assuming homogeneous electrical properties within the body). Newman commented that in their study both approaches had been considered. In the volume current approach, the number of unknowns is roughly proportional to the volume of the body; whereas in the surface current approach, the number of unknowns is proportional to the surface of the body. Thus for bodies with linear dimensions on the order of a wavelength, the volume current approach requires many more unknowns than the surface current approach. However, both approaches lead to matrix sizes which cannot be handled efficiently. At larger wavelengths, the volume current approach becomes more competitive. For bodies with dimensions on the order of a quarter wavelength or less, i.e., body sizes which can be treated accurately within the practical limit of 250 unknowns, the volume current approach requires about as many, or less, unknowns than the surface current approach and yields as good, or better, results.

The following comments based on experimental studies on body effects were contributed:

——Microwave irradiation experiments on rats under semi-far field conditions have indicated that the bone structure in biological bodies has a tendency to focus radiation and thus magnify the effects of irradiation. It appears extremely complicated to model biological structures with acceptable accuracy, and very difficult to draw conclusions. Even hazard levels appear to be rather arbitrary. Studies in cooperation with biologists to determine what constitutes a hazard by EM radiation are under way (contributor unidentified).

——Experiments with manpack sets indicate that the spinal column is a rather good conductor of electricity and does much to enhance or subtract from radiation, depending on excitation. Development of a model of the human body, more detailed than the currently used homogeneous model appears desirable. Under the conditions considered, for example, in the paper by Chen & Nyquist, ~12% of the power radiated by a manpack antenna would be absorbed by the operator's body. Experiments indicate that the actual percentage is higher (contributor unidentified).

GROUND EFFECTS

The electrical properties of antennas which are in close proximity to the ground are very difficult to compute. Available computer codes which take ground effects into account, usually by employing the reflection coefficient method, yield good approximations for the far field, but fail for near field calculations, in particular, they are unreliable for calculating the input impedance of the antenna, which requires application of the rigorous Sommerfeld theory. This theory, however, involves slowly converging integrals and is computationally inefficient (E).

The question was asked (Schwering) whether there is a technique available which combines both accuracy and computational efficiency in the modeling of near-field ground effects. Apparently no such technique is available at the present time (Mittra). According to the latest information, work in this area is under way at Lawrence Livermore Laboratories. LLL has found that in the case of a vertical electric dipole and a ground of large refractive index, the Norton formulas yield remarkably accurate results for the electric field strength, even for distances from the antenna substantially smaller than one wavelength, which in theory is the limit of the range of validity of Norton's approximation (Hansen, Medgyesi-Mitschang).

An example of the computational difficulties encountered in assessing ground effects accurately was discussed in connection with the paper by Lane, p. 81. The antenna considered was a ground-based vertical antenna, with a ground stake or a single wire counterpoise. In this case, a laborious semi-empirical method utilizing several approaches and involving curve-fitting was developed which gave good results in the MF and HF ranges. A computer program using the reflection coefficient method turned out to be very inaccurate (Lane).

An interesting experimental study on directional effects produced by small counterpoises consisting of a few short radial wires was reported by Belrose. The system studied used a 110" high center-loaded whip antenna radiating above sandy soil at 3.8 MHz; a counterpoise of a few symmetrically arranged radial wires $\lambda/4$ in length was used.

For counterpoises of three or more radials, little directivity was observed in the horizontal plane. When the number of radial wires was reduced to two, the field strength in the plane normal to these radials was marginally stronger (by 1.5 to 2 dB) than in the plane containing these radials. When only one radial was used, its orientation relative to the direction of incidence had a significant effect on the received signal strength. When the radial was oriented towards the direction of incidence, the signal strength was found to be 10 dB higher than when the radial was directed away from it. Similar directivity effects should be expected for vehicular antennas placed on one of the "corners" of the body of the vehicle. The study was conducted experimentally; a theoretical confirmation was not attempted (Belrose).

It appears that the theory of ground screens consisting of a few short wires is not well developed (Hansen).

BANDWIDTH OF SMALL ANTENNAS

Antennas used for Army tactical communications are usually of simple configuration, typically whips or loops. If these antennas are electrically small and operated in impedance match, as required to obtain high efficiency in the transmitting case, they are inherently narrow band devices. They may be tuneable over a wide frequency band, but their "instantaneous" bandwidth is small. However, there are Army applications where large instantaneous bandwidths are required. Examples are spread spectrum techniques and fast frequency hopping (FFH). The broad bandwidth requirement in these cases holds for both transmission and reception* (E).

Broad instantaneous bandwidth and small antenna size are conflicting requirements. The use of active antennas may provide a solution to this problem, as demonstrated for HF receiving antennas by the papers presented at this conference. Active transmitting antennas of rather small size and large bandwidth (but rather low power and efficiency) have been described by Mclean, et. al.†,§ The study of active antennas is thus of significant interest for Army tactical communications. In the case of transmitting antennas, the suppression of harmonics will be a problem; however, at the comparatively low power levels of typical tactical radio communication equipment (1 - 50 W), this problem is not likely to be critical (E).

The question was asked (Goubau) whether there is proof of the generally-accepted assumption that the bandwidth of a small antenna is determined by the ratio of stored energy and radiated plus internal-loss power (antenna Q).

---

*Instead of requiring broad band antennas, one may, of course, also consider fast (i.e., electronic) tuning methods for FFH.

†T. S. M. Maclean and P. A. Ramsdale, "Short active aerials for transmission," International Journal Electronics, vol. 34, no. 2, pp. 261-269, 1974.

§T. S. M. Maclean and G. Morris, "Short range active transmitting antenna with very large height reduction," IEEE Transactions Antennas & Propagation, vol. AP-23, pp. 286-287, March 1975.

This assumption is certainly correct if the antenna behaves as an ordinary LC circuit, as for example in the case of a small whip or loop. However, is it also correct when the antenna consists of a system of closely-coupled smaller radiating elements? The multi-element monopole antennas described in the paper by Goubau, p. 63, have a bandwidth which is a multiple of that of a single monopole of the same overall dimensions.

The question, in effect, remained unanswered. A possible approach was pointed out by Tai, who suggested that a study of the location of the poles and zeros of the impedance function of radiating systems is likely to provide useful information on the bandwidth problem. Fano in his papers on circuit theory* gives a good definition of bandwidth from the impedance point of view. His method could possibly be extended to the theory of broad band antennas, when more is known about the poles and zeros of their impedance function.

ACTIVE RECEIVING ANTENNAS

Responding to a request by the discussion moderator (Mittra), Lindenmeier discussed in some detail the difference in matching conditions for small passive and active antennas. In particular, he explained the relationship between the signal-to-noise bandwidth of a receiving system (i.e., frequency band in which S/N varies within a factor of 2), and the external noise level. He showed that an optimum antenna height (see Meinke, p. 35) can also be defined for broad-band antennas. Any larger antenna would increase the S/N ratio at the most by 3 dB. Due to the high external noise temperature in the HF and lower frequency bands, active antennas which combine small size and extremely large bandwidth can be designed. In Lindenmeier's words, "Active receiving antennas live on the high external noise temperature." Since it is not possible to summarize Lindenmeier's theory in a few sentences, reference is made to the pertinent literature.*,†,§

The optimum size of an active receiving antenna as defined by Meinke and Lindenmeier depends on the external noise temperature and the noise temperature of the active devices used in the preamplifier. Several comments centered around these two noise quantities:

---

*R. M. Fano, "Theoretical limitations on the broadband matching of arbitrary impedances," R.L.E. Technical Report No. 41, January 2, 1948.

**H. Lindenmeier, "Optimum bandwidth of signal-to-noise ratio of receiving systems with small antennas," Archiv für Elektronik und Übertragungstechnik, pp. 358-367, September 1976.

†H. K. Lindenmeier, "Relation between minimum antenna height and bandwidth of the signal-to-noise ratio in a receiving system," Presented at the 1976 International IEEE/AP-S Symposium & USNC/URSI Meeting, Oct. 10-15, 1976, Amherst, Mass.; published in Symposium Digest.

§H. K. Lindenmeier, "Design of electrically small broadband receiving antennas under consideration of nonlinear distortions in amplifier elements," Presented at the 1976 International IEEE/AP-S Symposium & USNC/URSI Meeting, Oct. 10-15, 1976, Amherst, Mass.; published in Symposium Digest.

——The range over which the external noise level varies is very wide. The CCIR curves commonly used to indicate upper and lower limits may not be applicable in all situations (Bedard).

——The CCIR curves have been found to give good predictions in open terrain (in southern Germany). On the other hand, cities have an incredibly high noise level; Munich was cited as an example (Meinke).

——Modern low noise transistors seem to have reached a fairly uniform noise temperature; all of these transistors are in practically the same class. Future developments, of course, may result in improvements which would allow further reduction in the optimum height of active receiving antennas. But it is felt that the h_{opt} defined today is already a basic quantity (Meinke).

——Cooling of the preamplifier would be an effective way to achieve a low electronic noise temperature, and thus reduce the optimum antenna size. The system noise temperature, of course, would be above the preamplifier noise temperature. Whether cooling is a reasonable approach from an engineering point of view is debatable, but substantial improvements can be achieved by this method (Bedard).

Further Comments

——Bedard pointed out and Lindenmeier confirmed the parallelism of the two active antenna methods described by Meinke-Lindenmeier, pp. 35 and 105, and by Welker-Bedard, p. 183, respectively. The first method applies to whip antennas and uses a high-impedance voltage amplifier; the second method applies to loop antennas and employs a low-impedance current amplifier. Both methods make use of the basic condition that the internal (electronics) noise of the active device should not exceed the external noise received by the antenna. Both approaches result in very broadband antenna designs, but at large dynamic ranges have to cope with the problem of nonlinearity. The noise temperature in the case of the Meinke-Lindenmeier antennas should be in the order of several hundred degrees Kelvin; in the case of the Welker-Bedard antennas, in the order of several degrees Kelvin (due to cooling). Hence, whereas the Meinke-Lindenmeier antennas can be used up to higher frequencies, the Welker-Bedard antennas can be used down to dc.

——The use of active antennas is likely to allow the design of antenna arrays with closer element spacing than considered up to now. The reason: reduced coupling between elements. Work conducted at Ohio State University in this area looks encouraging, but has not been carried through sufficiently far to permit definite conclusions (Walter in response to Bedard).

——The advantages of using active rather than passive elements in arrays may also be seen from the DF-array discussed in Lindenmeier's paper, p. 105. In addition to a substantial reduction in the height of the element antennas (in comparison to a passive array of equivalent sensitivity), the mutual coupling between elements is significantly smaller for two reasons: lower element height and the use of active, i.e., unmatched receiving networks (Lindenmeier).

——The S/N ratio of receiving antennas may be improved by the use of directive arrays. Directivity in the case of electrically small antennas

implies the use of *super*-directive arrays. Theoretical work on such arrays has been performed at Ohio State University. For example, it has been shown that circular arrays as small as 0.1λ in diameter may yield directivities up to 15 dB. The arrays considered consisted of passive elements. The use of active elements should facilitate the design of receiving arrays by reducing inter-element coupling (Walter and Newman in response to Lane).

ACTIVE TRANSMITTING ANTENNAS

No papers were presented on active antennas for transmission. The topic was only touched upon during the discussion sessions. According to Meinke, not much can be gained by using active devices integrated with transmitting antennas, at least not such fundamental improvements as were achieved in the case of receiving antennas. Solution of the tuning problem becomes easier and a somehwat better efficiency may be obtained if only a few components (and no transmission lines) are present between the power amplifier and the antenna. But no dramatic improvements are expected. The suppression of harmonics will be a problem, especially when the allowable limits on harmonic radiation are set in (absolute) field strength. The problem will be very difficult to solve for high power broadcast antennas, but for the moderate power commonly used in Army tactical communications (1 - 50 W), the suppression of harmonics should not pose a major problem (Meinke).

TRANSCEIVER ANTENNAS

Transceivers for tactical radio communication require antennas for both transmission and reception, as opposed, for example, to direction-finding, intercept, and navigation equipment, which operate with receiving antennas only. Since the electrical requirements for transmitting and receiving antennas are basically different--a fact very much in evidence in the case of electrically small antennas--the following question was raised: Is it more advantageous in the case of tactical transceivers to use two separate antennas optimized for transmission and reception, or a single antenna, possibly with two different feed networks, to be switched with the mode of operation? Tactical communication transceivers are usually operated in semi-duplex, i.e., they are alternately used for transmission and reception (at the same frequency), but are not concurrently operated in both modes (E).

At the University of Munich, experiments were made with U. S. Army standard communication manpack sets and two separate (though by necessity closely-spaced) antennas, i.e., a small active receiving antenna and a larger passive transmitting antenna. Improvements were obtained in comparison to conventional (single) Army whip antennas. These improvements, however, were brought about solely by the active receiving antenna; the transmitting antenna did not contribute noticeably to signal enhancement (Meinke).

The question was asked (Mittra): If a somewhat larger transmitting antenna is needed anyway, why not use it for reception also? No harm would be done by exceeding the optimum antenna height as defined by Meinke. In the ensuing discussion, the following observations were contributed:

——An active antenna which is too efficient may cause intermodulation problems in the presence of strong transmitters (Gibson).

——In the case of a duplex or semi-duplex communication system employing diversity reception, one transmitting antenna would be used at each station with several receiving antennas. No advantage is to be gained by trying to combine the transmitting with the receiving antennas (Lindenmeier).

——The use of separate antennas would help to decouple receivers from transmitters; in certain cases, it may just be more practical to use two antennas (Lindenmeier).

Editors' Comment. The use of only one antenna for transceivers has the advantage of structural simplicity. Furthermore, if this antenna is connected to a conventional variable-reactance tuning system designed to provide maximum efficiency in the transmit mode, then feeding the receiver through the same network (in the same tuning state) would not necessarily degrade the S/N ratio in comparison to that obtained with an active antenna, but might actually slightly enhance it. We are considering here the VHF-FM band. The instantaneous bandwidth is, of course, narrow, particularly in the case of an electrically small antenna. But since a variable tuning network is needed in the first place--to cover the specified frequency band in the transmit mode--, no advantage in principle is seen in using a separate antenna for reception, even if it is very small and has a very wide (instantaneous) bandwidth. Of course, practical aspects, as for instance, the problems involved in realizing an efficient passive variable tuning system operating over a large frequency band or the possibility of improving the S/N ratio of a given receiver by connecting it to an antenna with an integrated high quality preamplifier, may create conditions where the use of separate antennas would improve the system performance. In other words, for a given transceiver, it is entirely possible that the S/N ratio can be increased by the use of an active antenna for reception, as demonstrated by Meinke's experiments (see above).

DEFINITIONS AND STANDARDS FOR SMALL ANTENNAS

The term "electrically small antenna" commonly refers to a radiating structure which can be accommodated within a radian sphere, i.e., a sphere of diameter λ/π. In the case of monopole antennas, the "image" is to be considered as part of the antenna. A more stringent definition requires linear dimensions smaller than $\lambda/10$.

Comment by Schroeder. If small antennas have a broad bandwidth, as for example, the passive antenna described by Goubau, or the active antennas discussed by Meinke and Lindenmeier, then the above definitions need clarification: Should the condition that the linear dimensions be smaller than λ/π or $\lambda/10$, be applied at the lowest frequency of the band, at the center frequency, or where?

Schroeder furthermore suggested that an attempt be made to define active antennas. The standard dictionary of the IEEE does not offer such a definition. Opinions as to the need for, and approach to, defining active antennas differed widely:

——Hansen contended that the problem is no longer relevant. Every receiving antenna is active, since it is always connected to an amplifier; and with recent designs, it is very difficult to determine where the antenna terminates and the receiver begins.

——Gibson suggested that a performance standard for active receiving antennas be agreed upon. This standard should consider the whole system, including the receiver. For example, the S/N ratio of a given system might be compared to the S/N ratio of a standard reference system to provide an overall performance rating expressible in dB.

——Cottony: Related that a Standard on integrated antennas is already in existence. It has been prepared by the IEEE receiver group.

——Note by editors: Any definition of active antennas would necessitate a redefinition of antenna performance parameters. The antenna panel of The Technical Cooperation Program (TTCP), a working group set up by the defense departments of English-speaking nations, has been studying this question and seeking guidance from both the IEEE and the IEE. A final report has not yet been issued.

Gibson expanded his above remarks concerning a performance standard for active receiving antenna systems. An example for a reference standard would be a dipole antenna with a noise-free receiver operating under an assumed sky temperature of 290° K. Using the S/N ratio as the basis for comparison, the performance of any given antenna-receiver system could then be measured against the S/N ratio achievable with the reference standard. The figure of merit (performance in dB below standard) would involve all pertinent parameters, such as efficiency, noise figure, directivity, sky temperature, etc.

In response to a question by Walter regarding reference standards used by systems engineers, Gibson explained that for satellite communication systems, the G/T ratio is commonly used as performance parameter, i.e., the overall gain divided by the system temperature. However, for ground-based vehicular and airborne antennas, a performance standard which refers to a sky temperature of 290° K, rather than 0° K, appears more suitable (Gibson).

The comment was made that in the lower HF range and below the external noise temperature is so nigh that inconveniently large numbers would be obtained with the above suggested standard. Instead, the use of the equivalent noise field strength, which should be more convenient, was recommended. At higher frequencies where the external noise is low, it would be appropriate to base the performance standard on the noise figure, as suggested (Lindenmeier).

CONCLUSIONS AND RECOMMENDATIONS

The presentations and discussions of the Workshop clearly demonstrate that the present state-of-the-art in electrically small antennas is not sufficiently advanced to meet the requirements of Army tactical communications systems. We are referring here, specifically, to the requirements of reasonable efficiency and--in future systems--large instantaneous bandwidth. These requirements pose a difficult problem in the design of transmitting antennas, or more generally, the design of passive antennas for transceivers. The situation is different for antennas used solely for reception. For these antennas, the important performance parameter is not the radiation efficiency, but the S/N ratio; and, due to recent advances in active antenna techniques, the bandwidth problem can be regarded as solved.

The complexity of the problem in the case of passive antennas, arises from the fact that the requirements of large instantaneous bandwidth and high efficiency are in conflict with the constraint that the antenna system be small compared to a wavelength. However, small antennas mounted on helicopters, tanks, or shelters interact strongly with their platforms. The dimensions of these platforms are on the order of a wavelength in the upper HF and lower VHF bands, i.e., at about the center of the frequency range commonly used for tactical communication. Therefore, the actual radiating system, i.e., the combination of antenna and platform is not at all small in comparison with a wavelength in these Army applications. There appears to be no compelling reason why small antennas, or systems of small antennas, installed on platforms with dimensions in the order of a wavelength could not have good efficiency and large bandwidth. The fact that there are no efficient wide band vehicular antennas in existence should not be taken to mean that they are infeasible.

Although the problem of small, efficient vehicular antennas is the most urgent one at the present time, there are other problems involving small antennas for which an entirely satisfactory solution has not as yet been found. One of these problems is the development of antennas (including their tuning systems) for manpack radios operating in the VHF-FM range from 30 to 90 MHz. Since these antennas are used at the front lines, the requirement for low visibility is extremely important; and, since the available power is small, their radiation efficiency must be high. The problem is complicated by the fact that the radio operator is within the near field region of the antenna. He may stand, walk, or lie prone on the ground. In all these situations, an adequate transmission range is a necessity which imposes very demanding requirements, not so much on the antenna itself, but on the tuning system. Substantial progress has been made recently in the design of manpack antennas; but more work must be carried out to achieve a better understanding of proximity effects and--as far as possible--a reduction in their detrimental influence on antenna performance. The manpack antenna problem and various possible approaches to its solution were discussed in detail at a previous Workshop* held at ECOM in 1968.

---

*E. Berman, Editor, Proceedings of Antenna Workshop, U. S. Army Electronics Command, Fort Monmouth, N. J., 13-15 February 1968 (AD 833046 L).

Another problem to be mentioned in this context is the reduction of ground losses of small ground-based tactical HF antennas. Since these antennas must be transportable and easily installed, their ground systems cannot be bulky.

To meet the Army's requirements in the area of tactical communication antennas in the near future, intensified research efforts taking different paths of approach will be necessary. A number of problems and approaches which in the opinion of the editors merit special attention are listed below together with a few explanatory comments:

(1) Interaction of an electrically small monopole, or loop antenna, with a (metal) platform, having dimensions in the order of a wavelength.

The question of the extent and general direction in which typical Army platforms (and the location of an antenna on such platforms) modify input impedance, radiation, and antenna efficiency should be systematically investigated. The goal is to determine how platform effects can be utilized to improve antenna performance, possibly over an extended range of frequencies.

(2) Interaction between several small antennas mounted on the same platform.

Information should be derived on input impedance, radiation patterns, and the efficiency of the total system, including antennas, platform, and the network interconnecting the antennas. The objective of this study will be optimization of system performance by the use of several strategically-placed small antennas and the systematic utilization of platform effects. The goal will be to achieve reasonable efficiency and broad bandwidth, in addition to predictable, and in certain cases, steerable, patterns. An exploratory study related to problems (1) and (2) is presently under consideration at ECOM, where a spherical platform (or a hemisphere on a ground plane) excited by small antennas is analyzed. Such platforms allow a rigorous analytical treatment yielding qualitative information on interaction effects between small antennas and actual platforms, and an estimate of the order of magnitude of these effects. A similar study involving larger antennas was recently reported in the literature.*

(3) Development of a computer modeling code based on the patch model approach.

Typical Army antenna platforms such as helicopters, tanks, and armored personnel carriers, are complicated in structure. Hence, theoretical studies of platform effects, such as those suggested in (1) and (2), must, to a large extent, rely on computer modeling. Available computer codes, based

*F. M. Tesche and A. R. Neureuther, "The analysis of monopole antennas located on a spherical vehicle: Part I, Theory," IEEE Transactions on Electromagnetic Compatibility, vol. EMC-18, pp. 2-8, February 1976.

F. M. Tesche, A. R. Neureuther, and R. E. Stovall, "The analysis of monopole antennas located on a spherical vehicle: Part II, Numerical and Experimental Results, IEEE Transactions on Electromagnetic Compatibility, vol. EMC-18, pp. 8-15, February 1976.

on the wire grid model, require substantially more elements for numerically accurate modeling of Army platforms than can be handled economically with most of today's computers. The patch model approach can be expected to provide improved accuracy at substantially reduced cost. Development of a versatile code based on this approach is desirable.

(4) Development of an economical experimental method for measuring platform effects on antennas and antenna systems by use of scale models.

Such a method would offer not only an alternative to the computer modeling approach to problems (1) and (2), but is also needed to establish a data base of controlled experimental results, against which the accuracy of newly-developed computer codes can be checked.

(5) Investigation of multi-element monopole antennas.

The multi-element antennas discussed in Goubau's paper have very large bandwidth and high efficiency, despite comparatively small size. However, if present experimental models were scaled into the VHF range, they would be too large for placement on Army vehicles. At present, there is no theory available to predict their performance if their electrical size were reduced. A theory of multi-element antennas is therefore desirable. A number of different antenna configurations based on the same principle should be investigated.

(6) Fundamental study on the bandwidth of electrically small antennas.

The commonly accepted notion that the bandwidth of electrically small antennas is determined by the ratio of stored energy and radiated power plus internal loss may require revision. There appears to be no proof of this hypothesis except for the case of antennas of simple configuration (whips or loops), whose input impedance can be described by a simple LC circuit with a single resonance. In contrast, Goubau's antennas have several resonances within the operating band.

(7) Study of active transmitting antennas.

The state-of-the-art in the area of active receiving antennas is far advanced; but there is much too little information available on active transmitting antennas to predict their potential for Army applications. The subject was only very briefly touched upon during the discussion sessions, and no papers on active transmitting antennas were submitted for presentation. Although it is unlikely that drastic improvements in antenna performance will be obtained, there is the possibility that the use of active monopoles and loops for transmission will facilitate efficient broad-band excitation of platforms, such as tanks and helicopters.

(8) Development of very fast electronic tuning and switching circuits for small antennas.

The availability of such circuits would permit the use of fast frequency hopping (FFH) techniques, without necessitating antennas with large instantaneous bandwidth.

(9) Study of proximity effects on manpack antennas.

A better understanding is needed of the effects of interaction of manpack antennas with the human body, with manpack attachments, such as the microphone cord, and with the ground. Experimental evidence indicates that the nonuniform distribution of conductivity and permittivity throughout the body significantly affects interaction. Taking these inhomogeneities into account may render numerical modeling inefficient, and an experimental study appears to be the more promising approach at the present time. With regard to the investigation of ground effects, see Item (10).

(10) Development of an efficient numerical method for calculating ground effects on near-earth antennas.

In many situations, Army tactical communication antennas radiate in close proximity to the earth's surface. Currently-available computer codes for the study of such antennas use approximations to take earth effects into account. A consequence is that they become inaccurate when the antenna height above ground is decreased substantially below a quarter wavelength. (Computed radiation patterns may still be acceptable, but quantities strongly influenced by the antenna near field, such as the current distribution and input impedance, become unreliable.) On the other hand, codes using the rigorous Sommerfeld integrals are usually numerically inefficient. A numerical method which combines high accuracy with numerical efficiency is needed for near-earth antenna studies.

Note that small phase errors in the ground-reaction field strength may result in substantial errors in the input resistance and radiation efficiency of small antennas. (Since their input impedance is usually purely reactive, even a small phase error can lead to a large error in input resistance.) Hence, accuracy requirements may be stringent.

Specific applications include the investigation of earth effects on manpack antennas and the design of lightweight, transportable HF-whip antennas and their ground systems, which may typically consist of a few short radial wires. The effectiveness of a small counterpoise in reducing HF ground losses can be inferred from a recent study* on near-earth dipole antennas, which shows that the major portion of these losses occurs within a radial distance

*C. M. DeSantis, D. V. Campbell, and F. Schwering, "An array technique for reducing ground losses in the HF-range," IEEE Transactions Antennas & Propagation, vol. AP-21, pp. 769-773, November 1973.

$< 0.1\lambda$ about the antenna. Availability of an efficient computer method which accurately includes ground effects would facilitate the design of small tactical HF-antennas. For example, a trade-off study in terms of factors such as weight, ease of installation, and antenna efficiency could be conducted very economically.

ACKNOWLEDGMENTS

The Workshop was suggested and sponsored by the U. S. Army Research Office, Durham, N. C. The encouragement and assistance received from this Agency, and in particular from Dr. H. Wittmann, are gratefully acknowledged.

The organizers of the Workshop express their thanks to the moderators of the discussion periods, Dr. Hansen, Prof. Mittra, and Prof. Walter, for stimulating and guiding a thought-provoking exchange of ideas. Special thanks are due Prof. Mittra for reviving the spirits of the conference participants--exhausted after a long day of presentations and discussions--by his very entertaining after-dinner talk on the first day of the conference. The evening session of this day was as lively as the preceeding sessions, despite the late hours.

The organizers thank the invited speakers, Dr. Wheeler, Sgt. Donohue, Dr. Kvigne, and Prof. Walter, for presenting their informative overview papers. Special thanks are due Prof. Meinke and Dr. Lindenmeier, who came all the way from München to present invited papers on their pioneering work in the area of active antennas.

The assistance of the technicians of the Communications Research Technical Area of the Communications/ADP Laboratory, during the Workshop is gratefully acknowledged. The services of Messrs. M. Begala, W. Kennebeck, and A. Zanella contributed greatly to the smooth conduct of the conference; in particular, Mr. J. Wills played a key role in its organization. We thank our secretaries, Mrs. Jane Servilla, Mrs. Nellie Jones, and Miss Marg Vuksanic, for organizing, conducting, and gracing the registration desk. Mrs. Luella Bechmann's competent editing of these Proceedings is greatly appreciated.

The organizers thank the Fort Monmouth Officers' Club for having made their excellent Gibbs Hall Facilities available for the conference. The competent services and very cooperative assistance of Mr. J. Raczek, the catering manager of Gibbs Hall, are gratefully acknowledged. Thanks are due Messrs. S. Sroka, C. Exley, and J. Vonella of ECOM for installing and operating the audio-visual equipment, a job very well done.

We thank the IEEE for granting permission to reprint Dr. Wheeler's paper on electrically small antennas in these Proceedings.

WORKSHOP ON ELECTRICALLY SMALL ANTENNAS

ATTENDANCE LIST

Mr. M. Acker	ECOM, DRSEL-NL-RF-2 Fort Monmouth, NJ 07703
Mr. V. Alevizakos	ECOM, DRSEL-WL-D Fort Monmouth, NJ 07703
Mr. A.J. Bahr	Stanford Research Institute Menlo Park, CA 94025
Dr. F.D. Bedard	Lab for Phys Science College Park, MD 20740
Dr. J.F. Belrose	Comm Rsch Center Ottawa, Canada
Dr. H. Bennett	ECOM, DRSEL-NL-RO Fort Monmouth, NJ 07703
Mr. L. Black	Naval Surface Weapons Center
Mr. N. Brown	Cincinnati Electronics Corp Cincinnati, OH 45241
Mr. J. Brune	ECOM, DRSEL-VL-D Fort Monmouth, NJ 07703
Mr. J.E. Brunner	Cincinnati Electronics Corp Cincinnati, OH 45241
Mr. D. Campbell	ECOM, DRSEL-NL-RH Fort Monmouth, NJ 07703
Dr. J.R. Christian	ECOM, DRSEL-NL-RH Fort Monmouth, NJ 07703
Dr. H.V. Cottony	SELF, 5204 Wilson Lane Bethesda, MD 20014
Mr. W.P. Czerwinski	ECOM, DRSEL-NL-RH Fort Monmouth, NJ 07703

ATTENDANCE LIST (CONT'D)

Mr. J.D. Davis	DHV, Inc, P.O. Box 520 Mineral Wells, TX 67067
Mr. R. Deely	Applied Devices Corp.
Mr. C. DeSantis	ECOM, DRSEL-NL-RH Fort Monmouth, NJ 07703
Dr. R.J. Dinger	Naval Research Laboratory Washington, DC 20375
MSG A. Donohue	USA Signal School (ATSN-DCD-MS) Fort Gordon, GA 30905
Dr. D. Fessenden	NUCS
Dr. P.R. Franchi	RADC/ET, LG Hanscom Fld Bedford, MA 01730
Mr. R. Gallant	GTE-Sylvania
Dr. B. Gelernter	ECOM, DRSEL-CT-D Fort Monmouth, NJ 07703
Dr. J.J. Gibson	RCA Laboratories Princeton, NJ 08540
Mr. C.L. Golliday, Jr.	Naval Research Laboratory Washington, DC 20375
Dr. G. Goubau	ECOM, DRSEL-NL-RH Fort Monmouth, NJ 07703
Mr. J.R. Gruber	Cincinnati Electronics Corp Cincinnati, OH 45241
Dr. R.C. Hansen	R.C. Hansen, Inc., Box 215 Tarzana, CA 91356

ATTENDANCE LIST (CONT'D)

Prof. R.F. Harrington	ECE Dept, 111 Link Hall Syracuse Univ, Syracuse, NY 13210
Mr. S.J. Harris	Magnavox/General Atronics Philadelphia, PA 19118
Dr. J.A. Higgs	Motorola, Gov't Elect Div Scottsdale, AZ 85252
Mr. R.T. Hoverter	ECOM, DRSEL-NL-RH-4 Fort Monmouth, NJ 07703
Dr. K. Ikrath	ECOM, DRSEL-NL-RH-6 Fort Monmouth, NJ 07703
Mr. R. Ivone	ECOM, DRSEL-WL-D Fort Monmouth, NJ 07703
Mr. J.R. Jahoda	Bayshore Systems Corp Springfield, VA 22151
M.H.H. Jenkins	Engr Exp Station, GA Tech Atlanta, GA 30332
Dr. H.S. Jones, Jr.	Microwave Rsch & Dev Br, Harry Diamond Labs, Adelphi, MD 20783
Mr. J.L. Kerr	ECOM, DRSEL-CT-D Fort Monmouth, NJ 07703
Mr. R.T. Klopach	American Electronic Lab Colmar, PA 19446
Mr. M.C. Knight	GTE Sylvania, 77A St. Needham, MA 02194
Mr. S. Krevsky	ECOM, USACSA, CCM Fort Monmouth, NJ 07703
Mr. R.A. Kulinyi	ECOM, DRSEL-NL-RO Fort Monmouth, NJ 07703

ATTENDANCE LIST(CONT'D)

Dr. Marlan Kvigne	Navy Electronics Lab Center San Diego, CA 92152
Dr. Edwin F. Laine	Lawrence Livermore Lab Livermore, CA 94551
Mr. George Lane	USACEEIA, ATTN: CED-EMME Ft. Huachuca, AZ 85613
Dr. Stuart A. Long	Dept. of Elec Eng, University of Houston, Houston TX 77004
Dr. H. Lindenmeier	Techn. Univ of Munich 8 Muenchen 2, Arcisstr. 21, Germany
Mr. A. G. Loveberg	Navy Elec Lab Center San Diego, CA 92152
Prof. John A.M. Lyon	University of Michigan Ann Arbor, MI 48109
Mr. Alfred R. Lopez	Hazeltine Corp/Wheeler Lab Greenlawn, NY 11740
Mr. C. Masen	USACEEIA Ft. Huachuca, AZ 85613
Dr. W. McAfee	ECOM, DRSEL-RD-O Ft. Monmouth, NJ 07703
Prof. H.H. Meinke	Tech Univ of Munich 8 Muenchen 2, Arcisstr. 21, Germany
Dr. James W. Mink	ECOM, DRSEL-NL-RH Ft. Monmouth, NJ 07703
Dr. L. Medgyesi-Mitschang	McDonnell Douglas Rsch Labs St. Louis, MO 63166

ATTENDANCE LIST(CONT'D)

Prof. R. Mittra	University of Illinois Urbana, IL 61801
Mr. M.S. Moy	Dept. of Justice Washington, DC
Dr. Henry Mullaney	Ofc of Naval Rsch Arlington, VA 22217
Mr. E. Murphy	Motorola Corp.
Mr. Martin L. Musselman	Naval Rsch Laboratory Washington, DC 20375
Dr. E.H. Newman	Ohio State University Columbus, Ohio 43212
Dr. Dennis P. Nyquist	Michigan State University East Lansing, MI 48824
Mr. C. Payne	Naval Surface Weapons Center
Mr. J.H. Provencher	Naval Electronics Lab Center San Diego, CA 92152
Dr. F.H. Reder	CCOM, DRSEL-NL-RH Fort Monmouth, NJ 07703
Mr. Frank Reggia	Harry Diamond Labs Washington, DC 20438
Mr. Stephen J. Rosasco	Magnavox Company Philadelphia, PA 19118
Mr. R.K. Royce	Naval Rsch Laboratory Washington, DC 20375

ATTENDANCE LIST (CONT'D)

Mr. Robert Sainati	NUSC New London, CO 06320
Dr. William A. Sander	US Army Rsch Ofc Rsch Triangle Park, NC 27709
Mr. Frank Schiavone	Ball Brothers Rsch Boulder, CO 80302
Mr. Klaus P. Schroeder	Aerospace Corp. El Segundo, CA 90505
Dr. F. Schwering	ECOM, DRSEL-NL-RH-1 Ft. Monmouth, NJ 07703
Mr. Glen J. Seward	Cincinnati Electronics Corp. Cincinnati, OH 45241
Prof. L.C. Shen	University of Houston Houston, TX 77004
Mr. Panos P. Siatis	US Information Agency Washington, DC 20547
Mr. Larry D. Sikes	Engineering Experiment Station Georgia Institute of Technology Atlanta, GA 30332
COL D. Slingerland	ECOM, DRSEL-NL-D Fort Monmouth, NJ 07703
Prof. Glenn S. Smith	Georgia Institute of Technology Atlanta, GA 30332
Dr. Karl H. Steinbach	USAMERADCOM Fort Belvoir, VA 22060
Mr. E.K. Stodola	ECOM, Fort Monmouth, NJ 07703

ATTENDANCE LIST(CONT'D)

Mr. C.A. Strider	Hughes Aircraft Company Culver City, CA 90230
LTC Robert E. Swartwood	USMC LNO USAECOM, Ft. Monmouth, NJ 07703
Dr. Martin Sweeting	University of Surrey England
Prof. Chen-To-Tai	University of Michigan Ann Arbor, MI 48109
MAJ John M. Taylor, Jr.	SINCGARS TRASSO, HQ TRADOC ATTN: ATCD-SC-E Ft. Monroe, VA 23651
Mr. F. Triolo	ECOM, Ft. Monmouth, NJ 07703
Mr. Theodore H. Vea	Dept.of State Washington, DC 20520
MSG Jan L. Walker	10th Special Forces Group Ft. Devans, MA
CPT Gary C. Walker	US Army Armor Center, ATZK-CD-MS Ft. Knox, KY 40121
Prof. C.H. Walter	Ohio State University Electro Science Lab Columbus, OH 43212
Prof. Johnson J.H. Wang	Georgia Institute of Tech Atlanta, GA 30332
Mr. M. Weiner	ECOM, Ft. Monmouth, NJ 07703
Dr. Nancy K. Welker	Laboratory for Physical Sciences College Park, MD 20740

ATTENDANCE LIST(CONT'D)

Dr. Harold A. Wheeler	Hazeltine Corp Greenlawn, NY 11740
Dr. Gerald Whitman	NJ Institute of Technology Newark, NJ 07102
Dr. R.E. Whitman	ECOM, Ft. Monmouth, NJ 07703
Dr. Horst R. Wittmann	US Army Rsch Ofc Research Triangle Park, NC 27709
Mr. Andrew E. Zeger	Magnavox/General Atronics Philadelphia, PA 19118

AUTHORS' INDEX